Volledig recycleerbaar beton
voor een meer milieuvriendelijke bouwsector

Completely Recyclable Concrete
for a More Environment-Friendly Construction

Mieke De Schepper

UNIVERSITEIT
GENT

Acknowledgements

Elke en Kim om geduldig op al mijn vragen te antwoorden aangaande de papierwinkel bij het indienen van een doctoraat en praktische zaken voor de receptie.

A special thanks also to Dirk, Philip and Joris to join me in the final stages of becoming a PhD: the writing, the confrontation with the deadlines and the defences. The last months are the hardest, but with good company along the way it goes once so smooth.

And last but not least, thanks to all foreign colleagues to be a window to the world and all its cultures.

Uiteraard heb ik de afgelopen jaren niet alleen gewerkt, maar ook veel plezier gemaakt met vrienden en familie. Op de momenten dat ik het met mijn doctoraat wat moeilijker had was ons samenzijn eens zo belangrijk. Jullie hebben mij allemaal enorm gesteund en dat zal ik dan ook nooit vergeten.

Christine & Jan, Koen, Geertrui & Wouter, Petra & Tim, Jan & Jens, Timo & Marloes, Helena, Rita, Sven & Wes, Evelyne, Jo & Jolien en Sofie & Bart heel erg bedankt voor de vele gezellige dinertjes en (ont)spannende spelletjesavonden. Christine, aan jou een extra woord van dank om mij te blijven steunen toen ik worstelde met mezelf ook al had je het zelf niet altijd gemakkelijk.

Aan mijn vrienden van de wereldwinkel van Kieldrecht, Griet & Peter, Jan & Riet, Koen, Karlien & Mario, Helga, Babs, Sandy, Annemie en Karolien, een welgemeende dank je wel voor de fijne vergaderingen, inspirerende gesprekjes en bruisende activiteiten.

Mijn schoonfamilie verdient ook een woord van dank. Reeds van bij het prille begin hebben jullie mij met open armen ontvangen. Het doet deugd om samen met Tom en Line altijd welkom te zijn bij jullie.

Bomma en bompa, ook al is mijn leven sinds vroeger ontzettend druk geworden en heb ik veel te weinig tijd voor jullie: ik zie jullie nog even graag en ben enorm dankbaar voor alle uitstapjes die jullie vroeger met mij en mijn zus gemaakt hebben.

Katrien, je bent een geweldige zus en dat zeg ik wellicht veel te weinig. Hoewel het soms wel eens botst, als het moeilijk gaat kunnen we toch steeds bij elkaar terecht. Ik wens je nog veel succes in de toekomst en hoop dat je binnenkort niet alleen de job maar vooral ook de liefde van je leven tegen komt.

Mama en papa, jullie hebben mij de kans gegeven zorgeloos te studeren en in het leven te staan en mede daardoor heb ik dit doctoraat tot een goed einde kunnen brengen. Jullie hebben mij met veel zorg groot gebracht en hoewel ik intussen op

mijn eigen benen sta, kan ik nog steeds bij jullie terecht voor raad en daad. Dank je wel daarvoor.

Papa, voor jou nog een speciaal woordje. Terwijl ik de afgelopen zes maanden achter mijn computer mijn hoofd leeg typte, stak jij tijdens je vrije uren de handen uit de mouwen in ons huis om het klaar te maken voor onze komst. Dankzij jou verhuizen Tom, Line en ikzelf heel binnenkort naar ons eigen nestje. Een welgemeende dankjewel is dus zeker en vast op zijn plaats!

Tom, met jou aan mijn zij ben ik de gelukkigste vrouw ter wereld. We hebben al zeer mooie jaren achter de rug, en het blijft maar beter worden. Ik kijk enorm uit naar de verhuis naar ons eigen stekje en de mooie momenten die we er ongetwijfeld gaan meemaken met ons gezinnetje. Verder wil ik je enorm bedanken voor de steun van de afgelopen maanden. Terwijl ik alleen nog maar met mijn doctoraat bezig was, sloofde jij je uit om ons huishouden op orde te houden.

Line, bedankt om de schattigste dochter ter wereld te zijn. Zonder dat je het zelf besefte, was jij de afgelopen maanden de 'stille' kracht achter mijn relativerings- en doorzettingsvermogen. Een lach, een zoen of een knuffel van jou, meer heb ik niet nodig voor een *instant happiness* gevoel.

Mieke De Schepper, juni 2014

"It's not our job to toughen our children up to face a cruel and heartless world. It's our job to raise children who will make the world a little less cruel and heartless." – L.R. Knost

Table of contents

Notation index

ABBREVIATIONS

ADP	Abiotic depletion potential	NA	Natural Aggregate
AEA	Air Entraining Agent	ODP	Ozone depletion potential
AFm	Monosulphate	OPC	Ordinary Portland Cement
AFt	Ettringite	PC	Portland Clinker
AM	Alumina Modulus	POCP	Photochemical ozone creation potential
ANOVA	Analysis of variance	QCS	Quickly cooled granulated copper slag
AP	Acidification potential	RAC	Recycled Aggregate Concrete
BFS	Blast Furnace Slag	RCA	Recycled Concrete Aggregates
C2C	Cradle-to-Cradle	S	Sucrose
CA	Citric Acid	SAM	Salicylic Acid in Methanol
CDW	Construction and Demolition Waste	SCM	Supplementary Cementitious Materials
CR	Commercial Retarder	SCS	Slowly cooled broken copper slag
CRC	Completely Recyclable Concrete	SE	Solvent Exchange
cs	Casting surface	SM	Silica Modulus
DoS	Degree of Sulphatisation	SP	Superplasticizer
DT	Differential Thermal	ss	Sawn surface
EFCA	European Federation of Concrete Admixture Associations	SWOT	Strength, Weaknesses, opportunities, Threats
EP	Eutrophication potential	TAP	Apparatus for accelerated deterioration tests (Toestel voor versnelde AantastingsProeven)
FAETP	Fresh water aquatic ecotoxicity potential		
FD	Freeze Drying	TETP	Terrestrial ecotoxicity potential
GWP	Global warming potential	TG	Thermogravimetric
HM	Hydraulic Modulus	ts	Troweled surface
HTP	Human toxicity potential	XC4	Concrete environmental class: carbonation induced corrosion in a cyclic wet and dry environment
KOSH	Solution of KOH and Sucrose in water		
LCA	Life Cycle Assessment	XF4	Concrete environmental class: freeze-thaw attack with high water saturation and de-icing agent or sea water
LCS	Lime and Calcium sulphate		
LOI	Loss on ignition	XRD	X-Ray Diffraction
LSF	Lime Saturation Factor	XS3	Concrete environmental class: chloride induced corrosion from sea water in tidal, splash and spray zones
MAETP	Marine aquatic ecotoxicity potential		
mQCS	Milled QCS		
MSWI	Municipal Solid Waste Incineration		

CEMENT CHEMISTRY NOTATIONS

A	Aluminium oxide – Al_2O_3	CH	Portlandite – $Ca(OH)_2$
AH_x	Aluminate hydrate	C$\underline{S}$	Calcium sulphate – $CaSO_4$
C	Calcium oxide – CaO	C-S-H	Calcium silicate hydrate (C_xSH_y)
C	Carbondioxide – CO_2	C$\underline{S}H_{0.5}$	Bassanite – $CaSO_4.^1/_2H_2O$
$C_{12}A_7$	Mayenite – $Ca_{12}Al_{14}O_{33}$	C$\underline{S}H_2$	Gypsum – $CaSO_4.2H_2O$

C_2AS	Gehlenite – $Ca_2Al_2SiO_7$	C_xA_y	Calcium aluminate phase
C_2S	Belite – Ca_2SiO_4	F	Iron oxide – Fe_2O_3
C_3A	Aluminate – $Ca_3Al_2O_6$	H	Water – H_2O
C_3S	Alite – Ca_3SiO_5	K	Potassium oxide – K_2O
$C_4A_3\underline{S}$	Ye'elemite – $Ca_4(AlO_2)_6SO_4$	$K_{1.5}N_{0.5}\underline{S}$	Aphthitalite – $K_3Na(SO_4)_2$
$C_4AC_{0.5}H_{12}$	Calcium hemicarboaluminate – $Ca_4Al_2O_7(CO_2)_{0.5}.12H_2O$	$KC_2\underline{S}_3$	Calcium langbeinite – $K_2Ca_2(SO_4)_3$
C_4ACH_{11}	Calcium monocarboaluminate – $Ca_4Al_2O_7(CO_2).11H_2O$	$K\underline{S}$	Arcanite – K_2SO_4
C_4AF	Ferrite – $Ca_4Al_2Fe_2O_{10}$	M	Magnesium oxide – MgO
$C_4A\underline{S}H_{12}$	Calcium monosulphoaluminate (Kuzelite) – $Ca_4Al_2O_7(SO_3).12H_2O$	M_a	Magnesium oxide in alite
		M_c	Magnesium oxide in clinker
$C_6A\underline{S}_3H_{32}$	Ettringite – $Ca_6Al_2(SO_4)_3(OH)_{12}.26H_2O$	MH	Brucite – $Mg(OH)_2$
		N	Sodium oxide – Na_2O
CA	Monocalcium aluminate – $CaAl_2O_4$	$N\underline{S}$	Thenardite – Na_2SO_4
		S	Silicon oxide – SiO_2
C-A-H	Calcium aluminate hydrate (C_xAH_y)	$\underline{S}$	Sulphate – SO_3

SYMBOLS

A	Cross-sectional area [m^2]	T	Temperature [°C]
A	Aggregate content of 1 m^3 concrete [kg/m^3]	t	Time *(unit as mentioned)*
		U	Applied voltage [V]
$A_{agg,x}$	Water absorption coefficient of aggregate x [-]	V_a	Total aggregate volume for 1 m^3 concrete [m^3]
A_i	Amount of aggregate i to the total aggregate content [wt%]	V_{ai}	Volume of aggregate i for 1 m^3 concrete [m^3]
A_{sand}	Water absorption coefficient of sand [-]	V_{air}	Air volume of 1 m^3 concrete [m^3]
B	Binder content of 1 m^3 concrete [kg/m^3]	V_b	Total binder volume for 1 m^3 concrete [m^3]
B_i	Amount of binder i to the total binder content [wt%]	V_{bi}	Volume of binder i for 1 m^3 concrete [m^3]
C	Cement content of 1 m^3 concrete [kg/m^3]	$V_{concrete}$	Concrete volume [m^3]
c	CO_2 concentration [vol%]	V_f	Volume of filler for 1 m^3 concrete [m^3]
D	Non-steady-state migration coefficient [10^{-12} m^2/s]	V_w	Water volume of 1 m^3 concrete [m^3]
e	Porosity of the cement bed [-]	V_{water}	Water volume [m^3]
E/E_{ref}	Ultrasonic wave energy ratio [-]	W	Water content of 1 m^3 concrete [kg/m^3]
F	Filler content of 1 m^3 concrete [kg/m^3]	w_a	Weight of saturated specimen in air [kg]
FA	Fly Ash content of 1 m^3 concrete [kg/m^3]	w_d	Specimen weight after drying [kg]
$f_{agg,x}$	Mass of aggregate x [kg]	WL	Weight loss [wt%]
f_c	Compressive strength [N/mm^2]	wt%(x)	Weight percentage of x [wt%]
h	Specimen height [m]	w_w	Weight of saturated specimen in water [kg]
K	Gas permeability coefficient [m^2]	x	Carbonation depth [mm]
k	Carbonation coefficient [$mm/week^n$]	x_{cc}	Depth of the concrete cover [mm]
		x_d	Chloride penetration depth

L	Thickness of the specimen [mm]		(Diffusion test) [mm]
M	Molar mass [g/mol]	x_m	Chloride penetration depth (Migration test) [mm]
P	Applied pressure [N/m^2]		
P_a	Atmospheric pressure [101300 N/m^2]	x_t	Chloride penetration depth (TAP apparatus) [mm]
Q	Flow rate [m^3/s]	α_t	Hydration degree [-]
R	Hydration rate [1/days]	Δf_{sand}	Additional amount of sand to be added applying the MBE method [kg]
R90	Residue on a 90μm sieve [wt%]		
RH	Relative Humidity [%]	Δf_{water}	Additional amount of water to be added applying the MBE method [kg]
S	Amount of scaled material [kg/m^2]		
$S_{agg,x}$	Specific Surface Area of aggregate x [m^2/kg]	η	Dynamic viscosity of oxygen gas [2.02·10-5 N·s/m^2]
SSA	Specific Surface Area [m^2/kg]	ρ_i	Density of material i [kg/m^3]
S_{sand}	Specific Surface Area of sand [m^2/kg]	φ	Concrete porosity [%]

Dutch summary

Nederlandse samenvatting

Sinds de productie van het eerste industriële cement in de 19de eeuw is beton niet meer weg te denken uit onze maatschappij. Hoewel beton een duurzaam bouwmateriaal is, is de impact ervan op het milieu niet te onderschatten, mede door de hoge productiehoeveelheden. Behalve het gebruik en de productie van respectievelijk enorme hoeveelheden grondstoffen en afval, mag ook de bijdrage tot de opwarming van de aarde niet onderschat worden. De cementindustrie wordt geschat verantwoordelijk te zijn voor ongeveer 5-7% van de wereldwijde CO_2 uitstoot. Om voornoemde redenen focussen vele betonstudies zich op het recycleren van vaste afvalstoffen in beton. Deze vaste afvalstoffen kunnen gebruikt worden als granulaat (bv. slakken, glas, beton, ...), als alternatief bindmiddel (bv. slakken, bodem- of vliegassen, silica fume, ...) of als grondstof voor de klinkerproductie (bv. slakken, bodem- of vliegassen, residuen van grondstofdelving of raffinaderijen, ...). De meeste van deze recyclagemogelijkheden ontstaan vaak bij het zoeken naar nieuwe synergiën tussen meestal niet verwante industriële partners. Bovendien worden gerecycleerde producten vandaag vaak beschouwd als laagwaardig door een gebrek aan vertrouwen in de kwaliteit van deze materialen. Tot slot kan de kostprijs van deze gerecycleerde materialen wel eens hoger zijn dan wanneer deze producten vervaardigd werden met nieuwe materialen. Om recyclage naar een hoger niveau te tillen, kunnen producten idealiter ontworpen worden voor reïncarnatie, zoals beschouwd in het wieg-tot-wieg principe dat wereldwijd gepromoot wordt door McDonough en Braungart (2002). Als dit idee toegepast wordt op de productie van beton, valt het snel op dat de beton- en cementindustrie in grote mate dezelfde grondstoffen gebruiken. Van hieruit is het idee ontstaan om een volledig recycleerbaar beton te ontwerpen (Completely Recyclable Concrete, CRC), dat na afbraak als enig ingrediënt gebruikt kan worden binnen de cementproductie.

Ontwerp van de CRC-betonsamenstelling

Van bij het begin wordt het CRC-beton ontworpen om finaal te kunnen dienen als grondstof binnen de cementproductie. Dit laatste maakt het noodzakelijk dat de chemische samenstelling van het CRC gelijk is aan deze van een grondstoffenmengsel voor het vervaardigen van cement. De eisen die aan dit grondstoffenmengsel opgelegd worden, zijn goed gekend. Portlandklinker, het basisbestanddeel van Portlandcement, bestaat voor twee derde uit calciumoxide (CaO), wat het noodzakelijk maakt om kalksteengranulaten te gebruiken in CRC-beton. Een andere component die onontbeerlijk is voor de cementproductie is siliciumdioxide (SiO_2), wat gevonden wordt in bv. zand en vliegas. Tot slot kunnen de andere componenten zoals Al_2O_3 en Fe_2O_3 aangeleverd worden door porfiergranulaten, koperslak of calciumaluminaatcement.

In de eerste stap van het ontwerpproces werd een inventaris gemaakt van de beschikbare grondstoffen. Vervolgens werden enkele randvoorwaarden vastgelegd om

de betonkwaliteit te garanderen, met name de minimale hoeveelheid bindmiddel en een geschikte korrelverdeling van de granulaten. In een verdere ontwerpsamenstelling werd het k-waarde concept voor het gebruik van vliegas in beton [NBN EN 206-1 (2001)] toegepast om ook de duurzaamheid van het beton te garanderen. De bepaling van de chemische samenstelling in de laatste en belangrijkste stap in het ontwerpproces moet de recyclagemogelijkheden van het CRC-beton als grondstof voor de cementproductie, garanderen. Voor de optimalisatie van de chemische samenstelling werden de vier samenstellingsparameters van een grondstoffenmengsel voor het vervaardigen van cement gehandhaafd, met name de kalkverzadigingsfactor (Lime Saturation Factor, LSF), de Silica Modulus (SM), de Alumina Modulus (AM) en de Hydraulische Modulus (HM). Verder is het ook mogelijk om de potentiële mineralogische samenstelling van de uiteindelijke klinker te bepalen door gebruik te maken van de (aangepaste) Bogue-formules. Voor de vier samenstellingsparameters en de formules van Bogue werden literatuurwaarden nagestreefd.

Na het ontwerp van de CRC-betonsamenstelling werd het ontwerpproces geëvalueerd door de vooropgestelde en werkelijke (experimenteel bepaald m.b.v. XRF of ICP) chemische samenstelling van de klinkers te bepalen. Aanvaardbare verschillen werden waargenomen voor de chemische samenstelling en de samenstellingsparameters. De potentiële mineralogische samenstelling bepaald m.b.v. de Bogue formules bleek echter zeer gevoelig te zijn voor kleine verschillen in chemische samenstelling, en dan vooral de geschatte hoeveelheden aliet en beliet. Om deze reden waren de samenstellingsparameters doorslaggevend in het ontwerpproces, maar niet de Bogue-formules.

Uiteindelijk werden drie CRC-betonsamenstellingen ontworpen. In CRC1 en CRC2 werd silicium houdend vliegas gecombineerd met respectievelijk Portlandcement (CEM I 52.5 N) en hoogovencement (CEM III/A 42.5 N LA). Voor CRC3 werd gebruik gemaakt van drie bindmiddelen, met name silicium houdend vliegas, hoogovencement en calcium aluminaat cement. Kalksteen werd niet alleen gebruikt als zand en granulaat, maar ook als vulstof om de hoeveelheid CaO te verhogen. Indien nodig werden porfiergranulaten of koperslak aangewend om de ontwerpsamenstellingen te optimaliseren.

De kwaliteit en duurzaamheid van CRC

De kwaliteit en duurzaamheid van het CRC-beton zal voornamelijk beïnvloed worden door het gebruik van vliegas. Het is algemeen geweten dat het gebruik van vliegas in beton de sterkteontwikkeling zal vertragen, terwijl het carbonatatieproces zal versnellen. Andere aantastingsmechanismen, zoals de indringing van chloriden, zullen dan weer vertraagd worden door een dichtere poriënstructuur en de bindingscapaciteit van vliegas t.o.v. chloriden.

De druksterkte van CRC-beton op een ouderdom van 28 dagen was vergelijkbaar of zelfs hoger in vergelijking met het referentiebeton T(0.50) met een cementhoeveelheid van 320 kg/m^3, hoewel het k-waard concept voor het gebruik van vliegas volgens NBN EN

206-1 (2001) slechts van toepassing was voor de laatst ontworpen CRC-mengsels. Tussen een ouderdom van 1 en 3 maand werd voor de CRC-samenstellingen een sterktetoename van 4 tot 21% geregistreerd, terwijl voor de referentiemengsels slechts een toename van 5 tot 12% werd waargenomen. Deze sterktetoename op latere leeftijd voor de CRC-mengsels is toe te schrijven aan de puzzolane reactie van de vliegassen. Eén van de zelfverdichtende CRC-mengsels (CRC2) bleek een hoge-sterkte-beton. Dit resultaat werd wellicht bekomen door toepassing van het k-waarde concept enerzijds en het hoge gehalte aan poeder en dus betere korrelverdeling anderzijds. Uit de bekomen resultaten kan dus geconcludeerd worden dat de sterkteontwikkeling van CRC geen belemmering moet zijn voor het toekomstig gebruik ervan, zelfs indien een hoge sterkte beoogd wordt.

Drie duurzaamheidsaspecten van het CRC-beton werden onderzocht, met name de weerstand tegen carbonatatie, de indringing van chloriden en vorst-dooi cycli met dooizouten. Zoals verwacht was de weerstand tegen carbonatatie van het CRC-beton met significante vliegashoeveelheden slechter dan deze van het referentiebeton. Terwijl binnen het proefprogramma (tot 12 weken blootstelling aan een CO_2 concentratie van 10 vol%) geen carbonatatie kon worden opgemeten voor het referentiebeton, was dit wel het geval voor alle CRC-samenstellingen. Vanuit de literatuur werd verwacht dat de carbonatatieweerstand van het CRC-beton zou verhogen met de leeftijd van het beton, wat inderdaad bevestigd werd door de bekomen resultaten. Voor sommige CRC-samenstellingen bleek het model dat de carbonatatiediepte voorspelt in functie van de tijd niet toepasbaar (lage R^2 waarden voor de lineaire regressie). Om het effect van experimentele fouten te kunnen inschatten is een langere testperiode noodzakelijk, vooraleer het model in vraag gesteld kan worden. Voor de meeste samenstellingen bleek het model wel toepasbaar te zijn en werden aanvaardbare R^2 waarden bekomen.

De weerstand tegen de indringing van chloriden werd in eerste instantie getest door cyclische blootstelling aan een chloride-oplossing m.b.v. het TAP toestel. Op een ouderdom van 1 maand waren de resultaten van het CRC-beton vergelijkbaar met deze van het referentiebeton, of iets slechter. Op een ouderdom van 3 maanden waren de resultaten van de CRC-samenstellingen iets beter dan het referentiebeton of vergelijkbaar. Deze (beperkt) betere resultaten zijn wellicht te verklaren door een hogere verdichting van de poriënstructuur door de uitgestelde puzzolane reactie van het vliegas.

Aangezien geen duidelijke conclusies konden getrokken worden uit de bekomen resultaten bij cyclische blootstelling werd een diffusietest uitgevoerd op de finale CRC-betonsamenstellingen. Niettemin was het ook voor deze test niet mogelijk om tot eenduidige conclusies te komen. In eerste instantie bleek de chloride-indringing zoals verwacht af te nemen in functie van de ouderdom (tussen 1 en 3 maanden ouderdom). Indien de chloride-diffusie echter gestart werd op een leeftijd van 1 jaar bleek de chloride-indringing hoger te zijn. Het tegengestelde resultaat werd bekomen voor het referentiebeton. Eerst steeg de chloride-indringing met de ouderdom van het beton (tussen 1 en 3 maanden), waarna de chloride-indringing weer afnam (beton van 1 jaar

oud). Niettemin bleken de resultaten van het CRC- en referentiebeton beide binnen eenzelfde bereik te liggen.

De weerstand tegen vorst-dooi cycli met dooizouten was, zoals verwacht, sterk afhankelijk van het luchtgehalte van het verse beton. Het zijn inderdaad de luchtbelvormers in beton die de luchtholtes zullen creëren waarin het bevriezende water kan uitzetten zonder dat de trekspanning in de toplaag te sterk toeneemt. Dus indien vorst-dooi cycli met dooizouten verwacht worden, is het aangeraden luchtbelvormers te gebruiken om de weerstand van het beton hiertegen te verhogen. Van deze laatste stof wordt niet verwacht dat ze de chemische samenstelling van het CRC zal beïnvloeden. Luchtbelvormers zijn vaak organische componenten die tijdens het productieproces van cement zullen ontbinden. Bovendien zijn ook de toegevoegde hoeveelheden over het algemeen beperkt.

De combinatie van calciumaluminaatcement en hoogovencement voor één van de ontworpen CRC-betonsamenstellingen resulteerde in verwerkbaarheidsproblemen door een veel te snelle binding. Met het oog op het vertragen van het hydratatieproces werden verschillende bindingsvertragers op basis van gluconaat, sucrose of citroenzuur toegevoegd aan de mengsels, echter zonder succes. Uit de literatuur bleek dat de toevoeging van kalk en calciumsulfaat het verhardingsproces van deze mengsels beïnvloedt. De toevoeging van kalk en calciumsulfaat zorgde inderdaad voor beter verwerkbare mengsels. Een bijkomende verbetering werd waargenomen indien de toevoeging van kalk en calciumsulfaat gecombineerd werd met een bindingsvertrager. De vertraging van de binding werd vastgesteld gebruik makend van de Vicat naald, maar kon niet worden waargenomen m.b.v. ultrasone transmissie. Dit laatste is mogelijk gerelateerd aan de vorming van ettringiet, wat de p-golfsnelheid en de energiecurves zal beïnvloeden, maar slechts een beperkt effect heeft op de verharding van de cementpasta op jonge leeftijd. De hydratatiewarmte na 7 dagen was significant lager in vergelijking met de referentiemengsels. De druksterkte na 7 en 28 dagen van de CRC-mengsels met toevoeging van kalk en calciumsulfaat, met of zonder bindingsvertrager, was voldoende voor praktische toepassingen. Hoewel de binding van de CRC-samenstelling met calciumaluminaatcement en hoogovencement succesvol vertraagd werd, geniet dit mengsel niet de voorkeur. Een optimale combinatie van calciumsulfaat en kalk, en mogelijks een bindingsvertrager zal telkens weer gezocht moeten worden, wat het CRC-ontwerpproces complexer maakt.

Koperslak is een interessante bron van ijzer voor de productie van CRC-beton. Eerst en vooral zal het gebruik van dit industrieel bijproduct ervoor zorgen dat het grondstofverbruik enerzijds en de afvalproductie anderzijds zullen dalen. Verder wordt koperslak reeds gebruikt binnen de cementproductie als bron van ijzer. Twee mogelijke betontoepassingen van deze koperslak werden onderzocht, met name het gebruik als bindmiddel of als granulaat. Het gebruik als alternatief bindmiddel bleek niet veelbelovend, aangezien hoge hoeveelheden aan energie om de koperslak fijn te mailen noodzakelijk zijn voordat het materiaal puzzolane eigenschappen verkrijgt. Het gebruik van koperslak als granulaat is echter wel interessant. Het effect op de druksterkte, de

open porositeit, de gaspermeabiliteit en de weerstand tegen carbonatatie en chloride-indringing bleek aanvaardbaar, en zelfs een verbeterde prestatie van beton met koperslak werd waargenomen. Enkel de weerstand tegen vorst-dooi cycli met dooizouten bleek ondermaats te zijn. De prestaties in deze omgevingsklasse kunnen echter verbeterd worden door de hoeveelheid aanmaakwater aan te passen of door het toevoegen van een luchtbelvormer. Door de lage waterabsorptie van koperslakken is er eigenlijk een teveel aan water in het beton aanwezig. Dit is de belangrijkste parameter die de eigenschappen van beton met koperslakken beïnvloedt.

De kwaliteit van CRC-klinker en -cement

Het regeneratieproces van cement uit het CRC-beton was vergelijkbaar met het industriële cementproductieproces. Na het malen van het CRC-grondstoffenmengsel in een planetaire balmolen, werden hiermee tabletjes vervaardigd in een geperforeerde plaat. Deze tabletjes werden vervolgens verhit tot 1450 °C (@ 10 °C/min, gevolgd door een verblijfstijd van 1u bij 1450 °C) in een laboratoriumoven voor het sinteringsproces. De bekomen klinker werd vervolgens vermalen met calciumsulfaat voor de productie van CRC-cement. De klinkerkwaliteit werd onderzocht m.b.v. XRD/Rietveld, TGA/DTA en microscopische analyse. Isotherme calorimetrie, TGA en XRD/Rietveld-analyse werden gebruikt voor het bestuderen van het cementhydratieproces.

Voor één van de CRC-samenstellingen werden de reacties tijdens het sinteringsproces bestudeerd m.b.v. in situ (tot 1050 °C) en ex situ (1050-1450 °C) XRD analyse, aangevuld met TGA/DTA- en microscopische analyse. Aangezien de belangrijkste bron van CaO in CRC de kalksteengranulaten zijn, is het niet verwonderlijk dat de decarbonatatiereactie van calciet en dolomiet de reacties beneden een temperatuur van 1050 °C overheerst. Tijdens dit decarbonatatieproces worden significante hoeveelheden vrije kalk vrijgesteld. Deze vrije kalk zal vervolgens reageren met de beschikbare aluminaten, silicaten en beperkte hoeveelheden sulfaten voor de vorming van de tussenproducten, zijnde beliet en calcium(silicaat)aluminaten. De vorming van de finale klinkerfasen werd waargenomen vanaf een temperatuur van 1250 °C, waarbij de vorming van aliet, aluminaat en ferriet ten koste gaat van vrije kalk, beliet en calcium(silicaat)aluminaten. Hieruit kan geconcludeerd worden dat het sinteringsproces van CRC vergelijkbaar is met dit van een traditioneel grondstoffenmengsel, en dit zeker na ontbinding van de grondstoffen. De ontbindingsreacties van de grondstoffen zijn inderdaad inherent aan de samenstelling. Kalksteen mag dan wel de belangrijkste grondstof zijn voor beide, maar de materialen die SiO_2, Al_2O_3 en Fe_2O_3 aanleveren kunnen een verschillende oorsprong hebben. Vliegas, koperslak of porfiergranulaten werden gebruikt in het geval van CRC-beton, terwijl b.v. kleimineralen, schelpen, kalk en ijzererts gebruikt kunnen worden voor een traditioneel grondstoffenmengsel. De dehydratatie van de cementhydratatieproducten wordt eveneens verwacht bij het verhitten van een CRC-grondstoffenmengsel, hoewel dit experimenteel niet werd aangetoond door de verdunnende factor van cement in beton bovenop het vervangen van een deel van het cement door vliegas.

De potentiële mineralogische samenstelling van een klinker kan geschat worden met behulp van de (aangepaste) Bogue-formules. De bekomen experimentele resultaten (XRD/Rietveld-analyse en microscopie/puntentelling) toonden echter aan dat de werkelijke mineralogische samenstelling van de klinker in sterke mate kan verschillen van de theoretische. Dit laatste is te wijten aan het feit dat de vier belangrijkste klinkerfasen (aliet, beliet, aluminaat en ferriet) in belangrijke mate afwijken van hun stoichiometrische samenstelling en naast CaO, SiO_2, Al_2O_3 en Fe_2O_3 ook andere oxides kunnen bevatten, wat uiteraard ook de finale klinkersamenstelling zal bepalen. Hoewel de aangepaste Bogue-formules dit effect proberen te simuleren, blijft de verbetering beperkt. Dit is dan weer te wijten aan het feit dat zelfs bij gebruik van de aangepaste Bogue-formules de samenstelling van de verschillende fasen steeds een theoretische samenstelling blijft, dus een afwijking tussen de berekende en experimentele klinkersamenstelling kan niet vermeden worden.

De impact van de fijnheid van het grondstoffenmengsel op de klinkermineralogie en zijn reactiviteit werd onderzocht met behulp van respectievelijk XRD/Rietveld-analyse en isotherme calorimetrie. Voor de bestudeerde fijnheden (R90 variërend tussen 12 en 24 wt%) werd geen significante invloed gevonden. Bijkomend bleken de resultaten van een DT-analyse niet aan te duiden dat een hogere reactiviteit van het grondstoffenmengsel, bekomen door een hogere maalfijnheid, aanleiding zou kunnen geven tot significante energiebesparingen tijdens het sinteringsproces. Enkel in het lagere temperatuurgebied bleek dat bijkomend malen van de CRC-grondstoffenmengsels leidde tot een drogere grondstof. De eventueel hiermee gepaard gaande energiebesparingen zullen echter (gedeeltelijk) teniet gedaan worden door een hogere energieconsumptie die nodig is om de hogere maalfijnheid te bekomen.

Wanneer CRC-beton gebruikt wordt als grondstof voor cementproductie, kunnen zuren en zouten die binnengedrongen zijn in het beton het sinteringsproces beïnvloeden. Daar waar het gehalte aan MgO beperkt dient te worden om ongewenste expansie in het beton op latere leeftijd te vermijden, moeten de hoeveelheden van chloriden, sulfaten en alkaliën beperkt worden om problemen in de productie-installatie te voorkomen. Door de vluchtigheid van deze elementen ontstaan cycli van verdamping en condensatie in de draaioven, wat verstopping in de voorverwarmingsinstallatie of de vorming van ringvormige afzettingen op de wand van de draaioven kan veroorzaken. Beide zullen een periodiek onderhoud van de installatie vergen. Niettemin, kunnen magnesium, chloriden, sulfaten en alkaliën, indien goed gebalanceerd, ook een positief effect hebben op het sinteringsproces (bv. het stabiliseren van meer reactieve fasen en het reduceren van de viscositeit van de smelt) en het gebruik van aangetast CRC is dus zeker mogelijk indien het goed gedoseerd wordt.

De hydratatie van vier CRC-cementen en twee commerciële cementen (CEM I 52.5 N en CEM I 42.5 N LH HSR LA) werd bestudeerd. Drie verschillende klinkers werden gebruikt voor de regeneratie van CRC-cement. Voor één van deze klinkers werden twee fijnheden onderzocht. De verhoogde reactiviteit van cement door een verhoogde maalfijnheid bleek duidelijk uit de isotherme calorimetrie. Dit kan zeker interessant zijn om de

reactiviteit van cement met een lager alietgehalte te verhogen. Door middel van TGA en XRD/Rietveld-analyse kon het oplossen van de verschillende klinkermineralen en de vorming van de (kristallijne) hydratatieproducten gevisualiseerd worden. De hydratatiereacties van een cementpasta worden bij voorkeur gestopt door het aanwezige (vrije) water te vervangen door een solvent (bv. isopropanol), aangezien vriesdrogen de kristalliniteit van bv. ettringiet en gips beïnvloedt. De globale faseveranderingen tijdens het hydratatieproces waren vergelijkbaar voor CRC en traditioneel cement. Het belangrijkste verschil was wellicht de stabiliteit van anhydriet tot een ouderdom van 9u in een cementpasta met traditioneel cement. In het geval van CRC-cement werd het aanwezige calciumsulfaat onmiddellijk omgezet in gips.

De hydratatiereacties van alle cementen werden tevens gemodelleerd gebruik makend van het cementhydratatiemodel beschreven door Lothenbach & Winnefeld (2006). Dit model combineert het empirische dissolutiemodel van Parrot & Killoh (1984) met het thermodynamische evenwichtsmodel GEMS voor de berekening van de hierbij horende hydratatieproducten [Kulik et al. (2013)]. Over het algemeen zijn de gemodelleerde resultaten vergelijkbaar met de experimenteel bekomen resultaten. Niettemin werd de verhoogde reactiviteit voor een fijner cement niet gesimuleerd in het model. De gemodelleerde data zijn vooral interessant omdat deze de samenstelling van de niet of weinig kristallijne fasen kunnen voorspellen, in aanvulling tot de bekomen experimentele resultaten van de kristallijne fasen. Voor de calciumsilicaten is het mogelijk de samenstelling van de niet-kristallijne C-S-H-fase in te schatten. Voor de meer complexe hydratatie van aluminaat en ferriet is het dan weer mogelijk om de verdeling van de niet of weinig kristallijne calciumaluminaathydraten te voorspellen, dewelke verwacht worden aanwezig te zijn naast de kristallijne fasen ettringiet en kuzeliet.

De milieu-impact van CRC

Om daadwerkelijk het milieuvoordeel van het CRC-concept te kunnen inschatten is het nodig een levenscyclusanalyse (Life Cycle Assessment - LCA) uit te voeren. In deze studie werd de hele levenscyclus van beton beschouwd, van het ontginnen van de grondstoffen tot en met het recycleren of storten van het betonpuin. Bij de recyclage van het betonpuin werd rekening gehouden met de (positieve) impact die bekomen werd doordat het gebruik van natuurlijke grondstoffen beperkt kon worden. De functionele eenheid werd beschouwd als de hoeveelheid beton die nodig is om een sterkte van 1 MPa en een levensduur van 1 jaar te leveren. De functionele eenheid werd berekend gebruikmakend van de bekomen experimentele data (cfr. de kwaliteit en duurzaamheid van CRC).

Voor de inventarisatie van de levenscyclus werd gebruik gemaakt van de ecoinvent 2.0-databank samengesteld door het Zwitsers centrum voor de inventarisatie van levenscycli (Swiss Centre for Life Cycle Inventories). Deze databank wordt vaak samen gebruikt met de aangewende LCA software Simapro, ontwikkeld door Pré consultants (Product ecology consultants). Daar waar nodig werden aanpassingen gemaakt om de recyclagemogelijkheden van CRC en traditioneel beton te incorporeren, bv. het opsplitsen van een productieproces in het aanleveren van de grondstoffen en het

eigenlijke productieproces. Om de impact van de levenscyclus te onderzoeken werd de CML 2002 (Centrum voor Milieukunde Leiden) probleemgeoriënteerde impactmethode aangewend, waarbij volgende categorieën werden beschouwd: gebruik van abiotische bronnen, verzuringspotentieel, eutrofiëringspotentieel, broeikaspotentieel, ozonafbraakpotentieel, toxiciteit t.o.v. de mens en het milieu (zoetwater, zeewater en aarde), en fotochemische oxidantvormingspotentieel.

Zoals verwacht bleek de milieu-impact van de betonproductie hoofdzakelijk bepaald te worden door zijn gehalte aan bindmiddelen (voornamelijk cement, maar ook vliegas door middel van economische allocatie) en het benodigde transport. Ook de milieu-impact van de recyclage van beton bleek grotendeels toe te schrijven zijn aan transport, dewelke in het geval van CRC duidelijk hoger is. Het grootste milieuvoordeel van het recycleren van CRC-beton is gerelateerd aan de uitstoot van broeikasgassen. In vergelijking met een traditioneel grondstoffenmengsel voor cementproductie zal een CRC grondstoffenmengsel een zekere hoeveelheid CO_2-vrij CaO bevatten. Hierdoor kan de CO_2-uitstoot van de cementproductie dus gereduceerd worden.

Wanneer gekeken wordt naar de gehele levenscyclusanalyse van CRC en traditioneel beton blijkt dat de uitstoot van broeikasgassen met 66-70% gereduceerd kan worden indien een hoge-sterkte-CRC wordt geproduceerd met een laag klinkergehalte. In het geval van een CRC met normale sterkte en een hoger klinkergehalte bedraagt het voordeel 7 tot 35% indien een goede levensduur gegarandeerd kan worden. Voor de andere impactcategorieën zal enkel een CRC met hoge sterkte en een laag klinkergehalte de bijkomende transportkosten van het recyclageproces kunnen compenseren.

Conclusies

In dit onderzoek werd wetenschappelijk aangetoond dat het CRC-concept haalbaar is aangaande zijn sterkte en duurzaamheid en de regeneratie ervan binnen de cement productie. Bijkomend toonde een levenscyclusanalyse aan dat de uitstoot van broeikasgassen aanzienlijk gereduceerd kan worden. Niettemin zullen enkele logistieke en praktische probleem aangepakt moeten worden. Een weloverwogen systeem voor het traceren van CRC constructies, evenals het selectief slopen van constructies zal nodig zijn. Verder zijn de vereisten voor het grondstoffenmengsel voor de cement productie afhankelijk van de gebruikte brandstoffen wat ervoor zorgt dat er geen ideale samenstelling is voor het CRC. In vergelijking met de recyclagemogelijkheden voor betonpuin vandaag, is het CRC concept dus complexer. De opportuniteiten van het CRC concept zijn gerelateerd aan de mogelijkheid om (bepaalde) giftige afvalstoffen aanwezig in betonpuin te recycleren en ook aangetast betonpuin (na bv. blootstelling aan chloriden of sulfaten) kan gebruikt worden indien de concentraties hiervan gecontroleerd en beperkt worden indien nodig.

English summary

Since the first industrial cement was produced in the middle of the 19th century, concrete has become the most popular building material. Although it is a durable material, concrete has a big impact on the environment due to its high production volumes. Besides the use and the generation of enormous amounts of natural resources and waste respectively, the impact on global warming should equally be considered. The cement industry is estimated to emit about 5-7% of the global CO_2 emissions. For these reasons many studies in the field of concrete research focus on the recycling of solid waste in concrete. Solid waste can be used as concrete aggregate (e.g. slags, glass, concrete, …), cementitious binder (e.g. slags, bottom or fly ash, silica fume, …) or raw material for clinker production (e.g. slags, bottom or fly ash, mining waste, refinery residues, …). Most of the recycling opportunities, however, often arise from the search for new synergies between usually unrelated industrial partners. Also, recycled products still suffer from a low acceptability caused by a lack of trust in the quality of these products and in some cases by the higher cost of recycled materials compared to natural materials. To take recycling to a higher level, products could be 'designed for reincarnation' according to the Cradle-to-Cradle principle promoted by McDonough and Braungart (2002). Applying this idea on the production of concrete, it is easy to notice that the raw materials used for concrete and cement production share common base components. Hence the idea emerged to design a Completely Recyclable Concrete (CRC) which can be used as the only ingredient for cement production after its service life.

Design of the CRC concrete mix

From a predesign state, CRC is intended to be recycled as raw material within the cement production. This makes it necessary to aim for a chemical composition of CRC similar to the one of a cement raw meal, of which the requirements are well known. Portland Clinker consists for about two thirds of calcium oxide (CaO), which makes it necessary to incorporate limestone aggregates into CRC. The second most important oxide is silicon oxide (SiO_2) which is found in sand and fly ash. The other components, aluminium (Al_2O_3) and iron (Fe_2O_3) oxide, can be provided by porphyry aggregates, copper slag or calcium aluminate cement.

In the first step of the design process, the chemical compositions of the available raw materials were determined. Subsequently, boundary conditions were set to guarantee a minimal binder content and to obtain a suitable particle size distribution. Later on, also the k-value concept for the use of fly ash in concrete [NBN EN 206-1 (2001)] was applied in this stage of the design process to ensure the durability of the CRC mixture. The final step was most crucial towards the recycling opportunities of CRC, as its chemical composition was designed. For this purpose, four parameters normally used for the assessment of traditional cement raw materials were applied, namely the Lime Saturation Factor (LSF), the Silica Modulus (SM), the Alumina Modulus (AM) and the Hydraulic modulus (HM). Furthermore it was also possible to quantify the potential mineralogical composition using the (modified) Bogue calculations. For both the

compositional parameters and the Bogue formulas, typical values found in literature were aimed for.

Once the CRC mixtures were designed, the design process was evaluated by comparing the designed and the actual (experimentally determined by XRF or ICP) chemical composition of the clinkers. Acceptable differences were obtained regarding the chemical compositions and values for LSF, SM, AM and HM. However, the potential mineralogy according to the Bogue formulas was found to be very sensitive to small errors in the chemical composition, especially the estimated alite and belite contents. For these reasons the compositional parameters instead of the Bogue calculations were considered to be decisive in the design process.

Finally, three types of CRC mixtures were designed, each having different binder compositions. CRC1 and CRC2 combined siliceous Fly Ash with Ordinary Portland Cement (CEM I 52.5 N) and Blast Furnace Slag Cement (CEM III/A 42.5 N LA) respectively. Three types of binder were used for the production of CRC3, namely siliceous Fly Ash, Blast Furnace Slag Cement and Calcium Aluminate Cement. Limestone was not only used as sand and aggregate but also as filler to increase the CaO content. When necessary, porphyry aggregates or copper slag were added to optimize the designed chemical composition.

CRC quality and durability

The quality and durability of CRC will be influenced by the incorporation of Fly Ash. The use of Fly Ash as cementitious binder is known to delay the strength development of concrete and to reduce the carbonation resistance. Other deterioration mechanisms, such as the penetration of chlorides, are known to be delayed due to the densification of the pore structure and chloride binding.

The 28 day compressive strength of the CRC mixtures was comparable or even higher than the reference concrete T(0.50) with a cement content of 320 kg/m^3, although the k-value concept for the incorporation of fly ashes according to NBN EN 206-1 (2001) was only applicable for the latest CRC mixtures produced. The strength increase while curing between the first and third month varied between 4 and 21% for the CRC mixtures, while for the reference mixtures the strength gain varied between 5 and 12%. The higher strength gain for the CRC mixtures is related to the pozzolanic reaction of the fly ash at later ages. One of the self-compacting concretes (CRC2) was a high strength concrete, which is probably the result of the application of the k-value concept on the one hand and the high powder content improving the packing of the concrete on the other hand. From the results in this study it can thus be concluded that the strength development should not be an issue for CRC, even if a high strength performance is required.

Three durability aspects of CRC were studied, namely the resistance against carbonation, chloride ingress and freeze-thaw attack with de-icing agents. As expected, the carbonation resistance of the CRC mixtures containing significant amounts of fly ash

was lower compared to the reference mixtures. While for the reference mixtures, no carbonation was seen within the time frame of the study (up to 12 weeks exposure to a CO_2 concentration of 10 vol%), carbonation was observed for all CRC mixtures. From literature it was expected that the carbonation resistance would increase with curing age, which was indeed confirmed by the experimental results. For some mixtures, the applied model relating the carbonation depth to time seemed not applicable (low R^2 values for the linear regression). To exclude experimental errors, a longer test period should be considered before questioning the model. Indeed, for most mixtures the model seems applicable and acceptable R^2 values were obtained.

The resistance against chloride penetration was at first tested by cyclic exposure to a chloride solution using the TAP apparatus. After one month of curing the results were comparable to or slightly worse than the reference results. After another 2 months of curing, the results for the CRC mixtures were slightly better or comparable to the reference mixtures. The (slightly) improved results might be related to the densification of the pore structure due to the pozzolanic reaction of the Fly Ash.

As no clear conclusions could be drawn from this cyclic exposure to chlorides, a diffusion test was conducted on the final CRC designs. Nonetheless, it was not possible to come to solid conclusions. At first the chloride ingress of the CRC samples seemed to decrease with curing time (between 1 and 3 months of curing), but the chloride diffusion test after 1 year of curing resulted in a higher chloride penetration depth compared to 3 months curing. Regarding the reference mixture, the opposite was true and it seemed that the chloride penetration depth first increased (from 1 month curing to three months curing), and it again decreased after 1 year curing. Nonetheless, the results of both CRC and reference concrete mixtures were in the same range.

The resistance against freeze-thaw attack with de-icing agents was, as expected, strongly related to the air content of the fresh concrete. Indeed, air entraining agents will create the air bubbles necessary for the freezing water to expand without increasing the tensile stresses in the concrete top layer. Thus, when necessary the resistance against freeze-thaw attack with de-icing agents can be modified by air entraining agents. The latter is not expected to affect the chemical composition of the concrete, as these components are mostly organic and will be decomposed within the clinkering process. Also the added quantities remain limited.

The combination of Calcium Aluminate Cement and Blast Furnace Slag Cement in one of the designed CRC mixtures (CRC3) resulted in workability problems, as setting occurred very fast. To slow down the hydration process, different retarders based on gluconate, sucrose or citric acid were added to the mixtures, however without success. It was found in literature that lime and calcium sulphate affect the setting of cementitious mixtures. Applying this to the CRC mixtures, the addition of lime and calcium indeed resulted in workable mixtures. An additional improvement was observed when adding a retarder next to lime and calcium sulphate. The delay of the setting times was observed using a Vicat needle, but could not be registered by ultrasonic transmission measurements. The latter might be related to ettringite formation, affecting the p-wave velocity and energy

curves, although having only a limited effect on the stiffening of the cement paste at early age. The hydration heat after 7 days of hydration was significantly less compared to the reference mixtures. The compressive strength after 7 and 28 days of the CRC mixtures with the addition of lime and calcium sulphate, with or without retarder, was certainly sufficient for practical applications. Indeed, the setting of the CRC mixture combining CAC and BFSC was successfully slowed down, but this CRC mixture is not preferred. An optimal combination of calcium sulphate and lime, and maybe a retarder, should be searched for each time, making the design process more complex.

Copper slag was found to be an interesting iron source for the production of CRC. First of all, it is an industrial by-product and its application reduces the need for natural resources on the one hand and the production of waste on the other hand. Secondly, it is already used as an iron adjusting raw material in the cement production. Two possible applications of this solid waste were studied: as alternative cementitious binder or as concrete aggregate. It was concluded that the use of copper slag as alternative binder was of minor interest, as a high amount of energy will be required to reveal the pozzolanic properties of the waste material. The use of copper slag as aggregate replacement is however promising. The effects on the compressive strength, open porosity, gas permeability, resistance against carbonation and chloride ingress seemed acceptable and even an improved performance of the concrete was observed. Only the resistance to freeze-thaw attack with de-icing agents was inferior. The performance in such an environment might however be improved by adapting the water content of the concrete or by adding an air entraining agent. The excess water due to the lower water absorption of the copper slag was claimed to be the main parameter affecting the performance of the concrete.

CRC clinker and cement quality

The regeneration process of cement from CRC was comparable to the industrial production process. After milling the cement raw meal in a planetary ball mill, tablets were produced in a perforated plate. These tablets were subsequently heated up to 1450 °C (@ 10 °C/min with a dwell time of 1 hour) in laboratory furnace upon which the clinkering reactions took place. The obtained clinker was subsequently milled with calcium sulphate to produce the CRC cement. The clinker quality was studied by XRD/Rietveld, TG/DT and microscopic analysis. Isothermal calorimetry and TG and XRD/Rietveld analysis were used to assess the cement hydration process.

For a selected CRC, the clinkering reactions upon heating were documented using in situ (up to 1050 °C) and ex situ (1050–1450 °C) XRD analysis, accompanied by TG/DT and light microscopy analysis. As the main CaO source in CRC are limestone aggregates, the decarbonation reaction of calcite and minor dolomite dominates the reaction at temperatures below 1050 °C, resulting in important amounts of free lime. This free lime then recombines with aluminate, silicate and minor sulphate to form intermediate belite, gehlenite, mayenite and ye'elimite phases at temperatures up to 1150 °C. The formation of the final clinker phases are observed at 1250 °C and higher, when extensive formation of alite, aluminate and ferrite occurs at the expense of lime, belite and

intermediate Ca-aluminates. By this it could be concluded that the clinkering reactions of CRC are comparable to those of a traditional cement raw meal, and this certainly after the decomposition process. The latter is inherent to the raw meal composition. The main raw material, limestone, is common for both the CRC and traditional cement raw meal. The materials delivering the SiO_2, Al_2O_3 and Fe_2O_3 might however differ. Fly Ash, copper slag, or porphyry aggregate were used in case of CRC, but e.g. clay minerals, shells, chalk, and iron ore might be used in case of a traditional cement raw meal. Also, the dehydration of the cement hydration products should be expected upon heating the cement raw meal, although not experimentally proven due to the dilution factor of cement in concrete and partial substitution of cement by fly ash.

The potential mineralogy of a clinker can be estimated using the (modified) Bogue formulas. However, the experimental results (XRD/Rietveld analysis and microscopy/point-counting analysis) showed the actual clinker composition is significantly different. The latter is related to the fact that the four main clinker phases may contain substituent ions besides CaO, SiO_2, Al_2O_3 and Fe_2O_3, affecting the final mineralogy. Although the modified Bogue calculations try to simulate the effect of the minor elements on the phase compositions, the improvements remain rather limited. This is merely due to the fact that even in the modified Bogue calculations, the phase compositions remain estimations and errors between the calculations and the experimental results cannot be avoided.

The effect of raw material fineness on the clinker mineralogy and reactivity was studied by XRD/Rietveld analysis and isothermal calorimetry, respectively. For the studied ranges of raw mix fineness (R90 ranging from 12-24 wt%), no significant influence was noticed. Additionally, the results of a differential thermal analysis indicated that significant energy savings in the clinkering process due to an improved reactivity of a finer raw meal should not be expected. Only in the lower temperature range there might be a small effect, as additional milling seems to result in a slightly drier raw material. However, possible energy savings will be (partially) undone by a higher energy consumption to obtain the higher fineness.

When using CRC as cement raw material, the permeated acids and salts in deteriorated concrete will have an effect on the clinkering process. While the amounts of MgO should be limited to avoid a potential delayed expansion in hardened concrete, the amounts of chlorides, sulphates and alkali should be mainly limited to avoid problems in the kiln system. Due to the volatility of these elements, cycles of evaporation and condensation will be established in the clinker kiln. As a result of these cycles, the preheater might get clogged or kiln rings might appear on the kiln walls, both requiring periodic maintenance of the kiln system. Nonetheless, if properly balanced, magnesium, chlorides, sulphates and alkali can have a positive effect on the clinkering process (e.g. stabilisation of more reactive phases and decreasing the melt viscosity) and the use of deteriorated CRC raw meals is possible if properly diluted.

An assessment of the hydration reactions was made for four CRC cements and two commercial cements (CEM I 52.5 N and CEM I 42.5 N LH HSR LA). Three different

clinkers were used to produce the CRC cements. For one of them two different finenesses were tested. Isothermal calorimetry clearly showed that a higher fineness increases the cement reactivity. This can be interesting to improve the reactivity of a cement with a rather low alite content. The dissolution of the main clinker minerals and the formation of (crystalline) hydration products in time was visualized by TG and XRD/Rietveld analysis. The hydration of the cement paste is preferably stopped by solvent exchange, as freeze drying affects the crystallinity of e.g. ettringite and gypsum. The general phase changes upon hydration for both the CRC and reference cements were comparable. The main difference was perhaps the stability of anhydrite in the reference cements up to 9 hours of hydration, while in case of the CRC cements the calcium sulphate was immediately transformed into gypsum.

The hydration reaction of all cements was modelled using the cement hydration model described by Lothenbach & Winnefeld (2006). It combines the empirical model of clinker dissolution in time proposed by Parrot & Killoh (1984) and the thermodynamic equilibrium model GEMS for calculation of the corresponding hydrate assemblage [Kulik et al. (2013)]. In general the modelled and experimental data were comparable. However, the effect of the increased reactivity obtained for cements with a higher fineness did not show in the modelled data. In addition to the obtained experimental data, the modelled data can be interesting in predicting the composition of the non- or poorly crystalline fraction that could not be studied using XRD/Rietveld analysis. Regarding the hydration of the silicate phases, it is possible to predict the composition of the C-S-H phase. In case of the rather complex hydration process of the aluminate and ferrite phases, it is possible to indicate the distribution of the non- or poorly crystalline hydrate phases (AFm phases and hydrogarnets), which are expected to be present besides the experimentally observed crystalline phases ettringite (AFt) and kuzelite (AFm).

CRC sustainability

To assess the sustainability of the CRC concept, a Life Cycle Assessment (LCA) was conducted. Within this study, the whole life cycle of the concrete was considered, from the extraction of the raw materials up to the recycling and disposal of the demolished concrete structure, taking into account the (positive) impact of avoiding natural raw materials. The functional unit was set to be the total amount of concrete needed to deliver 1 MPa of strength and 1 year of service life. The data obtained from the strength and durability assessment of CRC were used for this purpose.

The life cycle inventory was based on the ecoinvent 2.0 database built by the Swiss Centre for Life Cycle Inventories which is commonly used in combination with the LCA software SimaPro developed by Pré consultants (Product ecology consultants) that was used in the present study. When needed, adaptations were made to take into account the recycling possibilities of both CRC and traditional concrete mixtures (e.g. splitting of the production process into the raw material delivery and the actual production process). For the life cycle impact assessment, the CML 2002 problem oriented impact method was used, and the following baseline impact categories were considered: abiotic

depletion, acidification, eutrophication, climate change, stratospheric ozone depletion, human toxicity, ecotoxicity (fresh water and marine aquatic and terrestrial) and photo-oxidant formation.

The environmental impact of the concrete production process was found to be strongly related to its binder content (mainly cement, but also fly ash by the economic allocation) and the required transport. Also the recycling opportunities of concrete are strongly affected by the required transport, which is in case of CRC expected to be higher, as transport to the cement plant is expected to be longer compared to the distance to a concrete recycling plant. The main environmental benefit of CRC recycling is related to its global warming potential. Compared to a traditional cement raw meal, CRC will contain a certain amount of CO_2 free CaO. Thus making use of CRC instead of a traditional cement raw meal for the manufacturing of clinker will avoid the emission of a certain amount of CO_2.

Looking at the complete life cycle of CRC and traditional concrete it was found that regarding the global warming potential a reduction of 66-70% is possible when a high strength CRC with a low clinker content is designed. In case of a normal strength CRC with a higher clinker content, the reductions can be up to 7-35% if a sufficient service life can be obtained. For most other impact categories (abiotic depletion, acidification, eutrophication, ozone layer depletion, photo-oxidant formation, human toxicity and ecotoxicity) only the performance of a high strength CRC with low clinker content could compensate for the additional transport required in the recycling process.

Conclusions

Within this study the feasibility of CRC regarding its strength and durability and its regeneration within the cement production was scientifically proven. Additionally it was shown through a life cycle assessment that the global warming potential can be reduced significantly. However, some logistic and practical problems will need to be tackled for the CRC concept to succeed. A well-considered tracking system and selective demolition will be required. Additionally the dependence of the raw material requirements on the used fuels in the clinkering process results in the non-existence of one ideal raw meal composition. In comparison with today's recycling opportunities for concrete, the CRC concept is thus more complex. The opportunities of the CRC concept however lay within the possibility of safely disposing (some) toxic wastes and the possibility to use deteriorated concrete if proper dilution is applied.

COMPLETELY RECYCLABLE CONCRETE
for a More Environment-Friendly Construction

I - The concept for Completely Recyclable Concrete

The flexibility in design that is given by concrete was already known to the designers and builders of ancient Rome. Water pipes and aqueducts, foundations and walls for buildings, all types of hydraulic structures for sea- and freshwater, and also bridges and palaces were built using *opus caementitium*. The first hydraulic binders probably comprised a mixture of lime and pozzolana (natural volcanic silica dust) [Meck (2006)]. One of the best-known concrete structures from that time, and still worth a visit, is probably the Pantheon (118-128 AD) in Rome (see Figure I.1). Although concrete was already made 2000 years ago, it was only in the middle of the 19th century that the first industrial cements would be made, first in shaft kilns, later on in rotary kilns [Schneider et al. (2011)]. Since the first half of the 20th century, designers use concrete for its sculptural possibilities. Besides its mechanical strength, freedom in design and relatively low cost, also the many environmental advantages, including durability, longevity, heat storage capability, and (in general) chemical inertness [ISO (2005)], make concrete the building material of the 20th and 21st century, which is shown by the annual production numbers of cement and concrete, about 3 and 10 billion tons respectively [Cembureau (2009); Meyer (2009); Schneider et al. (2011); U.S. Geological Survey (2011)].

Figure I.1 - Panoramic view of the Pantheon in Rome [Bauer (2005)]

The popularity of concrete goes hand in hand with an environmental cost, of which the three main aspects are marked in Figure I.2. Worldwide, the cement and concrete production industry is one of the most important consumers of primary raw materials. It is mainly the supply of conventional raw materials such as limestone for cement clinker production and aggregates for concrete that requires a massive extraction of primary resources (A in Figure I.2). At the opposite end of the concrete life cycle (C in Figure I.2), concrete demolition waste represents 12-21% of the total waste generated in the European Union [De Belie and Robeyst (2007); Fischer and Werge (2009)]. An additional environmental concern for the conventional cement used is related to the clinker manufacturing which releases about 0.85 kg of CO_2 per kg clinker (B in Figure I.2) [Gartner (2004)]. This is largely due to the calcination of limestone as main CaO source and to fuel combustion for reaching typical kiln clinkering temperatures of

1400-1450 °C. In total the cement industry is estimated to emit 5-7% of the global CO_2 emissions [Damtoft et al. (2008); Shi et al. (2011); Aranda Usón et al. (2013)].
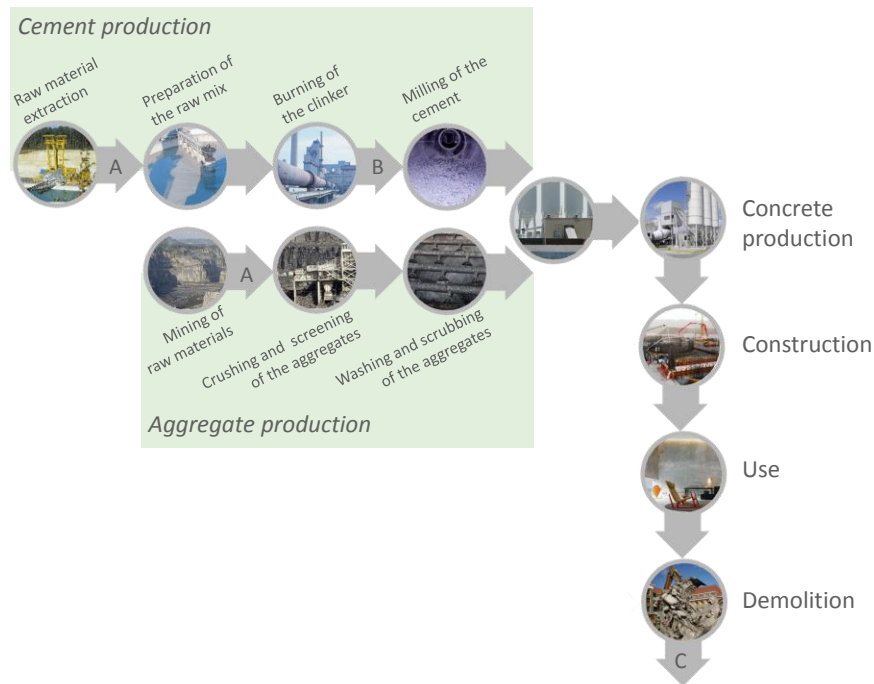
Figure I.2 – The (simplified) life cycle of a concrete construction. A: raw materials extraction requires massive extraction of primary resources. B: the clinker manufacturing process emits high amounts of CO_2. C: high amounts of construction and demolition waste are produced.

A. Reuse and recycling in concrete construction today

For the above-mentioned reasons, many studies in the field of concrete research are dealing with the reduction of the environmental impact of cement and concrete by means of recycling solid wastes. The following overview is based on the different concrete applications for these solid wastes. The focus of the overview is put on raw materials for concrete production, and extended to the use of alternative raw materials for clinker production. The use of solid waste as alternative fuel for the cement clinkering process will not be discussed, although it certainly increases the sustainability of cement manufacturing and thus concrete.

A.1. Solid waste as aggregate in concrete

In disregard of the environmental benefits and unless specific properties of waste material, absent in natural sand and gravel, can be exploited; the simple replacement of

fine or coarse aggregates by secondary aggregates extracted from waste, implies a certain degree of down cycling from an economical viewpoint [Meyer (2009)]. The use of rubber tires and recycled plastics is studied, but there is no real added value and they negatively affect the mechanical performance. The incorporation of different kinds of slags as aggregate in concrete seems however promising. Improved post-fire properties [Netinger et al. (2013)] and a reduced water absorption [Maslehuddin et al. (2003)] were observed for concrete with steel slag as aggregate. The increased compressive and tensile strength of concrete with copper slag as sand and aggregate replacement makes it a suitable alternative raw material in high strength concrete [Al-Jabri et al. (2009a); Al-Jabri et al. (2009b); Khanzadi and Behnood (2009)]. Also post-consumer glass can have an added value as aggregate in concrete [Jin et al. (2000); Meyer (2009)]. Glass is known to have a high hardness and good abrasion resistance combined with an excellent durability and chemical resistance, if its potential alkali-silica reaction (ASR) is properly controlled. Furthermore the aesthetic potential of coloured glass makes the glass a value-added product.

Also within the construction sector itself, recycling opportunities to reduce the impact of raw material mining exist. Construction and Demolition Waste (CDW) such as ceramics or masonry, but also concrete itself can be used as alternative aggregate in concrete [De Belie and Robeyst (2007); Medina et al. (2012)]. The latter is more interesting from a sustainable viewpoint as a closed material cycle can arise. Nonetheless, demolished concrete is mainly 'down cycled' as aggregates in granular base or sub-base applications, for embankment constructions and in earth construction works [Marinkovic et al. (2010)]. Indeed, the quality of these Recycled Concrete Aggregates (RCA) is lower than that of Natural Aggregates (NA), which limits their use for structural applications. The main problem is the mortar and cement paste attached to the old stone particles, which increase the water absorption and reduce the abrasion resistance [Marinkovic et al. (2010)]. Moreover, RCA can be contaminated by various sources of aggressive ions like chlorides and sulphates (e.g. from de-icing salts, sewage plants or seawater), which may have a significant impact on the durability of Recycled Aggregate Concrete (RAC) [Debieb et al. (2010)]. It has been intensively studied which quantities of recycled aggregates can be applied in concrete without negatively affecting the properties. These studies yielded towards replacement degrees of 20-30% having no significant impact on the new concrete's durability [Bonte and Van Laethem (2007); Chakradhara Rao et al. (2011)].

A.2. Solid waste as cementitious binder

The use of natural resources for concrete production cannot only be reduced by the use of recycled aggregates (see above), but also by using alternative binders with latent hydraulic or pozzolanic properties. The best known Supplementary Cementitious Materials (SCM) are probably blast furnace slag from the iron production [Meyer (2009); Gruyaert (2011); Lothenbach et al. (2011)], fly ash from coal power plants [Baert (2009); Meyer (2009); Lothenbach et al. (2011)] and silica fume from the production of (ferro)silicon alloys [Bentz (2000); Meyer (2009); Giner et al. (2011);

Lothenbach et al. (2011)]. These SCMs are as such no longer waste materials, but gained the status of a by-product. By replacing cement and clinker with SCMs not only the use of our earth's resources is being reduced, but also the CO_2 emissions associated with the cement clinkering process are strongly reduced.

New clinker substitutes that are studied are e.g. clays calcined at 600-850 °C. The calcination process depends on the origin and composition of the clays and the availability can be regionally limited [Fernandez et al. (2011); Schneider et al. (2011)]. The pozzolanic or latent hydraulic properties that might be derived from waste are highly depending on the lime content [Schneider et al. (2011)]. Waste materials with sufficient amounts of calcium, e.g. some vitrified waste materials or lignite ashes, might have sufficient amounts of calcium to be promising as latent hydraulic material. Other waste materials with a low calcium and high silica content might be more favourable as pozzolanic materials, e.g. waste sludge from the photovoltaic industry [Quercia et al. (2013)] or rice husk ashes [Zain et al. (2011)].

The challenges for SCMs are the slower strength development for the same fineness compared to OPC [Schneider et al. (2011)]. A slower hydration, however, goes hand in hand with lower levels of heat release and thus less internal tensions in massive structures. Also the dense microstructure improves the resistance against diffusion driven deterioration mechanisms such as chloride ingress. In comparison with OPC, they are however more susceptible to specific types of chemical attack (cf. fly ash and the carbonation mechanism [Papadakis (2000); Younsi et al. (2011); Van den Heede and De Belie (2014)]). Finally it should be noted, that as for most recycling cases, also for SCMs the sustainability depends highly on the local availability of these materials.

A.3. Solid waste as raw material for clinker manufacturing

The main raw materials for clinker production are limestone and clay, or their natural mixture marl. Alternative raw materials used in the clinker manufacturing process are mostly corrective materials to adjust the primary limestone feed composition [Schneider et al. (2011)]. The use of industrial by-products such as metallurgical slags or fly ashes has been evaluated [Monshi and Asgarani (1999); Chen and Juenger (2009)]. The elevated temperature and large production capacity of a clinker kiln can be exploited by producing clinker from a raw meal incorporating dilute amounts of waste materials such as municipal solid waste incineration (MSWI) ash [Shih et al. (2003); Pan et al. (2008)], mining waste [Potgieter et al. (2002); Kakali et al. (2003)] or refinery residues [Tsakiridis et al. (2004)], water purification [Chen et al. (2010)] or sewage sludge [Pan et al. (2004)], refuse glass [Chen et al. (2002)] and ceramic waste tiles [Puertas et al. (2008); Puertas et al. (2010)]. Replacement levels of waste for conventional raw materials are typically limited as most by-product and waste materials are relatively low in CaO compared with Portland clinker and can contain high levels of volatile heavy metals [van Oss and Padovani (2003)]. Higher utilization levels of secondary raw materials are therefore obviously only achievable when CaO rich waste materials are accessible. Non-carbonate CaO sources are of particular interest to reduce the calcination CO_2 emissions.

Also concrete waste materials can be used as raw material for clinker production. Cellular concrete is an interesting SiO_2 source for the clinker raw meal, but the presence of quartz impedes the grinding process [Schoon et al. (2013a)]. Waste fibre cement will reduce the CO_2 emissions due to the presence of non-carbonate CaO rich cement paste [Schoon et al. (2012)]. It should however be introduced in a hot point in the production process (e.g. the precalciner or preheater) to ensure the full thermal degradation of the organic fibres present. Finally also the fines from aggregate production can be used as raw material for cement production. These fines can originate from natural aggregates such as porphyry and dolomitic limestone [Schoon et al. (2013b)] or from concrete crusher sand [Schneider et al. (2011)]. The possible amounts of dolomitic limestone that can be provided to the clinker raw meal are limited due to the high level of MgO. However, when cautiously introduced with alkali and sulphates, the burnability of the raw mixture can be improved. In case of concrete crusher sand the dosage is often limited to an average of 3% due to the high silica content. In this case the production process can benefit from the presence of non-carbonate CaO in the cement paste on the one hand, but suffers from the presence of quartz increasing the energy needed for grinding.

B. The Cradle-to-Cradle concept for concrete

In general, recycling has an environmentally friendly image: it reduces the demand for new resources, it cuts down on production energy costs, and it recycles waste which would otherwise be lost as landfill [Edwards (1999)]. From the above it can be seen that today's recycling opportunities often arise from the search for new synergies between usually unrelated industrial partners. Producers of waste materials on the one hand, desire their waste products to be optimally used as material resources at the end of their life cycle. On the other hand producers are encouraged to improve the resource efficiency of their manufacturing process by the incorporation of waste materials. Above that, recycled products still suffer from a low acceptability, caused by a lack of trust in the quality of these products and in some cases by the higher cost of recycled materials compared to natural materials [F.I.R. (2005)].

To take recycling to a higher level of efficiency, the interest of both partners should be joined, and designers should think ahead and consider from as early as the design process the need for recycling the waste produced from their products. This idea of 'design for reincarnation', is also known as the Cradle-to-Cradle (C2C) concept, which is promoted worldwide by McDonough and Braungart (2002). In C2C production all material inputs and outputs are either seen as technical resources or as biological nutrients (see Figure I.3). Biological nutrients can be composted or consumed whereas technical resources can be recycled or reused without loss of quality.

When applying this idea on the production of concrete, it is easily noticeable that the raw materials used for concrete and cement production share common base components. Hence the idea emerged to design a Completely Recyclable Concrete (CRC) as a technical resource for cement production without the necessity to adjust the

ingredients. The latter is done by designing the chemical composition of CRC to be similar to that of the cement raw material mix. Hereby the concrete waste obtained after demolition becomes a valuable material for cement production. To obtain the desired raw meal composition, the concrete should contain limestone aggregates, and can also contain waste materials such as metallurgical slags or fly ash which additionally reduces the environmental impact of the CRC.
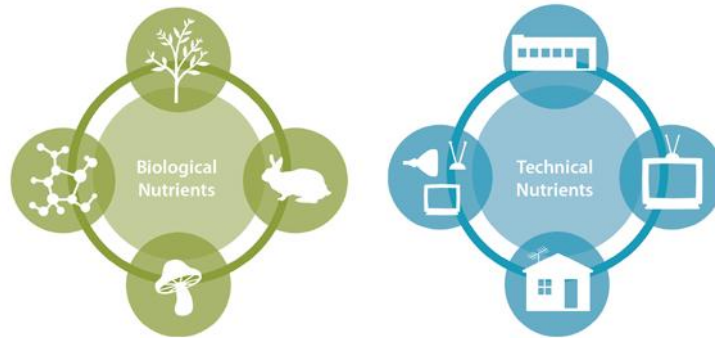
Figure I.3 - Visualisation of the Cradle-to-Cradle Principle [McDonough and Braungart (2003)]

C. Objectives of the study and outline of the thesis

The goal of this study is take the recycling of concrete to a higher level by creating Completely Recyclable Concrete (CRC). After pulling down the structure, concrete rubble is beginning a new life as raw material for cement production, without the necessity for ingredient adjustments. If CRC is then used on a regular basis, a concrete-cement-concrete material cycle will arise (see Figure I.4), which is completely different from the current life cycle of traditional concrete.

C.1. Design of the CRC concrete mix (PART I)

In preparation of the CRC design, a literature study is made on the composition and design parameters of Portland Clinker, of which the chemical composition is the required composition of CRC. Subsequently an overview of concrete raw materials is assembled to make a selection of potential raw materials for CRC. Finally, both are combined for designing CRC for reincarnation in the cement production.

C.2. CRC quality and durability assessment (PART II)

The aim is that the designed CRC fulfils the standard requirements of workability, strength and durability, and thus an experimental program is assembled. Experiments in the study are limited to these topics where there is still doubt about the performance of the CRC, or where durability problems are expected. During the course of the project, one of the designs combined calcium aluminate cement with blast furnace slag cement

which resulted in fast setting and thus a study towards the deceleration of the fast setting of this mixture was conducted. Also the possibilities of using copper slag in concrete, as SCM or aggregate, are assessed as it is was found to be an interesting Fe_2O_3 source for cement clinker production.
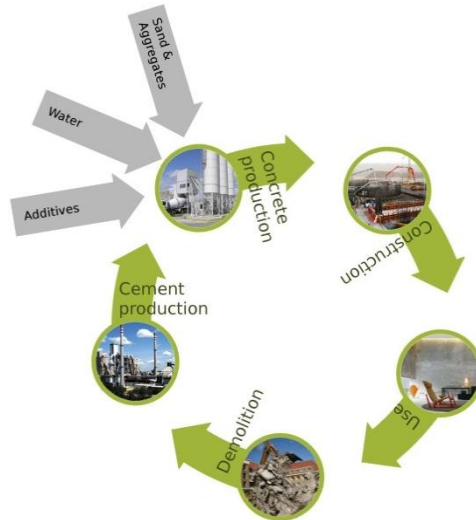
Figure I.4 - The concrete-cement-concrete material cycle of CRC

C.3. CRC clinker and cement quality assessment (PART III)

The clinker and cement regenerated from CRC should also be of sufficient quality. After a literature review of the chemistry of Ordinary Portland Cement manufacturing and hydration, the CRC clinker and cement quality are studied experimentally. Clinkering reactions and mineralogy are studied by means of in situ and ex situ XRD measurements, thermal analysis and clinker microscopy. Also the effect of burning deteriorated CRC on the clinker quality is assessed. Both thermal analysis and XRD measurements are used for investigation of the CRC cement hydration process. The applicability of an established OPC hydration model on the hydration of CRC cement is verified.

C.4. CRC sustainability assessment (PART IV)

In order to make a final evaluation of the feasibility and sustainability of the CRC concept, a life cycle assessment is required. The data obtained on the quality of CRC and its regenerated clinker will be used for this purpose. The life cycle assessment will focus on the use of natural resources, the energy consumption and its related CO_2 emissions and the use of land and space as those are the points where improvements are expected. After the life cycle assessment final conclusions on the CRC concept and perspectives for further research is formulated.

References

Al-Jabri, K. S., M. Hisada, S. K. Al-Oraimi and A. H. Al-Saidy (2009a). "Copper slag as sand replacement for high performance concrete." Cement and Concrete Composites 31(7): 483-488.

Al-Jabri, K. S., M. Hisada, A. H. Al-Saidy and S. K. Al-Oraimi (2009b). "Performance of high strength concrete made with copper slag as a fine aggregate." Construction and Building Materials 23(6): 2132-2140.

Aranda Usón, A., A. M. López-Sabirón, G. Ferreira and E. Llera Sastresa (2013). "Uses of alternative fuels and raw materials in the cement industry as sustainable waste management options." Renewable and Sustainable Energy Reviews 23(0): 242-260.

Baert, G. (2009). Physico-Chemical Interactions in Portland Cement - (High Volume) Fly Ash Binders. PhD Thesis. Ghent, Ghent University. PhD.

Bauer, S. (2005), Panoramic view of the Pantheon in Rome. Available from: www.ferras.at

Bentz, D. P. (2000). "Influence of silica fume on diffusivity in cement-based materials: II. Multi-scale modeling of concrete diffusivity." Cement and Concrete Research 30(7): 1121-1129.

Bonte, K. and K. Van Laethem (2007). Puingranulaten in stortbeton klassen C12/15 en C16/20. Vergelijkende prestatiestudie. Industriële Wetenschappen en Techniek. Oostende, KHBO.

Cembureau (2009) "Activity Report 2009."

Chakradhara Rao, M., S. K. Bhattacharyya and S. V. Barai (2011). "Behaviour of recycled aggregate concrete under drop weight impact load." Construction and Building Materials 25(1): 69-80.

Chen, G., H. Lee, K. L. Young, P. L. Yue, A. Wong, T. Tao and K. K. Choi (2002). "Glass recycling in cement production—an innovative approach." Waste Management 22(7): 747-753.

Chen, H., X. Ma and H. Dai (2010). "Reuse of water purification sludge as raw material in cement production." Cement and Concrete Composites 32(6): 436-439.

Chen, I. A. and M. C. G. Juenger (2009). "Incorporation of Waste Materials into Portland Cement Clinker Synthesized from Reagent-Grade Chemicals." International Journal of Applied Ceramic Technology 6(2): 270-278.

Damtoft, J. S., J. Lukasik, D. Herfort, D. Sorrentino and E. M. Gartner (2008). "Sustainable development and climate change initiatives." Cement and Concrete Research 38(2): 115-127.

De Belie, N. and N. Robeyst (2007). Recycling of construction materials. Environment-conscious construction materials and systems. State of the art report of TC 192-ECM. RILEM Report Nr. 37. N. Kashino, D. Van Gemert and K. Imamoto. Bagneux, RILEM Publications S.A.R.L.**:** 11-23.

Debieb, F., L. Courard, S. Kenai and R. Degeimbre (2010). "Mechanical and durability properties of concrete using contaminated recycled aggregates." Cement and Concrete Composites 32(6): 421-426.

Edwards, B. (1999). Sustainable architecture: European directives and building design. Oxford, Architectural Press.

F.I.R. (2005) "Information document on the effects of C&DW recycling." Prepared for DGEnvironment by the F.i.R. as input to the Thematic Strategy on Prevention and Recycling of Wate.

Fernandez, R., F. Martirena and K. L. Scrivener (2011). "The origin of the pozzolanic activity of calcined clay minerals: A comparison between kaolinite, illite and montmorillonite." Cement and Concrete Research 41(1): 113-122.

Fischer, C. and M. Werge (2009) "EU as a Recycling Society." European Topic Centre on Resource Waste Management, Working paper 2/2009.

Gartner, E. (2004). "Industrially interesting approaches to "low-CO_2" cements." Cement and Concrete Research 34(9): 1489-1498.

Giner, V. T., S. Ivorra, F. J. Baeza, E. Zornoza and B. Ferrer (2011). "Silica fume admixture effect on the dynamic properties of concrete." Construction and Building Materials 25(8): 3272-3277.

Gruyaert, E. (2011). Effect of Blast-Furnace Slag as Cement Replacement on Hydration, Microstructure, Strength and Durability of Concrete. Faculty of Engineering and Architecture. Ghent, Ghent University. PhD.

ISO (2005) "Business Plan." ISO/TC 71 Concrete, Reinforced Concrete and Prestressed Concrete.

Jin, W., C. Meyer and S. Baxter (2000). ""Glascrete" - Concrete with Glass Aggregate." ACI Materials Journal March-April: 208-213.

Kakali, G., S. Tsivilis, K. Kolovos, K. Choupa, T. Perraki, M. Perraki, M. Stamatakis and Vasilatos (2003). "Use of secondary mineralizing raw materials in cement production. The case study of a stibnite ore." Materials Letters 57(20): 3117-3123.

Khanzadi, M. and A. Behnood (2009). "Mechanical properties of high-strength concrete incorporating copper slag as coarse aggregate." Construction and Building Materials 23(6): 2183-2188.

Lothenbach, B., K. Scrivener and R. D. Hooton (2011). "Supplementary cementitious materials." Cement and Concrete Research 41(12): 1244-1256.

Marinkovic, S., V. Radonjanin, M. Malesev and I. Ignjatovic (2010). "Comparative environmental assessment of natural and recycled aggregate concrete." Waste Management 30(11): 2255-2264.

Maslehuddin, M., A. M. Sharif, M. Shameem, M. Ibrahim and M. S. Barry (2003). "Comparison of properties of steel slag and crushed limestone aggregate concretes." Construction and Building Materials 17(2): 105-112.

McDonough, W. and M. Braungart (2002). Cradle to cradle : remaking the way we make things. New York, North Point Press.

McDonough, W. and M. Braungart (2003), Towards a Sustaining Architecture for the 21st Century: The Promise of Cradle-to-Cradle Design. Available from: http://www.mcdonough.com/speaking-writing/toward-a-sustaining-architecture-for-the-21st-centurythe-promise-of-cradle-to-cradle-design/#!prettyPhoto

Meck, M. (2006). The evolution of reinforced concrete. DETAIL Practice Concrete. N. Kollmann, J. Liese and S. Schmid. Munich, Institut für internationale Architektur-Dokumentation GmbH & Co. KG**:** 8-9.

Medina, C., M. I. Sánchez de Rojas and M. Frías (2012). "Reuse of sanitary ceramic wastes as coarse aggregate in eco-efficient concretes." Cement and Concrete Composites 34(1): 48-54.

Meyer, C. (2009). "The greening of the concrete industry." Cement and Concrete Composites 31(8): 601-605.

Monshi, A. and M. K. Asgarani (1999). "Producing Portland cement from iron and steel slags and limestone." Cement and Concrete Research 29(9): 1373-1377.

Netinger, I., M. J. Rukavina and A. Mladenovič (2013). "Improvement of Post-fire Properties of Concrete with Steel Slag Aggregate." Procedia Engineering 62(0): 745-753.

Pan, J. R., C. Huang, J.-J. Kuo and S.-H. Lin (2008). "Recycling MSWI bottom and fly ash as raw materials for Portland cement." Waste Management 28(7): 1113-1118.

Pan, J. R., C. Huang and S. Lin (2004). "Reuse of fresh water sludge in cement making." Water science and technology 50: 183-188.

Papadakis, V. G. (2000). "Effect of supplementary cementing materials on concrete resistance against carbonation and chloride ingress." Cement and Concrete Research 30(2): 291-299.

Potgieter, J. H., K. A. Horne, S. S. Potgieter and W. Wirth (2002). "An evaluation of the incorporation of a titanium dioxide producer's waste material in Portland cement clinker." Materials Letters 57(1): 157-163.

Puertas, F., I. García-Díaz, A. Barba, M. F. Gazulla, M. Palacios, M. P. Gómez and S. Martínez-Ramírez (2008). "Ceramic wastes as alternative raw materials for Portland cement clinker production." Cement and Concrete Composites 30(9): 798-805.

Puertas, F., I. García-Díaz, M. Palacios, M. F. Gazulla, M. P. Gómez and M. Orduña (2010). "Clinkers and cements obtained from raw mix containing ceramic waste as a raw material. Characterization, hydration and leaching studies." Cement and Concrete Composites 32(3): 175-186.

Quercia, G., J. J. G. van der Putten, G. Hüsken and H. J. H. Brouwers (2013). "Photovoltaic's silica-rich waste sludge as supplementary cementitious material (SCM)." Cement and Concrete Research 54(0): 161-179.

Schneider, M., M. Romer, M. Tschudin and H. Bolio (2011). "Sustainable cement production—present and future." Cement and Concrete Research 41(7): 642-650.

Schoon, J., K. De Buysser, I. Van Driessche and N. De Belie (2013a). "Feasibility study on the use of cellular concrete as alternative raw material for Portland clinker production." Construction and Building Materials 48(0): 725-733.

Schoon, J., L. Van der Heyden, P. Eloy, E. M. Gaigneux, K. De Buysser, I. Van Driessche and N. De Belie (2012). "Waste fibrecement: An interesting alternative raw material for a sustainable Portland clinker production." Construction and Building Materials 36(0): 391-403.

Schoon, J., A. Vergari, K. De Buysser, I. Van Driessche and N. De Belie (2013b). "Fines extracted from porphyry and dolomitic limestone aggregates production: MgO as fluxing agent for a sustainable Portland clinker production." Construction and Building Materials 43(0): 511-522.

Shi, C., A. F. Jiménez and A. Palomo (2011). "New cements for the 21st century: The pursuit of an alternative to Portland cement." Cement and Concrete Research 41(7): 750-763.

Shih, P.-H., J.-E. Chang and L.-C. Chiang (2003). "Replacement of raw mix in cement production by municipal solid waste incineration ash." Cement and Concrete Research 33(11): 1831-1836.

Tsakiridis, P. E., S. Agatzini-Leonardou and P. Oustadakis (2004). "Red mud addition in the raw meal for the production of Portland cement clinker." Journal of Hazardous Materials 116(1–2): 103-110.

U.S. Geological Survey (2011). Mineral Commodity Summaries, Cement.

Van den Heede, P. and N. De Belie (2014). "A service life based global warming potential for high-volume fly ash concrete exposed to carbonation." Construction and Building Materials 55(0): 183-193.

van Oss, H. G. and A. C. Padovani (2003). "Cement Manufacture and the Environment Part II: Environmental Challenges and Opportunities." Journal of Industrial Ecology 7(1): 93-126.

Younsi, A., P. Turcry, E. Rozière, A. Aït-Mokhtar and A. Loukili (2011). "Performance-based design and carbonation of concrete with high fly ash content." Cement and Concrete Composites 33(10): 993-1000.

Zain, M. F. M., M. N. Islam, F. Mahmud and M. Jamil (2011). "Production of rice husk ash for use in concrete as a supplementary cementitious material." Construction and Building Materials 25(2): 798-805.

PART I
CRC Design

II - Portland Clinker

CRC is designed to become the only ingredient for the production of an Ordinary Portland Cement (OPC). Therefore the chemical composition of CRC should be similar to the one of a raw material for Portland Clinker (PC), the basic raw material for OPC production. OPC is used worldwide and is a well-known material, and its properties and performance are the topic of many courses, papers and books. The following is principally based on Taylor (1997), Hewlett (1998), BBG (2006) and Taerwe and De Schutter (2006) and gives a brief overview of the composition of both PC and its raw material.

A. Chemical and mineralogical composition

An ordinary Portland cement contains about 95-100% Portland clinker. This clinker contains the hydraulic components whereby cement will react with water to form a water insoluble product. To produce the clinker a raw mixture with a specific composition is heated. Table II.1 gives an overview of the required composition together with possible sources for the different oxides. About two thirds of this raw mixture is calcium oxide (CaO – C), whereby limestone is the main ingredient for clinker production. Another important oxide for the clinkering process is silicon oxide (SiO_2 – S), which is available in e.g. sand, fly ash and clay. The necessary amounts of aluminium (Al_2O_3 – A) and iron (Fe_2O_3 – F) oxide are limited and mostly already present in the raw materials delivering CaO and SiO_2. If necessary, minerals (e.g. iron ore) or industrial by-products (e.g. copper slag) can be added.

Table II.1 - Overview of the composition of a PC raw material and possible sources for the different oxides

	Weight percentages				Source
Oxide	BBG (2006)	Taylor (1997)	Huntzinger and Eatmon (2009)	Taerwe and De Schutter (2006)	Huntzinger and Eatmon (2009)
CaO	62-68	67	60-67	65	Limestone, shells, chalk
SiO_2	19-25	22	17-25	22	Sand, fly ash
Al_2O_3	2-9	5	2-8	5	Clay, shale, fly ash
Fe_2O_3	1-5	3	0-6	3	Iron ore
MgO	0-2	3			
$K_2O + Na_2O$	0.5-1.5				

During burning and subsequent cooling of the raw materials, the hydraulic components for cement hydration are formed. In Table II.2 a short overview of these components is given. The main component alite will generate the early strength of concrete, while belite will only contribute to the long term strength. Aluminate and ferrite will not significantly contribute to the strength development, but are still necessary ingredients. Due to the presence of Al_2O_3 and Fe_2O_3 a melt will be formed which facilitates the formation of alite from a temperature of 1300 °C onwards. As white cement can only be produced without colouring oxides such as iron, the production of white cement requires much higher burning temperatures. Aluminate has a limited influence on the strength development, but it however affects the stiffening and binding of the cement paste.

Table II.2 - Overview of the main hydraulic components of PC

Name	Chemical formula	Cement chemistry notation	Weight percentages		
			BBG (2006)	Taylor (1997)	Stephan and Wistuba (2006)
Alite or tricalcium silicate	Ca_3SiO_5 or $3CaO.SiO_2$	C_3S	40-75	50-70	52-85
Belite or dicalcium silicate	Ca_2SiO_4 or $2CaO.SiO_2$	C_2S	10-35	15-30	0-27
Aluminate or tricalcium aluminate	$Ca_3Al_2O_6$ or $3CaO.Al_2O_3$	C_3A	0-15	5-10	7-16
Ferrite or tetracalcium aluminoferrite	Ca_2AlFeO_5 or $4CaO.Al_2O_3.Fe_2O_3$	C_4AF	1-20	5-15	4-18

A.1. Alite

Alite or tricalcium silicate is the main hydraulic component in OPC (40-85%) responsible for the early strength. Depending on temperature, alite has different crystal structures. According to Taylor (1997) and Staněk and Sulovský (2002) it undergoes the following phase transitions:

$$T_1 \underset{\longleftarrow}{\overset{620\,°C}{\longrightarrow}} T_2 \underset{\longleftarrow}{\overset{920\,°C}{\longrightarrow}} T_3 \underset{\longleftarrow}{\overset{980\,°C}{\longrightarrow}} M_1 \underset{\longleftarrow}{\overset{990\,°C}{\longrightarrow}} M_3 \underset{\longleftarrow}{\overset{1070\,°C}{\longrightarrow}} R$$
$$(T = triclinic, M = monoclinic, R = rhombohedral)$$

(II-1)
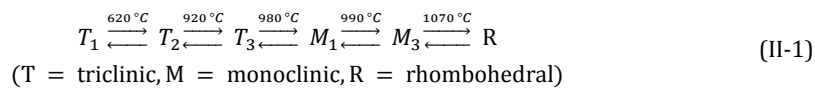
From the above it can be concluded that at room temperature, alite would be triclinic. However, at room temperature the monoclinic (M_1 and M_3) phase is mostly observed, and rarely the triclinic T_2 polymorph. Staněk and Sulovský (2002) and Stephan and Wistuba (2006) proved that the appearance of alite is influenced by the incorporation of substituents.

According to Taylor (1997) alite typically contains 3-4% of substituent oxides. From Table II.3 it can be concluded that MgO, Al_2O_3 and Fe_2O_3 are the main substituents. The influence of those elements on the crystal structure and the hydration heat of alite was studied by Stephan and Wistuba (2006). They concluded that the incorporation of MgO has the highest significance, although the influence on hydration seems of minor importance. The incorporation of Al_2O_3 is rather complex and leads to more defects. The latter could be a possible explanation for a higher hydration heat of alite containing Al_2O_3 in comparison with pure alite. Finally it seems that Fe_2O_3 causes only very small changes in the lattice parameters, while it has the biggest influence on the hydration heat. The hydration seems to be slowed down, but after 9 days of hydration the cumulative hydration heat is comparable with the one of pure alite.

According to Staněk and Sulovský (2002) the formation of the M_3 polymorph is favoured when the MgO to SO_3 ratio increases, while the opposite is true for M_1. Other parameters (e.g. the reactivity of the raw mixture, the intensity of the burning process or the addition of crystallization nuclei) seem to have a smaller influence on the appearance of alite. It was also observed that M_1 alite has a higher compressive strength by 10% compared to M_3. The transformation from M_3 to M_1 might be achieved by heating the clinker to 800 °C followed by a slow cooling process.

Table II.3 - The amount of substituents in alite in PC

Reference		Na_2O	MgO	Al_2O_3	P_2O_3	SO_3	K_2O	Fe_2O_3
Taylor (1997)		0.1	1.1	1.0	0.1	0.1	0.1	0.7
Stephan and Wistuba (2006)	Minimum	<0.1	0.1	0.6			<0.1	<0.1
	Maximum	1.2	2.1	2.7			0.9	4.5
	Typical	0.1	0.8	1.0			0.1	0.7

A.2. Belite

The amount of belite (0-35%), the other calcium silicate in PC, is a lot lower compared to alite. This is mainly because it has a very slow reaction degree, and the strength provided by belite is only comparable to the one of alite after one year. In parallel to alite, belite is known to have phase transitions due to temperature:

$$\alpha \underset{}{\overset{1425\,°C}{\rightleftarrows}} \alpha'_H \underset{}{\overset{1160\,°C}{\rightleftarrows}} \alpha'_L \underset{690\,°C}{\overset{630-680\,°C}{\rightleftarrows}} \beta \underset{}{\overset{<500\,°C}{\rightleftarrows}} \gamma$$

$$\underset{780-860\,°C}{}$$

(II-2)
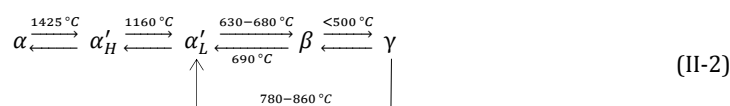
The arrangements of the ions are closely similar in α (Hexagonal), α'_H (Orthorhombic), α'_L (Orthorhombic) and β (Monoclinic) belite, while γ (Orthorhombic) belite is somewhat different. The much lower density of the γ polymorph compared to the others makes β belite crack and fall to a more voluminous powder upon cooling. To prevent this phenomenon, the belite structure needs substituents to stabilize the high temperature polymorphs. Such substituents are present in a cement raw mix and the

most important ones are Al_2O_3 (about 2.1%) and Fe_2O_3 (about 0.9%). Hereby the β polymorph is predominantly present.

Morsli et al. (2007) found that α belite is more reactive compared to the β polymorph. The addition of substituents such as alkalis and sulphates, or a specific heat treatment help to stabilize the α structure at room temperature. Furthermore, it is also possible to obtain a β belite with improved hydraulic properties by adding sulphates to the raw mixture. When sulphates are the only substituents present, they will not stabilize the α polymorph.

Compared to alite, belite has many advantages. Firstly, the production of belite cement will result in a lowered CO_2 emission. This is on the one hand due to the lower CaO content, and thus less $CaCO_3$ will be calcined. On the other hand a decrease of the burning temperature by about 100 °C is required for the production of such a cement, which will reduce the energy consumption and its related CO_2 emissions. Other advantages are the reduced hydration heat and improved durability. The main disadvantage is its high resistance to milling and the slow hydration process. The long hydration period can be reduced by stabilizing the more reactive α polymorph or by producing a more reactive β belite [Morsli et al. (2007)]. To ensure a minimal early strength it is however advised to aim for an alite content of about 15%.

A.3. Aluminate

A PC contains about 0-16% (tricalcium) aluminate. Aluminate is highly reactive and is known to result in fast setting. To control the reaction of aluminate, calcium sulphate is added to OPC. Pure aluminate is cubic and its appearance is not temperature dependent. Aluminate may contain Na^+ ions as substituent for Ca^{2+} which changes the formula to $Na_{2x}Ca_{3-x}Al_2O_6$. The incorporation of the Na^+ ions will not change the structure, as long as the limit of 1% Na_2O is not exceeded. Higher degrees of substitution lead to a series of variants of the structure, namely another cubic structure or to the orthorhombic or monoclinic polymorph. Also rapid cooling would stabilize orthorhombic aluminate.

A.4. Ferrite

The last main component of PC, ferrite or tetracalcium aluminoferrite, has a content varying from 1 to 20%. It is not known to have a significant effect on the strength development or the hydration process, but it does lower the temperature at which alite and belite are formed. At ordinary pressures and in absence of oxides besides CaO, Al_2O_3 or Fe_2O_3, it can have one of the following compositions: $Ca_2(Al_xFe_{1-x})_2O_5$ with $0<x<0.7$. C_4AF is thus only one composition with $x = 0.5$. Typically ferrite has about 10% of substituents where Fe^{3+} is replaced by Mg^{2+}, Si^{4+} and Ti^{4+}: $Ca_2AlFe_{0.6}Mg_{0.2}Si_{0.15}Ti_{0.05}O_5$. There are little or no substituents found for Ca^{2+}.

B. Tools to design a raw mixture for Portland clinker production

B.1. Compositional parameters for a PC raw mixture

For the composition of a raw mixture for Portland clinker production it is not only important that the necessary oxides are present, also the ratios between these oxides are of utmost importance. The weight ratios are expressed by means of the lime saturation factor (LSF), the silica modulus (SM), the alumina modulus (AM) and the hydraulic modulus (HM). An overview of target values found in literature is given in Table II.4.

Table II.4 - Typical values for LSF, SM, AM and HM

	Taylor (1997)[a]	Galbenis and Tsimas (2006)[a]		Kakali et al. (2003)[b]	Puertas et al. (2008)[b]	Binici et al. (2008)[b]
		Usual	Desired			
LSF	0.92-0.98	0.66-1.02	0.92-0.96	0.981	0.98	0.98-1.00
SM	2.0-3.0	1.9-3.2	2.3-2.7	2.42	2.30	2.0-2.1
AM	1.0-4.0	1.3-2.5	1.3-1.7	1.32	1.50	1.4
HM		1.7-2.3	~2	2.22		2.1

[a] Target values
[b] Values of realized raw meals

i. Lime saturation factor

The theory behind the lime saturation factor is found in Taylor (1997). Basically it comes down to the ratio of the available lime in the raw mixture to the lime chemically necessary for all the SiO_2, Al_2O_3 and Fe_2O_3 present in the raw mix to react. As such, the formula is as followed:

$$LSF = \frac{wt\%(CaO)}{2.8 \cdot wt\%(SiO_2) + 1.2 \cdot wt\%(Al_2O_3) + 0.65 \cdot wt\%(Fe_2O_3)} \tag{II-3}$$

A raw mixture with a LSF higher than 1 will result in an excess of lime whereby the clinker will have a certain amount of free lime. However, according to Taylor (1997) values up to 1.02 are acceptable in practice, without resulting in clinkers too high in free lime.

In alite, MgO is an important substituent for CaO. For this reason the lime content in formula (II-3) is replaced by:

$$wt\%(CaO) + 0.75 \cdot wt\%(MgO) \qquad \text{if } wt\%(MgO) \leq 2\% \tag{II-4}$$
$$wt\%(CaO) + 1.5 \qquad \text{if } wt\%(MgO) > 2\% \tag{II-5}$$

The upper limit for MgO is a result from the relation between the MgO content in alite (M_a) and clinker (M_c):

$$wt\%(M_a) = 0.67 \cdot wt\%(M_c) \qquad \text{if } wt\%(M_c) \leq 3\% \qquad \text{(II-6)}$$
$$wt\%(M_a) \approx 2.0 \qquad \text{if } wt\%(M_c) > 3\% \qquad \text{(II-7)}$$

From this it can be concluded that the MgO content of alite has a maximum of 2%. The difference between 0.67 (formula II-6) and 0.75 (formula II-4) is explained by the incorporation of MgO in the other hydraulic components (mainly belite).

ii. Silica and Alumina moduli

In contrast to LSF, having a theoretical basis, SM and AM are empirically based. These moduli are simply the following oxide ratios:

$$SM = \frac{wt\%(SiO_2)}{wt\%(Al_2O_3) + wt\%(Fe_2O_3)} \qquad \text{(II-8)}$$

$$AM = \frac{wt\%(Al_2O_3)}{wt\%(Fe_2O_3)} \qquad \text{(II-9)}$$

These parameters mainly influence the formation of the melt during the clinkering process (see chapter IX.A.2). From the broader range for the alumina modulus it can be concluded that the Al_2O_3 to Fe_2O_3 ratio is less crucial compared to the ratio of SiO_2 to Al_2O_3 and Fe_2O_3 (see Table II.4). In chapter IX.A.2 it will be seen that the silica modulus has a higher influence on the formation of the melt. The alumina modulus is only significant for the phase composition at lower temperatures.

iii. Hydraulic modulus

The hydraulic modulus is a tool to evaluate the potential hydraulic activity regarding strength development of the clinker. The hydraulic modulus is e.g. an additional parameter to estimate the compressive strength of mortar prisms based on microscopic analysis [Hewlett (1998)]. From a mathematical point of view the hydraulic modulus is the ratio between lime and the other main oxides:

$$HM = \frac{wt\%(CaO)}{wt\%(SiO_2) + wt\%(Al_2O_3) + wt\%(Fe_2O_3)} \qquad \text{(II-10)}$$

The target value is 2, whereby two thirds of the raw mixture should be CaO (ignoring the oxides besides CaO, SiO_2, Al_2O_3 and Fe_2O_3). Indeed, in Table II.1 it is seen that about 67% of CaO is typical for OPC raw mixtures.

B.2. The Bogue formulas

The aim of the Bogue formulas is to estimate the potential mineralogical composition of the Portland clinker based on the chemical composition of the raw mixture, only considering CaO, SiO_2, Al_2O_3 and Fe_2O_3. The formulas are based on the following assumptions [Taylor (1997)]:

- The compositions of the four major phases are C_3S, C_2S, C_3A and C_4AF
- Fe_2O_3 in the raw mixture occurs as C_4AF in the clinker
- The remaining Al_2O_3 in the raw mixture occurs as C_3A in the clinker
- The remaining CaO content in the raw mixture can be deducted from the amounts attributable to C_4AF, C_3A and free lime, to solve two simultaneous equations and obtain the contents of C_3S and C_2S in the clinker

From this, the Bogue formulas can be calculated as followed:

$$C_3S = 4.0710 \cdot C - 7.6024 \cdot S - 6.7187 \cdot A - 1.4297 \cdot F \tag{II-11}$$

$$\begin{aligned} C_2S &= -3.0710 \cdot C + 8.6024 \cdot S + 5.0683 \cdot A + 1.0785 \cdot F \\ &= 2.8675 \cdot S - 0.7544 \cdot C_3S \end{aligned} \tag{II-12}$$

$$C_3A = 2.6504 \cdot A - 1.6920 \cdot F \tag{II-13}$$

$$C_4AF = 3.0432 \cdot F \tag{II-14}$$

Target values can be found in Table II.2. It is important to know that the Bogue formulas only give an estimation of the potential mineralogical composition. When comparing the Bogue calculations with the mineralogy as obtained experimentally (e.g. by XRD/Rietveld analysis), the alite content is often overestimated, while the belite content is underestimated. The differences are mainly ascribed to the assumption of pure phases in the Bogue calculations, while studies have shown that clinker minerals contain significant amounts of substituent ions [Commission Chimique du CETIC (1978), Odler et al. (1981) and Herfort et al. (2010)]. As such modified Bogue calculations are proposed by Taylor (1997), taking into account the effect of minor elements on the composition of the major phases:

$$\begin{bmatrix} 0.716 & 0.635 & 0.566 & 0.475 \\ 0.252 & 0.315 & 0.037 & 0.036 \\ 0.010 & 0.021 & 0.313 & 0.219 \\ 0.33\,Fe_2O_3 & 0.009 & 0.051 & 0.214 \\ 0.67\,MgO & 0.005 & 0.014 & 0.030 \\ 0.001 & 0.001 & 0.010 & 0.001 \\ 0.001 & 0.009 & 0.007 & 0.002 \\ 0.001 & 1.23\,SO_3 + 0.24 & 0.000 & 0.000 \end{bmatrix} \cdot \begin{bmatrix} C_3S \\ C_2S \\ C_3A \\ C_4AF \end{bmatrix} = \begin{bmatrix} CaO \\ SiO_2 \\ Al_2O_3 \\ Fe_2O_3 \\ MgO \\ Na_2O \\ K_2O \\ SO_3 \end{bmatrix} \tag{II-15}$$

with C_3S, C_2S, C_3A and C_4AF the expected weight percentages [wt%] of alite, belite, aluminate and ferrite respectively and CaO, SiO_2, Al_2O_3, Fe_2O_3, MgO, Na_2O, K_2O and SO_3 the weight percentages of the concerned oxide in the clinker. Since there will always be some compositional variation in the solid solutions, also differences between theoretical calculations and experimental results cannot be avoided. Other sources of error are

related to the uncertainty of the bulk chemical analysis, the presence of free lime and insoluble residue (these components are not present in the four major phases) and compositional modifications during cooling, which reflect the absence of equilibrium [Stutzman et al. (2014)]. Stutzman et al. (2014) studied the uncertainty in Bogue-calculated phase compositions of hydraulic cements and calculated standard deviation values of about 9.6% for alite and belite, and 2.2% and 1.4% for aluminate and ferrite, respectively.

III - Concrete raw materials

The desired composition of CRC is now known, and in the following an overview of common concrete raw materials is given. From this it will be possible to select those materials that are interesting to use for CRC production. This overview is focussing on the Belgian cement and concrete production.

A. Cement

According to the European standard NBN EN 197-1 (2000) cement has 4 types of constituents: main constituents (>95%), minor additional constituents (<5%), additives (<1%, if organic <0.5%) and calcium sulphate. As such, the chemical composition of CRC will be mainly influenced by the main constituents. For this reason, only an overview for the main constituents based on NBN EN 197-1 (2000), Taerwe and De Schutter (2006) and BBG (2006) will be given.

There are 5 main constituents for cement: clinker, Blastfurnace Slag (BFS), pozzolanic materials, burnt shale and limestone. The Portland clinker was discussed earlier and as it is the desired composition for CRC, it can be considered as a neutral ingredient for the design of CRC. The other components are discussed hereafter and an indicative chemical composition is given in Table III.1.

Table III.1 - Overview of the chemical composition of OPC main constituents and calcium aluminate cement [wt%]

	Blastfurnace slag	Silica fume	Siliceous fly ash	Burnt shales	Calcium aluminate cement
SiO_2	35	90-96	56.5	55-60	0-8
CaO	40	0.1-0.5	4.9		20-42
Al_2O_3	15	0.5-3.0	25.5	15-25	36-80
Fe_2O_3	<1	0.2-0.8	8.1	5-10	0-20
MgO	10	0.5-1.5	1.7		0-1
Reference	BBG (2006)	BBG (2006)	BBG (2006)	Taylor (1997)	Hewlett (1998)

A.1. Blastfurnace slag

Granulated blastfurnace slag is made by rapid cooling of a slag melt obtained by smelting iron ore in a blastfurnace. This BFS has hydraulic properties when suitably activated. One of the possible activators is portlandite ($Ca(OH)_2$ or CH); one of the major hydration products from the calcium silicate phases in Portland clinker. For this reason BFS cements always contain a minimum content of PC. Blastfurnace slag consists for at least two-thirds out of CaO, MgO and SiO_2, besides Al_2O_3 and other minor components. As seen earlier, only a limited amount of MgO can be incorporated in the hydraulic components of PC. To prevent expansion, the remaining free MgO should be limited to

5% [BBG (2006)]. The danger to obtain a CRC containing too much MgO is however low. There is the dilution effect of the BFS in the whole binder content on the one hand and the rather low binder content of concrete compared to its aggregate content on the other hand.

A.2. Pozzolanic materials

Pozzolanic materials have a siliceous or silico-aluminous composition and form calcium silicate hydrates by consuming the portlandite from the hydration of alite and belite in Portland clinker. Natural pozzolana are usually materials of volcanic origin or sedimentary rocks having a suitable chemical or mineralogical composition. Natural calcined pozzolana are materials of volcanic origin, clays, shales or sedimentary rocks, which are activated by a thermal treatment.

Silica Fume (SF) and Fly Ash (FA) are both by-products having pozzolanic properties. SF is a by-product from the production of silicon and ferrosilicon alloys and contains at least 85 wt% amorphous silicon dioxide. FA is obtained by electrostatic or mechanical precipitation of dust-like particles from the flue gases from coal fired furnaces (e.g. for the production of electricity) and can be siliceous or calcareous in nature. Both types of FA have pozzolanic properties, the calcareous one is to a smaller extent also hydraulic. In Belgium the siliceous fly ash is commonly used, which will deliver SiO_2, Al_2O_3 and Fe_2O_3 to the CRC composition.

A.3. Burnt shale

Burnt (oil) shale is produced in a kiln at temperatures of about 800 °C. This component contains clinker phases such as dicalcium silicate and monocalcium aluminate, pozzolanic oxides (mainly SiO_2) and small amounts of free lime and calcium sulphate. Due to this composition it shows hydraulic as well as pozzolanic properties. In composition the burnt shale seems comparable to fly ash.

A.4. Limestone

Within cement, limestone can participate in the hydration reactions of aluminate (and ferrite) by forming hemi- or monocarbonate instead of monosulphate (AFm phases), and thus increasing the amount of ettringite in the hydrate assemblage. Due to this effect, the volume of hydrates increases in case of (low) limestone additions, which has a positive effect on compressive strength. Furthermore also the particle size distribution and physical properties of the limestone will affect the workability and the strength development of mixtures with this cement. A limestone that is suitable as main component in cement has a $CaCO_3$ content of at least 75%.

A.5. Calcium aluminate cement

Besides OPC, also Calcium Aluminate Cement (CAC) is a worldwide known cement. CAC is about 4 to 5 times as expensive as OPC [Scrivener et al. (1999)], and is therefore not used in everyday applications. Due to their special properties, such as rapid strength

development (even at low temperatures), high temperature resistance or refractory performance and resistance to a wide range of chemically aggressive conditions, they are used in specialist applications where the performance of OPC is insufficient [Taylor (1997), Hewlett (1998)]. The interest for this cement regarding the design of CRC is its high Al_2O_3 and CaO content (see Table III.1).

B. Aggregates

Besides cement that is a crucial ingredient, aggregates are the main constituents for concrete. Aggregates are mostly inert and have a natural or artificial origin. An overview of the chemical composition of some aggregates used in Belgium is given in Table III.2. The following overview is based on BBG (2006) and Taerwe and De Schutter (2006).

Table III.2 - Overview of the chemical composition of aggregates [wt%]

	Limestone	Porphyry	Granite	Blastfurnace Slag	Copper slag
SiO_2	10-25	65	72.04	30	25-41
$CaCO_3$	75-90				
CaO		2	1.82	45	0-11
Al_2O_3	0.5-5	16	14.42	15	0-16
Fe_2O_3	0.5-1.5	7	1.22		36-62
FeO			1.68	1.5	
$MgCO_3$	1-4				
MgO		2	0.71	4.5	0-4
Reference	*Taerwe and De Schutter (2006)*	*Taerwe and De Schutter (2006)*	*Blatt and Tracy (1997)*	*Taerwe and De Schutter (2006)*	*Shi et al. (2008)*

B.1. Natural aggregates

Gravel is an aggregate commonly used in Belgium and is found in or near rivers and the sea. As it is an alluvial material, it contains a variety of rocks and is therefore not included in Table III.2. Since *het grinddecreet* for the protection of natural resources the mining of gravel on land is stopped from 2005 onwards [BBG (2006)]. Due to this decree, it is only allowed to mine gravel if a river bed needs to be dredged or deepened.

Limestone is the most mined aggregate in Belgium, mainly in the Walloon region. If the amount of $MgCO_3$ exceeds the $CaCO_3$ content, it is called dolomite. The mined limestone is not only used as aggregate in concrete, but is also an important raw material for the production of lime and cement. For this reason it is an interesting aggregate to be used in CRC.

Sandstone is a rock that is used to a smaller extent in Belgium. It is hard to keep a constant quality because the layers of the sandstone quarries are strongly folded and

crossed by other layers. The high silicate content makes the use of this aggregate in CRC less favourable.

A final natural aggregate mined in Belgium is porphyry. It is an igneous rock that has the advantage of being free of pores. Due to its excellent mechanical and chemical properties, it is mainly used for high strength concrete and road construction. The Al_2O_3 content makes porphyry interesting to be used in CRC, although its high SiO_2 content will limit the possibilities.

To be complete, the chemical composition of granite is also added to Table III.2, which is an aggregate imported from Scotland and Norway to Belgium. As granite is also an igneous rock, it has the same advantages as porphyry. Also here the SiO_2 will limit its use in CRC.

B.2. Artificial aggregates

Slags, by-products from the metal industries, are the only artificial aggregates in Table III.2. According to BBG (2006) the disadvantage of using (blast furnace) slags as aggregates in concrete is the necessity of a pre-treatment to remove unwanted elements such as free lime. As mentioned earlier, blast furnace slag is a by-product from the iron industry. Copper slag on the other hand is obtained from the smelting and refining of copper. The blast furnace slag is interesting due to its relatively high CaO content, while copper slag is interesting as an Fe_2O_3 source for CRC.

Recycled Concrete Aggregates (RCA) are produced from the selective demolition of constructions. BBG (2006) uses 4 categories: concrete debris, masonry debris, mixed debris (concrete and masonry debris) and bituminous debris. The chemical composition of demolition waste is not given as it varies with its origin. Furthermore are RCAs only used for low value applications, at the moment not our intended application field (see chapter I).

Also lightweight aggregates, such as expanded clay, are only used in applications demanding low mechanical properties, due to their low density (600-900 kg/m^3). These lightweight aggregates have however other beneficial properties such as low weight and good heat insulation.

C. Additions and admixtures

The most used additions in Belgium are siliceous fly ashes, limestone filler, silica fume and blast furnace slag, which are all also used for cement production (see earlier and Table III.1). These additions are fillers (particle sizes < 80μm) and can be inert, pozzolanic or latent hydraulic. Due to their reactivity, fly ash, blast furnace slag and silica fume can be beneficial for concrete strength and its permeability when properly dosed into the concrete mix. The fine particle size distribution improves the properties of fresh concrete (good stability of the mixture, less bleeding). As a consequence, there is the higher water demand.

Admixtures are added to concrete to improve the properties of fresh and hardened concrete. As only a maximum of 5 wt% admixtures is allowed to be present in a concrete mixture, the chemical influence on CRC will be minimal and their composition will not be discussed. In the end, admixtures will only be used if it is otherwise impossible to meet the requirements for workability, strength and durability.

IV - CRC designed for reincarnation

From a predesign state, completely recyclable concrete is intended to be recycled as raw material for cement manufacturing. Therefore, the chemical composition of CRC is aimed to be identical to traditional cement raw materials, of which the requirements are well known (see chapter II). The design of CRC is divided into three steps: the making of an inventory, the establishment of boundary conditions and the determination of the chemical composition.

A. The design process

A.1. Inventory of CRC raw materials

Based on the overview of concrete raw materials (see chapter III), potential concrete raw materials were selected and analysed for their chemical composition. An overview of the concrete raw materials used in this study is assembled in Table IV.1. As seen in this table, 2 batches of limestone sand, CEM I 52.5 N and CEM III/A 42.5 N LA and 3 batches of fly ash were used during the course of the project.

A.2. Establishment of boundary conditions

In a second step the water W [kg/m^3] and total binder B [kg/m^3] content are determined, as these parameters are important for the production of a qualitative CRC. The binder content includes different types of cement and fly ash. Thereby the total volume of binders V_b [m^3], aggregates V_a [m^3] and fillers V_f [m^3] remain the only unknown parameters in the formula for 1 m^3 of concrete:

$$V_a + V_b + V_f + V_w + V_{air} = 1 \text{ m}^3 \tag{IV-16}$$

with V_w [m^3] the water volume (= W / 1000 kg/m^3) and V_{air} [m^3] the air content (= 0.02 m^3). The total volume of binders and aggregates can be calculated with the following formulas:

$$V_b = B \sum_{i=1}^{n} \frac{B_i}{\rho_i} \tag{IV-17}$$

$$V_a = A \sum_{i=1}^{n} \frac{A_i}{\rho_i} \tag{IV-18}$$

with B_i [-] and A_i [-] the amount of binder or aggregate i to respectively the total binder or aggregate content and ρ_i [kg/m^3] the density of aggregate or binder i. The ratios B_i and A_i, the total aggregate content A [kg/m^3] and the filler content F (= $V_f \cdot \rho_f$) [kg] will be determined aiming for an accurate chemical composition in the third step. For the determination of A_i the particle size distribution will also be considered, by aiming for the ideal curve of Fuller (by the least squares method) [Taerwe and De Schutter (2006)]. As filler only limestone filler was considered, mainly to increase the CaO content.

Table IV.1 - Overview of the chemical compositions of the used concrete raw materials [wt%]

Material	CaO	SiO$_2$	Al$_2$O$_3$	Fe$_2$O$_3$	MgO	Na$_2$O	K$_2$O	SO$_3$	Cl$^-$	LOI[a]	AT*
Copper slag 0/4	7.09	25.87	5.92	45.45	0.806	0.797[b]	0.191[b]		0.113	0.69	XRF
Limestone sand 0/4 - I	51.88	2.68	0.12	0.22	1.46	0.001	0.006				XRF
Limestone sand 0/4 - II	47.7	7.1	1.2	0.6	1.98	0.06	0.55	1.2		39.63	ICP
Limestone aggregate 2/6	44.7	15.3	1.26	0.51	0.71	0.06	0.5	0.6		36.05	ICP
Limestone aggregate 6/20	44.1	16.65	1.18	0.48	0.73	0.06	0.38	0.7		35.53	ICP
Porphyry aggregate 6/20	3.13	63.3	15.6	5.45	3.1	3.37	2.51	0.014	0.004	2.32[d]	XRF
Fly ash - I	2.42	47.99	33.5	3.8	0.47	0.23	1.56			4.98	XRF
Fly ash - II	4.7	50.3	29.5	4.26	1.12	0.347	1.35	0.721	0.002	3.49[d]	XRF
Fly ash - III	3.56	51.37	28.71	5.1	1.01	0.29	1.77	1.11[a]	0.001	3.6	XRF
CEM I 52.5 N - I	63.43	18.9	5.77	4.31	0.89	0.47	0.73				XRF
CEM I 52.5 N - II	62.2	18.65	5.91	4.12	0.84	0.47	0.89	3.2	0.061[c]	1.46	ICP
CEM III/A 42.5 N LA	52.73	28	8.92	2.67	4.06	0.36	0.5	3.05	0.05		XRF
Calcium aluminate cement	39.93	2.8	39.39	17.53	0.42	0.06	0.08			0	XRF
Limestone filler	54.2	0.59	0.22	0.08	0.91	0.02	<0.01	0.1		43.67	ICP

*the used analysis technique: X-ray fluorescence spectrometry (XRF) or inductively coupled plasma mass spectrometry (ICP), unless otherwise mentioned

[a] loss-on-ignition, according to NBN EN 196-2 (2005), unless otherwise mentioned
[b] according to CUR AANB. 89-6.2 (2006)
[c] by fusion-ion chromatography
[d] by thermogravimetric analysis

A.3. Determination of the chemical composition

The third step in the design process of CRC is crucial as it determines the chemical composition by outlining the proportions of all concrete materials. These proportions are determined by optimizing the compositional parameters or the Bogue formulas discussed earlier (see chapter II.B). Using the chemical compositions of the CRC raw materials, the composition of CRC is deducted by an iterations process calculating the above mentioned parameters and formulas and comparing them with typical values found in literature. The final aim is to achieve a CRC with an appropriate particle size distribution and more important a desired chemical composition.

B. Overview of the CRC compositions produced in this study

B.1. Concrete composition

The mixture proportions of the different CRCs produced in this study are shown in Table IV.2. As it is seen in this table, the main aggregate is limestone (CaO source), and when necessary, copper slag rich in Fe_2O_3 and SiO_2 (CRC1b, CRC1c and CRC2) or porphyry aggregates rich in SiO_2 and Al_2O_3 (CRC1b and CRC3b) were added to the mixture. Each CRC contained a certain amount of fly ash (for SiO_2 and Al_2O_3) and different kinds of cement were used. CRC1 and CRC2 are respectively produced with CEM I 52.5 N or CEM III/A 42.5 N LA. Calcium Aluminate Cement (CAC) was combined with CEM III/A 42.5 N LA in CRC3 as a source for Al_2O_3. As CRC2 required a high level of limestone filler, it was decided to aim for a self-compacting concrete.

The combination of CEM III/A 42.5 N LA and CAC in CRC3 resulted in fast setting of the concrete. In the first attempt to slow down the rapid setting of this concrete, calcium sulphate was added to the mixture. The desired effect was however not achieved for CRC3a. In an attempt to increase the workability by changing the particle size distribution of the aggregates, the chemistry of CRC3 changed and a small amount of porphyry aggregates was needed (CRC3b). In the end the concrete was still not workable, but the few specimens that could be produced were used for durability tests (see chapter VI) and the regeneration of cement (see chapter XI). More details on the setting and workability of CRC 3 are found in chapter VII.

Within the course of the project it was decided to produce CRC that fulfilled the requirements of the k-value concept for the use of fly ash in concrete [NBN EN 206-1 (2001)]: CRC1b, CRC1c and CRC2b. This concept enables the replacement of the W/C ratio by W/(C+k·*add*) and the use of pozzolanic or latent-hydraulic additions (*add*) such as fly ash and blast furnace slag are taken into account for the minimum cement content requirement. The k-values vary for the different types of addition and cement used; e.g. fly ash: 0.2 (CEM I 32.5 and CEM III/A) or 0.4 (CEM I 42.5 and higher) and blast furnace slag: 0.9 (CEM I 42.5 and higher). Additionally the replacement levels are limited; e.g. fly ash: FA/C ≤ 0.33 (CEM I) or 0.25 (CEM III/A) and blast furnace slag: BFS/C ≤ 0.45 or 0.20 depending on the exposure class. Finally also the reduction of the minimal cement

Table IV.2 - Overview of the mixture proportions of the different CRCs produced in this study [kg/m³ concrete]

Material	CRC1a	CRC1b	CRC1c	CRC2a	CRC2b	CRC3a	CRC3b
Copper slag 0/4		18	44	33	33		
Limestone sand 0/4 - I	614					611	850
Limestone sand 0/4 - II		769	764	790	844		
Limestone aggregate 2/6	378	313	443	494	361	376	510
Limestone aggregate 6/20	666	605	532	329	410	663	239
Porphyry aggregate 6/20		69					49
Fly ash - I	191			158		144	144
Fly ash - II		100					
Fly ash - III			100		85		
CEM I 52.5 N - I	293	300	300				
CEM I 52.5 N - II							
CEM III/A 42.5 N LA				293	325	261	261
Calcium aluminate cement						45	45
Limestone filler		36	53	50	177	50	50
Calcium sulphate						29	29
Water	180	160	153	180	154	180	180
W/B[a]	0.37	0.40	0.38	0.40	0.38	0.40	0.40
W/C	0.61	0.53	0.51	0.61	0.47	0.59	0.59
W/(C+k·FA)[b]		0.47	0.45	0.45	0.45		

[a] The water to binder ratio with fly ash and the different types of cement considered as binder; [b] The water to cement ratio corrected according to the k-value concept (NBN EN 206-1 (2001)); C_{min} = 340 kg/m³; k = 0.4 (CEM I 52.5 N) or k = 0.2 (CEM III/A 42.5 N LA)

content is limited; e.g. fly ash: $\Delta C < k \cdot (C_{min}-200)$ and blast furnace slag: $\Delta C < k \cdot (C_{min}-175)$. Fulfilling these requirements, the performance regarding strength and durability of the CRC mixtures should be guaranteed.

B.2. Chemical composition

The designed chemical compositions are shown in Table IV.3. The CaO and SiO_2 content vary around 65wt% and 22wt% respectively, which is around average according to literature (see Table II.1). The standard deviation on the designed CaO and SiO_2 contents for the different CRCs is limited to 0.71wt% and 0.74wt% respectively. The chemical compositions differ mostly in their Al_2O_3 and Fe_2O_3 content. Also these values are comparable with those found in literature (see Table II.1). The average values (with their standard deviations) are 5.88(±1.06) wt% and 2.25(±1.06) wt% for Al_2O_3 and Fe_2O_3 respectively. MgO and SO_3 are the most common minor components to be expected in the clinker, with contents of 1.34-2.44 wt% and 0.46-1.69 wt% respectively. The MgO values are high, but do not exceed the maximum MgO content that can be incorporated in the different clinker minerals. The value of 2wt% that can be taken up by the alite phase is however exceeded for CRC2, produced with blast furnace slag cement known for its higher MgO content. SO_3 is known as a mineralizer on the one hand and to stabilize the belite phase on the other hand (see chapter XI).

Regarding the compositional parameters shown in Table IV.3, the values for LSF, SM and HM show a good similarity with values found in literature. Only the LSF for CRC1b is rather low, while the values for SM tend towards the higher limits. In the end the values for AM were a bit too high in the first designs (CRC1a, CRC2a and CRC3). In the following designs (CRC1b and CRC1c and CRC2b) a lower AM was aimed for.

The potential mineralogical compositions calculated using the Bogue formulas are also shown in Table IV.3. Literature values are found in Table II.2. Except the final designs (CRC1c and CRC2b), all CRCs have a rather low alite content, and in consequence a rather high belite content. The amounts of aluminate and ferrite can be considered high and low respectively, but within the range of target values found in literature. For the final CRCs designed in this project (CRC1c and CRC2b), both a higher alite to belite and ferrite to aluminate ratio was aimed for, as seen in Table IV.3.

B.3. Designed versus actual composition

The chemical compositions of the produced clinkers (see chapter XI) were determined and are presented in Table IV.4, together with their compositional parameters and potential mineralogy. The differences between the designed and actual produced clinkers are visualized in Figure IV.1.

Comparing Table IV.3 and Table IV.4 it is seen that the differences between the designed and actual chemical compositions of the CRC clinkers are limited (see also Figure IV.1). Nonetheless, the differences for the potential mineralogy of the major clinker phases, alite and belite, are notable. The magnifying effect of small errors in chemical

composition on the potential mineralogy calculated with the Bogue formulas was already observed by many other authors [Aldridge and Eardley (1973), Commission Chimique du CETIC (1978), Aldridge (1982) and Le Saoût et al. (2011)]. The effect on the aluminate and ferrite phases seems limited. Also the effect on the compositional parameters LSF, SM, AM and HM seems acceptable. For this reason the compositional parameters are considered decisive in the design process, while the Bogue formulas give a rough estimation of the potential mineralogy. The consequences for the actual clinker mineralogy will be handled in detail later (see chapter XI).

Table IV.3 - Overview of the designed chemical compositions of the different CRCs with their compositional parameters and the Bogue formulas

	CRC1a	CRC1b	CRC1c	CRC2a	CRC2b	CRC3a	CRC3b
Chemical composition [wt%]							
CaO	65.1	63.6	65.6	65.3	65.9	65.0	65.1
SiO_2	22.3	23.1	21.2	21.5	20.9	22.1	21.4
Al_2O_3	6.3	5.1	4.5	6.2	4.8	6.9	7.3
Fe_2O_3	1.8	2.4	3.0	2.3	2.4	1.8	1.9
MgO	1.3	1.8	1.7	2.1	2.4	1.9	2.1
Na_2O	0.16	0.34	0.20	0.15	0.18	0.13	0.23
K_2O	0.64	0.89	0.83	0.52	0.73	0.54	0.56
SO_3	0.5	1.7	1.7	1.0	1.7	1.0	0.9
Cl^-		0.01	0.02	0.01		0.01	0.01
Compositional parameters [-]							
LSF	0.93	0.90	1.00	0.97	1.02	0.93	0.93
SM	2.75	3.06	2.81	2.51	2.88	2.53	2.53
AM	3.58	2.11	1.49	2.65	1.99	3.83	3.83
HM	2.14	2.08	2.28	2.18	2.34	2.11	2.11
Bogue formulas [normalized wt%]							
C_3S	53.1	48.7	75.2	60.4	77.7	49.3	53.4
C_2S	26.8	33.5	7.8	19.0	5.2	29.0	23.7
C_3A	14.4	10.0	7.3	13.1	9.3	16.0	16.7
C_4AF	5.6	7.8	9.8	7.5	7.9	5.7	6.2

Table IV.4 – Overview of the actual chemical compositions of the different CRCs with their compositional parameters and the Bogue formulas

	CRC1a	CRC1b	CRC1c	CRC2a	CRC2b	CRC3a	CRC3b
Chemical composition [wt%]							
CaO	65.7	64.7	63.7	63.6	64.8	63.6	63.5
SiO$_2$	22.3	22.8	21.7	21.8	21.0	22.3	21.5
Al$_2$O$_3$	6.1	5.1	4.8	6.3	4.9	6.5	7.0
Fe$_2$O$_3$	1.5	2.4	3.3	2.6	2.5	1.5	1.6
MgO	1.4	1.8	1.8	2.5	2.4	2.4	2.5
Na$_2$O		0.26	0.13		0.11		
K$_2$O		0.52	0.21		0.20		
SO$_3$	1.0[a]	1.1	0.7	1.1[a]	0.7	2.1[a]	1.9[a]
Cl$^-$	0.002	<0.005	<0.005	0.004	<0.005	0.002	0.002
*AT**	*XRF*	*ICP*	*ICP*	*XRF*	*ICP*	*XRF*	*XRF*
Compositional parameters [-]							
LSF	0.94	0.92	0.95	0.93	1.00	0.91	0.94
SM	2.97	3.03	2.68	2.44	2.85	2.79	2.50
AM	4.12	2.12	1.45	2.44	1.94	4.33	4.36
HM	2.20	2.13	2.14	2.07	2.28	2.10	2.11
Bogue formulas [normalized wt%]							
C$_3$S	62.8	61.0	64.7	57.4	71.1	55.4	57.4
C$_2$S	16.6	19.3	16.0	17.7	11.9	20.2	17.0
C$_3$A	15.5	11.1	8.0	15.2	9.1	18.6	19.6
C$_4$AF	5.1	8.6	11.3	9.7	8.0	5.8	6.1

*the used analysis technique: X-ray fluorescence spectrometry (XRF) or inductively coupled plasma mass spectrometry (ICP)
[a] according to NBN EN 196-2 (2005)
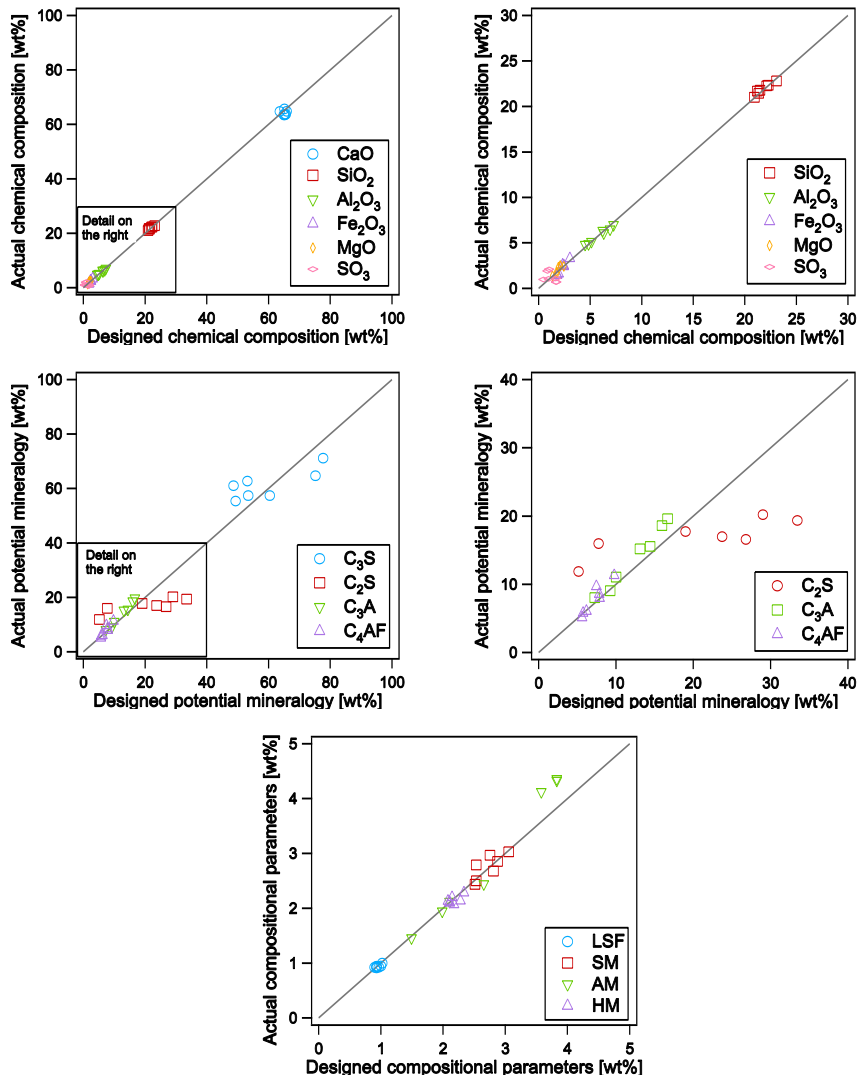
Figure IV.1 - Visualization of the differences between the designed and actual produced clinkers regarding the chemical composition (top), the mineralogical composition (middle) and the compositional parameters (bottom)

References

Aldridge, L. P. (1982). "Accuracy and precision of phase analysis in portland cement by Bogue, microscopic and X-ray diffraction methods." Cement and Concrete Research 12(3): 381-398.

Aldridge, L. P. and R. P. Eardley (1973). "Effects of analytical errorrs on the Bogue calculation of compound composition." Cement Technology 4(5): 177-182.

BBG (2006). Betontechnologie, De Belgische BetonGroepering.

Binici, H., I. H. Cagatay, T. Shah and S. Kapur (2008). "Mineralogy of plain Portland and blended cement pastes." Building and Environment 43(7): 1318-1325.

Blatt, H. and R. J. Tracy (1997). Petrology. New York.

Commission Chimique du CETIC (1978). "Détermination de la composition minéralogique du clinker par analyse microscopique et dissolution sélective des phases." Ciments Bétons Platres Chaux(4/78 (713)): 205-210.

Galbenis, C.-T. and S. Tsimas (2006). "Use of construction and demolition wastes as raw materials in cement clinker production." China Particuology 4(2): 83-85.

Herfort, D., G. K. Moir, V. Johansen, F. Sorrentino and H. B. Arceo (2010). "The chemistry of Portland cement clinker." Advances in Cement Research 22(4): 187-194.

Hewlett, P. C. (1998). Lea's Chemistry of Cement and Concrete (Fourth Edition). Oxford, Butterworth-Heinemann.

Huntzinger, D. N. and T. D. Eatmon (2009). "A life-cycle assessment of Portland cement manufacturing: comparing the traditional process with alternative technologies." Journal of Cleaner Production 17(7): 668-675.

Kakali, G., S. Tsivilis, K. Kolovos, K. Choupa, T. Perraki, M. Perraki, M. Stamatakis and Vasilatos (2003). "Use of secondary mineralizing raw materials in cement production. The case study of a stibnite ore." Materials Letters 57(20): 3117-3123.

Le Saoût, G., V. Kocaba and K. Scrivener (2011). "Application of the Rietveld method to the analysis of anhydrous cement." Cement and Concrete Research 41(2): 133-148.

Morsli, K., Á. G. de la Torre, M. Zahir and M. A. G. Aranda (2007). "Mineralogical phase analysis of alkali and sulfate bearing belite rich laboratory clinkers." Cement and Concrete Research 37(5): 639-646.

Odler, I., S. Abdulmaula, P. Nudling and T. Richter (1981). "Mineralogical and oxidic composition of industrial Portland-cement clinkers." Zement-Kalk-Gips 34(9): 445-449.

Puertas, F., I. García-Díaz, A. Barba, M. F. Gazulla, M. Palacios, M. P. Gómez and S. Martínez-Ramírez (2008). "Ceramic wastes as alternative raw materials for Portland cement clinker production." Cement and Concrete Composites 30(9): 798-805.

Scrivener, K. L., J.-L. Cabiron and R. Letourneux (1999). "High-performance concretes from calcium aluminate cements." Cement and Concrete Research 29(8): 1215-1223.

Shi, C., C. Meyer and A. Behnood (2008). "Utilization of copper slag in cement and concrete." Resources, Conservation and Recycling 52(10): 1115-1120.

Staněk, T. and P. Sulovský (2002). "The influence of the alite polymorphism on the strength of the Portland cement." Cement and Concrete Research 32(7): 1169-1175.

Stephan, D. and S. Wistuba (2006). "Crystal structure refinement and hydration behaviour of $3CaO \cdot SiO_2$ solid solutions with MgO, Al_2O_3 and Fe_2O_3." Journal of the European Ceramic Society 26(1-2): 141-148.

Stutzman, P., A. Heckert, A. Tebbe and S. Leigh (2014). "Uncertainty in Bogue-calculated phase composition of hydraulic cements." Cement and Concrete Research 61–62(0): 40-48.

Taerwe, L. and G. De Schutter (2006). Betontechnologie (Syllabus Concrete Technology), Ghent University.

Taylor, H. F. W. (1997). Cement Chemistry. London, Thomas Telford Publishing.

PART II
CRC Quality & Durability

V - Experimental procedures

The CRC concrete compositions designed in the previous part of this thesis should of course result in a concrete with good performance regarding workability, strength and durability. Different CRC compositions were tested regarding their compressive strength and resistance against carbonation, chloride penetration and freeze-thaw attack with de-icing agents. Furthermore the use of blast furnace slag cement in combination with calcium aluminate cement and the use of copper slag in concrete were the topic of additional studies. Hereafter the experimental procedures are discussed. The isothermal calorimetry, used for measuring the hydration heat in chapter VII and VIII, is described in chapter X. In the next chapters of this part the results of the different studies are presented and discussed.

A. Production of concrete

A.1. Reference concrete mixtures

To be able to evaluate the quality and durability performance of CRC concrete mixtures, reference mixtures were designed, produced and tested. These reference mixtures are designed according to the exposure classes and their corresponding concrete types defined in NBN EN 206-1 (2000) and NBN B 15-001 (2004). Three mixtures were produced as reference for the environmental classes XC4 (carbonation induced corrosion in a cyclic wet and dry environment), XS3 (chloride induced corrosion from sea water in tidal, splash and spray zones) or XF4 (freeze-thaw attack with high water saturation and de-icing agent or sea water), respectively T(0.50), T(0.45) and T(0.45)[A]. All these reference mixtures are produced with a CEM I 52.5 N as only binder. The water to cement ratio is mentioned between parentheses and the use of an air entraining agent is indicated by the capital A in superscript. A small letter after the mixture names indicates the different batches produced. For the different batches, different sand, aggregate and cement batches were used. The partitioning of the sand and the aggregates, which was set by aiming for the ideal curve of Fuller using the least squares method [Taerwe and De Schutter (2006)], was affected by the slightly changed particle size distributions for the different batches. The mixture proportions of the produced concretes are presented in Table V.1.

A.2. Production and curing of mortar and concrete samples

All concrete and mortar specimens were produced according to NBN B 15-001 (2004) and NBN EN 196-1 (2005), respectively. When applicable, superplasticizer was added without interrupting the mixing process, and mixing continued for an additional 2 minutes. If an air entraining agent was used, it was added together with the mixing water. Both concrete and mortar samples were stored in a climate chamber at 20±2 °C and RH >95% until testing.

Table V.1 - Overview of the reference concrete mixtures [kg/m³]

Material	T(0.50)	T(0.45)a	T(0.45)b	T(0.45)ᴬ
Siliceous sand 0/4	714	715	762	715
Gravel 2/8	515	515	450	515
Gravel 8/16	671	671	741	671
CEM I 52.5 N	320	340	340	340
Water	160	153	153	153
AEAᵃ				2
SPᵇ		5		5

[a] AEA = air entraining agent, Micro-Air 103 con. 4% (BASF), [mL/kg cement]
[b] SP = superplasticizer, Glenium 51 con. 35% (BASF), [mL/kg cement]

B. Applied test methods

B.1. Standard properties of mortar and concrete

i. Workability

The workability of fresh mortars was evaluated by determining their slump and flow about 20 minutes after mixing. The procedure to determine the flow is described in NBN EN 413-2 (2005). The slump was measured with a mini cone, which is similar to the Abrams cone for slump measurements of concrete [Schwartzentruber and Chatherine (2000)]. For the concrete mixtures the slump was determined according to NBN EN 12350-2 (1999). For CRC2, a self-compacting concrete, the slump flow was measured according to NBN EN 12350-8 (2010).

ii. Air content

The air content was measured according to NBN EN 12350-7 (2000). During the test also the density of the fresh concrete is quantified.

iii. Compressive strength

Compressive strength tests on mortar specimens (160x40x40 mm³) were performed according to NBN EN 196-1 (2005). Concrete cubes (150x150x150 mm³) were tested for their compressive strength according to NBN EN 12390-1 (2001).

B.2. Setting time

Ultrasonic p-wave transmission measurements were performed on concrete and mortar samples when studying the setting of CRC3 combining BFSC and CAC (see chapter VII). The FreshCon system developed at the University of Stuttgart [Reinhardt and Grosse (2004)] was used for this purpose (see Figure V.1). More details on the used test setup and conditions can be found elsewhere [Robeyst et al. (2008); Robeyst (2010)]. The FreshCon system also measures the frequency content of the received ultrasonic signals, but in this study the velocity and energy curves were considered for determining the

initial and final setting of the mixtures. From the velocity curves, the initial setting time was determined by its inflection point [Voigt et al. (2005); Robeyst (2010)]. The final setting time was set as the point at which the derivative of the velocity curve decreased to 20% of its maximum value [Robeyst (2010)]. For deducting the initial setting times from the energy curves the thresholds E/E_{ref} = 0.01 and 0.02 were used for concrete and mortar respectively [Robeyst (2010)]. Likewise the values E/E_{ref} = 0.07 and 0.13 were used to determine the final setting times for concrete and mortar samples. For the CRC mixtures, the setting behaviour was also monitored more traditionally using the Vicat needle, for which cement pastes were produced with a standard consistency [NBN EN 196-3 (2005)].
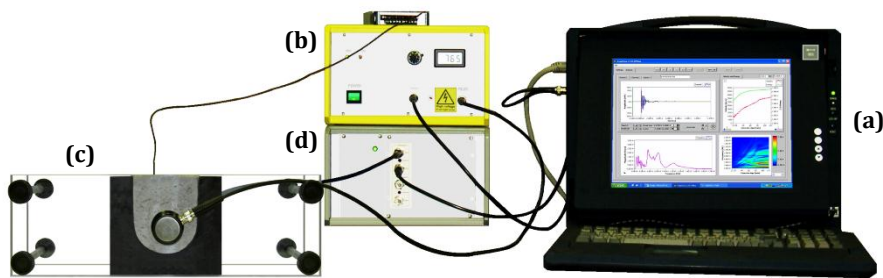
Figure V.1 – FreshCon measurement set-up: (a) computer with DAQ card, (b) amplifier, (c) container with piezoelectric sensor and (d) preamplifier [Robeyst (2010)]

B.3. Open porosity and gas permeability

Regarding durability, the accessibility of concrete to aggressive substances is a major issue. Important concrete characteristics regarding the ability of these substances to penetrate into concrete are its open porosity (a measure of the pores accessible to liquids) and gas permeability (a measure of the accessibility to gases). Both were determined for concrete with copper slag and reference T(045)b at a curing age of 1 month.

The open porosity of the concrete specimens (drilled cores d = 100 mm, h = 50 mm) was determined using the vacuum absorption test described in NBN B 05-201 (1976). After drying and weighing the samples (w_d [kg]), they were put under vacuum (2.7 kPa) for 3 h. Subsequently, the tank was filled with water and the samples were stored under water for 24 h. Finally the mass of the specimens was determined in air (w_a [kg]) and water (w_w [kg]). The porosity φ [vol%] of the sample could then be determined by calculating the volume of the pores filled with water:

$$\varphi = \frac{V_{water}}{V_{concrete}} = \frac{\dfrac{w_a - w_d}{\rho_{water}}}{\dfrac{w_d}{\rho_{concrete}}} = \frac{w_a - w_d}{w_a - w_w} \qquad (V\text{-}1)$$

with V_{water} and $V_{concrete}$ respectively the water and concrete volume [m³] and ρ_{water} and $\rho_{concrete}$ respectively the water and concrete density [kg/m³]. The samples were dried at 40 °C and 105 °C to estimate the capillary porosity and the total (capillary and gel) porosity respectively.

A gas permeability test was conducted on concrete cores (d = 150mm, h = 50mm) as described in the recommendation RILEM TC 116-PCD (1999) using a CEMBUREAU permeameter (see Figure V.2). After being saturated in water, the concrete specimens were dried at 40 °C until a constant weight was obtained (mass change < 0.05 wt% over 24h). The test specimens had a saturation degree of 42.0±0.69 wt%. During the measurement, the concrete specimens were placed in the permeameter cells as such that the oxygen gas was prevented from leaking. The first gas pressure was set at 2 bar and the flow rate was measured using the soap bubble flow meter when a steady-state regime was established (after about 30 minutes). Subsequently the measurement was repeated for gas pressures of 3 and 4 bar. The measurements were then redone for all concrete specimens after drying at 105 °C (saturation degree is nihil). The gas permeability coefficient K [m²] is calculated according to the following formula:

$$K = \frac{2 \cdot P_a \cdot Q \cdot h \cdot \eta}{A \cdot (P^2 - P_a^2)} \tag{V-2}$$

with P_a (101300 N/m²) the atmospheric pressure, Q [m³/s] the measured flow rate, h (0.05 m) the specimen height, A ($\pi \cdot (0.075m)^2$) the cross-sectional area, η ($2.02 \cdot 10^{-5}$ N·s/m²) the dynamic viscosity of oxygen gas and P [N/m²] the applied pressure.
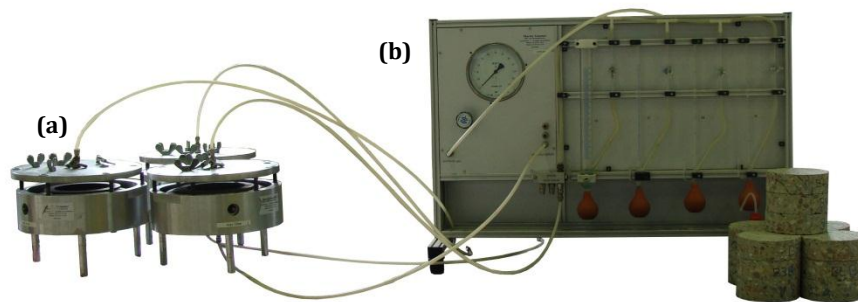
Figure V.2 - CEMBUREAU permeameter test set-up:
(a) permeameter cells and (b) bubble flow meter

B.4. Resistance against carbonation

The mechanism of carbonation consists of gaseous diffusion combined with chemical reaction. The carbonation reaction of CO_2 from the atmosphere with $Ca(OH)_2$, a cement

hydration product which buffers the pH, plays the most important role in the de-passivation phenomenon causing rebar corrosion [Sisomphon and Franke (2007)]. Pozzolanic materials, such as fly ash, are known to reduce the carbonation resistance of concrete. On the one hand, the quantity of $Ca(OH)_2$ will be significantly reduced since there is less cement present and the pozzolanic fly ash reaction consumes $Ca(OH)_2$. On the other hand, the slow rate of the pozzolanic reaction results in a higher porosity at early age, although a reduced porosity may be expected at later age. Since it is not clear which mechanism prevails, the carbonation resistance of e.g. CRC containing fly ash should be verified.

For this purpose, an accelerated carbonation test was performed by placing concrete cubes (100x100x100 mm^3) in a climate chamber (20±2 °C, RH 60±5%, 10 vol% CO_2). Five surfaces of each concrete cube were coated using an epoxy resin to ensure a unidirectional CO_2 ingress. Different exposure regimes were imposed during the course of the project. At first the most severe exposure class concerning carbonation according to NBN EN 206-1 (2000), namely a cyclic wet and dry environment (XC4) was simulated. The specimens were successively placed under water for one week and in the climate chamber for the other week. After every 2 cycles (2 weeks under water and 2 weeks in the climate room), the carbonation ingress was measured with phenolphthalein. The non-carbonated zone with a pH >9 will get a pink/purple colour, while the carbonated zones with a lower pH will show no colour change. The distance of the colour boundary from the exposed surface is measured every 10 mm, and the average result will be used as the carbonation depth. Later on the XC3 environment with moderate humidity (60±5%) was simulated and the specimens were placed in the climate chamber until measurement of the carbonation ingress by the phenolphthalein method. The sections needed to measure the carbonation ingress were obtained by sawing slices of the concrete cubes, or by splitting them in half. An overview of the experimental procedure for each concrete mixture is given in Table V.2.

**Table V.2 - Overview of the experimental procedures
for testing the resistance against carbonation**

Concrete mixtures	Exposed environment	Measurement surface	Curing age(s)	Exposure times
T(0.50), CRC1a, CRC2a, CRC3	Cyclic wet/dry	Sawn	1 month 3 months	4 weeks 8 weeks 12 weeks
T(0.45)b, concrete with copper slag	dry	Sawn	1 month	4 weeks 8 weeks 12 weeks
CRC1c, CRC2b	dry	Split	2 months 4 months 1 year	± 4 weeks ± 8 weeks ± 12 weeks

B.5. Resistance against chloride ingress

Rebar corrosion can not only be initiated by carbonation of the concrete, but also by the ingress of chlorides. These chlorides can be available in one of the concrete raw materials, e.g. cement. For this reason a maximum chloride content is prescribed for concrete raw materials. Another possibility is the ingress of chlorides in concrete by diffusion of a chloride containing fluid through its capillary pores. Also here, the corrosion will only be initiated if the chloride penetration front reaches the concrete reinforcement. To assess the resistance against the ingress of chlorides three different methods were used. An overview of the experimental procedure used for the different concrete mixtures is given in Table V.3.

Table V.3 - Overview of the experimental procedures
for testing the resistance against the ingress of chlorides

Concrete mixtures	Test method	Curing age(s)	Exposure times
T(0.45)a, CRC1a, CRC2a, CRC3	Simulation of a tidal zone	1 month 3 months	3 weeks 6 weeks 10 weeks
T(0.45)b, concrete with copper slag	Chloride migration	1 month	24 hours
T(0.45)a, CRC1c, CRC2b	Chloride diffusion	1 months 3 months 1 year	9 weeks

A first test simulates a tidal zone by putting cylindrical specimens (d = 230 mm, h = 70 mm) on a rotating horizontal shaft. In one hour, the specimens rotate one time around their axis. The lower part of the specimens are immersed in a salt solution (NaCl, 3.5 wt%). The TAP apparatus used for this test was developed at the Magnel Laboratory for Concrete Research by De Belie et al. (2002) (see Figure V.3 - left). After three, six and ten weeks, the chloride ingress x_t [mm] is measured by sprinkling a 0.1 mol/l $AgNO_3$ solution on six cross sections. The area containing the chlorides is indicated by a white precipitate that is formed due to the reaction of the silver and chloride ions to form silver chloride. The cross sections are produced by splitting the specimens into three likewise parts.

The resistance against the migration of chlorides can also be evaluated by a CTH test, described in NT Build 492 (1999) (see Figure V.3 – right). Before starting the actual test, the drilled cores (d = 100 mm, h = 50 mm) are vacuum saturated by a $Ca(OH)_2$ solution (4g/l). For actual testing, an external electrical potential is applied axially across the specimen to force chloride ions outside to migrate into the specimen. After a certain test duration (mostly 24h), again a silver nitrate solution is sprayed on to freshly split

sections and the chloride penetration depth x_m [m] is measured. From these results a non-steady-state migration coefficient D [10^{-12} m^2/s] can be calculated:

$$D = \frac{0.0239 \cdot (273 + T) \cdot L}{(U - 2) \cdot t} \left(x_m - 0.0238 \sqrt{\frac{(273 + T) \cdot L \cdot x_m}{U - 2}} \right) \qquad (V\text{-}3)$$

with U [V] the absolute value of the applied voltage, T [°C] the average value of the initial and final temperatures in the anolyte solution, L [mm] the thickness of the specimen, and t [h] the test duration.
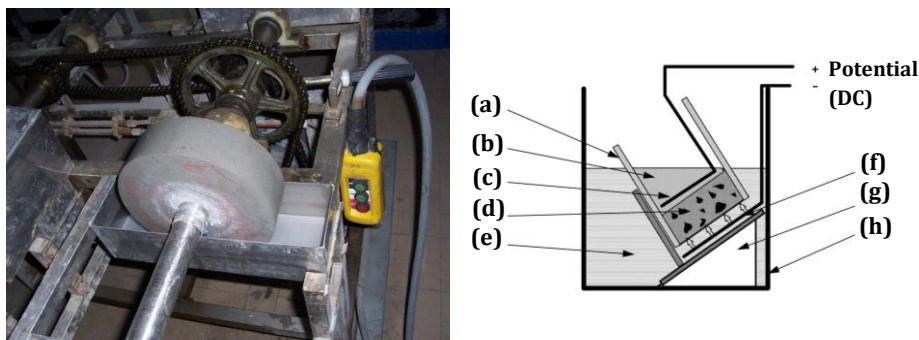
Figure V.3– *left:* The apparatus used for cycling immersion. TAP - 'Toestel voor versnelde AantastingsProeven' (Apparatus for accelerated Deterioration tests) *right:* CTH test-setup [NT Build 492 (1999)]: (a) rubber sleeve, (b) anolyte, (c) anode, (d) specimen, (e) catholyte, (f) cathode, (g) plastic support and (h) plastic box

Finally, the resistance against the penetration of chlorides can also be evaluated by an accelerated chloride diffusion test, based on NT Build 443 (1995). In preparation of the exposure to a chloride solution, the concrete specimen (a drilled core with d = 100 mm, h = 100 mm) was immersed in a saturated Ca(OH)$_2$ solution (4 g/l) until a constant weight is obtained (mass change < 0.1 wt% over 24h). Subsequently all faces of the concrete core are coated, except the exposure surface, which is a sawn surface 10 mm from the casting surface. After hardening of the coating, the specimens are again immersed in the Ca(OH)$_2$ solution until constant weight. Finally the samples are exposed to chlorides by immersion in a NaCl solution (165 g/l). After 63 days of exposure, the concrete core is split and a silver nitrate solution is sprayed on to the obtained sections and the chloride penetration depth x_d [mm] is measured.

B.6. Resistance against freeze-thaw attack with de-icing agents

Due to freeze-thaw cycles with de-icing agents, scaling can occur on concrete surfaces and material will be lost due to local flaking or peeling. This scaling alone does not pose a significant threat to the mechanical integrity of the concrete structure, but it is aesthetically undesirable. The resistance against freeze-thaw attack with de-icing agents

was tested according to appendix D of NBN EN 1339 (2003). A concrete test specimen (drilled core d=100mm, h=50mm) with a salt solution (NaCl, 3 wt%) on top was subjected to 28 freeze-thaw cycles (see Figure V.4). After every 7 cycles, the scaled material was collected, dried for at least 24h at 105±5 °C and weighed. This test was conducted on CRC1a, CRC2a, CRC3b and T(0.45)[A] at a curing age of 1 and 3 months and on the concrete mixtures with copper slag and T(0.45)b at a curing age of 1 month.
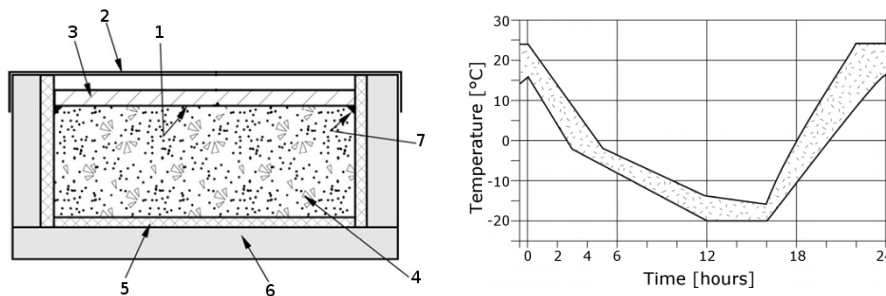
Figure V.4 – *left:* Test specimen for freeze-thaw attack with de-icing agents: (1) test surface, (2) cover of the test surface, (3) salt solution (NaCl, 3%), (4) concrete specimen, (5) PVC encapsulation, (6) thermal insulation, (7) sealing *right:* One time-temperature cycle for freeze-thaw attack with de-icing agents [NBN EN 1339 (2003)]

B.7. Statistical analysis

The software package SPSS Statistics was used for statistical analysis of the results. Analysis of variance (ANOVA) was used for comparison of mean values. The Tukey and Dunnett method were applied for post hoc testing when equal variances are respectively assumed or not assumed. An independent T-test was used when only two mean values were compared. For all tests a significance level of 0.05 was used.

VI - Strength and durability of CRC

In order to apply CRC at the same level of traditional concrete, it is inherent that its performance regarding workability, strength and durability should be of the same level. For this reason, different CRC compositions were tested for their strength and resistance against carbonation, chloride penetration and freeze-thaw attack with de-icing agents. In the previous chapter, the experimental procedures were introduced. In this chapter, the results will be presented and discussed. The concrete compositions of CRC and traditional concrete can be found respectively in Table IV.2 and Table V.1. Results of this chapter have been published in De Schepper et al. (2011).

A. Results

A.1. Standard properties of CRC

An overview of the standard properties of the CRC and reference mixtures is given in Table VI.1. As the water to binder and water to cement ratio are important factors regarding workability and strength, these values are also given.

Regarding workability CRC1 and CRC3 are aimed to be comparable to the reference concrete, which was for both measured by a slump test. It is seen that most mixtures have slump class S2. For T(0.50) this result was obtained due to a higher water to binder ratio, for CRC1 and the other reference mixtures, except T(045)b, a superplasticizer (SP) was used to improve the workability. The lower slump class S1 for T(0.45)b was a result of the decision to not use any SP. This not only had a consequence for the workability, but also for the strength. T(0.45)a and T (0.45)b have an average 28 days strength of 69.3±0.80 and 56.9±0.98 N/mm² respectively. The lower workability of CRC3 (slump class S1) is caused by combining blast furnace slag cement with calcium aluminate cement, what resulted in a very fast setting. More about this can be found in chapter VII.

Through the application of a high content of limestone filler in CRC2, a self-compacting concrete was aimed for. The quality of this self-compacting CRC2 was not studied in detail, and only the slump flow was measured as an indication. CRC2a had the slump flow class SF1. By increasing the amount of SP, the slump flow increased slightly whereby it could be categorized in the slump flow class SF2. Comparing the obtained values with the results in Desnerck (2011), which vary between 640 and 830 mm, this value is rather low. To obtain a CRC with better self-compacting properties, the composition should be optimized. This was however not the main goal of this research and a detailed study of this aspect was not conducted.

The lowest air contents were obtained for those concrete mixtures without air entraining agent (AEA), varying between 1.1 and 2.8% (CRC1c, CRC2b, T(0.50) and T(0.45)). For the mixtures with AEAs, the air content was higher and varied between 3.9 and 6.6% (CRC1a, CRC3 and T(0.45)[A]). On the one hand a variation on the results is expected due to variations characteristic for the applied test method. On the other hand

Table VI.1 - Overview of the fresh properties and compressive strength of CRC and reference mixtures

	CRC1a	CRC1c	CRC2a	CRC2b	CRC3a	CRC3b	T(0.50)	T(0.45)a	T(0.45)b	T(0.45)^A
W/B^a	0.37	0.38	0.40	0.38	0.40	0.40		0.45	0.45	0.45
W/C	0.61	0.51	0.61	0.47	0.59	0.59	0.50	0.45	0.45	0.45
W/(C+k·FA)^b	0.45	0.45		0.45						
Fresh concrete properties										
SP^c [mL/kg binder]	5	10	9	17	7	8		5	5	5
Slump [mm] (class)	70 (S2)	60 (S2)			30 (S1)	10 (S1)	70 (S2)	60 (S2)	10 (S1)	80 (S2)
Slump flow [mm] (class)			620 (SF1)	670 (SF2)						
AEA^d [mL/kg binder]	2		2		2	3				2
Air content [%]	4.0	1.1	6.6	1.8	3.9	4.4	2.6	2.8	2.1	6.0
Density [kg/m^3]	2319	2425	2238	2381	2313	2313	2369	2400	2406	2281
Compressive strength [N/mm^2]										
28 days	60.4^{B,C} (1.00)	65.1^{C,D} (1.40)	52.7^A (0.82)	84.2 (2.04)	59.6^B (0.88)	59.1^B (1.19)	57.8^{A,B} (0.28)	69.3^D (0.80)	56.9^{A,B} (0.98)	53.4^A (0.40)
3 months	72.9^{F,G} (0.26)	78.8^G (1.69)	59.3^E (0.86)	93.6 (0.24)	65.2^E (1.33)	61.3^E (1.63)	64.6^E (0.69)	72.6^F (0.41)	63.9^E (1.14)	59.6^E (1.99)
Strength class	C45/55	C50/60	C40/50	C60/75	C45/55	C45/55	C45/55	C55/67	C40/50	C40/50

^{a} The water to binder ratio with fly ash and the different types of cement considered as binder
^{b} The water to cement ratio corrected according to the k-value concept (NBN EN 206-1 (2001)) when applicable; C_{min} = 340 kg/m^3, k = 0.4 (CEM I 52.5 N)
or k = 0.2 (CEM III/A 42.5 N LA)
^{c} SP = superplasticizer, Glenium 51 con. 35% (BASF)
^{d} AEA = air entraining agent, Micro-Air 103 con. 4% (BASF)
A capital superscript denotes the groups for which the mean values do not differ significantly

also the composition of the concrete will have its effect. For example, the performance of AEAs will be affected by the presence of fly ash [Baltrus and LaCount (2001); Van den Heede et al. (2013)].

The compressive strength of concrete is influenced by many factors, such as water to binder and water to cement ratio, binder and cement content, workability, air content, the use of secondary cementitious materials (including fly ash, natural pozzolana, blast furnace slag, and silica fume), curing time etc.

While CRC2b has the highest compressive strength (28d) (significantly higher compared to all other mixtures), the lowest value was measured for CRC2a. Looking at the binder content, the one of CRC2a is higher, but it contains less cement and more fly ash. And although the water to binder ratio is comparable, it is only CRC2b that fulfils the requirements of the k-value concept according to NBN EN 206-1 (2001). Another possible explanation for the lower strength of CRC2a is its high air content (6.6% compared to 1.8% for CRC2b), as a result of the addition of an AEA. While the workability is only slightly higher, another property that works to the advance of the high compressive strength of CRC2b is a better packing due to a higher powder content. For 1m^3 concrete 177 kg lime stone filler was added, compared to 50 kg for CRC2a.

The compressive strength (28d) of CRC2a is not significantly different from the reference mixtures T(0.45)[A], T(0.45)b and T(0.50). T(0.45)[A] is a reference mixture with the lowest compressive strength, which also has the highest air content (6% compared to 2.6, 2.8 and 2.1% for respectively T(0.50), T(0.45)a and T(0.45)b). T(0.50) has a higher water to cement ratio and lower cement content, which are parameters known to result in lower compressive strength. This is however not true for T(0.45)a. The only difference between T(0.45)a and T(0.45)b is its workability, due to absence of a SP. This proves how workability can affect the strength of concrete.

While the results of CRC2a and CRC2b differ significantly, the results for CRC1a and CRC1c and CRC3a and CRC3b are similar (no significant difference). Compared to T(0.50) and T(0.45)b, CRC1a and CRC3 have similar compressive strengths (28d). While CRC1c has no significant difference with T(0.45)a. As mentioned earlier, the workability of CRC3 was rather low, due to a fast setting of the concrete as blast furnace slag cement and calcium aluminate cement were combined. Of course also its specific combination of binders (32% FA, 58% BFSC and 10% CAC) will influence the strength development.

At the age of 3 months, roughly the same conclusions as for 28 days can be made regarding the compressive strength. For the concrete mixtures with the lower compressive strengths, the differences become smaller, and no significant differences were noticed for CRC2a, CRC3 and all reference mixtures but T(0.45)a. The mean value for T(0.45)a became lower compared to CRC1, but not significantly for CRC1a. Probably the CRC1 mixtures benefit from the pozzolanic reaction of the fly ash at later age. The difference between CRC1a and CRC1c is not significant. Again, CRC2b performed significantly better compared to all the other concrete mixtures. Due to the good

performance regarding compressive strength of CRC2b (28 days and 3 months), it can be considered as a high strength concrete.

A.2. Resistance against carbonation

For evaluation of the carbonation resistance of CRC1a, CRC2a and CRC3b, a cyclic wet and dry environment was simulated. During the drying period the specimens were put in a climate chamber with high CO_2 concentration (10 vol%), while the samples were immersed in water during the wet period. An overview of the measured carbonation depths is given in Table VI.2. The results of the reference mixtures will not be discussed since no carbonation was observed during the time frame of the test.

Table VI.2 – Overview of the carbonation depths [mm] of CRC1a, CRC2a and CRC3b after 1 month or 3 months curing and an exposure time of 4, 8 or 12 weeks (for a cyclic wet and dry environment)

Exposure time	CRC1a		CRC2a		CRC3b	
	1 month curing	3 months curing	1 month curing	3 months curing	1 month curing	3 months curing
4 weeks	1.48[C,G] (0.10)	1.27[D,G] (0.11)	5.18 (0.13)	2.24 (0.17)	4.21 (0.19)	1.76 (0.11)
8 weeks	1.73[C,H] (0.21)	1.30[D,H] (0.11)	6.18[A] (0.22)	4.21[B,E] (0.22)	5.55[A,F] (0.27)	3.85[B] (0.18)
12 weeks	1.70[C,I] (0.08)	1.33[D,I] (0.18)	7.58 (0.29)	4.55[E] (0.17)	6.27[F,J] (0.26)	5.42[J] (0.36)

[x] by a capital superscript the groups are indicated for which the mean values do not differ significantly (ANOVA or independent T-test)

Looking at the results presented in Table VI.2, it is seen that CRC1a performs best regarding the resistance against carbonation. The carbonation depth does not even increase significantly in time. Compared to CRC1a, CRC2a and CRC3b have significantly higher carbonation depts. The difference between CRC2a and CRC3b is rather small. After eight weeks of curing, the difference between both mixtures is not significant, for both curing ages. Except for CRC2a (3 months curing) and CRC3b (1 month curing) between 8 weeks and 12 weeks, the increase of the carbonation depth is significant for CRC2a and CRC3b.

Looking at the effect of curing age onto the carbonation depth in time, it is seen that there is no difference for CRC1a. For the other mixtures there is a significant effect of the curing time, except for CRC3b after an exposure time of 12 weeks. The positive effect of a longer curing time on the rate of carbonation is possibly caused by the slow pozzolanic reaction, decreasing the porosity between one and three months, hindering the diffusion of CO_2 in the concrete samples.

The rate of carbonation also decreases in function of time, and is usually considered proportional to the square root of the exposure period. According to this theory, the

depth of carbonation x [mm] can be considered to be related to the exposure duration t [weeks], in accordance with the second law of Fick as shown in the following equation:

$$x = k\sqrt{t} \qquad\qquad\qquad \text{(VI-4)}$$

with k [mm/$\sqrt{\text{week}}$] the carbonation coefficient. This formula is based on a steady-state condition, with a constant carbonation coefficient. However, in reality, the carbonation itself blocks the air pores in concrete, and causes a reduction in gas diffusivity. For this reason, the carbonation coefficient should decrease with time. Simplifying the relation by still keeping k as a constant, the relation of the carbonation rate with respect to time can be written as follows:

$$x = k \cdot t^n \qquad\qquad\qquad \text{(VI-5)}$$

where n is the exponent value which is less than 0.5. The empirical exponent n was chosen to be 0.4 according to Sisomphon and Franke (2007).

In Figure VI.1, the carbonation depths are presented, together with the linear regression for determining the carbonation coefficient. In the different graphs, the formula for the carbonation depths with k and its standard error on the mean value is given together with the R^2 value. As for the results in Table VI.2, it is confirmed that the carbonation rate is higher for CRC2a and CRC3b, and an increase of the curing time has a positive effect resulting in lower carbonation coefficients. These k values will be used to calculate the service life of reinforced concrete exposed to CO_2 in chapter XIII.

The resistance to carbonation of CRC1c and CRC 2b was tested by placing the specimens in the carbonation chamber (CO_2 concentration of 10 vol%) during the whole exposure period. In Table VI.3 the measured carbonation depths are presented.

While CRC1a performed better compared to CRC2a, it seems that the opposite is true for the final batches produced (CRC1c versus CRC2b). However, care should be taken to quantitatively compare the results in Table VI.2 and Table VI.3 as different environments were studied. Tentatively, one could say that it seems that the dry environment results in higher carbonation coefficients. This difference can be explained as a result of a reduced exposure to CO_2 in the wet and dry environment as half of the time the specimen is stored in water and the pores are not accessible for CO_2. Also, at the start of the drying period, the water still hinders the ingress of CO_2, and the exposure will only start when the specimen is drying. Due to the unknown length of the drying period, it is not possible to exclude the wet period from the exposure time.

Focussing at the exposure time for CRC1c and CRC2b after different curing times, it is seen that the effect of the exposure time is not always significant, although the carbonation depth is expected to increase (significantly) with longer exposure times. One could attribute this to the variation on the exposure times, but it is not always the case that the lowest difference in exposure time leads to a non-significant difference.
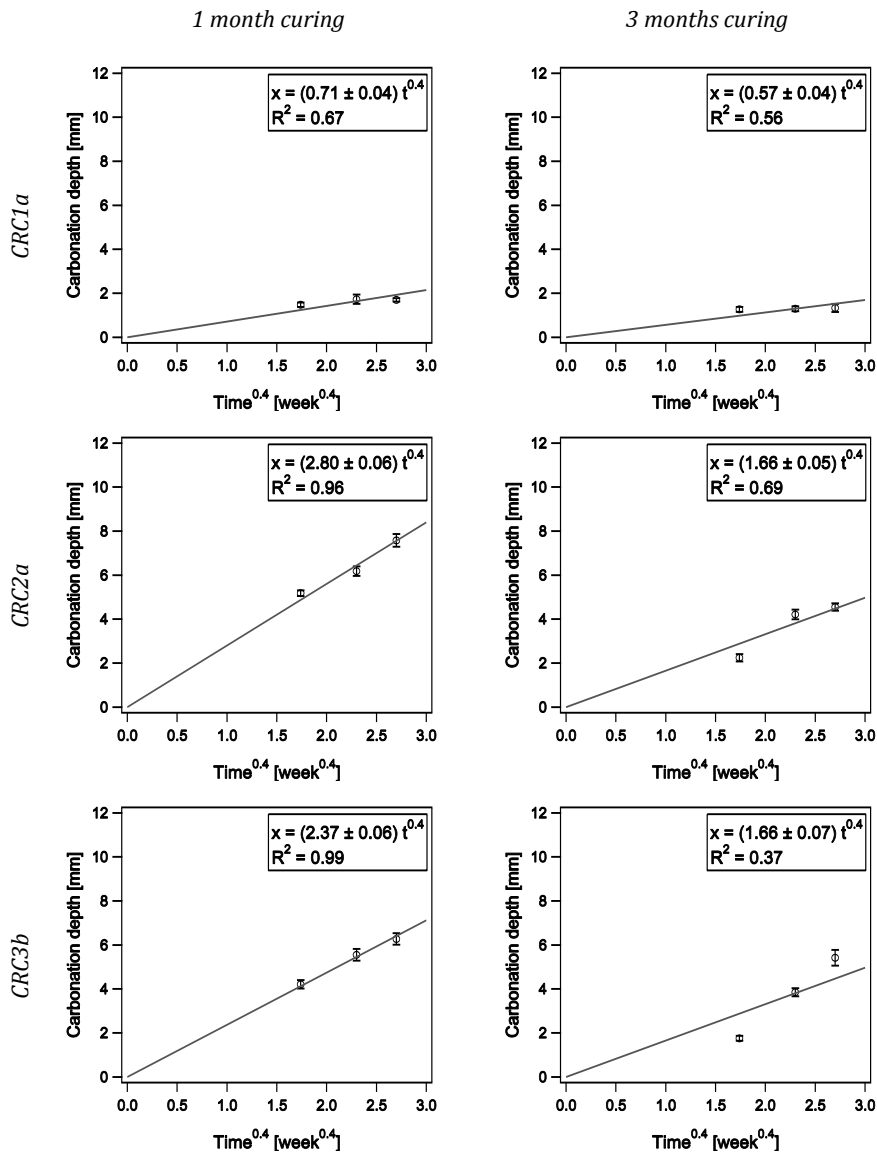
Figure VI.1 – Overview of the carbonation depths of CRC1a (top), CRC2a (middle) and CRC3b (bottom) after a curing time of 1 month (left) and 3 months (right). The mean values are plotted together with their standard error. The dark grey line plots the result of a linear regression used to determine the carbonation coefficient k, whereby no constant was included in the equation.

R^2 was calculated as followed: $\frac{\sum(\hat{x}-\bar{x})^2}{\sum(\hat{x}-\bar{x})^2+\sum(x-\hat{x})^2}$

Table VI.3 - Overview of the carbonation depths [mm] of CRC1c and CRC2b after 2 months, 4 months and 1 year curing and an exposure time of about 4, 8 or 12 weeks (for a dry environment)

	CRC1c			CRC2b		
	2 months curing	4 months curing	1 year curing	2 months curing	4 months curing	1 year curing
CD*	7.97[A] (0.34)	4.82 (0.39)	3.30[C] (0.16)	6.93[D] (0.42)	5.24[F] (0.32)	3.37 (0.14)
ET**	4.4	3.6	4	4.4	3.9	4
CD*	6.92[A] (0.65)	14.21[B] (0.92)	8.29 (0.65)	7.75[D,E] (0.36)	6.29[F] (0.39)	1.81[G] (0.29)
ET**	7.1	6.5	8	7.5	6.5	8
CD*	18.13 (0.89)	17.43[B] (1.24)	2.67[C] (0.22)	8.46[E] (0.38)	8.44 (0.48)	2.07[G] (0.26)
ET**	10.7	12.6	12	11.0	13.1	12

* CD = carbonation depth [mm] with standard errors on the mean values in parentheses
** ET = exposure time [weeks], differs for the different mixtures and curing ages due to a technical deficiency of the climate chamber
[x] by a capital superscript the groups are indicated for which the mean values do not differ significantly (ANOVA)

The effect of the curing age will not be evaluated from Table VI.3, as the exposure times differ for almost all curing ages and mixtures. Therefore the carbonation coefficients k were calculated and presented in Figure VI.2. Regarding the effect of the curing age for both mixtures, the results for CRC1c are unexpected as the carbonation first increases (5.09±0.25 after 2 months curing and 5.90±0.29 after 4 months curing), but later on decreases as expected (1.92±0.16 after 1 year curing). It should be noted that the R^2 values for the linear regressions are very low for these mixtures, and the k values should be used carefully. For CRC2b, a decreasing trend is noted, as expected, together with better R^2 values after 2 and 4 months curing.

CRC1c   _CRC2b_

2 months curing — top row:
- Left (CRC1c): $x = (5.09 \pm 0.25)\, t^{0.4}$, $R^2 = 0.15$
- Right (CRC2b): $x = (3.46 \pm 0.10)\, t^{0.4}$, $R^2 = 0.83$

4 months curing — middle row:
- Left (CRC1c): $x = (5.90 \pm 0.29)\, t^{0.4}$, $R^2 = 0.42$
- Right (CRC2b): $x = (3.01 \pm 0.10)\, t^{0.4}$, $R^2 = 1.00$

1 year curing — bottom row:
- Left (CRC1c): $x = (1.92 \pm 0.16)\, t^{0.4}$, $R^2 = 0.10$
- Right (CRC2b): $x = (1.00 \pm 0.08)\, t^{0.4}$, $R^2 = 0.14$
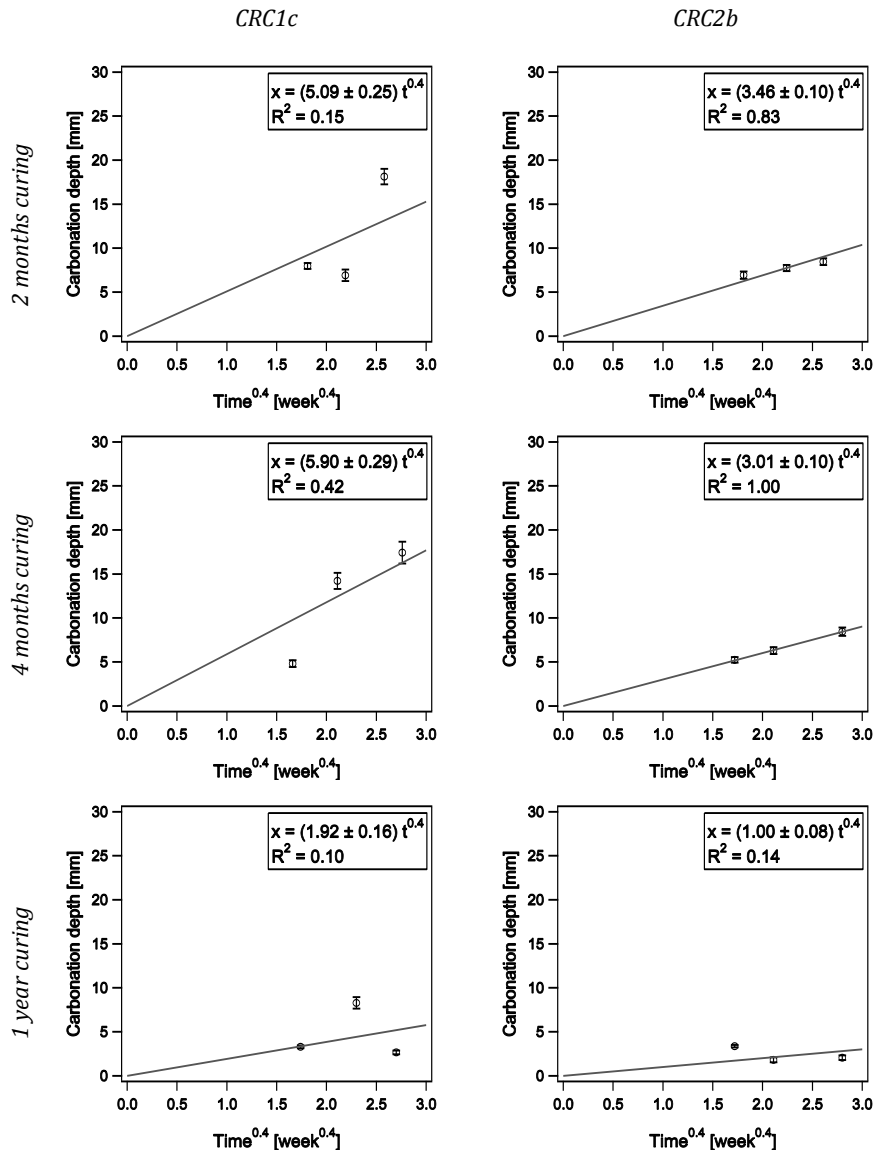
Figure VI.2 – Overview of the carbonation depths of CRC1c (left) and CRC2b (right) after a curing time of 2 months (top), 4 months (middle) and 1 year (bottom). The mean values are plotted together with their standard error. The dark grey line plots the result of a linear regression used to determine the carbonation coefficient k, whereby no constant was included in the equation.

R^2 was calculated as followed: $\dfrac{\sum(\hat{x}-\overline{x})^2}{\sum(\hat{x}-\overline{x})^2 + \sum(x-\hat{x})^2}$

A.3. Resistance against chloride ingress

For CRC1a, CRC2a, CRC3b and T(0.45)a, tides were simulated with the TAP apparatus and chlorides could penetrate into the concrete. The results of the cyclic chloride exposure are presented in Figure VI.3. No clear trend is observed in this graph and it seems that the results of the CRC mixtures do not differ that much with the values for the reference mixture, although significant differences were observed. As the goal is to evaluate the quality of CRC by comparing it to the reference, the results that not significantly differ with T(0.45)a are marked.

After 10 weeks of exposure, CRC1a has similar or better results compared to the reference. For CRC2a and CRC3b, the results are comparable (after 3 months curing) or are slightly worse (after 1 month curing). The improved results for CRC after 3 months curing are probably related to the pozzolanic reaction of the fly ash which is most significant between 1 and 3 months after casting. By this reaction the pore structure becomes denser, hindering the ingress of the chlorides.

Furthermore, it becomes clear that a sort of mean value exists around which the chloride ingress fluctuates with time. A possible explanation for the existence of a mean value is that during a drying period, the free chlorides are drawn back to the surface with the water front. For this reason chlorides need to travel the same distance every time again. Hereby, the chloride ingress does not increase in time, certainly not within the limited timeframe of the test.

As it was not possible to deduct a trend using this test setup, it was decided to perform an accelerated chloride diffusion test according to NT Build 443 (1995) for CRC1c, CRC2b and T(0.45)a. However, instead of profile grinding to determine the chloride concentration in function of the depth, the penetration depth of the chlorides was measured using silver nitrate. The results are presented in Figure VI.4.

It was thought that a better trend would be obtained, but again the trend is not obvious. Normally it would be expected that with curing age, the chloride ingress would decrease. This is not seen for T(0.45)a, the reference mixture. The rather strong decrease of the chloride ingress between 1 and 3 months curing for the CRC mixtures is again probably caused by the pozzolanic reaction of the fly ash in CRC. However, the significant increase of the chloride penetration front between 3 months and 1 year curing for mixture CRC1c, and to a smaller extent for CRC2b, is then unexpected and does not support this theory. Besides the aspect that there is no clear trend found for both experiments, we can say that both, CRC mixtures and the reference mixtures, have results in the same range, where the results of the CRC mixtures are one time better and the other time worse compared to the reference.
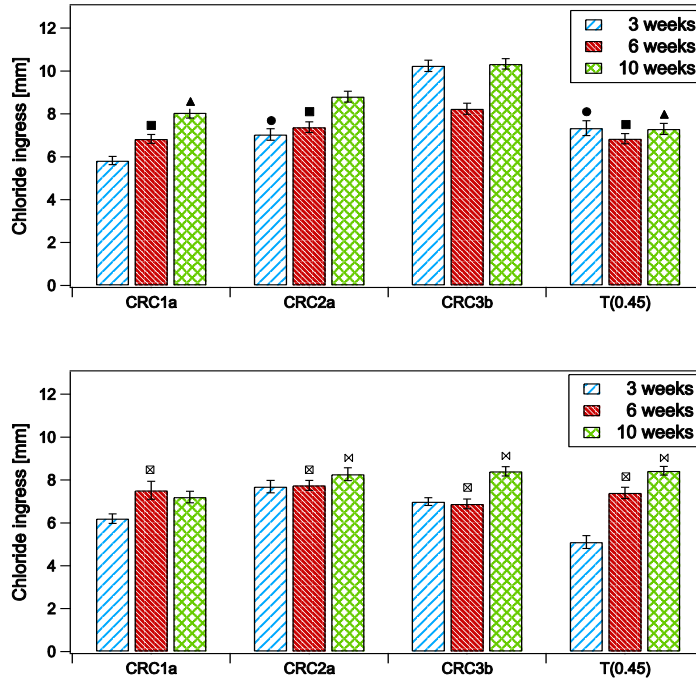
Figure VI.3 - Overview of the chloride ingress [mm] (with standard errors on the mean values) of CRC1a, CRC2a, CRC3b and T(0.45)a after a curing time of 1 month (top) or 3 months (bottom) and an exposure time of 3, 6 or 10 weeks to cyclic immersion in a chloride solution. The results of the CRC mixtures not significantly different from the reference are marked.
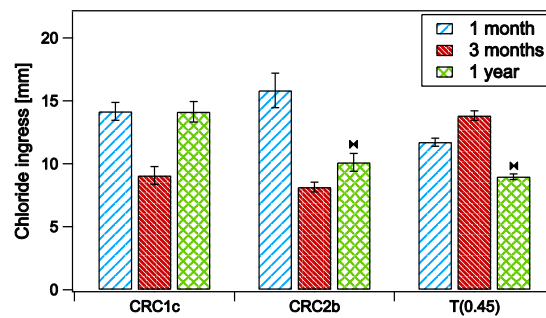
Figure VI.4 - The chloride ingress [mm] (with standard errors on the mean values) of CRC1c, CRC2b and T(0.45)a after 1 month, 3 months or 1 year curing obtained by an accelerated chloride diffusion test. The results of the CRC mixtures not significantly different from the reference are marked.

A.4. Resistance against freeze-thaw attack with de-icing agents

During the course of the freeze-thaw test with de-icing agents, scaled material was collected every 7 freeze-thaw cycles with a duration of 24 h, of which the results are presented in Table VI.4. After one month curing, it is only CRC3b that exceeds the limit of 1 kg/m^2 scaled material after 28 freeze-thaw cycles. After three months, the performance of CRC1a decreases significantly, and it also exceeds the limit. The reference concrete T(0.45)[A] has the best performance, but CRC2a also fulfils the requirements of NBN EN 1339 (2003), both after 1 and 3 months curing. The better performance of CRC2a and T(0.45)[A] compared to CRC1a and CRC3b regarding this durability issue is probably due to the higher air content of the fresh concretes (see Table VI.1). The air contents of CRC1a and CRC3b, respectively 4.0% and 4.4%, are just over the limit of the European standard NBN EN 206-1 (2000) and the Belgian standard NBN B 15-001 (2004) being 4% for a nominal maximum aggregate size of 20 mm. While the air contents of CRC2a and T(0.45)[A], respectively 6.6% and 6.0%, also meet the more strict American standard ACI 201.2R (2008) which requires an air content of 6-7%.

Table VI.4 – Overview of the material loss [kg/m^2] during a freeze-thaw test with de-icing agents, with standard errors on the mean values between parentheses.

Exposure time	CRC1a	CRC2a	CRC3b	T(0.45)[A]
1 month curing				
7 cycles	0.24 (0.07)	0.04 (<0.01)	0.96 (0.12)	<0.01 (<0.01)
14 cycles	0.38 (0.07)	0.07 (0.01)	1.24 (0.19)	0.03 (0.01)
21 cycles	0.43 (0.08)	0.09 (0.01)	1.30 (0.21)	0.05 (0.01)
28 cycles	0.48 (0.08)	0.21 (0.02)	1.36 (0.22)	0.06 (0.01)
3 months curing				
7 cycles	0.43 (0.05)	0.21 (0.03)	0.59 (0.14)	0.03 (0.01)
14 cycles	0.81 (0.05)	0.39 (0.04)	0.91 (0.18)	0.07 (0.02)
21 cycles	1.16 (0.07)	0.53 (0.08)	1.21 (0.20)	0.11 (0.03)
28 cycles	1.35 (0.10)	0.69 (0.07)	1.40 (0.22)	0.13 (0.03)

B. Discussion

One of the goals of this study was to evaluate the performance of CRC concrete mixtures, in comparison with some reference concrete mixtures. All CRC mixtures had one thing in common, besides being completely recyclable, they contained fly ash. CRC1 and CRC3 were produced as traditional concrete, for which Ordinary Portland cement (CEM I 52.5 N) and blast furnace slag cement (CEM III/A 42.5 N) were used as cementitious binder. CRC3 also contained some calcium aluminate cement. CRC2 was produced with CEM III/A 42.5 N as binder and aimed to be self-compacting. The mixtures T(0.50), T(0.45)a and T(0.45)^A were respectively produced to set a reference for concretes exposed to CO_2, chlorides or freeze-thaw attack with de-icing agents.

Looking at possible applications towards practice, CRC3 is not a first choice. Due to the use of calcium aluminate cement and blast furnace slag cement, the concrete is almost immediately unworkable due to fast setting. In chapter VII, this phenomenon was studied, and the workability could be increased, but an optimal combination of additives to avoid the fast setting should be searched for each time. This means that not only the chemical composition should be optimized each time, but also an optimal combination of (retarding) additives. Due to this practical issue, CRC3 is excluded from further discussion as a future for this CRC3 is very unlikely.

CRC1 and CRC2 were more successful and promising. Regarding the self-compacting properties of CRC2, an optimization of the concrete mix design towards the workability still needs to be done. Regarding strength, CRC2a performed less then all concretes made in this study, but the second batch, CRC2b can be classified as a high strength concrete. Possible parameters which resulted in this improvement might be the higher cement content, the fact that the k-value concept according to NBN EN 206-1 (2001) was applicable, a lower air content and a better packing. For CRC1, the strength results for both batches (CRC1a and CRC1c) were not significantly different, and comparable with T(0.45)a. From these results it can be concluded that strength performance will not be an issue for CRC.

Regarding durability, the resistance against carbonation, chloride ingress and freeze-thaw attack with de-icing agents was tested. Although no carbonation was observed for the reference mixtures, all CRC mixtures showed carbonation, which was expected as all mixtures contained fly ash. While in the first tests (wet/dry cycles), CRC1a performed better compared to CRC2a, the opposite was true for CRC1c and CRC2b (continuously moderate humidity). Regarding the ingress of chlorides, no clear trend was found for both experiments (cyclic immersion or continuous immersion). Nonetheless it was seen that all concrete mixes, CRC and reference, had about the same range of chloride penetration depths. Looking at the final durability aspect tested, CRC2a and T(0.45)^A both fulfil without problem the limits of NBN EN 1339 (2003) set for the freeze-thaw resistance with de-icing agents. CRC1a meets the limit of 1 kg/m^2 after 1 month curing, but exceeds it after 3 months curing. It was seen that when exposed to freeze-thaw attack with de-icing agents, the air content of the fresh concrete is an important

parameter. It is thereby advised to aim for a fresh air content of 6-7%, as demanded in the American standard ACI 201.2R (2008), if it is permitted by the required strength performance.

Finally it should be noted that the latest produced CRC mixtures, CRC1c and CRC2b, are designed according to the k-value concept to be classified as a T(0.45), which can be used in a wide range of environmental classes. For this reason, no durability problems should be expected on the condition that the concrete is used in an appropriate environmental class. In order to meet the requirements of a concrete exposed to freeze-thaw attack with de-icing agents (T(0.45)[A]), also the air content of the fresh concrete should be optimized by adding a sufficient amount of air entraining agent. The durability characteristics as determined in this chapter will be used for a life cycle assessment of CRC, which can be found in chapter XIII.

VII - CRC with blast furnace slag cement and calcium aluminate cement

CRC3, one of the designed compositions in PART I, combines a blast furnace slag cement (CEM III/A 42.5 N LA) with CAC (see Table IV.2). The combination of BFSC and CAC resulted in fast setting, which made the concrete unworkable within about 15 minutes. In this chapter, a theoretical background for this early initial set is given, together with the results of a search towards the deceleration of the hydration of this CRC. On the one hand different retarders were tested, but also the effect of lime and calcium sulphate addition was investigated. Finally the combination of both methods was tried out. The experimental work focused on achieving a good workability (slump and flow) and setting time (ultrasonic transmission measurements and Vicat), but also the strength development (compressive strength tests) and hydration behaviour (isothermal calorimetry) were studied.

A. Theoretical background

A.1. CAC hydration

Calcium Aluminate Cements (CAC) were studied by many authors (e.g. the chapters in Hewlett (1998) and Taylor (1997)), and a short summary is given hereafter. CAC is considerably more expensive compared to Ordinary Portland Cement (OPC), about 4 to 5 times the cost of OPC [Scrivener et al. (1999)], and is therefore not used in everyday applications. However, due to its special properties, such as rapid strength development (even at low temperatures), high temperature resistance or refractory performance and resistance to a wide range of chemically aggressive conditions, it is used in specialized applications where the performance of OPC is insufficient [Taylor (1997); Hewlett (1998)], such as refractory concrete or concretes exposed to acid attack and biogenic corrosion [Scrivener et al. (1999)]. Chemically a CAC contains mainly calcium (17-48%) and aluminium (36-82%) oxides, besides iron (up to 20%), silicon (up to 8%) and other minor oxides such as TiO_2, MgO, Na_2O, K_2O and SO_3 [Taylor (1997); Hewlett (1998)]. Regarding its mineralogy [Taylor (1997); Hewlett (1998)], CAC is composed for the greater part of monocalcium aluminate (CA, > 40%) as hydraulic phase. Depending on the alumina content, CA_2 and $C_{12}A_7$ may be present and α-Al_2O_3 might be added after sintering. C_3A is not a normal constituent for CAC and CA_6 is rarely present. The C_4AF content will vary between 20-40%, depending on the iron content [Taylor (1997)].

CA and $C_{12}A_7$ are the only phases which react significantly at early ages. However, recent findings proved hydration of CA_2 starts as soon as the hydration of CA has reached its maximum speed [Klaus et al. (2013)]. For the hydration of CA, there are 5 possible reactions and analogous reactions may be written for $C_{12}A_7$ [Edmonds and Majumdar (1988); Hewlett (1998); Scrivener et al. (1999)]:

$$CA + 10H \rightarrow CAH_{10} \qquad \qquad \text{(VII-6)}$$

$$2CA + 11H \rightarrow C_2AH_8 + AH_3 \qquad \qquad \text{(VII-7)}$$

$$3CA + 12H \rightarrow C_3AH_6 + 2AH_3 \qquad\qquad (VII\text{-}8)$$

$$2CAH_{10} \rightarrow C_2AH_8 + AH_3 + 9H \qquad\qquad (VII\text{-}9)$$

$$3C_2AH_8 \rightarrow 2C_3AH_6 + AH_3 + 9H \qquad\qquad (VII\text{-}10)$$
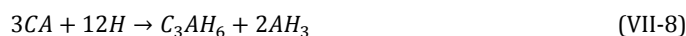
The hydration of CAC is highly temperature dependent and e.g. the setting [Bushnell-Watson and Sharp (1986); Bushnell-Watson and Sharp (1990)] and the composition of the hydrates [Edmonds and Majumdar (1988); Edmonds and Majumdar (1989); Scrivener et al. (1999)] are influenced by the temperature. At later hydration stages conversion reactions are known to take place. Below 10 °C the formation of CAH_{10} dominates (equation VII-6) and between 10 and 27 °C, CAH_{10} (equation VII-6) and C_2AH_8 (equation VII-7) are formed together. Above these temperatures CAH_{10} is no longer stable and C_3AH_6 occurs. It has been claimed that, at first, C_3AH_6 is preceded by the formation of some C_2AH_8 and that direct formation of C_3AH_6 (equation VII-8) takes only place after some C_3AH_6 has been nucleated. The conversion rate of the metastable phases (equations VII-9 and VII-10) is depending on temperature, moisture state, and possibly other variables such as water/cement ratio. At ambient temperature the formation of C_2AH_8 is favoured by the higher C/A ratio of $C_{12}A_7$ compared to CA. Generally the stable hydrates are also formed earlier in case of $C_{12}A_7$.

A.2. The hydration of C_3A in OPC

The aluminate phase in Portland clinker is very reactive and results in a fast setting. The exact composition of the calcium aluminate hydrates is not known and often referred to as C-A-H. The hydration reaction without calcium sulphate (C$\underline{S}$) is [Quennoz and Scrivener (2012)]:

$$2C_3A + nH \rightarrow C_4AH_x + C_2AH_{n-x} \qquad\qquad (VII\text{-}11)$$
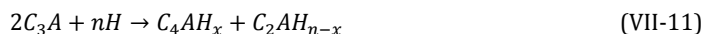
It would be mainly the formation of large C_4AH_x crystals that causes the fast setting of fresh mortar or concrete as it bridges the pores filled with water [Locher et al. (1976)].

To control the fast setting of the calcium aluminate phase in OPC, C$\underline{S}$ is added. There are four possible explanations for the retardation mechanism of C$\underline{S}$ [Mehta (1976); Collepardi et al. (1978); Brown and LaCroix (1989); Bullard et al. (2011)]. The first mechanism is based on an ettringite layer that is formed around the C_3A grains acting as a diffusion barrier [Schwiete et al. (1966) cited in Brown and LaCroix (1989); Collepardi et al. (1978); Kuzel (1996)]. However some authors [Mehta (1976); Bullard et al. (2011)] question this theory as the ettringite crystals around the C_3A grain do not appear to be dense enough to account for the retardation by a protective-coating mechanism. According to Mehta (1976) the reduced solubility of C_3A in solutions saturated with sulphate is an adequate explanation for the retardation mechanism. This theory is however confuted by Collepardi et al. (1978) as their experiments showed no retardation effect when Na_2SO_4 is added instead of a C$\underline{S}$ source. Nonetheless, both Collepardi et al. (1978) and Mehta (1976) agree on the effect of $Ca(OH)_2$ addition to the C_3A-C$\underline{S}$ system, which reduces the size of the ettringite crystals. According to Collepardi et al. (1978) this explains the improved retardation when C$\underline{S}$ and $Ca(OH)_2$ are both

added to OPC for controlling C_3A hydration. Indeed an ettringite layer with smaller crystals will fit better to the irregular shape of the C_3A grain and by this becomes more effective. Other authors also explain the retardation mechanism by a diffusion barrier, but consisting of other phases, e.g. an aluminium gel layer [Corstanje et al. (1973); Corstanje et al. (1974a); Corstanje et al. (1974b)] or a layer of small thin C_4AH_x crystals [Gupta et al. (1973) cited in Collepardi et al. (1978); Plowman and Cabrera (1984)]. A last possible explanation is an alumina gel layer on which sulphate ions are adsorbed, blocking the dissolution sites [Feldman and Ramachandran (1966); Skalny and Tadros (1977) cited in Brown and LaCroix (1989)].

Nevertheless, most authors agree that the first hydration reaction of C_3A with the addition of $C\underline{S}$ results in the formation of ettringite [Pommersheim and Chang (1988); Kuzel (1996); Baert (2009)]:

$$C_3A + 3C\underline{S} + 36H \rightarrow C_6A\underline{S}_3H_{36} \qquad \text{(VII-12)}$$

In the above stoichiometric expression of ettringite, 36 moles of water are written. In literature this amount can however vary between 30 and 36 moles of water [Baert (2009)]. When all $C\underline{S}$ is consumed ettringite will become unstable and will react with the additional calcium aluminate to form monosulphoaluminate [Pommersheim and Chang (1988); Kuzel (1996); Baert (2009)]:

$$2C_3A + C_6A\underline{S}_3H_{36} + 6H \rightarrow 3C_4A\underline{S}H_{14} \qquad \text{(VII-13)}$$
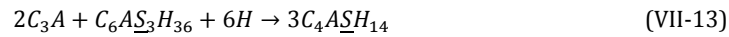
In some literature reports, only 12 moles of water instead of 14 moles are used for the stoichiometric expression for monosulphoaluminate [Pommersheim and Chang (1988); Kuzel (1996); Baert (2009)]. When all the ettringite is converted into monosulphoaluminate, calcium aluminate can further react with water to form hydrogarnet (VII-14), according to Baert (2009), or hexagonal and cubic aluminate hydrates (VII-15 and VII-16), according to Pommersheim and Chang (1988):

$$C_3A + CH + 12H \rightarrow C_4AH_{13} \qquad \text{(VII-14)}$$
$$2C_3A + 21H \rightarrow C_2AH_8 + C_4AH_{13} \qquad \text{(VII-15)}$$
$$C_2AH_8 + C_4AH_{13} \rightarrow 2C_3AH_6 + 9H \qquad \text{(VII-16)}$$
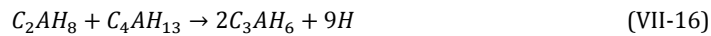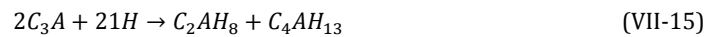
A.3. CAC-OPC hydration

When combining OPC and CAC, the reaction mechanism of both systems will interfere. OPC/CAC mixtures are known to have a poor strength development in the absence of additives [Amathieu et al. (2001)] and strength reduction at later ages due to delayed or secondary ettringite formation [Gawlicki et al. (2010)], which limits their use. The factors affecting the early strength development of these OPC/CAC mixtures are the formation of ettringite, the main hydration product of these systems [Gawlicki et al. (2010)], and the delayed hydration of OPC [Gu et al. (1994); Gu et al. (1997)]. The importance of the ettringite formation in such systems is explained in detail by Amathieu et al. (2001). The formation of ettringite from Al^{3+}, SO_4^{2-} and Ca^{2+} ions in the

solution dominates the early hydration reactions. As mentioned earlier the rapid hydration of the aluminate phase in OPC is controlled by adding calcium sulphate to the clinker. When combining CAC and OPC, SO_4^{2-} ions from OPC will react with Al^{3+} ions from CAC. Due to this reaction, ettringite will be formed in the body of the paste and not on the surface of C_3A particles. Hereby the retardation mechanism of C_3A is reversed. According to Evju and Hansen (2001), this ettringite is more stable in OPC/CAC mixtures, compared to ettringite from an OPC mixture, which would be due to changes in the chemical composition. The calcium aluminate in CAC (CA and $C_{12}A_7$) is different from the one in OPC (C_3A), which would hinder the change from ettringite to monosulphoaluminate. Amathieu et al. (2001) defines three parameters influencing the ettringite formation. The first and most important one being the type of calcium sulphate added. If calcium sulphate is present as anhydrite, being less rapidly soluble than CAC, rapid set will occur already at low amounts of CAC added. If the type of calcium sulphate added is more rapidly soluble than CAC, in case of hemihydrate or gypsum, sulphate ions have the time to migrate to the C_3A blocking its reaction, before significant dissolution of CAC occurs. Thus in case of gypsum or hemihydrate, large amounts of CAC need to be added to result in rapid setting. Additionally, the higher the C_3A content is, the easier it is to produce rapid setting as the SO_3 content of Portland cement does not increase proportionally with its C_3A content. When CAC destabilises the inhibition of the C_3A the latter produces more hydrates, contributing to rapid set. Also the addition of free lime will influence the setting of OPC/CAC mixtures [Bayoux et al. (1990)]. A small addition will accelerate the precipitation of ettringite from CAC-calcium sulphate mixtures, whereas a large one leads to a dramatic reduction of the hydration kinetics.

B. Mix design

B.1. MBE method

Different additions were studied to slow down the fast hydration of the studied CRC. To minimise the material cost and effort, the tests were carried out on equivalent mortar mixtures. The compositions of these mortars were calculated according to the MBE method (Mortier de Béton Equivalent) [Schwartzentruber and Chatherine (2000)]. To obtain a workability behaviour of the MBE mortar, identical to that of the corresponding concrete mixture, the total amount of coarse aggregates was replaced by an amount of sand Δf_{sand} [kg]:

$$\Delta f_{sand} = \frac{f_{agg,1} \cdot S_{agg,1} + f_{agg,2} \cdot S_{agg,2}}{S_{sand}} \qquad \text{(VII-17)}$$

with $f_{agg,x}$ [kg] the mass of aggregate x and $S_{agg,x}$ [m^2/kg] and S_{sand} [m^2/kg] the specific surface area of respectively aggregate x and sand. The amount of water was also corrected with Δf_{water} [kg]:

$$\Delta f_{water} = -f_{agg,1} \cdot A_{agg,1} - f_{agg,2} \cdot A_{agg,2} + \Delta f_{sand} \cdot A_{sand} \qquad \text{(VII-18)}$$

with $A_{agg,x}$[-] and A_{sand}[-] the absorption coefficient of respectively aggregate x and sand. In Table VII.1 the composition of the MBE mortars for the CRC mixture and two reference mixtures T(0.50) and T(0.45) are presented.

Table VII.1 - Overview of the MBE mortar compositions [kg/m³] for CRC3b (see Table IV.2) and the reference mixtures T(0.50) and T(0.45) (see Table V.1)

Material	CRC3b	T(0.50)	T(0.45)[a]
Limestone sand 0/4	1318		
Siliceous sand 0/4		1424	1427
Limestone filler	70		
Fly ash	200		
CEM I 52.5 N		563	598
CEM III 42.5 N LA	363		
Calcium Aluminate Cement	63		
Water	236	261	249

[a] Batch T(0.45)a was used as reference

B.2. Setting retarders

In a first attempt to slow down the hydration process three types of retarders were added to the system, namely a commercial retarder on the basis of gluconate (CR; 1000 cc per kg binder), sucrose (S; 0.10m% of the binders) and citric acid (CA; 0.10m% of the binders). As it was found that lime and calcium sulphate have an influence on the setting of OPC/CAC hydration (see chapter VII.A), also the combined addition of lime (Ca(OH)$_2$; 4 wt% of the binders) and calcium sulphate (2/3 CaSO$_4$·½H$_2$O and 1/3 CaSO$_4$; 6 wt% of the binders) was tested (LCS). Initially three mixtures of lime and calcium sulphate were tested with CH/C$\underline{S}$ ratios of 2.7/4, 3.3/5 and 4/6. As the latter gave the best results regarding slump and flow, only this one was used for further testing. Finally both methods were combined and each type of retarder was combined with the lime and calcium sulphate addition (LCS/CR, LCS/S and LCS/CA). All mixtures were tested for their workability (by slump and flow tests) and their hydration heat (by isothermal calorimetry). After these first tests, the setting times (by ultrasonic transmission and Vicat needle measurements) and the strength development were studied for three CRC mixtures, namely those with the commercial retarder (CR), the lime and calcium sulphate addition (LCS) and the combination of both (LCS/CR).

C. Results

C.1. Workability

The workability of the mixtures was determined by slump and flow tests 20 minutes after mixing, of which the results are presented in Figure VII.1. At first three retarders were tried separately to slow down the fast setting of the CRC mixtures: a commercial retarder, sucrose and citric acid. As seen in Figure VII.1, no slump or flow was measured.

As it was found that lime and calcium sulphate have an influence on the fast setting of mixtures with OPC and CAC, this effect was also tested. Although a slump and flow could be measured, the effect disappeared soon (see VII.C.3). When combining a retarder with the addition of lime and calcium sulphate, the results improved significantly and the setting time was postponed enough to meet practical requirements.
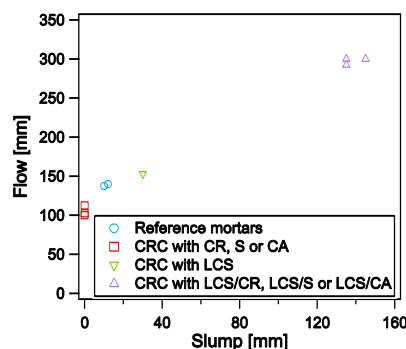
Figure VII.1 - The slump and flow measured 20 min after mixing of reference mortars (T(0.45) and T(0.50)) and CRC mortar with a retarder (CR, S and CA), lime and calcium sulphate addition (LCS) or a combination of both (LCS/CR, LCS/S and LCS/CA)

C.2. Hydration heat

The hydration heat of cement pastes was measured using isothermal calorimetry (see chapter X). Each paste contained 4 g water and 10 g binder (BFSC/CAC/fly ash in case of CRC; CEM I 52.5 N in case of T(0.45) and T(0.50)) and the studied retarder. The left graphs of Figure VII.2 show the (cumulative) heat evolution of the CRC mixtures with a retarder or combined lime and calcium sulphate addition. It is seen that already during the first hour a lot of heat is produced, but after the first hours all reactions slowed down. Also the characteristic peak from alite hydration around 10 hours is missing from all CRC curves.

The hydration heat during the first hours seems controllable for the CRC mixtures which combine the addition of a retarder with lime and calcium sulphate addition (see right graphs of Figure VII.2). For the first 10 hours the cumulative hydration heat of the CRC mixtures is close to the curves of the reference mixtures. However after this period the alite hydration starts for the reference mixtures, and this process seems to be slowed down significantly for the CRC mixtures.

The mixtures containing the commercial retarder (with or without lime and calcium sulphate addition) show a peak after about 1 hour of hydration, which is missing for the mixtures with sucrose and citric acid. It is possible that this peak results from the hydration of the aluminate phases of the BFSC and/or CAC. One could also think of early alite hydration, but this would be rather fast and only a very small amount of the total alite content would have been hydrated considering the small contribution to the

cumulative heat production. In the end, the origin of this peak was not examined as it was not within the scope of this study.
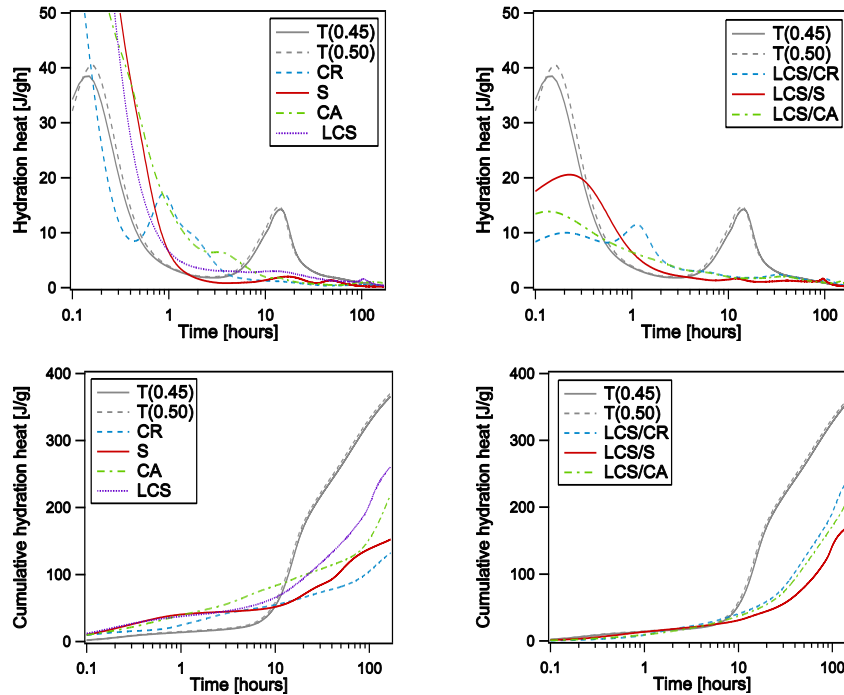
Figure VII.2 - The hydration heat and cumulative hydration heat of reference mixtures T(0.45) and T(0.50) and CRC mixtures with a retarder (commercial retarder (CR), sucrose (S) or citric acid (CA)), lime and calcium sulphate addition (LCS) or a combination of both (LCS/CR, LCS/S and LCS/CA)

C.3. Setting times

The setting times of the reference mixtures and the CRC mixtures with the commercial retarder, the combined lime and calcium sulphate addition and the combination of both are presented in Table VII.2. Regarding the results for the CRC mixture with lime and calcium sulphate, it was not possible to deduct the setting times from the velocity curves as no inflection point was obtained. For the energy curves it was not possible to deduct the final setting time for the CRC mixture with the commercial retarder as the threshold of 0.13 was not reached within the first 48 hours. Earlier research [Robeyst et al. (2011)] showed that the energy curves are preferred over the velocity curves to determine setting times if admixtures are used. For this reason only the energy curves are presented (see Figure VII.3).

Table VII.2 - Overview of the setting times [hours] as determined from the p-wave velocity or energy curve from ultrasonic transmission measurements on concrete (c) or mortar (m) samples or by using the Vicat needle on pastes.

Mixture	p-wave velocity		p-wave energy		Vicat	
	Initial setting	*Final setting*	*Initial setting*	*Final setting*	*Initial setting*	*Final setting*
T(0.45)	3.55 (c)	5.43 (c)	5.44 (c)	10.27 (c)		
T(0.50)	3.22 (c)	4.56 (c)	5.38 (c)	12.97 (c)		
CRC-CR	0.70 (m)	1.15 (m)	0.7 (m)	n/a	1.30	1.50
CRC-LCS	n/a	n/a	2.95 (c)	8.7 (c)	4.40	7.58
CRC-LCS/CR	0.18 (m)	0.98 (m)	1.08 (m)	13.9 (m)	6.83	10.33

In Table VII.2 it is seen that there is a high variability for the results obtained by the different techniques. The setting times deducted from the velocity curves did not confirm the expectations from the workability and hydration tests. Looking at the energy curves, the final setting times are significantly later compared to the ones from the velocity curves. The difference for the initial setting times is however limited. In Figure VII.3 it is seen that for all CRC mixtures the initial rise of the energy ratios is much stronger compared to the reference mixtures. For the CRC concrete mixture with lime and calcium sulphate addition (LCS) it is seen that eventually it reaches the same energy ratio as the reference mixtures.
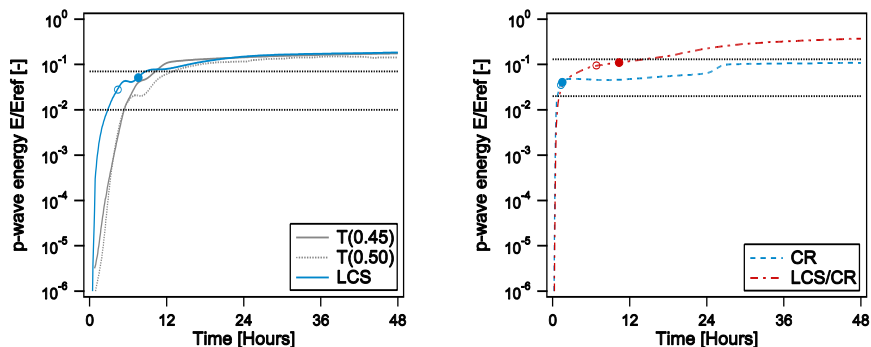
Figure VII.3 - Ultrasonic p-wave energy curves for concrete (left) and mortar (right) mixtures. Reference mixtures T(0.45) and T(0.50) were tested besides CRC mixtures with a commercial retarder (CR), lime and calcium sulphate addition (LCS) or a combination of both (LCS/CR). The initial and final setting times obtained by Vicat needle are presented by the open and closed bullets respectively. The horizontal lines present the energy ratio thresholds for determining initial (lowest) and final (highest) set.

As admixtures and Supplementary Cementitious Materials (SCMs) are known to influence the velocity and energy curves from ultrasonic transmission measurements [Robeyst et al. (2008); Robeyst et al. (2009); Robeyst (2010); Robeyst et al. (2011)], the setting times were determined more traditionally using a Vicat needle. For these tests

the expected improvement of the setting times can be seen for the lime and calcium sulphate addition, with or without the commercial retarder. When projecting the results of the Vicat measurements on the energy curves, it is seen that the thresholds for the initial and final setting times as proposed by Robeyst et al. [Robeyst et al. (2008); Robeyst et al. (2009); Robeyst (2010)] seem not applicable for the CRC mixture with CAC and BFSC. It seems however not possible to propose new thresholds, as the energy ratios corresponding with initial and final set have a high variability.

Although the presence of admixtures and SCMs in the CRC mixtures will probably have their effect on the velocity and energy curves, there might also be another explanation for the differences between the ultrasonic transmission measurements and the Vicat needle. In CAC/OPC mixtures, ettringite is formed during the first hours of cement hydration in the shape of stubby crystals or thin needles [Amathieu et al. (2001)]. Depending on the W/C ratio and the chemical composition of the system, ettringite has no or merely a small influence on the stiffening of the cement paste [Aïtcin and Neville (2003)]. Nevertheless, in contrast to the setting behaviour, the p-wave velocity and energy are strongly affected by the formation of ettringite. The crystals do not create bonds between the cement particles at early hydration times, but they fill pore space that was previously occupied by water, and thus the velocity will increase. As the formation of ettringite is limited in OPC mixtures, the influence on the velocity will also be minimal. In a CAC/OPC mixtures with lime and calcium sulphate added, a lot more ettringite will be formed and this effect is probably seen in the ultrasonic transmission measurements.

C.4. Strength development

Besides workability, which is related to the setting time of concrete mixtures, the compressive strength is also an important parameter for practical applications. Looking at the results of the isothermal calorimetry, it is seen that after 7 days, the total hydration heat for the CRC mixtures is significantly lower than the reference mixtures. As the hydration heat is known to be related to the hydration degree of cement pastes, mortars or concrete, the question arose whether the compressive strength of the CRC mixtures was sufficient for practical applications. The results of the compressive strength tests on 2, 7 and 28 days of the CRC mixture with a commercial retarder, the combined lime and calcium sulphate addition or a combination of both are presented in Figure VII.4.
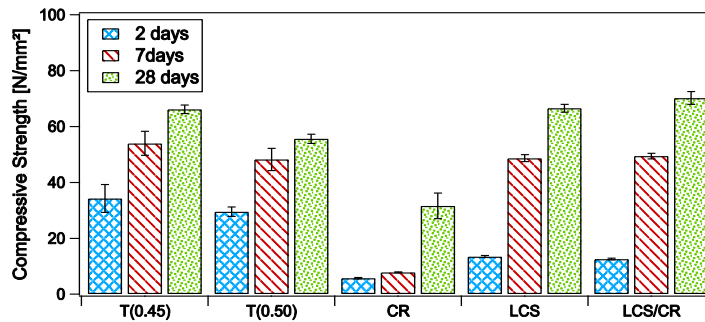
Figure VII.4 - Strength development of reference mixtures T(0.45) and T(0.50) and CRC mixtures with a commercial retarder (CR), lime and calcium sulphate addition (LCS) or a combination of both (LCS/CR)

From the compressive strength tests it can be concluded that after 2 days the strength for all CRC mixtures is significantly lower compared to the reference mixtures. Indeed, retarders do not only delay the early hydration of the aluminate phases and thus setting, but are also known as strong retarders for the alite hydration. For the CRC mixture with the commercial retarder the compressive strength at later ages, 7 and 28 days, is inferior compared to the reference mixtures. It should be noted here that the total cement content of the CRC mixture is lower compared to the reference mixtures (about 70 and 75 wt% for T(0.45) and T(0.50) respectively) and that the fly ash will mainly contribute to the strength development on the long term. The results at 7 and 28 days for the CRC mixtures with lime and calcium sulphate, with or without commercial retarder, are both comparable with the reference mixtures showing that the addition of lime and calcium sulphate significantly improves the strength development of the CRC mixture.

D. Discussion

The aim of this study was to produce a CRC combining CAC and BFSC with an appropriate workability and setting time, comparable to the one of OPC concrete. For this purpose, different retarders based on gluconate, sucrose or citric acid were added to the mixtures, but without success. In literature it was found that the addition of calcium sulphate, especially in combination with lime, affects the setting of such CAC/OPC mixtures. The beneficial effects of lime and calcium sulphate addition on the workability were proven by slump and flow tests. The results even improved more when the lime and calcium sulphate addition was combined with a retarder. Notwithstanding these good results, the effect was not observed by the ultrasonic transmission measurements using the FreshCon system, probably due to the formation of significant amounts of ettringite affecting the p-wave velocity and energy curves. The latter has however no or merely a small influence on the stiffening of the cement paste at early age. On the other hand, when using the Vicat needle to study the setting times of the mixtures, the advantageous effect on the setting times was observed.

Although the desired workability was obtained, the cumulative hydration heat of all CRC mixtures measured during the first 7 days of hydration was significantly lower compared to the reference mixtures. As the strength development is related to the hydration heat, the compressive strength was checked after 2, 7 and 28 days of hydration. The early strength (2 days) was significantly lower for the mixtures with lime and calcium sulphate addition, but after 7 and 28 days the strength development was comparable to the one of the reference mixtures.

Despite the fact that we succeeded to produce a CRC combining Blast Furnace Slag Cement and Calcium Aluminate Cement with an appropriate workability, we may not ignore the fact that the optimal combination of calcium sulphate, lime and maybe also a retarder should be selected over and over again. The latter will make the whole concept of CRC, which is designed for reincarnation in cement production, even more complex. For this reason we concluded that it is wiser to use such fast setting mixtures only when fast setting is actually one of the requirements for application. Indeed, OPC/CAC mixtures, are often used for e.g. flooring installations, rapid wall construction and concrete repair (sealing of leaks, road pavement repair, …) due to their unique properties: adjustable setting time, rapid hardening and drying, dimensional stability, good adhesion and compatibility with existing concrete and corrosion resistance [Gu et al. (1994); Gu et al. (1997); Amathieu et al. (2001)].

VIII - The use of copper slag in concrete

This chapter focuses on the use of copper slag in CRC production. As mentioned in PART I, copper slag is interesting for the production of CRC. On the one hand it is a source of Fe_2O_3, on the other hand, it is a by-product which will reduce the environmental impact of CRC. Also its lower melting point compared to iron ore, resulting in a lower calcination temperature [Shi et al. (2008)], should create additional benefits for the environment (lower energy consumption and reduced CO_2 emissions). The question remains how this copper slag is preferably used in our CRC. The effect of partial cement replacement by copper slag was studied on cement pastes and mortars. The influence of replacing aggregates by copper slag was studied for mortars and concrete. Results of this chapter will be published in the Journal of Materials in Civil Engineering [De Schepper et al. (accepted for publication May 2014)]

A. Copper slag

Copper slag is a by-product obtained during smelting and refining of copper. Today, common management options are recycling, recovering of metal and production of value added products (e.g. abrasive tools, roofing granules, cutting tools, tiles, glass, road-base construction, rail-road ballast and asphalt pavements) [Shi et al. (2008)]. Still, huge amounts are disposed in dumps or stockpiles. One of the greatest potential applications is in cement and concrete [Shi et al. (2008)]. In cement production it can be used as an iron adjusting material or as partial cement replacement [Goñi et al. (1994); Tixier et al. (1997); Gorai et al. (2003); Taha et al. (2004); Zain et al. (2004); Al-Jabri et al. (2006); Taha et al. (2007); Shi et al. (2008); Najimi et al. (2011)]. Regarding the latter, a major concern is the leaching of heavy metals; however, studies have shown that this is within regulatory limits. Copper slags can also be used as fine and coarse aggregates in concrete production [Gorai et al. (2003); Shi et al. (2008); Al-Jabri et al. (2009a); Al-Jabri et al. (2009b); Khanzadi and Behnood (2009); Wu et al. (2010a); Wu et al. (2010b); Al-Jabri et al. (2011); Thomas et al. (2012)]. The density of this copper slag is higher compared to natural aggregates and varies with the Fe_2O_3 content between 3.16 and 3.87 g/cm^3 according to Shi et al. (2008). Furthermore the water absorption is very low (0.15-0.55% [Shi et al. (2008)]) and also the glass-like smooth surface has implications towards the design of concrete mixtures with copper slag. Copper slag has however also favourable mechanical properties such as excellent soundness, good abrasion resistance and good stability [Shi et al. (2008)].

B. Mix design

B.1. Used raw materials

The copper slag used in this research is a secondary slag from a Belgian copper, lead, tin and nickel producer who uses waste products (e.g. old copper wires, dust from the tin production, old televisions and computers and radiators from cars) as raw materials. On the one hand a quickly cooled granulated copper slag (QCS) was used for the

replacement of the fine aggregates (= sand) in concrete and as a material for cement replacement. A slowly cooled broken copper slag (SCS) was utilized to replace the coarse aggregates. Before using the copper slag as a substitution for cement, QCS was milled 3 times during 4 minutes at 300 rpm in a planetary ball mill (mQCS). A CEM I 52.5 N was used throughout all experiments as cementitious binder. An overview of the chemical and mineralogical composition of the cement and copper slag is given in Table VIII.1 and Table VIII.2. In Table VIII.2 and Figure VIII.1 it is seen that, as expected, the quickly cooled granulated copper slag QCS has a higher 'other' amorphous fraction in comparison with the slowly cooled broken copper slag SCS.

B.2. Copper slag as cement replacement

The effect of using copper slag as cement replacement was tested on cement pastes (isothermal calorimetry) and mortars (compressive strength). Cement pastes were produced with increasing copper slag contents from 0 to 60 wt% in steps of 10 wt%. For each paste 10 g of powder (n g mQCS with (10-n) g CEM I 52.5 N) was mixed with 4 g of water. The reference composition of the mortars was a standard mortar with cement:sand:water equal to 6:2:1, for which the copper slag content replacing the cement was increasing in steps of 20 wt% from 0 to 60 wt%. A CEN sand in accordance with NBN EN 196-1 (2005) was used to produce these mortars.

Table VIII.1 - Chemical composition [wt%] of the used copper slag and cement (by XRF analysis).

Oxide	QCS	SCS	CEM I 52.5 N
CaO	7.09	5.18	63.12
SiO_2	25.87	29.33	18.73
Al_2O_3	5.92	3.23	4.94
Fe_2O_3	45.45	50.72	3.99
MgO	0.81	0.47	1.02
Na_2O	0.80	1.99	0.41
K_2O	0.19		0.77
SO_3	0.37	0.24	3.07
P_2O_5	0.82	0.41	
TiO_2	0.31	0.10	
ZnO	8.8	5.13	
MnO	0.74	0.41	
Cr_2O_3	0.73	0.36	
CuO	0.35		
PbO	0.36		

Table VIII.2 - Mineralogical composition [wt%] of the used copper slag and cement (by XRD/Rietveld analysis).

Mineral	QCS	SCS	CEM I 52.5 N
Alite			53.6
Belite			17.0
Ferrite			11.2
Aluminate			6.2
Gypsum			0.8
Bassanite			0.9
Anhydrite			2.1
Aphthitalite			0.3
Arcanite			0.5
Syngenite			0.7
Zincite	0.4	0.6	
Hematite		0.8	
Wuestite	1.6	0.4	
Fayalite	4.1	45.5	
Hercynite	4.0	3.9	
Other	89.9	48.8	6.8
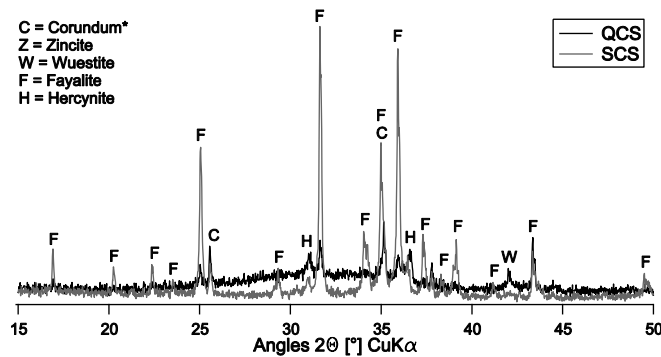
Figure VIII.1 - Observed XRD patterns of QCS and SCS between 15 and 50 °2θ. The large bump in the 20-40 °2θ range in case of QCS results from the scatter from the amorphous fraction.

B.3. Copper slag as aggregate replacement

For evaluation of the aggregate replacement by copper slag, mortars (for compressive strength tests) and concrete (for compressive strength and durability evaluation) were made. Due to the higher density of copper slag compared to the one of natural aggregates, the replacement levels are volume based and the density of the concrete will

increase. The copper slag QCS and SCS used in this study had a density of respectively 3.61 and 3.98 g/cm^3. Standard mortars were produced, and the sand was replaced by QCS from 0 to 100 vol% in steps of 20 vol%. Based on these results, the replacement levels for the concrete were fixed, namely 20 and 40 vol% of the total aggregates volume. On the one hand the fine aggregates were replaced by QCS (QCS-20 and QCS-40). On the other hand the coarse aggregates were substituted by SCS (SCS-20 and SCS-40). An overview of the concrete mixtures is given in Table VIII.3. The particle size distribution of most raw materials is given in Figure VIII.2.

Table VIII.3 – Overview of the concrete compositions with copper slag [kg/m^3]

Concrete raw material	CS-0	QCS-20	QCS-40	SCS-20	SCS-40
River sand 0/4 (kg/m^3)	762	383		786	837
QCS 0/4 (kg/m^3)		403	848		
SCS 8/20 (kg/m^3)				403	858
Gravel 2/8 (kg/m^3)	450	464	488	312	170
Gravel 8/16 (kg/m^3)	741	765	805	514	280
CEM I 52.5 N (kg/m^3)	340	340	340	340	340
Water (kg/m^3)	153	153	153	153	153
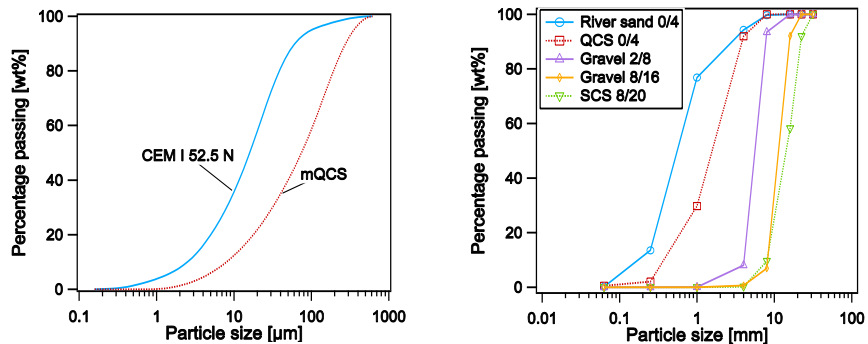
Figure VIII.2 - Particle size distributions of the used materials determined by laser diffraction (left) or sieving (right)

C. Results

C.1. Copper slag as cement replacement

i. Isothermal calorimetry of cement pastes

The hydration heat was measured by isothermal calorimetry at 20 °C during 7 days. In Figure V.1 the heat production rate and cumulative heat production per gram of powder are presented for cement pastes with varying mQCS content. It is seen that the

maximum of the heat production rate and the cumulative heat production decrease with increasing mQCS content. It can be observed that the maximum of the heat production rate moves further in time when more CEM I 52.5 N is replaced by mQCS. To estimate the possible contribution of the mQCS to the heat production, the heat production rate and cumulative heat production per gram of CEM I 52.5 N are presented in Figure VIII.4. It is seen that the maximum values of the heat production rate are similar for all mixes, but the maximum moves further in time with increasing mQCS content. It is also observed that the cumulative hydration heat of the cement pastes with mQCS increases more compared to the reference mixture without mQCS.
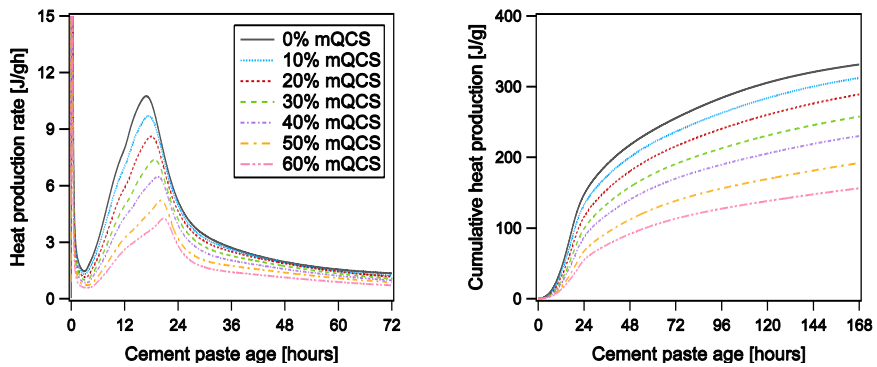
Figure VIII.3 - The heat production rate (left) and cumulative heat production (right) per gram of powder (both CEM I 52.5 N and mQCS) with varying mQCS contents
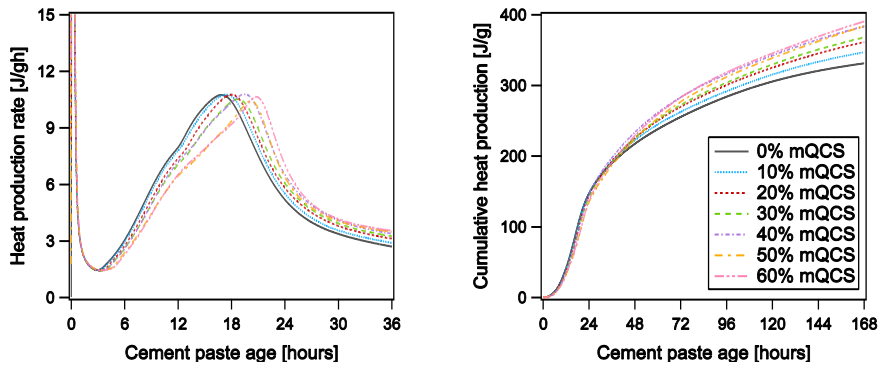
Figure VIII.4 - The heat production rate (left) and cumulative heat production (right) per gram of CEM I 52.5 N with varying mQCS contents

ii. Compressive strength of mortars

The compressive strength of mortars with increasing mQCS content to replace CEM I 52.5 N are presented in Table VIII.4. While the compressive strength test after 7 days indicated that the addition of 20wt% mQCS seems beneficial and results in a higher strength compared to the reference, the reference mortar is the strongest after a curing period of 28 days. Except for the good result after 7 days for 20wt% mQCS addition, it can be observed that the compressive strength decreases with increasing mQCS content, for both curing times of 7 and 28 days.

Table VIII.4 - The average results of the compressive strength tests [N/mm²] on mortar samples with copper slag as cement (mQCS) or sand (QCS) replacement. Standard errors on the mean values are added between parentheses

Amount and type of copper slag	7 days	28 days
Reference mortar	31.5 (0.90)	61.5 (0.92)[D,E]
20wt% mQCS	36.8 (0.51)	44.7 (0.49)
40wt% mQCS	26.1 (0.17)	34.3 (0.25)
60wt% mQCS	13.9 (0.10)	17.2 (0.27)
20vol% QCS	54.2 (0.66)[A]	63.4 (0.66)[E,F]
40vol% QCS	50.3 (1.08)[B,C]	66.9 (0.84)[G]
60vol% QCS	53.3 (0.40)[A,B]	65.3 (0.44)[F,G]
80vol% QCS	52.7 (0.25)[A,B]	62.7 (0.64)[E,F]
100vol% QCS	48.4 (0.70)[C]	58.2 (0.82)[D]

A capital superscript denotes the groups for which
the mean values do not differ significantly

C.2. Copper slag as aggregate replacement

i. Compressive strength of mortars

Mortars with increasing QCS content in replacement of standard sand were tested for their compressive strength, and the results are presented in Table VIII.4. For all mortar samples with QCS, the compressive strength after 7 days of curing is comparable for the different amounts of copper slag; although some results have significant differences between the mean values (see Table VIII.4). Compared to the reference mortar, all results for the copper slag mixtures are significantly higher. For the tests after a curing period of 28 days, the compressive strength results are similar for the reference mortar and the mortars with QCS, but again results might differ significantly. The mortars with 40 and 60 vol% QCS give the best results after 28 days, while the mortar with 100 vol% QCS has the lowest strength, although not significantly different from the reference mortar.

ii. Compressive strength of concrete

The results of the compressive strength tests on concrete with varying copper slag contents are presented in Table VIII.5. For the mixtures with 20 vol% copper slag (QCS-20 or SCS-20), the results are comparable for all curing ages (no significant differences). For the mixtures with 40 vol% copper slag (QCS-40 and SCS-40), the results are only comparable after 28 and 84 days of curing, and the compressive strength of SCS-40 is significantly higher after 2 and 7 days of curing. Compared to the reference mixture, the results for concrete with 20 vol% and 40 vol% copper slag are similar or higher (except for SCS-20 after 2 days curing). Thus, from the compressive strength tests on concrete it can be concluded that the use of copper slag as aggregate results in comparable or even better results.

iii. Durability of concrete

The durability of concrete with copper slag as aggregate replacement was studied by testing several parameters, of which the results are presented in Table VIII.5. Looking at the results of the open porosity, the effect caused by the copper slag seems to be acceptable. The capillary porosity of QCS-20 and SCS-40 is comparable to the reference mixture, while the capillary porosity of SCS-20 and QCS-40 is respectively significantly higher or lower. For the total porosity there is no significant difference for QCS-20 and QCS-40, which is also true for QCS-40, SCS-40 and the reference mixture. Again the total porosity of SCS-20 is significantly the highest. Nonetheless, the differences with the reference mixture seem minimal for all mixtures. The gas permeability of all mixtures with copper slag is lower compared to the reference and this for all pressures and both drying temperatures. This improvement is however only significant for mixtures SCS-20 and SCS-40 after being dried at 105 °C. After drying at 40 °C the reduction is significant for SCS-20 and SCS-40 for an applied pressure of 3 bar, for SCS-40 also at 4 bar.

Both the reference concrete and the mixtures with copper slag were subjected to a high CO_2 concentration (10%). All mixtures showed negligible carbonation up to 84 days. For the reference concrete and SCS-40 the first limited carbonation was observed after 84 days of exposure. For the other mixtures with copper slag, limited carbonation was measured after the first 28 days of carbonation. The ingress occurred locally, explaining the high variability. E.g. where carbonation was measured after 28 and 56 days for QCS-20, no carbonation was measured after 84 days for the same mixture on different samples.

The migration of chlorides into concrete was tested by a CTH test. The chloride migration coefficient for all mixtures with copper slag was lower compared to the reference mixture. Except for QCS-20, this improvement was also significant.

Different surfaces (casted, sawn and troweled) of most mixtures were tested for the resistance against freeze-thaw attack with de-icing agents. The results of SCS-20 are not available as the test specimens were destroyed due to a technical defect and the same

Table VIII.5a - Results of compressive strength and durability tests on concrete containing copper slag QCS. Standard errors on the mean values are added between parentheses.

Tested parameter	CS-0	QCS-20	QCS-40
Fresh properties			
Slump [mm]	60	50	20
Air content [%]	2.8	2.2	1.2
Compressive strength [N/mm^2]			
2 days	34.7 (0.31)[A]	33.6 (0.26)[A,B]	33.7 (0.15)[A]
7 days	49.3 (0.88)[C,D]	48.2 (0.18)[C]	51.8 (0.78)[D]
28 days	57.0 (0.98)[E]	57.7 (1.16)[E]	63.7 (1.49)[F]
84 days	63.9 (1.14)[G,H]	59.9 (1.61)[G]	69.3 (1.61)[H]
Open porosity [vol%]			
Capillary porosity (40°C)	7.5 (0.12)[I]	7.9 (0.15)[I]	6.9 (0.05)
Total porosity (105 °C)	12.6 (0.13)[K]	11.9 (0.08)[J]	12.3 (0.08)[J,K]
Gel porosity (105°C-40°C)	5.1 (0.16)[M,N]	4.0 (0.13)[L]	5.5 (0.12)[N]
Gas permeability coefficient [10^{-17} m^2] – after drying at 40 °C			
2 bar	6.7 (0.44)[O]	5.9 (0.29)[O]	5.5 (0.61)[O]
3 bar	4.5 (0.29)[P]	3.9 (0.16)[P,Q]	3.5 (0.38)[P,Q]
4 bar	4.1 (0.27)[R]	3.5 (0.13)[R,S]	3.1 (0.31)[R,S]
Gas permeability coefficient [10^{-17} m^2] – after drying at 105 °C			
2 bar	43.3 (2.39)[T]	39.0 (0.96)[T]	37.4 (1.32)[T]
3 bar	28.7 (1.47)[V]	25.5 (0.67)[V]	24.3 (0.89)[V]
4 bar	24.5 (1.27)[X]	21.2 (0.62)[X]	20.0 (0.75)[X]
Carbonation depth [mm]			
28 days exposure	-[a]	0.76 (0.17)	0.30 (0.08)
56 days exposure	-[a]	0.12 (0.08)	0.18 (0.13)
84 days exposure	0.24 (0.09)	-[a]	0.52 (0.16)
Chloride migration coefficient [10^{-12} m^2/s]			
	13.0 (1.0)[Z]	12.5 (1.6)[Z]	9.3 (1.1)
Scaled material due to freeze-thaw attack with de-icing agents – CS [kg/m^2]			
7 cycles	0.04 (0.01)	0.53 (0.15)	0.06 (0.01)
14 cycles	0.34 (0.10)	1.41 (0.02)	0.15 (0.04)
21 cycles	0.70 (0.16)	2.03 (0.07)	0.42 (0.12)
28 cycles	1.14 (0.24)	2.78 (0.14)	n/a[b]
Scaled material due to freeze-thaw attack with de-icing agents – SS [kg/m^2]			
7 cycles	0.17 (0.23)	0.11 (0.02)	0.24 (0.03)
14 cycles	0.34 (0.05)	0.34 (0.03)	0.62 (0.05)
21 cycles	0.63 (0.13)	0.90 (0.09)	1.08 (0.09)
28 cycles	1.04 (0.23)	1.63 (0.20)	n/a[b]
Scaled material due to freeze-thaw attack with de-icing agents – TS [kg/m^2]			
7 cycles	0.45 (0.06)	0.07 (0.01)	0.84 (0.07)
14 cycles	0.70 (0.11)	0.63 (0.07)	1.88 (0.08)
21 cycles	0.85 (0.14)	1.56 (0.10)	2.54 (0.07)
28 cycles	1.08 (0.19)	2.24 (0.14)	n/a[b]

[a] no carbonation observed

[b] due to a technical defect the test specimens were destroyed and the same mixture could not be tested again

[X] by a capital superscript the groups are indicated for which the mean values do not differ significantly (for the results of the compressive strength, open porosity, gas permeability and chloride migration)

Table X.5b - Results of compressive strength and durability tests on concrete containing copper slag SCS. Standard errors on the mean values are added between parentheses.

Tested parameter	CS-0	SCS-20	SCS-40
Fresh properties			
Slump [mm]	60	40	50
Air content [%]	2.8	2.4	2.0
Compressive strength [N/mm²]			
2 days	34.7 (0.31)[A]	32.2 (0.48)[B]	40.4 (0.25)
7 days	49.3 (0.88)[C,D]	47.9 (0.73)[C]	56.2 (0.47)
28 days	57.0 (0.98)[E]	59.2 (0.23)[E]	65.6 (0.31)[F]
84 days	63.9 (1.14)[G,H]	64.0 (1.47)[G,H]	69.0 (3.11)[H]
Open porosity [vol%]			
Capillary porosity (40°C)	7.5 (0.12)[I]	8.9 (0.20)	8.1 (0.16)[I]
Total porosity (105 °C)	12.6 (0.13)[K]	13.6 (0.14)	12.6 (0.16)[K]
Gel porosity (105°C-40°C)	5.1 (0.16)[M,N]	4.7 (0.15)[M]	4.5 (0.16)[L,M]
Gas permeability coefficient [10⁻¹⁷ m²] – after drying at 40 °C			
2 bar	6.7 (0.44)[O]	5.2 (0.25)[O]	5.1 (0.08)[O]
3 bar	4.5 (0.29)[P]	3.4 (0.15)[Q]	3.3 (0.07)[Q]
4 bar	4.1 (0.27)[R]	3.2 (0.15)[R,S]	3.1 (0.06)[S]
Gas permeability coefficient [10⁻¹⁷ m²] – after drying at 105 °C			
2 bar	43.3 (2.39)[T]	37.4 (1.32)[T]	30.2 (0.94)[U]
3 bar	28.7 (1.47)[V]	24.3 (0.89)[V]	19.8 (0.64)[W]
4 bar	24.5 (1.27)[X]	20.0 (0.75)[X]	16.6 (0.53)[Y]
Carbonation depth [mm]			
28 days exposure	-[a]	0.06 (0.04)	-[a]
56 days exposure	-[a]	0.12 (0.07)	-[a]
84 days exposure	0.24 (0.09)	-[a]	0.24 (0.08)
Chloride migration coefficient [10⁻¹² m²/s]			
	13.0 (1.0)[Z]	11.1 (0.6)[AA]	11.1 (0.9)[AA]
Scaled material due to freeze-thaw attack with de-icing agents – CS [kg/m²]			
7 cycles	0.04 (0.01)	n/a[b]	0.02 (0.01)
14 cycles	0.34 (0.10)	n/a[b]	0.44 (0.10)
21 cycles	0.70 (0.16)	n/a[b]	1.24 (0.20)
28 cycles	1.14 (0.24)	n/a[b]	2.13 (0.25)
Scaled material due to freeze-thaw attack with de-icing agents – SS [kg/m²]			
7 cycles	0.17 (0.23)	n/a[b]	0.17 (0.03)
14 cycles	0.34 (0.05)	n/a[b]	0.63 (0.06)
21 cycles	0.63 (0.13)	n/a[b]	1.23 (0.09)
28 cycles	1.04 (0.23)	n/a[b]	1.85 (0.16)
Scaled material due to freeze-thaw attack with de-icing agents – TS [kg/m²]			
7 cycles	0.45 (0.06)	n/a[b]	0.65 (0.12)
14 cycles	0.70 (0.11)	n/a[b]	1.60 (0.15)
21 cycles	0.85 (0.14)	n/a[b]	2.47 (0.37)
28 cycles	1.08 (0.19)	n/a[b]	3.79 (0.50)

concrete batch could not be tested again. The technical defect also made it impossible to have the results for SCS-40 after 28 cycles. The results presented in Table VIII.5 clearly show that the resistance against freeze-thaw attack with de-icing agents is worse for concrete with copper slag aggregates compared to the reference concrete. While the effect of testing different surfaces is rather limited for the reference mixture; there is a higher variability for the mixtures with copper slag. However, there is no surface type showing consequently a better or worse performance for the different amounts and types of copper slag addition.

D. Discussion

D.1. Copper slag as cement replacement

From the results obtained within this study, it can be concluded that the contribution of ground copper slag to the hydration degree of a cement paste is negligible. The hydration heat reduces with increasing mQCS content when plotted per gram of powder due to a decreasing cement content. The increase of the hydration heat when presented per gram of CEM I 52.5 N is probably caused by the increase of the water to cement ratio, as cement is replaced by an almost inert powder. The higher the water to cement ratio, the more water will be available for hydration, resulting in a higher ultimate hydration degree α_u, which can be calculated according to the following formula [Mills (1966) cited in Baert (2009)]:

$$\alpha_u = \frac{1.031 \cdot {W}/{C}}{0.194 + {W}/{C}} \qquad \text{(VIII-19)}$$

For all mixtures the ultimate hydration degrees were calculated using their water to cement ratio and the above mentioned formula. For comparison, the hydration degree after seven days was calculated as the ratio of the total measured heat to the potential heat of the cement. The latter was calculated using the mineralogical composition of the cement (see Table VIII.2) and the potential heat release of the different clinker minerals: 500 J/g, 260 J/g, 1673 J/g and 42 J/g for alite, belite, aluminate and ferrite respectively. It was found that the calculated hydration degrees after 7 days of hydration are comparable with the calculated ultimate hydration degrees (see Figure VIII.5). Comparable hydration degrees after 7 days were obtained in Baert (2009), where the effect of the water to cement ratio on the heat release of ordinary Portland cement pastes was studied. This confirms the presumption that the measured increase of the hydration heat per gram of cement can be attributed to the variation in water to cement ratio and the effect of the copper slag is nihil. The delay of the main hydration peak can be explained by the set-inhibiting properties of heavy metals in copper slag [Zain et al. (2004)]. The reduction in compressive strength with increasing copper slag content is explained by the lower cement content of the mixtures.

Looking into the literature, it is seen that most researchers use much lower replacement levels of up to 15 wt% [Tixier et al. (1997); Taha et al. (2004); Zain et al. (2004); Al-Jabri

et al. (2006); Shi et al. (2008)]. Their conclusion is that the effect of using copper slag on compressive strength is limited and only in some cases small improvements were noticed. Some researchers used activators such as cement by-pass dust and/or lime, which had no effect [Al-Jabri et al. (2006)] or only a limited effect [Taha et al. (2004)]. In Tixier et al. (1997) a positive effect on the compressive strength from adding copper slag was noticed. This copper slag was well crystallized and the fineness of the copper slag was comparable to the one of cement, which is not the case for the copper slag mQCS used in this study (see Figure VIII.2). In further research it might be interesting to start from the SCS instead of QCS, and higher fineness should be aimed for.
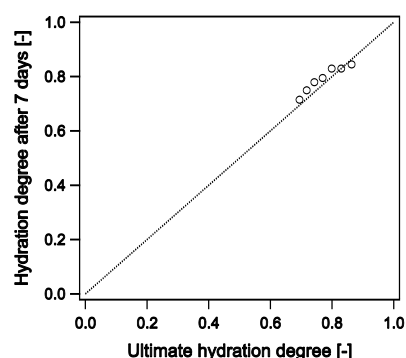
Figure VIII.5 - Comparison of the calculated ultimate hydration degree and hydration degree based on the measured hydration heat after 7 days for cement pastes with varying mQCS content

Finally it is worth mentioning that the replacement of cement by copper slag results in a better resistance regarding sulphate attack [Najimi et al. (2011)]. The replacement with copper slag up to 15% led to more than 50% decrease in sulphate expansion, accompanied with less strength degradation. Microstructure studies showed that ettringite, present in the control samples, was absent in the samples with copper slag. The results were explained as follows [Najimi et al. (2011)]: a reduced C_3A content due to the replacement with copper slag, a reduction of soluble calcium hydroxide (if copper slag would show a mediocre pozzolanic reactivity) or a less permeable microstructure due to the copper slag addition.

D.2. Copper slag as aggregate replacement

From the compressive strength test results, it was concluded that the replacement of sand by copper slag had no significant effect on the strength performance of the mortars. As the compressive strength of mortars with 40 vol% QCS was the highest and literature suggests replacement levels of about 40-50% [Shi et al. (2008); Al-Jabri et al. (2009a); Al-Jabri et al. (2011)], the replacement levels for concrete were chosen to be 20 and 40 vol%, for both the fine fraction (with QCS) and the coarse fraction (with SCS). Regarding the compressive strength of this concrete compared to the reference, it was concluded that the results were similar or even better. Similar or slightly improved compressive

strengths were expected from literature [Shi et al. (2008); Wu et al. (2010a); Wu et al. (2010b); Al-Jabri et al. (2011)] and are related to the physical properties of the copper slag. Copper slag has a better compressibility than natural aggregates, partially relieving the stress concentration, if natural sand is still the dominant fine aggregate holding the concrete matrix together. Also the angular sharp edges of the copper slag can improve the cohesion of the concrete matrix, although the glassy surface of the copper slag can have a negative effect on the cohesion. Furthermore copper slag as aggregate replacement can have a negative effect on the compressive strength due to their low water absorption, leaving excess water as discussed later in this paper.

The performance of the concrete with copper slag was compared with the reference concrete by means of durability indices (DI) [Kaid et al. (2009)]. These indices are formulated as such that values higher than 1 indicate that copper slag concrete performs better than the reference concrete. The results are presented in Figure VIII.6.
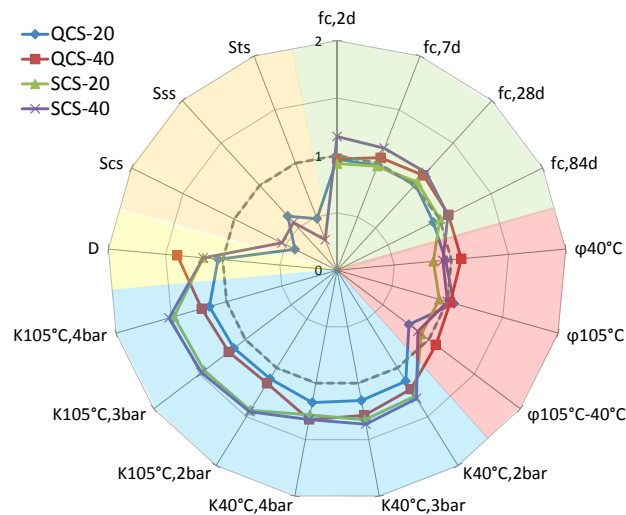
Figure VIII.6 – Durability indices [-] to compare the performance of concrete with copper slag to the reference concrete: (fc,xd) x days compressive strength, (φx°C) open porosity after drying at x °C, (Kx°C,nbar) gas permeability coefficient after drying at x°C with an applied pressure of n bar, (D) non-steady-state chloride migration coefficient , (Sxs) Scaled material after 28 cycles for the casting (cs), sawn (ss) or troweled (ts) surface

It was found that the effect of aggregate replacement levels of 20 and 40 vol% was limited regarding the open porosity and gas permeability. For SCS-20 and SCS-40 the gas permeability was even reduced compared to the reference. Regarding carbonation and chloride migration, the performance of the concrete with copper slag is comparable with the one of the reference concrete. However, in the test for freeze-thaw attack with de-icing agents, the concretes with copper slag performed worse compared to the reference and the surface scaling after 28 standardized freeze-thaw cycles increased significantly. Depending on the tested surface and mixture, scaling increased by 57 to 252% due to

the addition of copper slag. As required by NBN EN 1339 (2003) the amount of scaled material should not exceed the limit of 1 kg/m². In Table VIII.5 it is seen that even the reference mixture is slightly exceeding the limit. The performance regarding freeze-thaw attack with de-icing agents is strongly related to the air content of fresh concrete. As can be seen in Table VIII.5 the air contents are rather low for both the reference and copper slag concrete. The European standard NBN EN 206-1 (2001) and the Belgian standard NBN B 15-001 (2004) require an air content of at least 4% for a nominal maximum aggregate size of 20 mm. In the American standard ACI 201.2R (2008) requires even an air content of 6-7%. It is thus advised to improve the resistance against freeze-thaw attack with de-icing agents by means of e.g. air entraining agents.

An effect on strength and durability from the addition of copper slag was expected, as the low water absorption and glass-like smooth surface create a water excess and thus a risk for bleeding [Shi et al. (2008); Al-Jabri et al. (2009b); Wu et al. (2010a)], since the water to cement ratio is kept constant. This excess water is water that is not absorbed by the aggregates and becomes available in the cement matrix which results in a higher content of voids, micro cracks and capillary channels, especially when the substitution rate exceeds 20% [Wu et al. (2010a)]. This has of course its consequences for the performance of the concrete. From the results reported in this paper it was concluded that mainly the performance regarding freeze-thaw attack with de-icing agents of the copper slag concrete was reduced compared to the reference concrete. In case of the copper slag concrete it might thus not be only the air content of the fresh concrete that resulted in the inferior performance, but also the quality of the concrete surfaces is expected to be reduced due to an excess of water and thus a risk for bleeding and segregation [Shi et al. (2008)]. In order to compensate for this excess in water, less water could be added. Al-Jabri et al. (2009b) replaced sand by copper slag keeping the workability constant and adapting the water to cement ratio. They concluded that a 100% replacement of the sand by copper slag results in a water reduction of 22%. In this study both the water to cement ratio (0.45) and amount of superplasticizer (2ml/kg binder) of the copper slag concrete were kept constant. As observed in Table 5, the slump of the copper slag mixtures is rather low, although the risk for bleeding was observed. A detailed study on the water demand of the mixtures is required. The optimum should allow a sufficient slump of the concrete, without the risk for bleeding.

References

ACI 201.2R (2008). "Guide to Durable Concrete. Reported by ACI Committee 201."

Aïtcin, P. C. and A. M. Neville (2003). "How the water-cement ratio affects concrete strength." Concrete International 25(8): 51-58.

Al-Jabri, K. S., A. H. Al-Saidy and R. Taha (2011). "Effect of copper slag as a fine aggregate on the properties of cement mortars and concrete." Construction and Building Materials 25(2): 933-938.

Al-Jabri, K. S., M. Hisada, S. K. Al-Oraimi and A. H. Al-Saidy (2009a). "Copper slag as sand replacement for high performance concrete." Cement and Concrete Composites 31(7): 483-488.

Al-Jabri, K. S., M. Hisada, A. H. Al-Saidy and S. K. Al-Oraimi (2009b). "Performance of high strength concrete made with copper slag as a fine aggregate." Construction and Building Materials 23(6): 2132-2140.

Al-Jabri, K. S., R. A. Taha, A. Al-Hashmi and A. S. Al-Harthy (2006). "Effect of copper slag and cement by-pass dust addition on mechanical properties of concrete." Construction and Building Materials 20(5): 322-331.

Amathieu, L., T. A. Bier and K. L. Scrivener (2001). Mechanisms of Set Acceleration of Portland Cement Through CAC Addition. International conference on Calcium Aluminate Cements (CAC), Edinburgh, Scotland**:** 303-317.

Baert, G. (2009). Physico-Chemical Interactions in Portland Cement - (High Volume) Fly Ash Binders. PhD Thesis. Ghent, Ghent University. PhD.

Baltrus, J. P. and R. B. LaCount (2001). "Measurement of adsorption of air-entraining admixture on fly ash in concrete and cement." Cement and Concrete Research 31(5): 819-824.

Bayoux, J. P., A. Bonin, S. Marcdargent and M. Verschaev (1990). Study of the Hydration Properties of Aluminous Cement and Calcium Sulphate Mixes. Calcium Aluminate Cements, E & F. N. Spon, London, U.K.**:** 320-334.

Brown, P. W. and P. LaCroix (1989). "The kinetics of ettringite formation." Cement and Concrete Research 19(6): 879-884.

Bullard, J. W., H. M. Jennings, R. A. Livingston, A. Nonat, G. W. Scherer, J. S. Schweitzer, K. L. Scrivener and J. J. Thomas (2011). "Mechanisms of cement hydration." Cement and Concrete Research 41(12): 1208-1223.

Bushnell-Watson, S. M. and J. H. Sharp (1986). "The effect of temperature upon the setting behaviour of refractory calcium aluminate cements." Cement and Concrete Research 16(6): 875-884.

Bushnell-Watson, S. M. and J. H. Sharp (1990). "Further studies of the effect of temperature upon the setting behaviour of refractory calcium aluminate cements." Cement and Concrete Research 20(4): 623-635.

Collepardi, M., G. Baldini, M. Pauri and M. Corradi (1978). "Tricalcium aluminate hydration in the presence of lime, gypsum or sodium sulfate." Cement and Concrete Research 8(5): 571-580.

Corstanje, W. A., H. N. Stein and J. M. Stevels (1973). "Hydration reactions in pastes C3S+C3A+CaSO4.2aq+H2O at 25°C.I." Cement and Concrete Research 3(6): 791-806.

Corstanje, W. A., H. N. Stein and J. M. Stevels (1974a). "Hydration reactions in pastes C3S+C3A+CaSO4.2aq+water at 25°C. II." Cement and Concrete Research 4(2): 193-202.

Corstanje, W. A., W. N. Stein and J. M. Stevels (1974b). "Hydration reactions in pastes C3S + C3A + CaSO4 .2aq. + water at 25°C.III." Cement and Concrete Research 4(3): 417-431.

De Belie, N., J. Monteny and L. Taerwe (2002). "Apparatus for accelerated degradation testing of concrete specimens." Materials and Structures 35(251): 427-433.

De Schepper, M., P. Van den Heede, C. Windels and N. De Belie (2011). The resistance of Completely Recyclable Concrete to carbonation, chloride penetration and freeze-thaw attack with de-icing agents. 12th International Conference on Durability of building materials and components, Porto**:** 2061-2068.

De Schepper, M., P. Verlé, I. Van Driessche and N. De Belie (accepted for publication May 2014). "The use of secondary slags in Completely Recyclable Concrete." Journal of Materials in Civil Engineering.

Desnerck, P. (2011). Compressive, Bond and Shear Behaviour of Powder-Type Self-Compacting Concrete. Ghent, Ghent University. PhD.

Edmonds, R. N. and A. J. Majumdar (1988). "The hydration of monocalcium aluminate at different temperatures." Cement and Concrete Research 18(2): 311-320.

Edmonds, R. N. and A. J. Majumdar (1989). "The hydration of Secar 71 aluminous cement at different temperatures." Cement and Concrete Research 19(2): 289-294.

Evju, C. and S. Hansen (2001). "Expansive properties of ettringite in a mixture of calcium aluminate cement, Portland cement and β-calcium sulfate hemihydrate." Cement and Concrete Research 31(2): 257-261.

Feldman, R. F. and V. S. Ramachandran (1966). "The influence of CaSO4.2H2O upon the hydration character of 3CaO.Al2O3." Magazine of Concrete Research 18(57): 185-196.

Gawlicki, M., W. Nocuń-Wczelik and Ł. Bąk (2010). "Calorimetry in the studies of cement hydration." Journal of Thermal Analysis and Calorimetry 100(2): 571-576.

Goñi, S., M. P. Lorenzo and J. L. Sagrera (1994). "Durability of hydrated portland cement with copper slag addition in NaCl + Na2SO4 medium." Cement and Concrete Research 24(8): 1403-1412.

Gorai, B., R. K. Jana and Premchand (2003). "Characteristics and utilisation of copper slag—a review." Resources, Conservation and Recycling 39(4): 299-313.

Gu, P., J. J. Beaudoin, E. G. Quinn and R. E. Myers (1997). "Early Strength Development and Hydration of Ordinary Portland Cement/Calcium Aluminate Cement Pastes." Advanced Cement Based Materials 6(2): 53-58.

Gu, P., Y. Fu and J. J. Beaudoin (1994). "A study of the hydration and setting behaviour of OPC-HAC pastes." Cement and Concrete Research 24(4): 682-694.

Gupta, P., S. Chatterji and J. W. Jeffery (1973). Cement Technology 4: 1-4.

Hewlett, P. C. (1998). Lea's Chemistry of Cement and Concrete (Fourth Edition). Oxford, Butterworth-Heinemann.

Kaid, N., M. Cyr, S. Julien and H. Khelafi (2009). "Durability of concrete containing a natural pozzolan as defined by a performance-based approach." Construction and Building Materials 23(12): 3457-3467.

Khanzadi, M. and A. Behnood (2009). "Mechanical properties of high-strength concrete incorporating copper slag as coarse aggregate." Construction and Building Materials 23(6): 2183-2188.

Klaus, S. R., J. Neubauer and F. Goetz-Neunhoeffer (2013). Calculation of heat flow from QXRD data for the hydration of a synthetic calcium aluminate cement. 1st International Conference on the Chemistry of Construction Materials, Berlin**:** 89-92.

Kuzel, H. J. (1996). "Initial hydration reactions and mechanisms of delayed ettringite formation in Portland cements." Cement and Concrete Composites 18(3): 195-203.

Locher, F. W., W. Richartz and S. Sprung (1976). "Erstarren von Zement - Teil I: Reaktion und Gefügeentwicklung (Setting of cement - Part I: Reaction and development of structure)." Zement-Kalk-Gips 29: 435-442.

Mehta, P. K. (1976). "Scanning electron micrographic studies of ettringite formation." Cement and Concrete Research 6(2): 169-182.

Mills, R. H. (1966). Factors influencing cessation of hydration in water-cured cement pastes. Special Report No.90. Symposium on the Structure of Portland Cement Paste and Concrete, Washington D.C.**:** 406.

Najimi, M., J. Sobhani and A. R. Pourkhorshidi (2011). "Durability of copper slag contained concrete exposed to sulfate attack." Construction and Building Materials 25(4): 1895-1905.

NBN B 15-001 (2004). "Supplement to NBN EN 206-1 - Concrete - Specification, performance, production and confirmity."

NBN EN 206-1 (2001). "Concrete - Part 1 : Specification, performance, production and conformity."

Plowman, C. and J. G. Cabrera (1984). "Mechanism and kinetics of hydration of C3A and C4AF. Extracted from cement." Cement and Concrete Research 14(2): 238-248.

Pommersheim, J. and J. Chang (1988). "Kinetics of hydration of tricalcium aluminate in the presence of gypsum." Cement and Concrete Research 18(6): 911-922.

Quennoz, A. and K. L. Scrivener (2012). "Hydration of C3A–gypsum systems." Cement and Concrete Research 42(7): 1032-1041.

Reinhardt, H. W. and C. U. Grosse (2004). "Continuous monitoring of setting and hardening of mortar and concrete." Construction and Building Materials 18(3): 145-154.

Robeyst, N. (2010). Monitoring Setting and Microstructure Development in Fresh Concrete with the Ultrasonic Through-Transmission Method. Ghent, Ghent University.

Robeyst, N., G. De Schutter, C. Grosse and N. De Belie (2011). "Monitoring the effect of admixtures on early-age concrete behaviour by ultrasonic, calorimetric, strength and rheometer measurements." Magzaine of Concrete Research 63(10): 707-721.

Robeyst, N., C. U. Grosse and N. De Belie (2009). "Measuring the change in ultrasonic p-wave energy transmitted in fresh mortar with additives to monitor the setting." Cement and Concrete Research 39(10): 868-875.

Robeyst, N., E. Gruyaert, C. U. Grosse and N. De Belie (2008). "Monitoring the setting of concrete containing blast-furnace slag by measuring the ultrasonic p-wave velocity." Cement and Concrete Research 38(10): 1169-1176.

Schwartzentruber, A. and C. Chatherine (2000). "La méthode du mortier de béton équivalent (MBE) - un nouvel outel d'aide à la formulation des bétons adjuvantés." Matériaux et Construction 33: 475.

Schwiete, H. E., U. Ludwig and P. Jager (1966). Investigations in the system 3CaO.Al2O3-CaSO4-H2O. Spec. Rept. Highway Research Board. 90**:** 353-366.

Scrivener, K. L., J.-L. Cabiron and R. Letourneux (1999). "High-performance concretes from calcium aluminate cements." Cement and Concrete Research 29(8): 1215-1223.

Shi, C., C. Meyer and A. Behnood (2008). "Utilization of copper slag in cement and concrete." Resources, Conservation and Recycling 52(10): 1115-1120.

Sisomphon, K. and L. Franke (2007). "Carbonation rates of concretes containing high volume of pozzolanic materials." Cement and Concrete Research 37(12): 1647-1653.

Skalny, J. and M. E. Tadros (1977). "Retardation of Tricalcium Aluminate Hydration by Sulfates." Journal of the American Ceramic Society 60: 174-175.

Taerwe, L. and G. De Schutter (2006). Betontechnologie (Syllabus Concrete Technology), Ghent University.

Taha, R., A. Al-Rawas, K. Al-Jabri, A. Al-Harthy, H. Hassan and S. Al-Oraimi (2004). "An overview of waste materials recycling in the Sultanate of Oman." Resources, Conservation and Recycling 41(4): 293-306.

Taha, R. A., A. S. Alnuaimi, K. S. Al-Jabri and A. S. Al-Harthy (2007). "Evaluation of controlled low strength materials containing industrial by-products." Building and Environment 42(9): 3366-3372.

Taylor, H. F. W. (1997). Cement Chemistry. London, Thomas Telford Publishing.

Thomas, B. S., S. Anoop and V. S. Kumar (2012). "Utilization of Solid Waste Particles as Aggregates in Concrete." Procedia Engineering 38(0): 3789-3796.

Tixier, R., R. Devaguptapu and B. Mobasher (1997). "The effect of copper slag on the hydration and mechanical properties of cementitious mixtures." Cement and Concrete Research 27(10): 1569-1580.

Van den Heede, P., J. Furniere and N. De Belie (2013). "Influence of air entraining agents on deicing salt scaling resistance and transport properties of high-volume fly ash concrete." Cement and Concrete Composites 37(0): 293-303.

Van den Heede, P., M. Maes, R. Caspeele and N. De Belie (2012). Chloride diffusion tests as experimental basis for full probabilistic service life prediction and life-cycle assessment of concrete with fly ash in a submerged marine environment. 3rd International symposium on Life-cycle Civil Engineering (IALCCE 2012) : Life-cycle and sustainability of civil infrastructure systems. A. Strauss, D. M. Frangopol and K. Bergmeister. Vienna, Austria, CRC Press**:** 913-920.

Voigt, T., C. Grosse, Z. Sun, S. P. Shah and H. W. Reinhardt (2005). "Comparison of ultrasonic wave transmission and reflection measurements with P- and S-waves on early age mortar and concrete." Materials and Structures 38(282): 729-738.

Wu, W., W. Zhang and G. Ma (2010a). "Mechanical properties of copper slag reinforced concrete under dynamic compression." Construction and Building Materials 24(6): 910-917.

Wu, W., W. Zhang and G. Ma (2010b). "Optimum content of copper slag as a fine aggregate in high strength concrete." Materials & Design 31(6): 2878-2883.

Zain, M. F. M., M. N. Islam, S. S. Radin and S. G. Yap (2004). "Cement-based solidification for the safe disposal of blasted copper slag." Cement and Concrete Composites 26(7): 845-851.

PART III
CRC clinker & cement quality

IX - The chemistry of Ordinary Portland Cement

In part I, several CRC mixtures were designed for reincarnation within the cement production. With CRC as the only ingredient, OPC will be produced in a laboratory setting simulating the industrial process. An overview of the industrial production process and its chemical reactions are given in this chapter. For evaluation of the cement quality, the hydration process of the CRC cement was compared to the one of OPC. The OPC hydration process is also presented in this chapter. Detailed descriptions can be found in Taylor (1997) and Hewlett (1998).

A. The production of Ordinary Portland Cement

A.1. The industrial production process

The cement production process can be divided into three phases: the preparation of a cement raw meal, the burning of the raw mixture for Portland Clinker production and the milling of the clinker (with additives) for the production of cement. In Figure IX.1 possible process flow sheets with different kiln systems for a cement plant are presented. According to Hewlett (1998) the choice for a certain rotary kiln system depends on the available raw materials, the fuel consumption, the required output and the available capital investment. In practice the moisture content of the raw materials is crucial. Indeed, when too high, only the wet or semi-wet production processes remain possible. As a consequence, the output per day decreases (from 100-8500 t/day to 100-3340 t/day), the fuel consumption increases (900-2200 kcal/kg clinker instead of 800-950 kcal/kg clinker) and the required investment becomes higher due to the need for a longer rotary kiln (up to 232 m instead of up to 110 m).

i. The preparation of a cement raw meal

The origin of the raw materials not only defines the rotary kiln system, it mostly also defines the location of a cement plant. As lime (CaO), mostly available as calcite ($CaCO_3$), is the main ingredient for cement production, a cement plant is preferably located close to a limestone quarry reducing the costs related to transportation as only a conveyor belt is needed. For the other ingredients, such as shells, chalk, sand, clay, fly ash, ore etc. stockpiles are gathered at the cement plants. Unless these materials can also be mined near the factory and transportation by a conveyor belt is possible, these materials are transported preferably by boat or train and otherwise by truck.

The wet process

The wet process is ideal for soft and moist raw materials which can be dredged, e.g. limestone, marl and clay (see Figure IX.2). As they are soft and moist in nature and can easily be mixed with water, a fine homogeneous slurry is prepared (see Figure IX.3), which is then brought to the kiln for the clinkering process. Although the preparation of a wet raw meal has its advantages when used for the proper soft and moist raw materials, its low fuel efficiency makes the process less common these days.
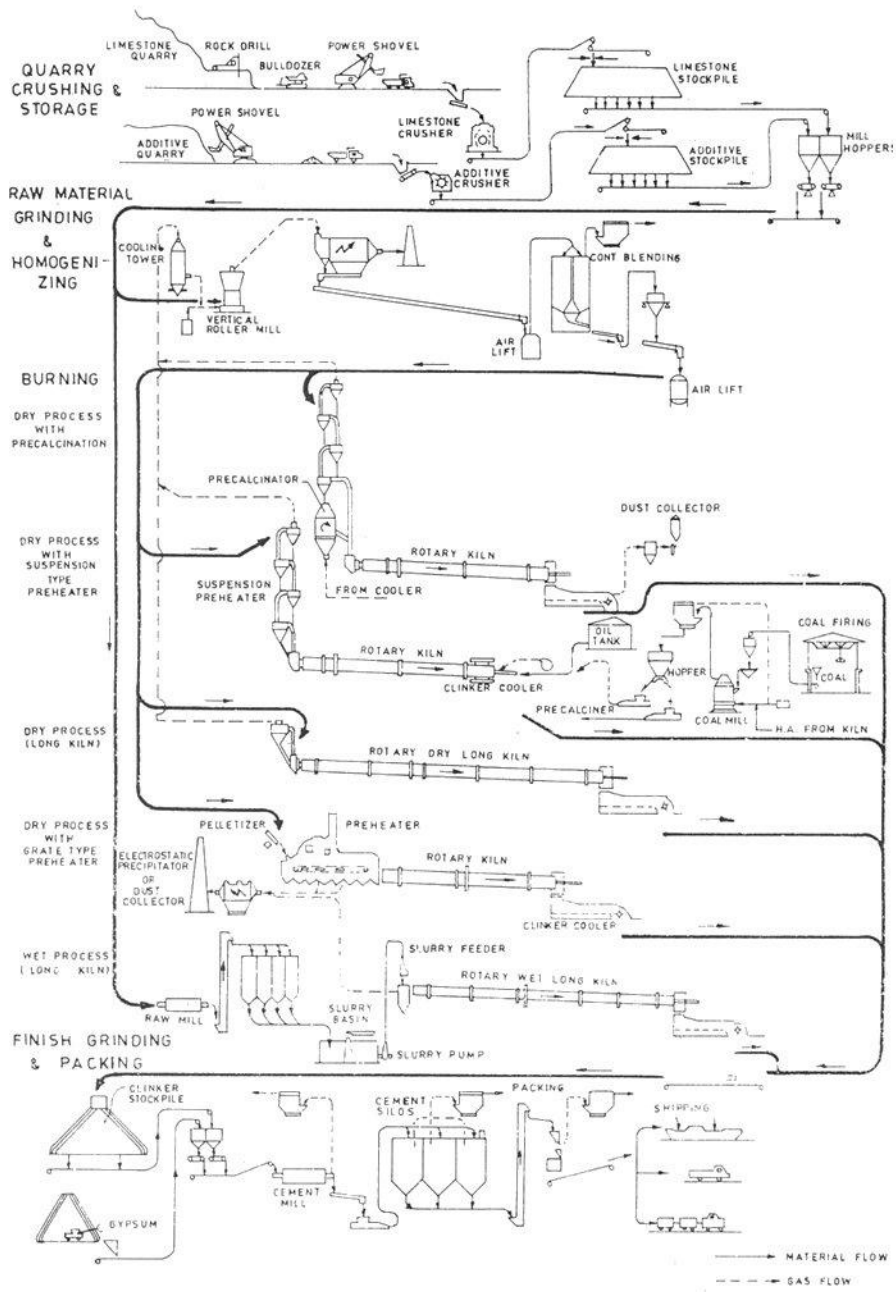
Figure IX.1 – Overview of possible process flow sheets for cement production [Department of Science and Industrial Research et al. (1988)]

Figure IX.2 – The dredging of soft limestone [Holcim Belgium (2013a)]

Figure IX.3 – The preparation of the slurry [Holcim Belgium (2013a)]

The dry process

When hard raw materials are available, they first pass through a series of crushing, stockpiling, milling and blending stages. From the obtained fine powder, typically 85% passes through a 90 μm sieve. The raw meal will then be preheated, and frequently also passes a precalciner before entering the actual burning process in the kiln. In a preheater, the powder falls through a series of cyclones in less than one minute, whereby the powder is dispersed in a stream of hot gas coming from the kiln. Entering the kiln, the powder has a temperature of about 800°C and about 40% of the $CaCO_3$ is already decarbonated. The presence of this preheater shortens the length of the kiln, reducing the capital investment needed and accelerating the production process. Between the preheater and the kiln, a precalciner can be used to optimize the thermal pre-treatment. After its passage through the precalciner 90-95% of the raw meal will be decarbonated, wherefore the precalciner uses 50-65% of the fuel. One of the advantages of the precalciner is that part of the fuel is burnt at a lower temperature, releasing less NO_x.

The semi-wet and semi-dry process

To increase the fuel efficiency of the kiln process if only moist raw materials are available, part of the water can be pressed out. The obtained raw meal with a water

content somewhat below 20% can then continue towards the wet or dry process. In the semi-dry process, the raw meal is made into nodules with a water content just over 10%, which are fed to a moving grate preheater. The process is thus comparable to the dry process, but the fuel efficiency of a preheater with the cyclones is higher.

ii. The production of a Portland Clinker by heating the raw meal

The homogeneous raw meal entering the rotary kiln as a slurry, a powder or pellets is gradually heated to about 1450 °C. The kiln itself is a cylindrical tube lined with refractory bricks on the inside, rotating around its longitudinal axis (see Figure IX.4). Due to the inclination to the horizontal, the raw meal slowly moves towards the flame. At the entrance of the furnace the raw meal is heated by contact with the combustion gas, while towards the end of the furnace also the radiation of the flame will heat the raw materials. The upper zone of a wet rotary kiln has a temperature of 100 to 500 °C as the combustion gasses lost already a lot of heat along the way. In this zone, the raw meal is dehydrated. The decarbonation process takes place between 800 and 1100 °C. For the dry rotary kiln with a preheater this process starts already in the cyclones, when also a precalciner is used, the raw meal enters the furnace almost completely decarbonated. Ultimately, the Portland Clinker is formed in the zone of the kiln with a temperature of about 1450 °C. This Portland Clinker is a round grey particle with a diameter of 3-25 mm (see Figure IX.5).

Figure IX.4 - A rotary kiln for the wet process [Holcim Belgium (2013a)]

iii. The production of Ordinary Portland Cement by milling the Portland Clinker

Once the Portland Clinker is manufactured, it is fed to a store to obtain a measure of blending and to allow it to cool to ambient temperature. Once at ambient temperature the clinker is milled together with calcium sulphate as setting regulator. Although this final step seems simple, it is a crucial one and has an important influence on the hydration process and strength development of the ultimate mortar or concrete. The finer the cement, the higher the hydration degree and the better the strength development. As generally known, the addition of calcium sulphate is necessary to control the hydration of C_3A, but it will also affect the hydration of the strength giving calcium silicates [Amathieu et al. (2001)]. The added amount of calcium sulphate is

therefore a compromise between the quantity needed for controlling the hydration of the aluminate phase and the one required for a desired strength development.
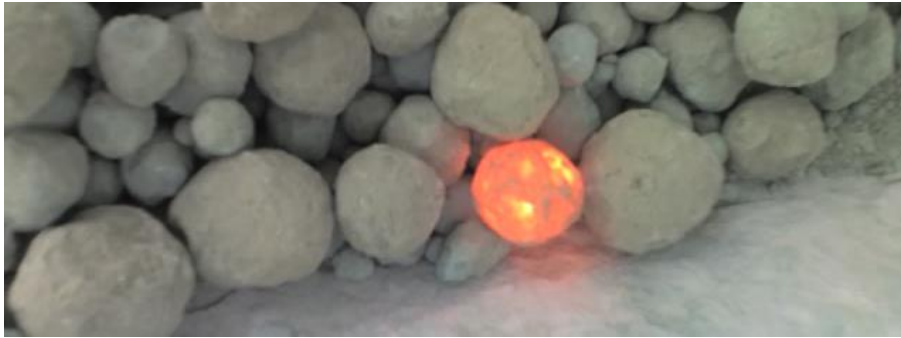
Figure IX.5 - Typical clinker nodules [Wikipedia (2009)]

Earlier, a ball mill was used at most manufacturing plants (see Figure IX.6). To obtain the fine powder, the milling process is normally divided in at least two stages. For the larger clinker lumps, large balls (90-100 mm) are needed to break them down, while small balls (13 mm) are required to obtain the fine cement powder. Therefore a cement plant has two or more ball mills, or one ball mill with at least two compartments. A separator might be used to select coarse particles for additional milling.

However, technological developments over the years resulted in three additional types of grinding systems used today: a vertical roller mill, high pressure grinding rolls (HPGR) and a horizontal roller press mill [Sorrentino (2011)]. The vertical roller mill uses approximately 40% less power compared to a traditional ball mill, and with an integral separator it is mostly used for finish grinding. The HPGR is used for primary grinding and semi-finish grinding in combination with ball mills. Both HPGR and the horizontal roller press mills can be used for a single-stage grinding process. The horizontal roller press mill uses 50% or 20% less energy compared to respectively the ball mill or the vertical mill.

Figure IX.6 - The inside of a ball mill [Holcim Belgium (2013a)]

A.2. The chemical reactions of the clinkering process

In the manufacturing process of Portland Clinker, (mostly) inert materials are converted into a hydraulic binder. To obtain a qualitative hydraulic binder, there are strict requirements for the chemical composition of the raw materials (see PART I). Figure IX.7 gives an overview of the typical phases during the formation of Portland Clinker.
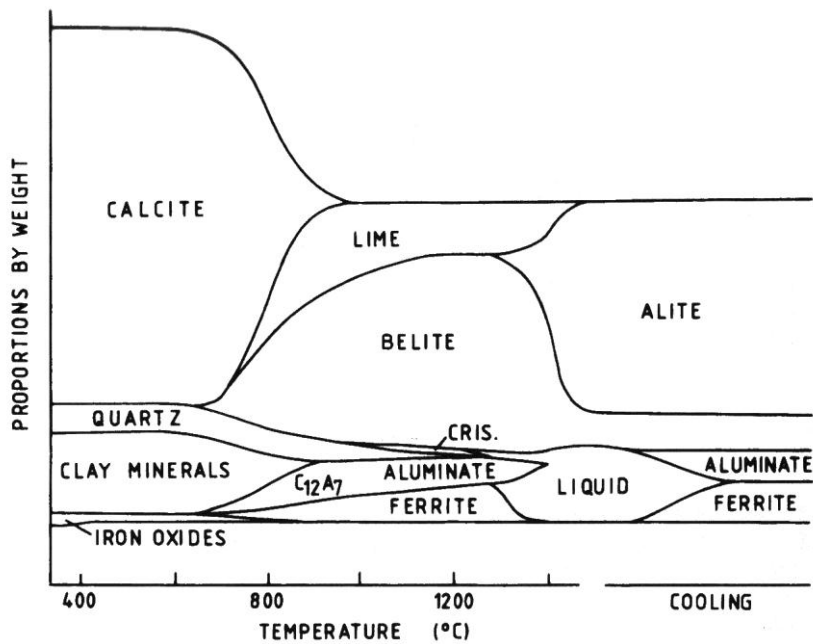
Figure IX.7 – Schematic diagram showing the variation in typical contents of phases during the formation of Portland cement clinker [Taylor (1997)]

i. Reactions below 1300 °C

A big weight loss is observed for the reactions below 1300 °C, which results from the release of water vapour and carbon dioxide. Besides the loss of free water, water will evaporate upon the decomposition of clay minerals. The behaviour upon heating of clay minerals depends on structure, composition, crystal size and degree of crystallinity. Around a temperature of 100-250 °C interlayer and adsorbed water will be released. The first dehydroxylation reactions of clay minerals begin at 300-400 °C, and are rapid at 500-600 °C.

The loss of CO_2 gas is the result of the dissociation of carbonate materials, such as calcite ($CaCO_3$) and dolomite ($CaMg(CO_3)_2$). The decarbonation rate of calcite is significant at 500-600 °C if the partial pressure of CO_2 is sufficiently low or if the calcite is intimately mixed with materials such as quartz and decomposition products of clay minerals. The rapid decomposition of dolomite begins in air at about 750 °C. Initially periclase and a

carbonate of higher Ca/Mg ratio will be formed. Nonetheless, the decomposition temperature is much affected by the presence of other substances.

As mentioned before, the decarbonation of calcite is stimulated by the presence of quartz or the decomposition products of clay minerals. Indeed, CaO easily reacts with SiO_2, Al_2O_3 and Fe_2O_3. This is not only beneficial for the carbonation process, but it also results in the formation of the first hydraulic components such as ferrite (C_4AF), but with a lower Al/Fe ratio, and belite (C_2S). Although tricalcium aluminate (C_3A) can form at 850 °C, the early aluminate phases present are monocalcium aluminate (CA), mayenite ($C_{12}A_7$) and less frequently gehlenite (C_2AS). $C_{12}A_7$ will precipitate in the final clinker, if the Al_2O_3/Fe_2O_3 ratio exceeds 1.7 [Sorrentino (2011)].

ii. Reactions from 1300 °C to 1450 °C

Between 1300 and 1450 °C, a melt of aluminate, ferrite and some belite is formed. The clinker will have a liquid content of 20-30% around 1450 °C, enabling the formation of alite from belite and free lime. As the melt is the medium in which the crucial calcium silicate alite is formed, the importance of the silica and alumina moduli comes forward. The amount of liquid formed is strongly dependent on the Al_2O_3 and Fe_2O_3 content, and to a smaller extent also MgO, K_2O and Na_2O. If the silica modulus is too high, less melt will be available to facilitate the diffusion of CaO towards belite to form alite. The alumina modulus will have its main influence at low clinkering temperatures, because from 1400 °C onwards the quantity of liquid is not depending on the Al_2O_3/Fe_2O_3 ratio.

iii. Reactions during cooling

Upon cooling, the liquid will crystallize whereby aluminate and ferrite will be present as interstitial material around the alite and belite crystals. Slow cooling, especially between 1450 to 1200 °C, should be avoided as alite might partially be transformed into belite, C_3A will crystallise from the flux in a form which is more reactive leading to setting problems, and in clinker high in magnesia, periclase might crystallise from the flux resulting in long term unsoundness. Alite and belite will undergo the phase transformations described in chapter II-A. The ultimate appearance of alite (mostly monoclinic, rarely triclinic) and belite (mostly the β polymorph) will however be dependent on the incorporation of substituent ions.

iv. Enthalpy changes in clinker formation

While the dehydroxylation and decarbonation reactions are endothermic, the formation of the clinkering minerals is exothermic. An overview of the standard enthalpies of common reactions in a cement kiln is presented in Table IX.1. It is seen that the decarbonation of calcite consumes most of the energy. The theoretical enthalpy requirement for burning a cement clinker is about 1800 MJ/t. At the moment, the most efficient clinker kiln (short kiln with a multistage preheater and cooling system) consumes 3000 MJ/t of clinker [Sorrentino (2011)]. This energy requirement is however more a punctually short term performance, and not an annual average. Although there

are still margins for improvement, the efficiency has improved significantly from the old wet process in a long kiln (5000-6000 MJ/t of clinker).

Table IX.1 - Standard enthalpies of clinkering reactions [Taylor (1997)]

Reaction	ΔH (kJ)	For 1kg of
$CaCO_3$ (calcite) $\rightarrow$ CaO + CO_2 (g)	+1782	$CaCO_3$
AS_4H (pyrophyllite) $\rightarrow$ α-Al_2O_3 + 4 SiO_2 (quartz) + H_2O (g)	+224	AS_4H
AS_2H_2 (kaolinite) $\rightarrow$ α-Al_2O_3 + 2 SiO_2 (quartz) + H_2O (g)	+538	AS_2H_2
2 FeO·OH (goethite) $\rightarrow$ α-Fe_2O_3 + H_2O (g)	+254	FeO·OH
2 CaO + SiO_2 (quartz) $\rightarrow$ β-C_2S	-734	C_2S
3 CaO + SiO_2 (quartz) $\rightarrow$ C_3S	-495	C_3S
3 CaO + α-Al_2O_3 $\rightarrow$ C_3A	-27	C_3A
4 CaO + α-Al_2O_3 + α-Fe_2O_3 $\rightarrow$ C_4AF	-105	C_4AF

Values for starting materials and products at 25 °C and 0.101 MPa. The value for C_4AF is for 20 °C.

B. The hydration of Ordinary Portland Cement

B.1. The chemical reactions of a hydrating Ordinary Portland Cement

The hydration process of cement is a dissolution-precipitation process. Most studies of the cement hydration processes focus on the hydration of the alite and aluminate phases, as these are most reactive [Scrivener and Nonat (2011)]. After 1 day, 40-60% and 20-80% of respectively the alite and aluminate phases have reacted. The high variability for aluminate is probably due to differences in microstructure of the interstitial phases and sulphate content. Belite clearly shows only little reaction, with a hydration degree less than 20% after 7-10 days. The reactivity of ferrite should however not be underestimated, as a degree of hydration around 40% after 1 day was observed in the study of Kocaba (2010).

The hydration reactions of the silicates are as follows [Hewlett (1998)]:

$$C_3S + (3 - x + y)H \rightarrow C_xSH_y + (3 - x)CH \qquad \text{(IX-1)}$$
$$C_2S + (2 - x + y)H \rightarrow C_xSH_y + (2 - x)CH \qquad \text{(IX-2)}$$
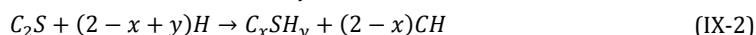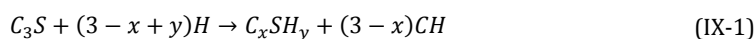
The strength of a hydrated cement paste is ascribed to the poorly crystalline calcium silicate hydrate C_xSH_y, having the properties of a rigid gel. Its composition varies and depends on the Ca/Si ratio of the system, the water to cement ratio, the temperature and the hydration degree, and for this reason the phase is often written as C-S-H. The portlandite (CH) from the reaction of alite and belite does not contribute to the strength of the concrete, but gives concrete its high pH, preventing the corrosion of rebars. When Supplementary Cementitious Materials (SCM) are used, portlandite will participate in activating the slag reaction (in case of e.g. blast furnace slag) or enabling the pozzolanic reaction (in case of e.g. fly ash or silica fume).

The hydration of the aluminate phase is described in detail in chapter VII-A.2. The hydration products of the ferrite phases are similar to those formed from aluminate, but the rates of reaction differ and seem to be depending on the Al/Fe ratio. Generally the reactivity declines with increasing Fe content [Taylor (1997)].

The hydration reactions of OPC are associated with a heat release. The enthalpy of hydration for each clinker mineral is given in Table IX.2. Although the hydration enthalpy of the aluminate phase has the highest values, it is the hydration heat of the alite phase that dominates, as it is the main constituent of OPC.

Table IX.2 - Enthalpy of hydration of pure clinker minerals [Hewlett (1998)]

Starting phase	Reaction product	Enthalpy of (complete) hydration	
		kJ/kg	kJ/mol
C_3S (+ H)	CSH + CH	520	118
β-C_2S (+ H)	CSH + CH	260	45
C_3A (+ CH + H)	C_4AH_{19}	1160	314
C_3A (+ H)	C_3AH_6	910	245
C_3A (+ CSH_2 + H)	C_4ASH_{12} (AFm)	1140	309
C_3A (+ CSH_2 + H)	$C_6AS_3H_{32}$ (AFt)	1670	452
C_4AF (+ CH + H)	$C_3(A,F)H_6$	420	203

The rate of heat evolution during the hydration of an OPC is thus dominated by the one of alite, which is given in Figure IX.8. An initial sharp hydration peak is followed by a rapid slowdown (stage 1) ending in an induction or dormant period (stage 2), which is of great practical importance for transportation and placing of concrete. According to Scrivener and Nonat (2011), a slow dissolution period after an initial rapid reaction with water is the norm, rather than the exception for complex iono-covalent minerals. In case of alite, the addition of water to the cement results in a high under saturation, which provides the needed energy for the formation of etch pits on the alite surface. Once a certain threshold is exceeded, the dissolution rate slows down rapidly and dissolution can only take place step by step from the existing defects. In case of the aluminate phases the adsorption of sulphate ions on the reactive sites will inhibit the dissolution of the mineral and ettringite will start to form slowly.

The pattern of the main hydration peak, with its acceleration (stage 3) and deceleration period (stage 4), can be seen in most cementitious systems and is also typical for many metallurgical reactions. This pattern can be described by the Avrami equation [Scrivener and Nonat (2011)]. At first, the surface of the precipitates grows, and thus the rate of hydration. Later on the surfaces of the precipitates start to impinge and the available surface for reaction decreases, together with the rate of hydration. Ultimately, the hydration process will slowly continue (stage 5).
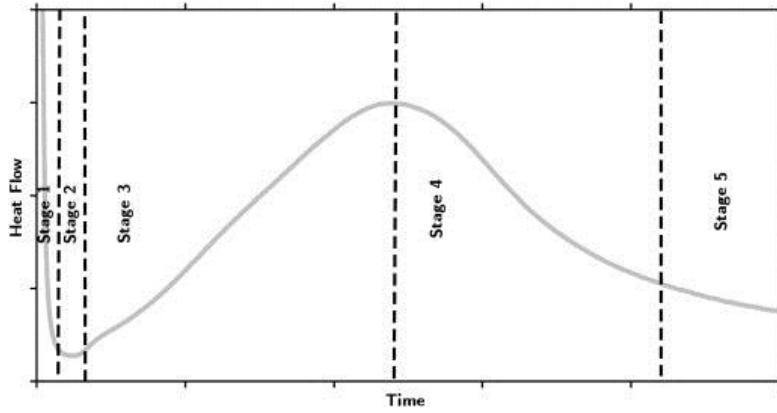
Figure IX.8 - Rate of heat evolution during hydration of alite, (w/c =0.4). Stages 1 and 2, slowdown in dissolution and induction period; stage 3 acceleration period; stage 4 deceleration period; stage 5 slow ongoing hydration [Scrivener and Nonat (2011)]

B.2. Modelling the hydration of Ordinary Portland Cement

The cement hydration model used in this study is described in detail elsewhere [Lothenbach and Winnefeld (2006)]. This model is based on an empirical approach that describes the dissolution of the clinker phases as a function of time for OPC [Parrot and Killoh (1984)], in combination with a thermodynamic equilibrium model that calculates the hydrate assemblages as a function of time using GEMS 3 [Kulik et al. (2013)].

The degree of hydration α_t [-] at time t [days] can be expressed as:

$$\alpha_t = \alpha_{t-1} + \Delta t \cdot R_{t-1} \tag{IX-3}$$

with Δt [days] the time interval and R_{t-1} [1/days] the rate of hydration. The approach of Parrot and Killoh (1984) to describe the dissolution rate R_t [1/days] of the individual clinker phases at time t is based on three equations:

Nucleation and growth
$$R_t = \frac{K_1}{N_1}(1 - \alpha_t)(-\ln(1 - \alpha_t))^{(1-N_1)} \tag{IX-4}$$

Diffusion
$$R_t = \frac{K_2(1 - \alpha_t)^{2/3}}{1 - (1 - \alpha_t)^{1/3}} \tag{IX-5}$$

Formation of hydration shell
$$R_t = K_3(1 - \alpha_t)^{N_3} \tag{IX-6}$$

The lowest value of R, the rate controlling value, is selected to calculate the degree of hydration α_t. At first, nucleation and the growth of the formed nuclei will determine the rate of hydration, and later on the reaction becomes diffusion controlled. Ultimately, the hydration rate will be influenced by the development of a coating around the grains of

unhydrated cement, which creates a barrier that slows down the transport of dissolved species and is empirically represented within equation IX-6 by Parrot and Killoh (1984). Here Scrivener and Nonat (2011) agree that a slowdown of the hydration rate exists with the increase of the reaction degree, but there could be several explanations, e.g. reduction of surface area of reactive phases available or the space filling effect as described by the Avrami equation.

The original values of K_1, N_1, K_2, K_3 and N_3 as given by Parrot and Killoh (1984) were used for modelling, but with an adaptation of the values of K_2 and K_3 for belite as given by Lothenbach et al. (2008a). An overview of the values is given in Table IX.3.

Table IX.3 - Overview of the parameters used to model the dissolution of the clinker minerals from Parrot and Killoh (1984), adapted by Lothenbach et al. (2008a)

Parameter	Alite	Belite	Aluminate	Ferrite
K1	1.5	0.5	1.0	0.37
N1	0.7	1.0	0.85	0.7
K2	0.05	0.02	0.04	0.015
K3	1.1	0.7	1.0	0.4
N3	3.3	5.0	3.2	3.7
H	1.8	1.35	1.6	1.45

The hydration rate of cements especially with low water/cement ratios is significantly reduced at later ages, which can be explained by a lack of larger pores for hydration products to form [Parrot and Killoh (1984)]. This effect is taken into consideration by a factor f(w/c) [-] from a critical degree of hydration onwards:

$$if\ \alpha_t > 1.333 \cdot w/c$$
$$f(w/c) = (1 + 4.444(w/c) - 3.333\alpha_t)^4 \tag{IX-7}$$

According to Lothenbach et al. (2008a) this effect is also depending on the considered clinker mineral, wherefore the factor is reconsidered to be:

$$if\ \alpha_t > H \cdot w/c$$
$$f(w/c) = (1 + 3.333(H \cdot (w/c) - \alpha_t))^4 \tag{IX-8}$$

The H values for determining the critical degree of hydration according to Lothenbach et al. (2008a) and used in this study are also given in Table IX.3. The influence of the specific surface area SSA (m^2/kg) on the initial rate of hydration, during nucleation and growth, is included using [Parrot and Killoh (1984)]:

$$f(SSA) = \frac{SSA}{385\ m^2/kg} \tag{IX-9}$$

In the end, thermodynamic modelling is carried out using the Gibbs free energy minimization program GEMS 3 [Kulik et al. (2013)]. Besides the w/c ratio and the composition of the studied cementitious system, the above mentioned dissolution rates,

together with the thermodynamic data from the PSI-GEMS thermodynamic database and the cement specific database CEMDATA07.3 [Babushkin et al. (1985); Hummel et al. (2002); Thoenen and Kulik (2003); Lothenbach and Winnefeld (2006); Matschei et al. (2007); Lothenbach et al. (2008b); Möschner et al. (2008); Schmidt et al. (2008); Möschner et al. (2009)] are used as input for the modelling in GEMS. As output, the phase composition of a cement paste (in mass or volume) and the different ion concentrations in the pore solution during the hydration process can be obtained.

X - Experimental procedures

During the course of this study, clinker and cement was regenerated from CRC. Not only is the regeneration process discussed in this chapter, but also the methods used for analysing the quality of the regenerated material. The clinker quality was studied by XRD/Rietveld, TG/DT and microscopic analysis. The cement hydration process was studied by isothermal calorimetry and TG and XRD/Rietveld analysis. For the latter hydration of several cement pastes was stopped after predefined curing ages.

A. The cement regeneration process

An overview of the cement regeneration process from CRC applied in this study is given in Figure X.1 and Table X.1. Within the regeneration process, the industrial cement manufacturing process was simulated in the laboratory. Like in industry, the production of cement occurred in three steps: the preparation of a raw meal by milling CRC, the production of clinker by burning the raw meal and finally the making of cement by milling the clinker with calcium sulphate.
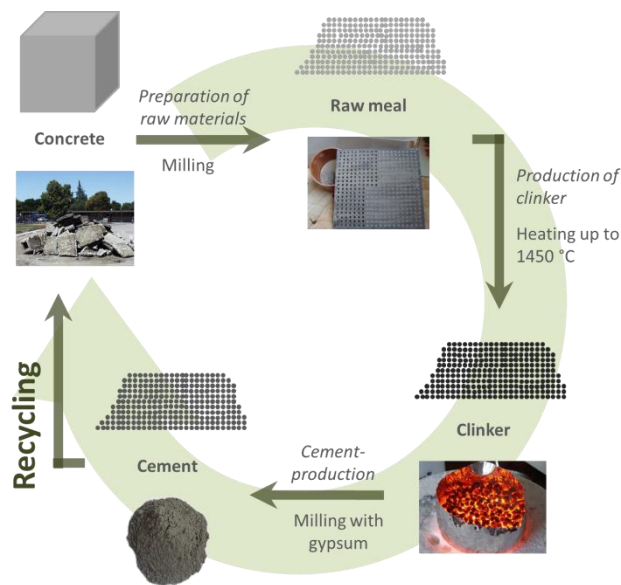
Figure X.1 – Overview of the clinker regeneration process from CRC

A.1. Preparation of the raw meal

CRC rubble from the compressive strength tests was used for the preparation of the cement raw meal. Before grinding the concrete in a planetary ball mill during 4 min at 300 rpm, it was broken in a jaw crusher (resulting particle size < 10 mm). Afterwards the resulting powders were mixed with water to form a paste that was brought into a perforated PVC-plate. By drying, at least 1 day at room temperature or 2 hours at 60 °C,

small tablets (d = 5 mm, h = 5 mm) were formed. After removing the tablets from the perforated plate, a raw meal was ready to be sintered. For CRC1c and CRC2b, the effect of the raw material fineness was evaluated by preparing clinkers from CRC ground during 4, 6 and 8 min.

Table X.1 - Overview of the production parameters of the cement regeneration process

Production parameters	CRC1a CRC2a CRC3a CRC3b	CRC1b	CRC1c	CRC2b
Raw meal preparation				
Milling time raw material [min]	4	4	4 6 8	4 6 8
Clinker production				
Heating rate [°C/min]	15	10	10	10
Burning temperature [°C]	1350 1400 1450	1450	1450	1450
Dwell time in furnace [min]	30	60	60	60
Cement production				
Milling time of clinker [min]		4	4	4
Amount of C$\underline{S}$ added [wt%]		2	3.7[b]	3.8[b]
Milling time with C$\underline{S}$ [min]		6	6	2 6

[b] wt%(SO_3) = 1.841 + 0.095·wt%(C_3A) + 1.6364·wt%($Na_2O_{equivalent}$) [Hewlett (1998)]

A.2. Burning of the cement clinker

In the industry, the raw meal would then be burned in a rotary kiln tube and thus gradually heated by shifting down towards the flame at the end of the furnace. In this study, a high temperature electric furnace (Carbolite BLF 1800) was used for simulating the burning process. For the first experiments (CRC1a, CRC2a, CRC3a and CRC 3b), the raw meals were gradually (15 °C/min) heated up to 1350, 1400 and 1450 °C followed by a dwell time of 30 min. After these first experiments the following heat treatment was decided upon: at 10 °C/min up to 1450 °C with a dwell time of 1 hour. After burning, the clinkers were always immediately air-cooled by removal from the furnace.

Using a laboratory furnace, some conditions of the industrial kiln cannot be simulated. The very fast temperature increase in the preheater or precalciner due to dispersion of the raw meal in hot gasses could not be simulated, and thus the applied heat treatment is most comparable with the long wet process. On the other hand also the effect of the flame is missing. As fuels, more traditional ones can be used such as coal, gas and oil, but since the evolution towards more sustainability, also combustible wastes are used:

rubber tires, paper, wood, used solvents and lubricants, agricultural residues, etc. [Glasser (2004)]. The use of different fuels has however an impact on the composition of the clinker, as combustion ashes enter the cement kiln. In an industrial kiln, the raw material balance should be corrected for this. Furthermore, in a real kiln, material is transported within the vapour phase, and a complex sulphur cycle is known to exist [Glasser (2004)].

A.3. Milling of the cement

In the final step of the regeneration process, cement is produced by milling the clinker with calcium sulphate. The clinkers were first ground in a planetary ball mill during 4 minutes before adding the calcium sulphate. An overview of the added amounts of calcium sulphate ($2/3$ $CaSO_4.^1/_2H_2O$ + $1/3$ $CaSO_4$) can be found in Table X.1. Together with the calcium sulphate the clinker was ground an additional 6 minutes to obtain the regenerated cement powder. In order to study the effect of cement fineness, CRC2b was ground only 2 minutes after the addition of the calcium sulphate, in order to obtain a coarser cement.

A.4. Stopping the cement hydration process

To study the hydration process of the regenerated cement in time by XRD and TG analysis, it was necessary to stop hydration after predetermined time periods (1, 3, 6 and 9 hours and 1, 2, 3, 7 and 28 days). For this purpose small amounts of paste (w/c = 0.4) were introduced into 125 mL conical PP-containers, resulting in discs (d = 45 mm, h = about 5 mm). Once closed, these containers were stored in a climate chamber (20 °C, RH >95%). Two methods to stop hydration were tested: freeze drying and solvent exchange.

i. Freeze Drying

When the Freeze Drying (FD) technique was applied, less damage to the structure and no change of the hydration product are observed according to Zhang and Scherer (2011). A disadvantage of this technique is the degradation of ettringite and monosulphate. For stopping hydration, cement paste discs were crushed, placed in aluminium sample holders and submerged in liquid nitrogen for about 2 minutes. Subsequently, the samples were dried in a Mini Lyotrap Freeze Drying machine (LTE Scientific Limited) until constant mass ($\Delta m < 0.1$ wt% in 24 h).

ii. Solvent Exchange

The benefit of Solvent Exchange (SE) is the reduced damage to the pore structure, nonetheless it might partly dehydrate the C-S-H and ettringite phases [Zhang and Scherer (2011)]. Also, the solvent might be sorbed into the cement phases. The use of isopropanol as solvent is preferred, as it causes the least reaction in cement [Zhang and Scherer (2011)]. The method used for solvent exchange is based on Winnefeld and Lothenbach (2010). The samples were crushed and ground with a mortar and pestle to obtain a powder. About 15 g powder was submerged in about 200 mL isopropanol for

15 min. After filtering and washing with isopropanol and diethyl ether, the powder was dried for about 8 min at 40 °C.

B. Analysis

B.1. Fineness

i. Sieving

There are no real standards for determining the fineness of a cement raw meal. In literature it was found that mostly the residue on a sieve with a certain sieve opening (e.g. R90 [wt%] for the residue on a 90 μm sieve (mesh 170)) is used to quantify the fineness of a raw meal. The requirements are mostly empirical and depending on the used kiln system. Some target values can be found in literature: R90 = about 17 wt% [Kakali and Tsivilis (1993)]; R90 = 15 wt% [Taylor (1997)]; R90 = 10-15 wt% [Sorrentino (2011)]; R88 = 15 wt% and R212 = 1.5-2.5 wt% [Chatterjee (2011)]. Chatterjee (2011) states that in some improved burning systems R88 = 30 wt% and R212 = 6% might be acceptable. It should be mentioned that regarding the burnability of a raw mix, the top size of some minerals should be limited (see Table X.2). In this study the raw material fineness of CRC1c and CRC2b was assessed by determining R90.

Table X.2 - Top sizes for mineral phases in a cement raw meal [Chatterjee (2011)]

Mineral	Top size [μm]
Silica minerals (e.g. quartz, chert, acid insoluble residue, etc.)	44
Shale particles	50
Silicate minerals (e.g. feldspar)	63
Carbonate minerals (e.g. calcite and dolomite)	125

ii. Blaine method

The fineness of a cement powder is commonly evaluated by determining its Specific Surface Area (SSA [m^2/kg]). Using the Blaine method, the time is measured wherein a fixed volume of air passes through a cement bed. Ultimately, the specific surface area is calculated from the measured time, the density of the cement, and the porosity and dimensions of the cement bed.

$$SSA = \frac{1}{10} \cdot \frac{K}{\rho} \cdot \frac{\sqrt{e^3}}{(1-e)} \cdot \frac{\sqrt{t}}{\sqrt{10\eta}} \qquad \text{(X-10)}$$

with K the apparatus constant, e the porosity of the bed (0.5), t the measured time [s], ρ the density of the cement [g/m^3] and η the viscosity of air at the test temperature [Pa·s]. Bentz et al. (2008) report that many cements available have a fineness of 400-420 m^2/kg. The production certificates of Holcim Belgium (2013b) report average values of 333 m^2/kg (CEM I 42.5 N), 375-433 m^2/kg (CEM I 52.5 N) and 439-520 m^2/kg (CEM I 52.5 R).

B.2. XRD/Rietveld analysis

i. Clinkering reactions during firing of CRC

The clinkering reactions of CRC from 25 to 1050 °C were investigated by in situ heating experiments (Figure X.2), and complemented by ex situ heating experiments (Figure X.3) by burning at 10 °C/min up to 1050, 1150, 1250, 1350, 1450 and 1550 °C with a dwell time of 1 hour. Preparation of the samples and the measurement conditions for the ex situ experiments are similar as described below ('*Mineralogy of the regenerated clinker – Methodology 2*'). The in situ heating experiment was conducted on a Bruker AXS D8 Discover Diffractometer with a custom built high-temperature chamber [Rampelberg et al. (2011)]. The clinker raw meal powders were mounted on a zero background (511) silicon wafer and heated at a 10 °C/min rate in a static air atmosphere. Data were continuously read out over a fixed range of 24.5-44.5 °2θ (CuKα radiation) using a VÅNTEC-1 detector.
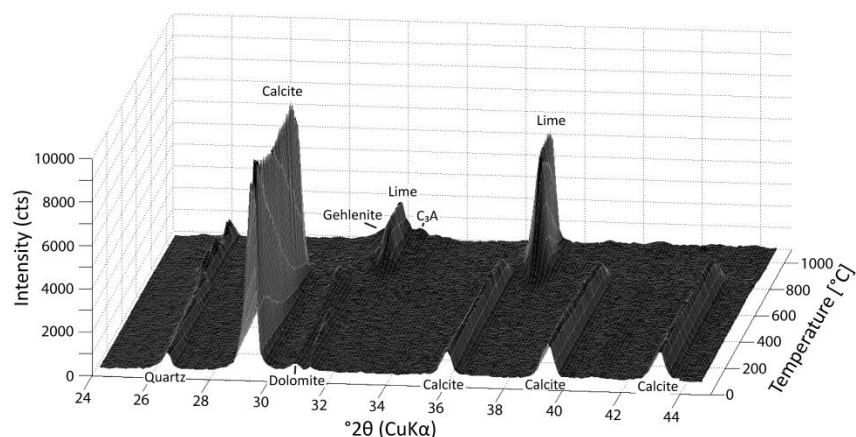
Figure X.2 - Overview of the XRD patterns obtained by the in situ heating experiment, as an example given for the CRC raw meal [Snellings et al. (2012)]

The XRD data collected during the heating experiments were sampled at 5 °C temperature intervals and were subjected to a parametric Rietveld refinement (using Topas Academic V4.1 software [Coelho (2007)]) in which the ensemble of diffraction data was fitted by a set of evolving structural models [Stinton and Evans (2007)]. This approach offers significant advantages in fitting a set of data in which certain parameters such as the diffractometer zero error can be fitted to all patterns simultaneously. In a first step, phase identification as a function of temperature was necessary to determine temperatures of first formation or disappearance of minerals stable at high or low temperature, respectively. Next, both global and phase specific parameters were refined for the entire data set covering the 25-1050 °C temperature range. No internal standard was added to the raw clinker meal to prevent possible interactions of the standard in the high-temperature reactions. To take into account the

amount of non-crystalline components or crystalline components below detection limits, the in situ Rietveld quantification outcome at initially ambient temperature was rescaled to the raw meal composition as determined by Rietveld analysis of the XRD data collected ex situ using the measurement conditions reported below ('*Mineralogy of the regenerated clinker – Methodology 2'*). An additional difficulty in obtaining quantitative results of the in situ heating experiments is that thermal decomposition and volatilization of hydrate and carbonate compounds occurs. The samples are thus not constant in chemical composition and total scattering mass may vary during heating. Therefore, the XRD results are complemented and compared with TG analyses that monitor the weight loss as a function of temperature as determined by TG.
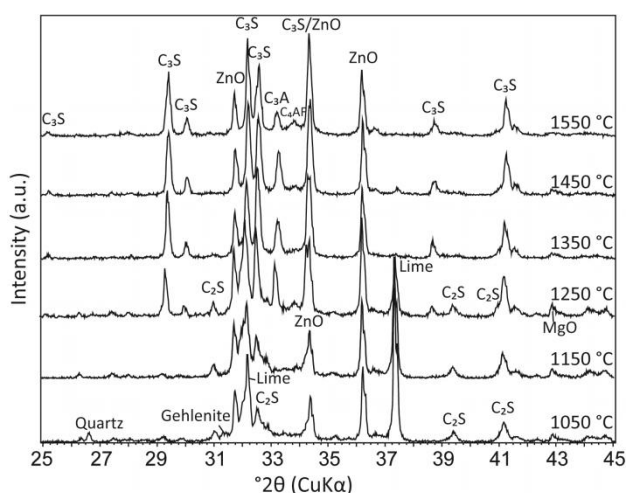
Figure X.3 – Overview of the XRD patterns obtained by the ex situ heating experiment, as an example given for the CRC raw meal [Snellings et al. (2012)]

ii. Mineralogy of the regenerated clinker

The fired clinkers were prepared for XRD analysis by crushing the pellets to pass a 500 μm sieve in a mortar and pestle, followed by fine grinding in a water-free ethanol medium in a planetary ball mill to reduce the clinker particle size distribution below a d_{50} of 10 μm. The ethanol grinding medium was immediately evaporated in a rotary evaporator to minimize carbonation of the suspended clinker powder. The XRD data were collected on a Thermo Scientific ARL X'tra Diffractometer equipped with a Peltier cooled detector.

Methodology 1

Data were collected for 18-130 °2θ (CuKα radiation) in θ-2θ geometry, using a step size of 0.02 and a 1 s/step counting time. For Rietveld analysis of the patterns, the Fullprof Suite software 1.10 [Rodriguez-Carvajal (1993)] was used. The following parameters were refined: background (a cosine Chebyshev function of 12 polynomial terms),

measurement specific or global zero error, scaling factor, cell parameters and Pseudo-Voight peak shape and FWHM parameters.

Methodology 2

To increase the accuracy and lower the detection limits of the quantitative phase analysis by XRD, selective dissolution methods were used to reduce reflection peak overlap in the XRD patterns and concentrate the characteristic residue fraction. A solution of salicylic acid in methanol (SAM extraction) was used to dissolve the clinker calcium silicates and a solution of KOH and sucrose in H_2O (KOSH extraction) to remove mainly the C_3A, C_4AF and soluble sulphate phases. The dissolution procedures are described elsewhere [Gutteridge (1979)].

Additionally, the internal standard approach was selected for absolute phase quantification and estimation of the amorphous or non-identified phase content by XRD analysis [Bish and Howard (1988); Martín-Márquez et al. (2009)]. A 10wt% ZnO internal standard was added to the untreated clinker powder. Finally the powders were side-loaded into sample holders to reduce preferred orientation effects.

Samples were measured in θ-2θ geometry over an angular range of 5-70 °2θ (CuKα radiation) using a 0.02 °2θ step size and 1 s/step counting time. Topas Academic V4.1 software was used for Rietveld refinement [Coelho (2007)]. The phase quantification routine for the fired clinkers initiated with the identification of major and minor phases in the SAM and KOSH treated samples. Subsequently, peak shape and unit cell parameters of the major clinker phases were refined and used as fixed input for the final quantitative phase analysis of the untreated clinker samples as described in Le Saoût et al. (2011). Also the clinker C_3A/C_4AF weight ratio was taken from the analysis of the SAM treated residue. This procedure strongly reduces parameter correlation during refinement of the untreated sample. Overall, the refined parameters were the measurement specific or global zero error and cosine Chebyshev function of 12 polynomial terms and the phase specific scale factors, unit cell parameters and Lorentzian peak shape broadening parameters. An indication of the accuracy of the Rietveld refinement of XRD patterns can be found in Table X.3 [Scrivener et al. (2004)]. An overview of the crystal structures used in this study is given in Table X.4.

Table X.3 - Typical values and accuracies for the determination of phases present in anhydrous cement [wt%] by XRD analysis [Scrivener et al. (2004)]

Phase	Typical value with accuracy	Typical value with accuracy
Alite	60 ± 2.0	2 ± 0.3
Belite	15 ± 1.5	2 ± 0.3
Ferrite	4 ± 0.6	2 ± 0.3
Aluminate	4 ± 0.6	1 ± 0.3
Free lime	1 ± 0.3	1 ± 0.3
Periclase	1 ± 0.3	1 ± 0.3

Table X.4 - Overview of the crystal structures used in this study

Mineral	Formula	ICSD code
Alite	Ca_3SiO_5	94742
Belite	Ca_2SiO_4	79550
Aluminate	$Ca_3Al_2O_6$	1841
Ferrite	$Ca_2Al_2O_6$	51265
Calcite	$CaCO_3$	20179
Aphthitalite	$K_3Na(SO_4)_2$	26018
Arcanite	K_2SO_4	2827
Thenardite	Na_2SO_4	28056
Ca-langbeinite	$Ca_2K_2(SO_4)_3$	40989
Syngenite	$K_2Ca(SO_4)_2.H_2O$	26829
Periclase	MgO	9863
Dolomite	$CaMg(CO_3)_2$	27540
Gypsum	$CaSO_4.2H_2O$	27221
Bassanite	$CaSO_4.^1/_2H_2O$	380286
Anhydrite	$CaSO_4$	27474
Zincite	ZnO	31052
Portlandite	$Ca(OH)_2$	202229
Kuzelite	$Ca_2Al(OH)_6.(SO_4)_{0.5}(H_2O)_3$	100138
Ettringite	$Ca_6Al_2(SO_4)_3(OH)_{12}(H_2O)_{26}$	155395
Quartz	SiO_2	174
Fluorite	CaF_2	44937
Mullite	$Al_{4.52}Si_{1.48}O_{9.74}$	66451

iii. Phase composition of hydrated cement pastes

Studying cement hydration, XRD analysis was performed on cement pastes for which hydration was stopped after predefined curing times. In preparation of the measurement, the samples were crushed and ground using a mortar and pestle to achieve a powder with a maximum grain size of 74 μm (mesh 200). The measurement conditions were as described earlier ('*Mineralogy of the regenerated clinker – Methodology 2*'); however no SAM and KOSH extractions were performed on the hydrated samples. During Rietveld refinement, the clinker minerals alite, belite, aluminate and ferrite were considered besides gypsum and the hydration products portlandite, ettringite and kuzelite (a crystalline calcium monosulfoaluminate). Other hydration products, such as C-S-H, hydrogarnet, hydrotalcite and other AFm phases (calcium monosulfoaluminate and calcium hemi- or monocarboaluminate) are (often) poorly crystalline [Scrivener et al. (2004); Lothenbach and Winnefeld (2006); Lothenbach et al. (2008a)] and are therefore comprised within the 'other' fraction.

Effect of sample preparation

The presented manual grinding of the samples was necessary to preserve the hydration products sensitive for rough grinding techniques such as a planetary ball mill. Due to the lower fineness of the samples, the accuracy of the Rietveld analysis is reduced [Le Saoût et al. (2011)]. Furthermore, it seemed that the amount of ZnO was overestimated. This was observed after testing an unhydrated sample for which both preparation methods were followed (see Table X.5). To both samples, 20% of ZnO was added to the sample, while the refinement of the XRD patterns resulted in ZnO contents of 20.9 and 23.9 wt% for respectively the ideal sample preparation using a ball mill and the manual soft preparation procedure.

The difference between both measurements might be explained by a 'rocks in dust effect' (see Figure X.4), whereby the coarse clinker or cement particles are covered by the fine zincite particles, resulting in an overestimation of the ZnO content. After normalization of the results (without ZnO), it is seen that the effect on the quantification of the different phases is acceptable, keeping in mind the accuracy of XRD/Rietveld analysis (see Table X.3 [Scrivener et al. (2004)]), but obviously the effect becomes more significant for phases present in lower amounts. As a correction for this effect during quantification of the hydrated samples, the amount of 'other' phases was calculated using the ZnO content measured for an unhydrated sample that followed the preparation procedure of a hydrated sample (only manual grinding), instead of the ZnO content added to the sample.

Table X.5 - Effect of sample preparation on the quantification by Rietveld analysis [wt%]

Mineral	Ball mill		Mortar and Pestle	
	With ZnO	*Normalized*	*With ZnO*	*Normalized*
Zincite	20.9	-	23.9	-
Alite	52.9	66.9	52.7	69.3
Belite	10.5	13.3	9.6	12.7
Ferrite	7.1	8.9	6.7	8.8
Aluminate	2.1	2.7	2.0	2.6
Calcite	0.3	0.3	0.2	0.3
Bassanite	2.3	3.0	2.5	3.2
Anhydrite	1.3	1.6	1.3	1.7
Aphthitalite	0.6	0.7	0.5	0.6
Syngenite	1.3	1.7	0.3	0.4
Ca-Langbeinite	0.0	0.0	0.1	0.1
Periclase	0.7	0.9	0.2	0.2

Figure X.4 - Visualisation of the 'rock in dust effect'

B.3. Clinker microscopy

The clinker texture and microstructure were examined on polished sections by reflected light optical and back-scattered electron microscopy. Polished sections were prepared by impregnating the sintered clinker pellets with a low viscosity epoxy resin to fill the connected pore network. The epoxy resin was hardened at 40 °C for at least 48 h and clinker sections were ground on a rotating wheel using a SiC abrasive paper (No. 320-grit) and water. These sections were subsequently polished to a fineness of 0.25 μm using first SiC abrasive paper of 500, 1200, 2400 fineness and DP-lubricant brown (Streurs) for water sensitive materials and finally 3 to 0.25 μm diamond polishing pastes.

To allow better phase identification by optical microscopy the clinker surfaces were etched by immersion for 10 sec in water at 40°C, followed by a 10 sec nital (1 mL HNO_3 in 99 mL isopropyl alcohol) etch. Alite crystals can hereby be recognized as brown, blue, red, green or yellow angular crystals, while belite is round and brown to blue. Possible explanations for the different colours of the alite and belite crystals are differences in crystallographic orientation, chemical composition, structural state (monoclinic or triclinic) or a combination of the above mentioned factors [Campbell (1999)]. The interstitial material, containing aluminate and ferrite, is crystallized between the alite and belite crystals as the molten liquid cooled down after the burning process. The water etch simplifies the identification of the interstitial phases. Aluminate is turned blue to brown, while ferrite remains white.

In preparation of point-counting analysis, microscopic images of the clinkers were taken on the crossings of a regular grid. These images were then studied by means of JMicroVision [Roduit (2008)]. For each clinker at least 1000 points were investigated by point counting. In addition the crystal size distribution of alite and belite was measured for some clinkers.

Support for the phase analysis by optical microscopy and XRD was obtained by electron microscopy images of carbon-coated, non-etched polished sections acquired on a SEM XL30-I (FEI) with W filament in BSE mode in combination with energy dispersive X-ray (EDX) microanalysis.
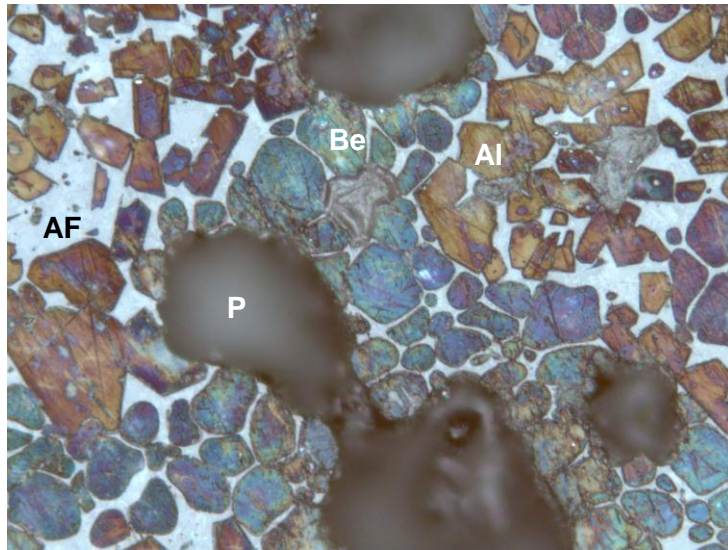
**Figure X.5 - Micrograph of a polished CRC clinker section etched with nital.
Al = alite; Be = belite; AF = interstitial phase of aluminate and ferrite; P = pore.**

B.4. TG/DT analysis

Thermogravimetric (TG) and Differential Thermal (DT) analysis were carried out using a Netzsch STA 449F3 apparatus. TG analysis was used to study the hydration process of the regenerated cements, while both TG and DT were used to study the clinkering process.

i. Clinkering process

Data were recorded during heating at 10 °C/min up to 1450 °C and subsequent cooling at 25 °C/min up to 1000 °C in a 50 mL/min dry air flow to study both heating and cooling reactions in the clinkering process. To more adequately separate between sample and baseline DT signals, TG/DT data were recorded twice for a single sample, but with differing sample weights of 25 and 50 mg. Subtraction of both curves then results in improved singling out of the sample DT signal and reduction of both apparatus and sample contributions to the asymmetric heat profile, thus enabling better peak assignment [Yang and Roy (1999)].

ii. Hydration process

The measurements were performed on about 50 mg of powdered cement paste with a nitrogen gas flow of 50 mL/min and a heating rate of 10 °C/min up to 1050 °C. The amount of chemically bound water was determined from the weight loss between 105 and 1050 °C [Pane and Hansen (2005); Gruyaert (2011)]. The weight loss between 400 and 520 °C can be attributed to the dehydroxylation of portlandite ($Ca(OH)_2$). The amount of portlandite was quantified by the weight loss between these temperatures

[Lothenbach et al. (2008a)]. Additionally, a tangential method [Baert (2009); Gruyaert (2011)] was used for determination of the water loss due to portlandite dehydroxylation. Within this method, the concurrent release of chemical bound water from the other cement hydrates is not taken into account [Pane and Hansen (2005)].

Due to limited carbonation of the samples, a small mass loss in the range of 600-780 °C was observed, which is due to the release of carbon dioxide, mainly from carbonated portlandite [Pane and Hansen (2005)]. For this reason the portlandite content $m(Ca(OH)_2)$ (wt%) should be corrected:

$$wt(Ca(OH)_2) = WL(Ca(OH)_2)\frac{M(Ca(OH)_2)}{M(H_2O)} + WL(CaCO_3)\frac{M(Ca(OH)_2)}{M(CO_2)} \qquad \text{(X-11)}$$

with $WL(Ca(OH)_2)$ en $WL(CaCO_3)$ the weight loss (in wt%) due to the decomposition of $Ca(OH)_2$ and $CaCO_3$, respectively, and $M(Ca(OH)_2)$, $M(H_2O)$ and $M(CO_2)$ the molar masses of $Ca(OH)_2$, H_2O and CO_2, respectively. This however gives a small overestimation of the portlandite content, as also the C-S-H gel in a hydrated cement paste is known to carbonate [Borges et al. (2010)].

B.5. Isothermal calorimetry

The hydration heat of the regenerated cements was studied by isothermal calorimetry. For this purpose, cement pastes were prepared with a water to cement ratio of 0.4. About 10 g of the cement paste was mounted into glass vials, which were then placed in an isothermal calorimeter (TAM AIR) at 20 °C to measure the hydration heat during the first 7 days of hydration. Since mixing occurred outside the calorimeter, the first hydration peak could not be registered entirely. Because this peak only amounts to a few percent of the total heat liberated [De Schutter (1999)], and is possibly influenced by inserting the sample inside the calorimeter, disturbing the thermal equilibrium, it will not be considered in further analysis. The hydration heat of the very first hydration peak is associated with the wetting of cement and the hydration of free lime, aluminate and calcium sulphates at the moment of mixing the samples [Mostafa and Brown (2005)].

XI - The regeneration of CRC clinker

For a selected CRC, the clinkering reactions during firing were documented using in situ and ex situ XRD analysis, accompanied by TG/DT analysis and light microscopy. For the other regenerated clinkers, the mineralogy was studied by XRD/Rietveld analysis and light microscopy. Later on also the effect of raw meal fineness on the clinker quality was assessed. Finally the use of deteriorated CRC and its effect on the clinkering process was studied. Results of this chapter have been published in Snellings et al. (2012) and De Schepper et al. (2013).

A. The clinkering reactions during firing of CRC

A.1. Starting materials

The clinker reactions during firing were not only studied for a CRC, but also for a hydrated cement paste (CP). As CRC, CRC2a was used with an adapted CaO content by adding 7% limestone filler. Both the chemical and mineralogical composition of the raw materials are presented in Table XI.1. The cement paste contains lower SiO_2, CaO, and MgO concentrations and higher Fe_2O_3 and SO_3 levels. It should be noted that the SO_3 level in the cement paste raw material is outside typical limits used in Portland clinker production. Elevated SO_3 levels are known to result in excessive clogging of the clinker kiln by volatilization and reprecipitation of alkali sulphates that form rings in lower temperature zones of the kiln [Glasser (2004)]. Moreover, excessive SO_3 unbalanced by equivalent amounts of alkalis is reported to stabilize belite over alite by preferential replacement of Si by S in belite compared to alite [Horkoss et al. (2011)]. Although in production practice, hydrated cement residue is unlikely to be used as sole or principal component of clinker raw meal, this study documents the implications of firing a hydrated cement paste on the clinkering process.

Table XI.1 - Overview of the chemistry and mineralogy of the studied raw materials [wt%] [Snellings et al. (2012)]

Chemistry[A]	CRC	CP	Mineralogy[B]	CRC	CP
CaO	65.0	62.2	Calcite	61.5	3.3
SiO_2	21.0	18.7	Quartz	5.2	
Al_2O_3	6.1	5.9	Dolomite	4.9	
Fe_2O_3	2.5	4.1	Fluorite	0.6	
MgO	2.5	0.1	Mullite	1.2	
SO_3	1.0	3.2	Belite	1.1	10.7
LSF	0.96	1.00	Ferrite		4.6
SM	2.44	1.87	Portlandite		17.1
AM	2.44	1.44	Ettringite		3.1
HM	2.20	2.17	Other	25.4	61.2

[A] by inductively coupled plasma mass spectrometry
[B] by XRD/Rietveld analysis

The mineralogy highlights important differences in raw material constitution. Most notable is that the source of CaO for the clinkering reactions in the CRC is primarily calcite together with a smaller amount of C-S-H contained in the 'other' phases fraction, as it is not directly quantifiable by XRD due to a lack in long-range order. In case of the cement paste raw material, the main CaO suppliers are portlandite and an important amount of C-S-H. The calcite in the CRC raw meal is largely derived from the aggregate fractions and of course the added amount of lime stone filler. Mullite and belite are derived from the unreacted cementitious materials in the CRC, i.e. from the fly ash and the Portland cement, respectively. Crystalline cement hydrates in the CRC raw material could not be detected by XRD due to the dilution factor of the cement in the concrete and the partial substitution of the cement by fly ash and limestone filler. The addition of fly ash is expected to result in a reduction of the portlandite content due to the pozzolanic reaction. In contrast, in the hydrated cement paste, significant amounts of crystalline cement hydrates are found. In addition to portlandite, ettringite and AFm phases were detected. The latter were however not separately quantified but included into the 'other' phases fraction for the in situ heating experiment. Belite and ferrite were not entirely consumed in the hydration reactions and remain as relict phases in the cement paste raw meal.

A.2. In situ XRD measurements: reactions from 25 up to 1050 °C

i. CRC

The results of the in situ heating experiments on CRC are presented in Figure XI.1. It should be noted that the low angular resolution and restricted angular range of the in situ XRD measurements impeded the quantification of minor phases identified in the raw meals such as fluorite, mullite and belite. Calcite decarbonation and dolomite decarbonation are clearly observed and start around 670 and 730 °C respectively. The first lime XRD reflections appear at 680 °C and the rate of lime crystallization is closely related to the carbonate decomposition rate. However, also the content in non-crystalline and unidentified 'other' phases increases sharply. Calcite and dolomite are completely decomposed at respectively 860 and 810 °C. Also the lime content in the CRC raw meal reaches a maximum at 860 °C. In addition to lime, several minor calcium (alumina-)silicate phases start to crystallize. Mayenite ($C_{12}A_7$) and tricalciumaluminate (C_3A) are formed from about 800 °C onwards. Belite (α-C_2S), gehlenite (C_2AS), and ferrite (C_4AF) start to develop at somewhat higher temperatures of respectively 890, 940 and 980 °C. Quartz levels in the heated raw meal remain relatively constant up to 850 °C, further heating results in a slightly decreasing quartz content up to 1050 °C. In this temperature range, silica and alumina for the formation of the high-temperature phases are therefore considered to be derived primarily from decomposed calcium silicate and aluminate hydrates and from unreacted constituents such as copper slag and fly ash present in the concrete raw meal.
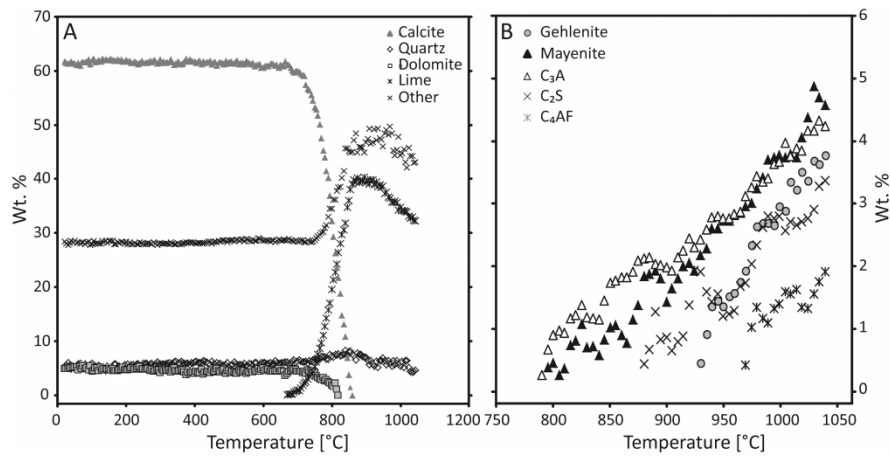
Figure XI.1 - Rietveld XRD quantification results for the in situ heating experiment of the CRC. On the left, the weight fraction evolution of the major phases is shown. On the right, the formation of minor Ca-silicate and aluminate phases in the range 700-1050 °C are presented [Snellings et al. (2012)].

ii. Cement paste

As can be expected from the differences in raw meal mineralogy, thermal transformations in the cement paste raw meal deviate considerable from the phase evolution in the CRC. From the cement industry point of view, in fact the CRC is closer to the traditional raw meal composition. In the cement paste sample the first observable reaction in the in situ heating experiment is the dehydroxylation of portlandite to form lime starting around 440-460 °C (Figure XI.2). Portlandite is decomposed completely at 520 °C. Interestingly, a considerable part of the lime is carbonated to calcite in static air conditions of the furnace and does not participate in the formation of intermediate temperature calcium aluminates and silicates. This carbonation reaction is also expected to occur in production kilns or precalciners as the hot kiln air arriving in counter current flow at the low temperature parts of the furnace will be enriched in CO_2 due to calcite decarbonation and fuel combustion. This means that even though noncarbonated calcium (silicate) hydrates may be used as kiln feed, the temperature profiles in the production kilns still need to allow for calcite decarbonation. Thermal decomposition of the calcite initiates around 680 °C, closely followed by increasing lime weight fractions and the incipient formation of intermediate temperature calcium silicates i.e. gehlenite and belite. In contrast to the CRC sample, lime contents are rather low, and belite abundantly crystallizes in the heated cement paste. The enhanced rate of reconversion of the non-crystalline phases into belite indicates an improved burnability of the cement paste below melting temperatures and possible stabilization of belite due to the presence of abundant SO_3 [Herfort et al. (2010)]. No formation of calcium aluminate phases was resolved in the in situ heating measurements; this is likely due to the relatively low A/F ratio of the regenerated cement paste.
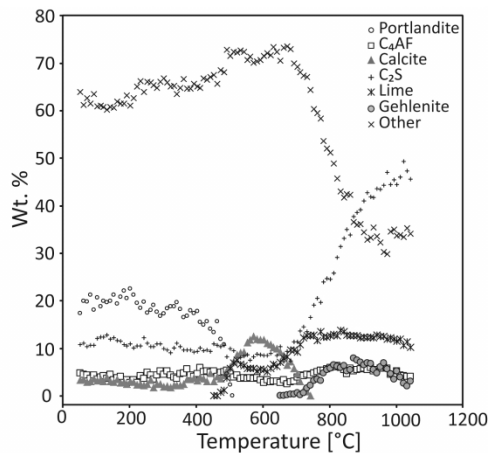
Figure XI.2 - Rietveld XRD quantification results for the in situ heating experiment of the CP. Lime formed in the dehydroxylation of portlandite is partially carbonated below 670 °C. Above this temperature, the formed calcite is decomposed and extensive formation of belite and gehlenite is observed [Snellings et al. (2012)].

A.3. Ex situ XRD measurements: reactions from 1050 up to 1450 °C

i. CRC

The ex situ heated samples show very similar mineral assemblages at the lower temperatures of 1050 °C and 1150 °C compared to the in situ heating experiment in the highest temperature range (Figure XI.3 - left). However, the amount of non-crystalline or unidentified phases is much lower. This is partially due to the optimized sample preparation and data collection procedure that allows identifying minor phases such as periclase and alkali sulphates in the diffractogram, but also due to the 1 h dwell time at peak temperature which allowed further crystallization of the high-temperature phases such as belite (C_2S). In addition to the previously mentioned phases, also ye'elemite ($C_4A_3\underline{S}$) was found in the samples heated at 1050 °C and 1150 °C. In the CRC sample a major transformation of the phase assemblage occurs between 1150 and 1250 °C. Alite is formed at the expense of lime, belite and gehlenite. Lime is completely consumed in the CRC heated at 1350 °C, while belite levels are progressively lowered upon increasing dwell time temperature. The calcium aluminate fraction undergoes a marked change. Mayenite, gehlenite and ye'elemite contents decrease with temperature and disappear at 1250 °C to be replaced by C_3A. Eventually at 1550 °C, ferrite and alite partially replace C_3A and belite.
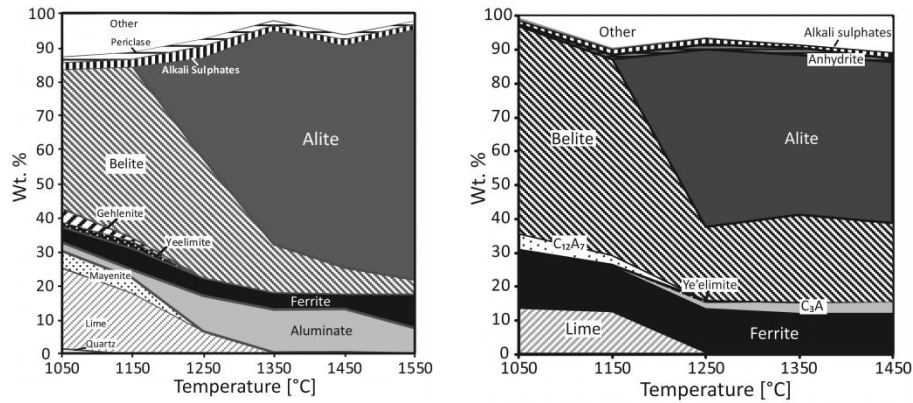
Figure XI.3 - Overview of the phase changes upon (ex situ) heating of CRC (left) or CP (right) raw meal [Snellings et al. (2012)].

ii. Cement paste

The enhanced resolution and lowered detection limits of the ex situ measurements do indicate the occurrence of mayenite at 1050 and 1150 °C (Figure XI.3 - right). In comparison with the in situ experiments at 1050 °C, ferrite contents are higher, gehlenite is decomposed and the amount of unidentified or amorphous phases is lower. As in the CRC, the extended high-temperature retention time resulted in extensive crystallization of the unidentified and unknown phase fraction. The Ca-sulphate phases identified in the cooled clinkers were anhydrite and Ca-K sulphates such as langbeinite and syngenite. Minor volatilization of sulphates and alkalis was observed at temperatures above 1350 °C. Even though the cement paste contains higher amounts of sulphate, no ye'elemite formation was observed at 1050-1150 °C. The cement pastes fired at 1250 °C and above show the formation of alite and C_3A at the expense of belite and lime and of mayenite, respectively. Compared with the CRC, the fired cement paste contains considerably more belite at 1450 °C. This is in part due to a lower LSF and in part due to the thermodynamic stabilization of belite by incorporation of S [Herfort et al. (2010)].

A.4. Differential Thermal Analysis

The DT curves recorded during heating and cooling show considerable differences in the endothermal and exothermal signals detected (Figure XI.4). In the CRC raw meal the main endothermal peak at 854 °C is clearly related to carbonate decomposition. In the cement paste two endotherms appear, a broad cement hydrate dehydration peak at 150 °C and a narrow peak at 487 °C related to the dehydroxylation of portlandite. Carbonation and decarbonation of the lime formed in the latter reaction (cf. in situ XRD experiment) were not observed due to the continuous air-flushing of the TG furnace.
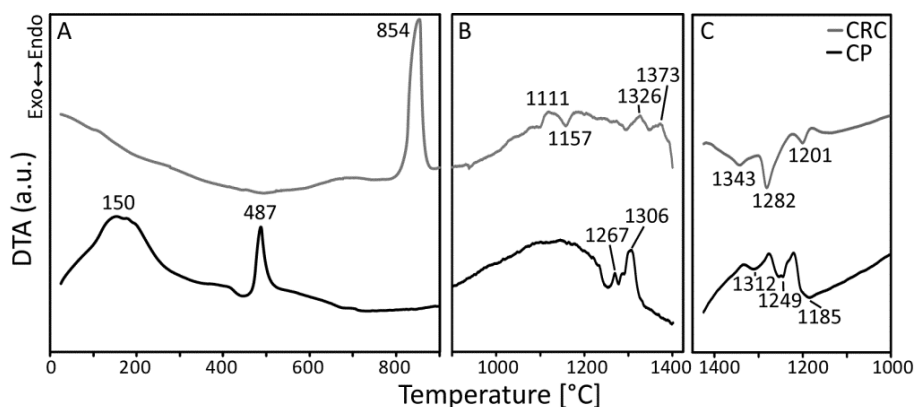
Figure XI.4 - DT curves for heating (A, B) and cooling (C) of the CRC and CP raw meals. In (A) the main endothermal signals of decarbonation (CRC) and dehydration (CP) can be observed. Above 900 °C several minor endo- and exothermal signals occur in (B) and (C); with an expanded vertical scale compared to (A) [Snellings et al. (2012)].

Above calcination temperatures, the interpretation of the curves is not straightforward due to an increasing effect of the temperature drift. Indeed, the applied technique from Yang and Roy (1999) was intended to be used within a range of 30 to 600 °C, the typical range for a DSC measurement. An endothermal signal can be expected around 1160 °C related to the polymorphic transition of the early formed α_L belite to the α_H polymorph structure. Exothermal signals during CRC heating can be related to the reaction of intermediate temperature calcium aluminates and aluminosilicates (mayenite, ye'elemite and gehlenite) to C_3A and belite. Furthermore, endothermal signals between 1250 and 1350 °C can be related to the melt formation. As the reaction of lime and belite to alite is spread out over a wide range of temperature, a well-defined exothermal peak due to alite crystallization is not to be expected. Upon cooling, several conspicuous exothermal peaks related to the crystallization of C_3A and ferrite from the melt and polymorphic transitions of α-belite to α'_H-belite and eventually to α'_L-belite can be expected.

A.5. Visualisation by clinker microscopy

Clinker microscopy was used to evaluate the spatial distribution of the clinker minerals and the overall burning conditions. Figure XI.5 presents the micrographs of the clinker made by burning a CRC and a cement paste at 1250 and 1450 °C. At 1250 °C more melt and alite is formed in the cement paste clinker. The related better burnability of the cement paste clinker is also observed at burning temperatures of 1450 °C. The clinker is less porous with mainly closed pores and the main clinker minerals, alite and belite, are better dispersed in the melt, indicated by less fused alite in the cement paste clinker (see also Table XI.2). The better burnability of the cement paste is attributed to the larger amount of melt phases formed and the higher SO_3 content. The former enhances melt phase diffusion of reactants, while the latter lowers the temperature of the melt

formation and reduces the melt viscosity [Taylor (1997)]. However, as mentioned earlier, SO_3 stabilizes belite at the expense of alite.

Alite crystal size distributions show an average of 24.2 and 35.1 μm for the CRC and cement paste clinker, respectively (Table XI.2). Of the measured alite crystals, 38% and 79% for the CRC and cement paste clinker, respectively, range between 25 and 65 μm, which is the normal alite size according to Campbell (1999). Nevertheless, for reactivity, alite crystals are ideally 15-20 μm in size. In the clinker produced from CRC, belite is mostly present as inclusions in alite, and rarely as clusters or single crystals dispersed in the melt phase. The clinker originating from the cement paste on the other hand contains mostly belite clusters. The average belite size in the cement paste clinker is 26.8 μm; the average size of a belite cluster is 114.1 μm. A typical belite size is 25-40 μm, which is the case for 52% of the belite crystals in the cement paste clinker [Taylor (1997); Campbell (1999)].

SEM/EDX analyses confirmed that the angular and round shaped crystals (Figure XI.5) were alite and belite respectively. For the clinker obtained from the cement paste a high SO_3 content in the belite phase was observed, also for the belite inclusions in alite, supporting belite stabilization by S incorporation. In the cement paste clinker the sulphate phases were also studied, which contained mainly CaO and K_2O and little Na_2O and are thus conform to the X-ray identification of langbeinite and syngenite.
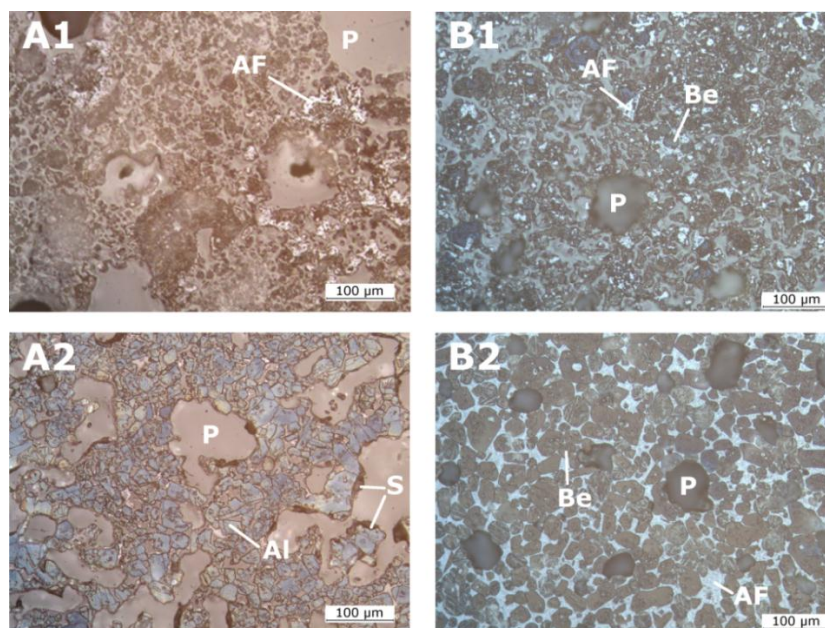
Figure XI.5 - Micrographs of clinker obtained by burning a CRC (A) and a cement paste (B) at 1250 °C (1) and 1450 °C (2). Al = alite; Be = belite; AF = interstitial phase of aluminate and ferrite; P = pore; S = alkali sulphates [Snellings et al. (2012)]

Table XI.2 - Mineralogy and microstructure analysis of regenerated clinker from a CRC and a CP raw meal by light microscopy [Snellings et al. (2012)]

	CRC	CP
Mineralogical composition of the clinker phases [wt%]		
Alite	72.5 (2.1)	50.5 (1.8)
Belite	4.7 (0.9)	22.2 (2.0)
Aluminate	15.6 (1.6)	6.7 (1.1)
Ferrite	7.2 (1.4)	20.7 (2.1)
Clinker porosity [vol%]		
Open pores (grey, filled with epoxy)	24.4	0.2
Closed pores (dark, epoxy could not enter)	0.3	11.3
Alite characteristics		
Fused [wt%]	77.0 (2.4)	58.5 (4.2)
With inclusions [wt%]	71.1 (2.6)	94.3 (1.6)
Average size [μm]	24.2 (0.5)	35.1 (0.6)
Minimum size [μm]	4.9	10.3
Maximum size [μm]	73.7	75.7
<25 μm [%]	61	20
25 μm < x < 65 μm [%]	38	79
>65 μm [%]	1	1

B. Mineralogy of the regenerated clinker

The mineralogy of a Portland cement clinker can easily be determined from its chemical composition by the Bogue calculations (see PART I, Table IV.4). However, the results obtained from these formulas only give an estimation of the potential mineralogical phases present (alite, belite, aluminate and ferrite). Furthermore, the original Bogue calculations (II-11-14) estimate the pure phases, while the real clinker phases are solid solutions containing substituent ions [Commission Chimique du CETIC (1978); Odler et al. (1981); Herfort et al. (2010)]. For this reason modified Bogue calculations (II-15) are proposed in Taylor (1997), using the chemical composition of a phase from a typical clinker instead of the chemistry of the pure phase.

Experimentally, the mineralogy of a clinker was studied by XRD/Rietveld analysis and light microscopy. XRD/Rietveld focuses on the crystal structure and quantification of the phases. Microscopy gives an idea of the spatial distribution of the clinker phases and the overall burning conditions (see chapter XI.A.5). Additionally quantification of the phases is possible by point-counting analysis of micrographs.

B.1. XRD/Rietveld analysis

The results obtained from XRD/Rietveld analysis on the regenerated clinkers are presented in Table XI.3. By making use of selective dissolution for better refinement of

the crystal structures and better detection of minor phases such as (alkali) sulphates and periclase and due to the addition of an internal standard for quantification, the results of the XRD/Rietveld analysis of CRC1b, CRC1c and CRC2b have a higher accuracy. Furthermore, by analysing the patterns using Topas Academic, instead of Fullprof Suite, more phases could be fitted in one pattern, improving the quality of the analysis.

Table XI.3 - Overview of the mineralogy of the regenerated clinkers from CRC [wt%] according to XRD/Rietveld analysis. As a comparison the mineralogy of the clinkers CRC1c and CRC2b was also determined using point-counting analysis of micrographs [wt%]. The values in parentheses are the estimated errors on the weight percentages of the individual refinements.

Rietveld analysis by...	Methodology 1				Methodology 2[*]		
Mineral	**CRC1a**	**CRC2a**	**CRC3a**	**CRC3b**	**CRC1b**	**CRC1c**	**CRC2b**
Alite	57.9 (0.37)	60.8 (0.50)	43.2 (0.39)	47.9 (0.36)	48.2 (1.17)	63.8 (1.90)	70.2 (2.12)
Belite	26.2 (0.26)	21.3 (0.30)	40.3 (0.38)	34.9 (0.32)	31.5 (0.93)	17.4 (0.96)	13.6 (0.98)
Aluminate	13.1 (0.13)	10.2 (0.14)	10.1 (0.15)	11.4 (0.14)	1.8 (0.08)	1.1 (0.06)	2.8 (0.15)
Ferrite	2.0 (0.11)	6.0 (0.14)	4.0 (0.15)	3.6 (0.14)	9.3 (0.38)	10.1 (0.50)	9.2 (0.48)
Aphthitalite					0.1 (0.04)	0.5 (0.22)	0.6 (0.22)
Syngenite					1.5 (0.28)	0.8 (0.38)	1.9 (0.40)
Calcite					0.6 (0.23)	0.6 (0.32)	0.9 (0.23)
Lime	0.3 (0.04)	0.2 (0.04)	0.0 (-)	0.2 (0.04)			
Periclase	0.5 (0.06)	1.5 (0.08)	2.4 (0.09)	2.0 (0.07)	0.3 (0.10)	0.5 (0.15)	0.9 (0.19)
Other					6.6	4.7	0.0
Results from point-counting analysis of micrographs							
Alite						70.2 (3.1)	75.8 (1.2)
Belite						14.7 (3.8)	7.0 (1.5)
Aluminate						2.8 (0.5)	4.0 (0.6)
Ferrite						12.3 (1.4)	13.2 (1.0)

[*] To improve accuracy of the results an internal standard was used for absolute quantification and estimation of the amorphous and non-identified phases ('other' phase). Also selective dissolutions were applied for improvement of the refinement of the crystal structures.

Regarding the calcium silicates, the distribution is not optimal for CRC3a, CRC3b and CRC1b, all having a rather low alite and high belite content. The other clinkers have an average (CRC1a, CRC2a and CRC1c; about 60 wt%) or a high (CRC2b; about 70 wt%) alite content, and the belite content is thus reduced to more acceptable values. The effect of adding copper slag, rich in iron and resulting in lower values for AM (see Table IV.3), is clearly seen on the aluminate to ferrite ratio for CRC1b, CRC1c and CRC2b. The amount of aluminate phases is very low. Although it is of great interest to increase the alite content of a clinker, care should be taken this is not at the expense of the melt phases aluminate and ferrite affecting the burnability of the material. Besides the main clinker phases, other minor phases such as (alkali) sulphates, calcite, lime and periclase were detected. The accurate quantification of these elements is however doubtful, and the values are presented as an indication of their presence. By the use of an internal standard the amount of 'other' phases was calculated, indicating the presence of amorphous phases or phases below the detection limits.

B.2. Light microscopy

Compared to XRD/Rietveld analysis, quantification using point-counting analysis of micrographs is more time consuming. Although both techniques require a careful sample preparation asking about the same effort, there is absolutely a difference in the analysis of the obtained data. Regarding XRD/Rietveld analysis, once you have a good analysis of the first sample which can require some time, the analysis of similar samples goes rather easy. Point-counting of the micrographs requires the same effort for each sample. Furthermore, less information on the minor phases is withdrawn from light microscopy, as identification of them is not straightforward and requires experience and a more in depth study by SEM/EDX analysis.

Nonetheless, to compare the results obtained from Rietveld analysis with another experimental quantification technique, micrographs of CRC1c and CRC2b were studied using point-counting, of which the results are also presented in Table XI.3. From the results it can be concluded that the alite and ferrite content are rather high for a traditional clinker. The belite content of CRC2b, and too smaller extent also CRC1c is rather low. And as for the XRD analysis it can be concluded that again the aluminate content is low.

B.3. Comparison of the different quantification methods

The mineralogy of the cement clinkers as determined by the different methods are visualized in Figure XI.6. Within this graph it is seen that there are big differences between the mineralogy as calculated theoretically with the Bogue calculations (original or modified), and those determined experimentally (XRD/Rietveld and microscopic analysis). It is seen that although the modified Bogue calculations take into account the effect of minor elements on the composition of the major phases, the improvement of the results is limited. The phase compositions used in the modified Bogue calculations remain estimations, and thus errors between these calculations and experimental results from XRD/Rietveld or microscopic analysis cannot be avoided. In Figure XI.7

both experimental techniques are compared. The quantification data are broadly comparable for both methods; however, the belite content tends to be lower in the microscopic analysis.
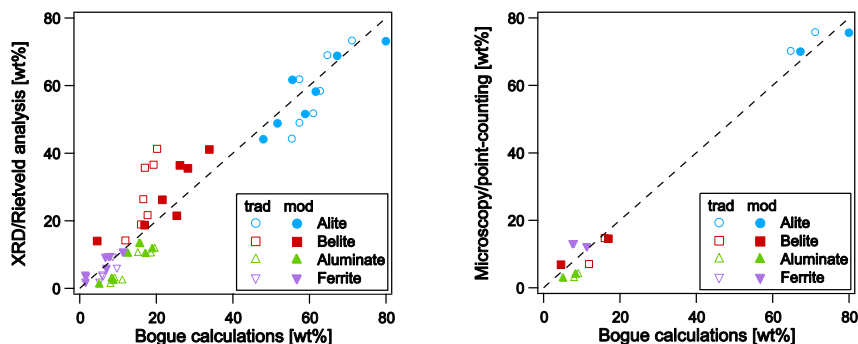
Figure XI.6 – Comparison of the clinker mineralogy according to the traditional (empty markers) and modified (filled markers) Bogue calculations and the mineralogy obtained from XRD/Rietveld analysis (left) or microscopic analysis (right) using point-counting.
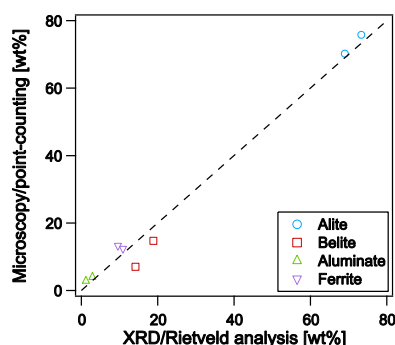
Figure XI.7 – Comparison of the experimental methods to quantify the clinker mineralogy: XRD/Rietveld analysis versus microscopic analysis using point-counting.

C. Effect of burning temperature on clinker mineralogy

The influence of the maximum burning temperature was studied by heating the cement raw meals up to 1350, 1400 and 1450 °C at a constant heating rate (15 °C/min) with a dwell time of 30 min. The results of the XRD analysis are presented in Table XI.4. Within this table the major increase of the alite content due to increasing the burning temperature from 1350 to 1400 °C is seen for CRC1a and CRC2a, while for CRC3a and CRC3b it is seen between 1400 and 1450 °C. As expected, the increase of the alite content is associated with a belite decrease, since alite is formed from belite and free lime. From these results it can be concluded that for CRC1a and CRC2a, burning at 1400

°C is sufficient as the alite content does not increase when burned at 1450 °C, while CRC3a and CRC3b are preferentially burned at 1450 °C to maximize the alite content. After these experiments, the burning temperature was fixed at 1450 °C to assure the highest alite content.

Table XI.4 - The mineralogical composition [wt%] of the regenerated clinkers burned at 1350, 1400 and 1450 °C according to Rietveld analysis of the measured XRD spectra. In parentheses, the estimated error on the weight percentages of the individual refinements is shown.

	CRC1a			CRC2a		
Burning temperature [°C]	*1350*	*1400*	*1450*	*1350*	*1400*	*1450*
Alite	51.9 (0.37)	57.6 (0.46)	57.9 (0.37)	54.2 (0.40)	61.6 (0.51)	60.8 (0.50)
Belite	32.34 (0.31)	26.1 (0.33)	26.2 (0.26)	26.5 (0.31)	19.9 (0.29)	21.3 (0.30)
Aluminate	12.8 (0.14)	12.8 (0.16)	13.1 (0.13)	11.8 (0.14)	10.9 (0.15)	10.2 (0.14)
Ferrite	2.3 (0.13)	2.2 (0.14)	2.0 (0.11)	5.5 (0.13)	5.8 (0.14)	6.0 (0.14)
Lime	0.4 (0.04)	0.2 (0.01)	0.3 (0.04)	0.3 (0.04)	0.3 (0.05)	0.2 (0.04)
Periclase	0.3 (0.06)	1.1 (0.08)	0.5 (0.06)	1.7 (0.08)	1.4 (0.08)	1.5 (0.08)
	CRC3a			CRC3b		
Burning temperature [°C]	*1350*	*1400*	*1450*	*1350*	*1400*	*1450*
Alite	36.3 (0.37)	34.4 (0.35)	43.2 (0.39)	42.6 (0.32)	41.5 (0.39)	47.9 (0.36)
Belite	47.2 (0.44)	48.4 (0.42)	40.3 (0.38)	39.3 (0.32)	39.0 (0.38)	34.9 (0.32)
Aluminate	11.1 (0.16)	11.8 (0.16)	10.1 (0.15)	13.4 (0.14)	13.7 (0.17)	11.4 (0.14)
Ferrite	2.9 (0.15)	2.8 (0.15)	4.0 (0.15)	2.5 (0.12)	3.1 (0.15)	3.6 (0.14)
Lime	0.0 (0.00)	0.0 (0.00)	0.0 (0.00)	0.3 (0.04)	0.0 (0.00)	0.2 (0.04)
Periclase	2.5 (0.09)	2.5 (0.09)	2.4 (0.09)	2.0 (0.07)	2.7 (0.09)	2.0 (0.07)

The content of aluminate and ferrite in the clinker was found to be rather stable, which is expected, as the aluminate and ferrite phases are formed at temperatures below 1300 °C. The quantities of lime and periclase are rather low, and mere an indication of their presence than an accurate quantification.

Four micrographs of CRC3b burned at 1450 °C are shown in Figure XI.8. It is clearly seen that the clinker is rather heterogeneous, which was the main conclusion for all clinkers

regenerated from CRC1a, CRC2a, CRC3a and CRC3b. The heterogeneity of the clinkers is not only affected by the heterogeneity and chemistry of the cement raw meal, but also by the applied heat treatment. It was found plausible that the static heating causes a temperature gradient between the inner and outer part of the rather big sample (about 150 g). Micrograph B in Figure XI.8 indeed indicates that the clinker could be overburned locally, which increases the alite size by recrystallization [Taylor (1997)]. To exclude the effect of such a temperature gradient resulting in heterogeneous clinkers, the clinkers can be burned in a laboratory rotary kiln, if available and when large amounts of clinker are needed, e.g. for the production of cement. Another option is to reduce the effect of the temperature gradient in a static furnace by heating smaller samples (about 100 g) and slowing down the heating rate (e.g. 10 °C/min). To avoid the effect of a static heat treatment on the heterogeneity of the clinker, the heat treatment was adapted accordingly for further clinkering experiments. Additionally, the dwell time in the furnace was increased to about 1 hour.
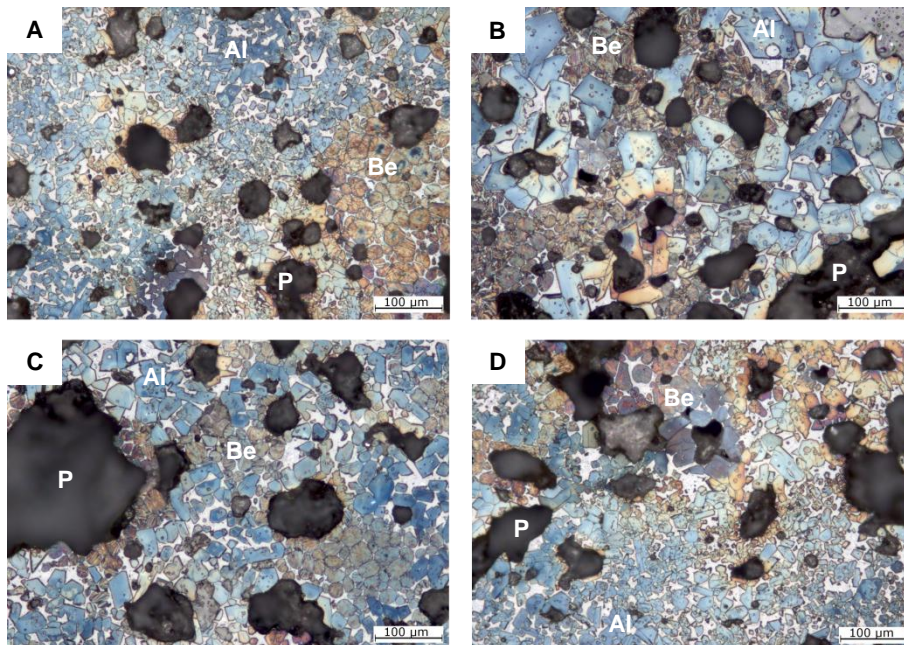
Figure XI.8 - Micrographs of the clinker regenerated from CRC3b with a maximum burning temperature of 1450 °C. Al = alite; Be = belite; P = pore.

D. Effect of raw material fineness on CRC clinker quality

The burnability of a cement raw meal is not only affected by its chemistry, but also by the particle size of the raw mix, and especially by the contents of coarse particles [Kakali and Tsivilis (1993); Chatterjee (2011); Sorrentino (2011)]. E.g. large particles of siliceous materials will result in belite crystals. These large particles mainly determine

the time required for the free lime content to reach its final value. The top sizes for different minerals were already mentioned in chapter X.B. Furthermore, the nature, microstructure and homogeneity of a raw meal will influence the burnability of a cement raw meal [Taylor (1997)]. The nature of our CRC as cement raw meal is a given fact, the fineness and homogeneity can however be changed by varying the grinding time for the raw meal preparation.

D.1. Clinker mineralogy and reactivity

To study the effect of raw material fineness, CRC1c and CRC 2b were ground in a planetary ball mill for respectively 4, 6 and 8 minutes. The obtained R90 values are given in Table XI.5. Subsequently the raw materials were burned to obtain the clinkers of which the quality was assessed by XRD/Rietveld analysis and the reactivity by isothermal calorimetry.

The results of the XRD/Rietveld analysis are presented in Table XI.5. Focussing on the normalized results for the four main clinker phases, some variation on the amounts of calcium silicate phases was noticed, nonetheless the effect seems minimal. For CRC1c, first one would think the amount of alite would increase with the fineness of the raw material (4 minutes versus 6 minutes). However, the clinker from the raw meal ground during 8 minutes is again similar to the one ground for 4 minutes. For CRC2b, there is a trend for an increased alite content with an increasing fineness; the significance of this trend is however questioned. Also the amount of aluminate and ferrite phases remains constant despite variation of the raw meal fineness.

Another point of interest was the reactivity of the clinker phases. For this purpose isothermal calorimetry was performed on the clinkers mixed with calcium sulphate. The amount of calcium sulphate added was calculated from the C_3A and Na_2O content of the clinkers (see Table X.1); the total grinding time was 10 minutes. The measured heat flows are presented in Figure XI.9. As expected from the limited effects of the raw material fineness on the clinker mineralogy, also the effect on the reactivity of the clinker phases is non-existent.

D.2. Differential Thermal Analysis

Since the effect of the raw material fineness on the clinker mineralogy and reactivity was rather limited, a DT analysis was conducted on the raw meals of CRC2b to see whether the clinkering reactions were promoted by increasing the raw meal fineness. The obtained results are presented in Figure XI.10 (DT analysis) and Figure XI.11 (TG analysis).

As mentioned earlier, for CRC, the main endothermic peak is around a temperature of 850 °C, namely the decarbonation peak of the limestone. This reaction seems not to be influenced by the raw material fineness. For the CRC raw meal, milled for only 4 minutes, an (unexpected) exothermic peak around 243 °C might be observed. However, considering the results of the TG analysis, a bigger mass loss for this raw meal

was registered from a temperature of about 170 °C onwards. It might thus be possible that an endothermic peak should be seen on a decreasing baseline. This endothermic peak is then probably related to the loss of e.g. water from the cement paste in the CRC. Inherent to this interpretation, it seems that by increasing the milling time, part of the bound water is already released in the milling process, due to a combination of the impact of milling, damaging e.g. the crystal structure of the C-S-H gel, and the heat produced upon milling. Above all, by increasing the fineness, more surface becomes available for dehydration of the CRC. From the TG data it can be concluded that only an additional amount of about 2wt% of bound water might be lost due to the increased milling time (4 minutes compared to 6 and 8 minutes). As far as an interpretation of the endo/exothermal peaks in the high temperature range is possible, also these peaks seem not to be influenced that much by the increased fineness of the raw meals.
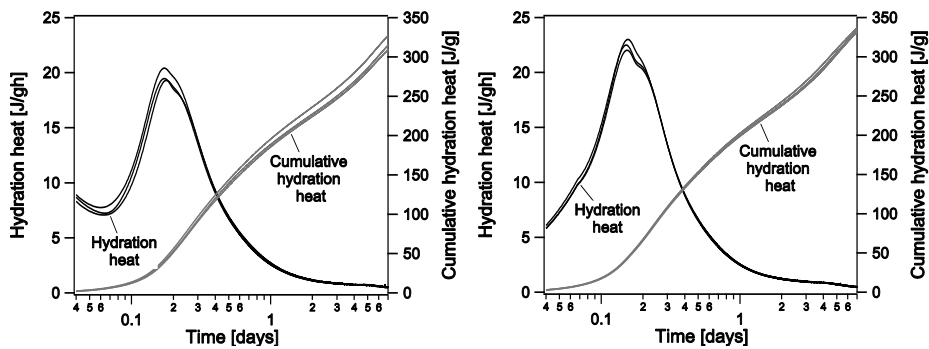
Figure XI.9 - Hydration heat and cumulative hydration heat of CRC1c (left) and CRC2b (right) clinkers with different raw material fineness
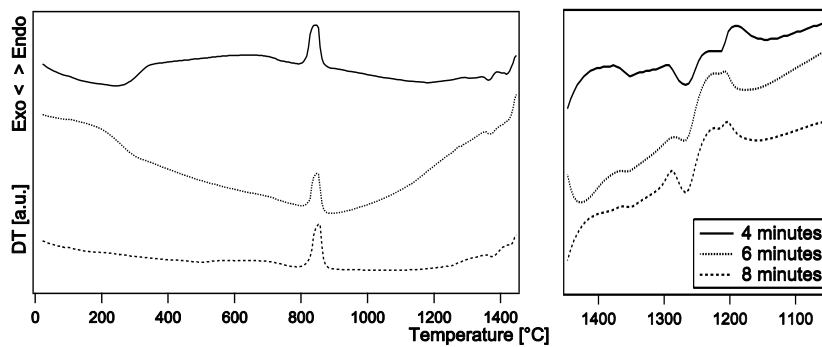
Figure XI.10 - DT data for heating (left) and cooling (right) of CRC8 with different finenesses after milling during 4, 6 or 8 minutes. The vertical scale of the cooling process (right) was expanded compared to the heating process (left).

Table XI.5 – Fineness parameters (milling times and R90 values), together with the clinker mineralogy of the burned clinker for CRC1c and CRC2b. The values in parentheses are the estimated errors on the weight percentages of the individual refinements.

	CRC1c			CRC2b		
Raw material fineness						
Milling time [min]	4	6	8	4	6	8
R90 [wt%]	24	17	12	19	15	12
Clinker mineralogy by XRD/Rietveld analysis [wt%]						
Alite	63.8 (1.90)	71.8 (2.19)	68.0 (2.09)	70.2 (2.12)	69.5 (2.02)	70.0 (1.84)
Belite	17.4 (0.96)	12.5 (0.93)	16.5 (1.00)	13.6 (0.98)	10.9 (0.83)	8.9 (0.73)
Aluminate	1.1 (0.06)	1.5 (0.08)	1.4 (0.07)	2.8 (0.15)	3.1 (0.16)	3.1 (0.15)
Ferrite	10.1 (0.50)	10.2 (0.52)	10.6 (0.54)	9.2 (0.48)	9.1 (0.46)	8.6 (0.40)
Aphthitalite	0.5 (0.22)	0.4 (0.21)	0.8 (0.23)	0.6 (0.22)	0.8 (0.22)	0.6 (0.19)
Syngenite	0.8 (0.38)	1.3 (0.39)	1.6 (0.39)	1.9 (0.40)	1.8 (0.39)	1.4 (0.35)
Ca-langbeinite	0.4 (0.26)	0.1 (0.25)	0.2 (0.26)	0.0 (0.16)	0.2 (0.25)	0.3 (0.23)
Calcite	0.6 (0.32)	1.4 (0.36)	0.4 (0.34)	0.9 (0.23)	0.5 (0.29)	0.4 (0.29)
Periclase	0.5 (0.15)	0.8 (0.20)	0.5 (0.19)	0.9 (0.19)	0.9 (0.18)	0.6 (0.15)
Other	4.7	0.0	0.0	0.0	3.1	6.1
Normalization of the 4 main clinker phases to 100 wt% [wt%]						
Alite	69.0	74.8	70.5	73.3	75.0	77.3
Belite	18.8	13.1	17.1	14.2	11.8	9.8
Aluminate	1.2	1.5	1.4	2.9	3.3	3.4
Ferrite	10.9	10.6	11.0	9.6	9.9	9.5
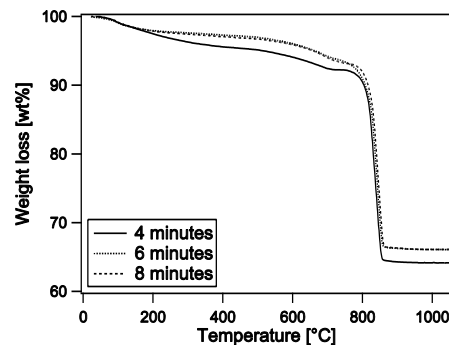
Figure XI.11 - TG data upon heating of CRC 8 with different finenesses after milling during 4, 6 or 8 minutes.

E. Effects of burning deteriorated concrete on the regeneration process

E.1. Theoretical background

The degradation of a CRC structure can affect the future clinkering process of the CRC rubble and thus its regenerated clinker. Carbonation will mainly affect the CO_2 emissions during the production of the regenerated cement. Since this CO_2 was captured from the atmosphere during the life cycle of concrete, this additional CO_2 release can be considered neutral in a life cycle assessment (see chapter XIII). The effect of the permeation of acids and salts (alkalis, Cl^-, SO_4^{2-}, Mg^{2+}) in CRC on the regenerated cement however, should be considered differently. Their effect may be positive or negative, depending on the concentration. For all of these components, proper dilution might thus be required to avoid problems during the clinkering process or in the final cement. A short literature overview of the effect of magnesium, chlorides, sulphates and alkalis is given hereafter. The effect of sulphate additions on the clinker mineralogy was assessed using XRD/Rietveld analysis (see chapter XI.E.2).

Magnesium

Magnesium will affect the mineralogy of the clinker, as it is an important substituent for CaO in the clinker minerals, especially alite. Magnesium will affect the crystal structure of alite on the one hand (see chapter II.A.1), and the lime saturation factor for designing a cement raw meal on the other hand (see chapter II.B.1). Although the crystal structure of alite is affected by the incorporation of magnesium, it was found that the influence on its hydration was of minor importance. The concentration of magnesium should however be limited (see Table II.1), since only a limited amount of magnesium oxide can be incorporated in the clinker minerals. The remaining MgO present in a clinker mostly crystallises as periclase, which is undesirable since it is a potential cause of delayed expansion in hardened concrete [Glasser (2004)].

Chlorides

Chlorides trapped in the clinker are known to reduce concrete strength and may speed up the corrosion of the reinforcement [Taylor (1997)]. Another reason to limit the chloride content of cement raw meals is related to the high volatility of chlorides. Large fractions of chlorides are volatilized at about 980 °C and travel up the kiln to cooler regions to finally precipitate. In particular chlorides, but also sulphates, can condensate resulting in preheater clogging or the formation of kiln rings on the kiln walls [Pradip et al. (1990); Gadayev and Kodess (1999); Aouad et al. (2012); Aranda Usón et al. (2013)].

Although the amount of chlorides in a cement raw meal is limited, mainly to reduce the maintenance costs, it also has positive effects on the clinkering reactions. In the presence of chlorides, the appearance of a liquid was observed from 600 °C [Gadayev and Kodess (1999)]. This liquid based on the $CaCl_2$-KCl-$NaCl$ salt system has a low viscosity and contributes to the decomposition of the raw materials. The alkali oxides released from the raw materials react with $CaCl_2$ to release alkali chloride (RCl) and CaO. This free lime can be used to form the first clinker minerals. At 1000-1200 °C RCl evaporates and an alkali cycle is established. In high concentrations, this cycle of volatiles results in the earlier mentioned problems of clogging in the preheater and the formation of kiln rings.

Apart from the earlier formation of C_2S and $C_{12}A_7$, the addition of $CaCl_2$ can also result in the formation of new minerals such as $C_{11}A_7.CaCl_2$ and $2C_2S.CaCl_2$ [Gadayev and Kodess (1999)]. The latter intermediate mineral will decompose at about 1000-1200 °C to produce C_2S and a new highly alkaline calcium chlorosilicate, alinite ($6C_3S.C_3A.CaCl_2$). Since the hydration characteristics of alinite were found superior to alite [Pradip et al. (1990); Gadayev and Kodess (1999)], the production of alinite cement was found promising in the nineties. Additional benefits are the lower burning temperatures (1150 °C compared to 1450 °C) and a less energy intensive grinding process (the resulting clinker is more friable). Nonetheless all these benefits could not compensate for the practical issues in the kiln system requiring periodic maintenance whereby production time is lost.

Sulphates and alkali

The effect of sulphur on the clinkering process is also related to the alkalis present, and both will participate in cycles of evaporation and condensation in the clinker kiln [Glasser (2004)]. The sulphates, originating from the raw materials or the fuels, introduced in the clinkering process must eventually appear in one of the three output streams: clinker, cement kiln dust or gaseous emissions. As for the chlorides, also sulphate may be retained in the kiln as annular deposits, and contribute to the formation of kiln rings, interrupting the normal downslope flow of the cement raw meal.

Alkalis affect the clinkering process by modifying the physicochemical properties of the melt, and may have an adverse effect on the phase composition of the clinker [Jawed and Skalny (1977)]. In the presence of sulphur, the volatility of the alkali during clinker formation is reduced. The alkali sulphates hereby present in the melt can decrease its

viscosity, but even a small stoichiometric excess of alkali oxide over SO_3 increases it. A low viscosity of the melt is favoured as it stimulates the formation of alite by accelerating dissolution and diffusion through the liquid of lime and belite.

When the molar $SO_3/(K_2O+Na_2O)$ are in balance, almost all of the sulphur and alkalis are present in the clinker as alkali sulphates (arcanite (K_2SO_4), aphthitalite ($K_3Na(SO_4)_2$), thenardite (Na_2SO_4)), and very little of the sulphate or alkalis can be incorporated in the clinker phases. A separated liquid phase is formed in the burning zone, which is immiscible with the normal aluminate/ferrite liquid phase [Glasser (2004)]. If alkalis are present in excess of sulphate, the excess Na_2O and K_2O are available to be incorporated in the clinker minerals, particularly C_3A. The latter results in the formation of so called 'alkali aluminate', or orthorhombic C_3A, which is more reactive compared to cubic C_3A and can result in faster setting times. If there is an excess of sulphate present, potassium sulphate will associate with calcium sulphate to form calcium langbeinite. The occurrence of anhydrite in the cement clinker is related to both the SO_3 and alkali (especially K_2O) content.

The amount of alkali sulphates present in the clinker will affect the setting times of the cement, and thus the amount of calcium sulphate added during the milling process should be adapted accordingly [Torréns-Martín and Fernández-Carrasco (2013)]. Increased concentrations of soluble alkalis also have an effect on cement strength, increasing early strength while potentially lowering late strength.

E.2. The effect of sulphate additions on the clinker mineralogy

i. Mix design

Calcium sulphate was added to the CRC mixtures to simulate the effect on the clinkering process of using CRC from a construction that suffered sulphate attack. It is difficult to find appropriate SO_3 concentrations since a considerable scatter on the results is expected. The degradation process starts at the surface of the concrete by crack propagation, which is initiated by the formation of ettringite and other expansive products. The concentrations are thus depending on the ratio of the exposed surface to the concrete volume and the SO_3 contents will be diluted in the concrete matrix.

In a study of the sulphate ingress in mortar samples produced with Portland cement, conducted by Schmidt et al. (2009), the sulphate concentrations as a function of depth were studied. The effect of the sulphate ingress was observed up to about 5 mm for exposure times of 56 and 270 days. In that zone, the sulphate concentrations measured vary with the concentration of the sulphate solution and the exposure time. The SO_3 concentrations varied from 5 to 20 wt% in case the mortar samples were exposed to a 44 g/l Na_2SO_4 solution (high concentration). In Weritz et al. (2009) different concrete cores obtained from sewage treatment plants that suffered sulphate attack were analysed for their sulphate content. Although the zones with affected sulphate concentrations were higher, up to 15 mm, the measured sulphate concentrations were lower, up to 6 wt%.

Different amounts of CaSO₄ were added to both CRC1c and CRC2b clinker raw meals, before starting the laboratory clinkering process as described in chapter X. After 3 minutes milling of the cement raw meal, CaSO₄ was added. The adapted raw meal was subsequently milled for 1 minute, before preparing the raw meal tablets. The studied range of sulphate content in the CRC raw meals was 1.6-5.3 wt% and 1.6-5.9 wt% for CRC1c and CRC2b respectively (see Table XI.6). The chemical compositions of the produced raw meals and regenerated clinkers are given in Table XI.6 and Table XI.7 respectively. In Table XI.7 it is seen that a significant amount of SO_3 is lost as gaseous emission in the clinkering process, as the measured SO_3 content of the clinker is significantly lower compared to the expected SO_3 content.

Table XI.6 - Chemical composition of the produced raw materials with different amounts of CaSO₄ added [wt%]; with LOI = Loss on Ignition

	CRC1c				CRC2b			
CaO	44.4	44.7	44.3	44.3	43.4	44.2	44.0	43.5
SiO_2	14.1	14	13.7	13.0	13.6	13.6	13.2	12.6
Al_2O_3	3.3	3.0	3.0	2.9	3.1	3.0	3.1	2.9
Fe_2O_3	2.1	1.9	1.9	1.8	1.4	1.4	1.3	1.3
MgO	1.3	1.2	1.2	1.2	1.6	1.5	1.6	1.5
Na_2O	0.08	0.06	0.07	0.06	0.02	0.01	0.02	0.01
K_2O	0.42	0.39	0.39	0.37	0.43	0.42	0.43	0.40
SO_3	1.6	1.9	3.2	5.3	1.6	2.0	3.7	5.9
Cl^-	0.018	0.045	0.016	0.017	0.022	0.025	0.024	0.022
LOI	31.8	32.2	31.2	30.2	33.6	33.6	32.4	31.1

Table XI.7 - Chemical composition of the regenerated clinkers with different amounts of CaSO₄ added [wt%]

	CRC1c				CRC2b			
CaO	65.1[a]	65.9[a]	64.4[a]	63.5[a]	68.7	68.5	68.3	66.7
SiO_2	21.6	21.5	21.1	19.8	21.5	21.2	20.8	19.9
Al_2O_3	4.7	4.1	4.3	4.2	4.1	4.1	4.3	4.0
Fe_2O_3	3.3	2.8	2.9	2.9	2.2	2.1	2.2	2.1
MgO	1.9	1.8	1.8	1.8	2.4	2.4	2.3	2.2
Na_2O	0.11	0.09	0.11	0.11	0.02	0.02	<0.01	0.04
K_2O	0.26	0.28	0.38	0.41	0.29	0.31	0.28	0.52
SO_3	0.9	1.1	2.0	4.4	0.8	0.9	1.3	4.6
Cl^-	<0.005	<0.005	<0.005	<0.005	0.011	0.012	0.010	0.011
Expected SO_3*	2.3	2.9	4.7	7.6	2.4	3.1	5.5	8.5

* Calculated from the raw material sulphate content by exclusion of the LOI
[a] The CaO contents were calculated from the raw material composition by exclusion of the LOI

The effect of the sulphate additions on the clinker mineralogy was studied by XRD/Rietveld analysis. The XRD/Rietveld analysis of the SAM extraction was used to evaluate the distribution of the sulphate phases qualitatively. Quantitative analysis from XRD/Rietveld analysis of the whole clinker was not possible for all sulphate phases due to their presence under the detection limits related to their low concentrations. The effect of sulphate additions on the major phases was studied quantitatively by XRD/Rietveld analysis of the whole clinker sample.

Distribution of the sulphate phases

The XRD patterns obtained from the SAM extractions are shown in Figure XI.12 and Figure XI.13. For the lower sulphate concentrations (0.9% and 1.1% for CRC1c and 0.8% and 0.9% for CRC2b), limited amounts of sulphates are found, namely arcanite and Ca-langbeinite. For higher sulphate concentrations (2.0% and 4.4% for CRC1c and 1.3% and 4.6% for CRC2b), significant amounts of the calcium sulphate anhydrite were observed. Some H_2O bearing calcium sulphate phases (bassanite ($CaSO_4.^1/_2H_2O$) and gypsum ($CaSO_4.2H_2O$)) were observed. The uptake of this water probably occurred during the sample preparation.
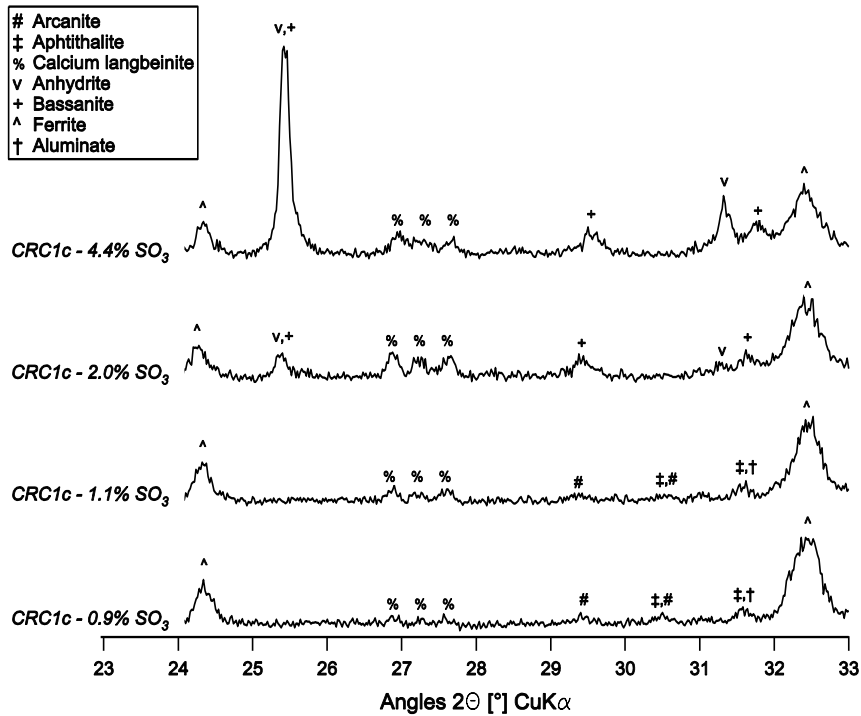
Figure XI.12 - Observed XRD patterns of the SAM extractions obtained from the CRC1c clinker with varying sulphate contents
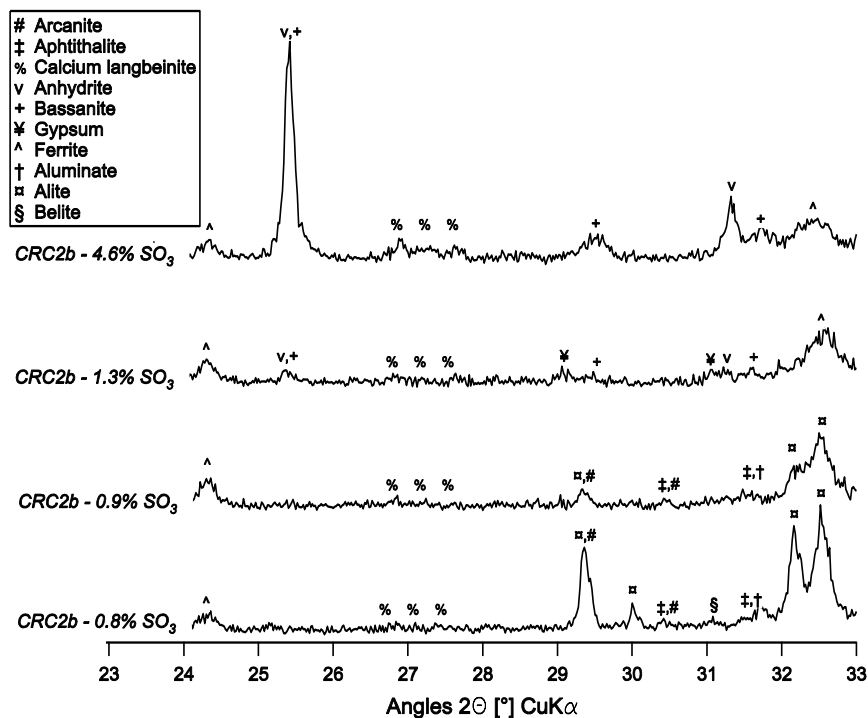
Figure XI.13 - Observed XRD patterns of the SAM extractions obtained from the CRC2b clinker with varying sulphate contents

In some of the samples certain amounts of alite and belite were left after the SAM extraction. No thenardite and only a limited amount of aphthitalite was found present in the CRC clinkers. The absence of significant amounts of sodium sulphates can be expected due to the low sodium concentrations of the clinkers.

For both calcium langbeinite and bassanite, the reflections slightly shift in the 2θ range. Rietveld analysis of the XRD patterns indeed showed that the cell parameters of both phases are affected by the sulphate concentration of the clinker. Probably the sulphate concentration slightly affects the composition of the phases and thus the cell parameters. In case of bassanite also the water content might be responsible for the observed shift.

Effect on the major clinker phases

The results of the XRD/Rietveld analysis of the whole clinker samples are presented in Table XI.8. For CRC1c, the formation of alite seemed to be stimulated by a lower viscosity of the melt when the sulphate concentration was about 1.1%. A further increase of the sulphate concentrations resulted in the stabilisation of belite due to the uptake of SO_3. For CRC2b, the alite content seems rather stable for sulphate concentrations of 0.8%, 0.9% and 1.3%. Again, the uptake of SO_3 in the belite structure resulted in lower alite contents for a SO_3 content of about 4.6%.

In Table XI.9, the distribution of the four main clinker phases obtained by XRD/Rietveld analysis is compared with the potential mineralogy as calculated with the modified Bogue formulas. The increased amount of alite observed for CRC1c with a 1.1% SO_3 concentration is also obtained within the modified Bogue calculations. Since these calculations do not take into account the effect of alkali and/or sulphates on the viscosity of the melt and thus the burnability of the clinker, the increased alite content might be a result of rather limited changes in raw meal composition. In the end it is probably the combined effect of SO_3 on the melt viscosity and the raw meal composition that explains the increased alite content in the clinker of CRC1c with 1.1% SO_3. The stabilisation of belite by the incorporation of SO_3 is taken into account in the modified Bogue calculation. This effect is seen in the calculations for both CRC1c and CRC2b with the highest SO_3 content, having a significantly higher belite content at the expense of alite.

Table XI.8 - Mineralogical composition of the regenerated clinkers with different amounts of CaSO$_4$ added [wt%] by XRD/Rietveld analysis

	CRC1c				CRC2b			
SO_3	0.9	1.1	2.0	4.4	0.8	0.9	1.3	4.6
Expected SO_3*	2.3	2.9	4.7	7.6	2.4	3.1	5.5	8.5
Alite	65.6	71.2	67.2	60.7	72.5	76.0	76.1	62.5
Belite	16.3	11.2	21.7	22.9	7.9	6.9	10.0	15.5
Aluminate	1.3	1.1	1.0	0.8	3.1	2.6	2.6	3.4
Ferrite	11.5	9.7	9.2	9.4	8.6	7.4	9.0	5.9
Anhydrite				4.2				4.2
Calcite	0.7	0.7	0.8	1.4	0.3	1.3	1.5	2.6
Periclase	0.4	0.1	0.1	0.6	0.4	0.4	0.8	0.6
Other	4.3	6.1			7.2	5.4		5.3

*Calculated from the raw material sulphate content by exclusion of the LOI

iii. Discussion

From literature it was concluded that the effect of an increasing sulphate content is highly depending on the alkali content. Since the alkali content of the studied clinkers is rather low, it was observed that an increasing sulphate content resulted in the formation of more CaO containing sulphates such as calcium langbeinite and anhydrite. The reasoning could be made that the consumption of CaO by the formation of calcium langbeinite and anhydrite will reduce the alite formation since less CaO is available. The latter is however not expected in this study, as the sulphates are added as calcium sulphate. Since a significant amount of sulphate was lost due to emissions in the clinkering process, a limited enrichment of the CaO content is more likely.

The experimental results obtained in the present study (low alkali content) showed, that the effect of SO_3 concentrations up to 2% on the clinker mineralogy are limited. For sulphate concentrations up to 4.4-4.6%, the high SO_3 content seemed to stabilize belite

at the expense of alite. This effect is certainly not favoured, although the resulting alite contents are certainly acceptable for a modern clinker, since the alite content of the clinker to start from was rather high (see Table XI.3).

Table XI.9 - Clinker mineralogy of the regenerated clinkers with different amounts of CaSO₄ added [wt%]: experimental quantification by XRD/Rietveld analysis versus potential mineralogy using the modified Bogue calculations

	CRC1c				CRC2b			
SO_3	0.9	1.1	2.0	4.4	0.8	0.9	1.3	4.6
*Expected SO₃**	2.3	2.9	4.7	7.6	2.4	3.1	5.5	8.5
XRD – normalized for four main clinker phases								
Alite	69.3	76.5	67.8	64.8	78.7	81.8	77.9	71.6
Belite	17.2	12.0	21.9	24.5	8.6	7.4	10.3	17.8
Aluminate	1.3	1.1	1.0	0.8	3.4	2.8	2.7	3.9
Ferrite	12.1	10.4	9.3	0.8	9.3	8.0	9.2	6.7
Modified Bogue – normalized for four main clinker phases								
Alite	73.9	82.7	74.3	62.1	86.6	86.4	85.3	71.4
Belite	10.2	3.6	10.7	20.9	-a	-a	-a	13.0
Aluminate	5.0	4.5	5.4	6.8	6.9	7.6	8.2	9.1
Ferrite	10.9	9.2	9.5	10.1	6.6	6.1	6.5	6.5

* Calculated from the raw material sulphate content by exclusion of the LOI
a Negative values for belite were obtained and this phase was excluded from the calculations

In practice, the sulphate content of a clinker raw meal should be limited in order to avoid clogging of material on the sides of the clinker kiln. Depending on the kiln installation, the sulphate content of the final clinker should be limited to 1.1-1.4% [Schoon et al. (2012)]. These more strict practical limitations will also avoid problems related to mineralogy as discussed above. Additionally, in practice, a stoichiometric balance is imposed on the sulphate and alkali content, expressed as the Degree of Sulphatisation (DoS) [Schoon et al. (2012)]:

$$\text{DoS} = \frac{77.41 \cdot wt\%(SO_3)}{(wt\%(Na_2O) + 0.658 \cdot wt(K_2O)}$$

(XI-12)

calculated using the chemical analysis of the final clinker. DoS levels between 80 and 120 wt% are recommended to avoid damage to the kiln system. In case of the current study, the alkali contents are rather low, resulting in an imbalance between the sulphates and alkali. In order to meet the practical requirements, the SO₃ and alkali content should thus be decreased or increased respectively.

Finally, it should be noted that the behaviour of alkalis and sulphates in the real clinkering process could not be simulated in the static furnace used. This study only showed how an increasing sulphate content (with constant alkali content) affects the clinker mineralogy. The effect of an increasing sulphate content of a cement raw meal on

the clinker processing of a real kiln is expected to result in more strict limitations. An optimisation of the $SO_3/(K_2O+Na_2O)$ balance in case of the studied CRC raw meals will be required. In the end it can be concluded that the use of concrete that suffered sulphate attack will not harm the clinkering process, if properly diluted.

F. Conclusions

The clinkering process for a CRC and a hydrated cement paste as alternative raw material was studied. The main CaO sources in CRC are the limestone aggregates. Decarbonation of the calcite and minor dolomite results in the formation of important amounts of free lime (CaO) at temperatures below 1050 °C. This free lime is recombined with aluminate, silicate and minor sulphate to form intermediate belite, gehlenite, mayenite and ye'elemite phases at temperatures up to 1150 °C. The formation of the final clinker phases are observed at 1250 °C and higher, when extensive formation of alite, aluminate and ferrite occurs at the expense of lime, belite and intermediate Ca-aluminates. In the cement paste lime was mainly formed around 450 °C during the dehydroxylation of portlandite. Partial carbonation of the lime to calcite occurred over the temperature range of 450-650 °C. Above 650 °C extensive and rapid formation of belite, lime and gehlenite was observed. In general, thermal reactions during heating of the cement paste were observed to occur more rapidly and to initiate at lower temperatures.

The improved burnability of the cement paste clinker can be related to the larger amount of melt forming phases. However, below melting temperature, it is mainly the elevated levels of sulphate and the very fine intermixing of the decomposed Ca-silicate and Ca-aluminate hydrate phases that promote the onset and completion of thermal transformations and reactions. Sulphate acts as a flux by lowering melting temperatures and melt viscosity, but also as a mineralizer by promoting the formation of belite. Substantial substitution of sulphate into the belite lattice shows, however, the negative effect of lowering the alite to belite ratio in the clinker.

The experimental quantification of the CRC clinkers by XRD/Rietveld analysis revealed that the effect of other elements besides CaO, SiO_2, Al_2O_3 and Fe_2O_3 may not be neglected. The observed mineralogy of the clinkers differed from the one theoretically expected from the Bogue calculations. Although the modified Bogue calculations try to simulate the effect of the minor elements on the phase compositions, the improvements remain rather limited. This is merely due to the fact that even in the modified Bogue calculations the phase compositions remain estimations and errors between the calculations and the experimental results cannot be avoided.

From the clinker mineralogy and reactivity, studied by XRD/Rietveld analysis and isothermal calorimetry respectively, it was concluded that the raw material fineness had no significant influence. Obviously this conclusion only applies for the studied ranges of the raw mix fineness (R90 ranging from 12-24 wt%). However, as the alite content was already satisfying for the clinker from the raw mix with the lowest fineness, it was

concluded that a lower fineness might be favoured as this will be beneficial for the energy consumption of the raw meal preparation. The results of a differential thermal analysis indicate that significant energy savings in the clinkering process due to an improved reactivity of the raw meal should not be expected. Only in the lower temperature range there might be a small effect as additional milling seems to result in a slightly drier raw material.

When using CRC as cement raw material, the permeated acids and salts in deteriorated concrete will have an effect on the clinkering process. While the amounts of MgO should be limited to avoid a potential delayed expansion in hardened concrete, the amounts of chlorides, sulphates and alkali should be mainly limited to avoid problems in the kiln system. Due to the volatility of these elements, cycles of evaporation and condensation will be established in the clinker kiln. As a result of these cycles, the preheater might get clogged or kiln rings might appear on the kiln walls, both requiring periodic maintenance of the kiln system. Nonetheless, if properly balanced, magnesium, chlorides, sulphates and alkali can have a positive effect on the clinkering process (e.g. stabilisation of more reactive phases and decreasing the melt viscosity) and the use of deteriorated CRC raw meals is possible if properly diluted.

XII - The hydration of CRC cement

In total, the hydration of four CRC cements was tested, besides the hydration of two commercial cements (CEM I 52.5 N and CEM I 42.5 N LH HSR LA). An overview of the produced CRC cements is given in Table XII.1. The mineralogy of CEM I 52.5 N and CEM I 42.5 N LH HSR LA are presented in Table XII.2. Hereafter, CEM I 42.5 N will refer to the CEM I 42.5 N LH HSR LA used in the study. Results of this chapter have been published in De Schepper et al. (2014).

Table XII.1 – Overview of the CRC samples used for the assessment of the cement hydration process

Cement	Raw material	Alite content [wt%][a]	CaSO$_4$ added [wt%]	Grinding time [min]	SSA [m^2/kg]
CRC1b_CS2_GT10	CRC1b	48	2	10	400
CRC1c_CS4_GT10	CRC1c	64	3.7	10	410
CRC2b_CS4_GT10	CRC2b	70	3.8	10	410
CRC2b_CS4_GT6	CRC2b	70	3.8	6	350

[a] see Table XI.3

Table XII.2 – The mineralogy by XRD/Rietveld analysis [wt%] and the specific surface area (SSA) by Blaine [m^2/kg] of the commercial cements used as reference within the hydration study of the CRC cements

Phase	CEM I 52.5 N	CEM I 42.5 N LH HSR LA
Alite	52.5	57.9
Belite	18.2	21.9
Aluminate	5.0	1.1
Ferrite	10.9	10.9
Anhydrite	2.2	0.9
Gypsum	0.4	
Calcite	2.5	2.3
Other	8.4	5.1
SSA	380	350

A. Experimental results

A.1. Hydration heat

The heat release during hydration of the different cement pastes was measured by isothermal calorimetry, of which the results are presented in Figure XII.1. Neglecting the very first hydration peak, it is seen that for CRC1c_CS4_GT10 and CRC2b_CS4_GT10 the first hydration peak, mainly related to the hydration of alite, occurs sooner (after about 4 hours) and reaches a higher maximum value, about 19 and 22 J/gh for respectively

CRC1c_CS4_GT10 and CRC2b_CS4_GT10. For the other CRC cements, the dormant period is a bit longer and the first hydration peak reaches a maximum after about 8 and 9 hours of 11 and 12 J/gh for respectively CRC2b_CS4_GT6 and CRC1b_CS2_GT10. Finally, the commercial cements reach their maximum after about 11 hours. For CEM I 52.5 N and CEM I 42.5 N the measured maximum values are respectively about 12 and 8 J/gh. As CEM I 42.5 N is a low heat cement, a lower value was indeed expected. The smaller heat release obtained is due to the difference in fineness on the one hand, and the difference in mineralogy on the other hand. The lower aluminate content of CEM I 42.5 N might indeed affect the hydration heat measured.

The cements of CRC2b prove how the fineness of a cement affects its reactivity. CRC2b_CS4_GT10 shows a high narrow first hydration peak, significantly earlier compared to the low broader first hydration peak of CRC2b_CS4_GT6, where the only difference between both cements is their fineness. As the hydration peak of the latter is more similar compared to the commercial one (CEM I 52.5 N), it seems however that the lower fineness might be good enough for practical applications. Also the clinker mineralogy will affect the reactivity of a cement paste. It is seen that a higher cement fineness compensates the rather low alite content of CRC1b_CS2_GT10. Hereby the obtained hydration curve also approaches the curve of the commercial cement (CEM I 52.5 N).
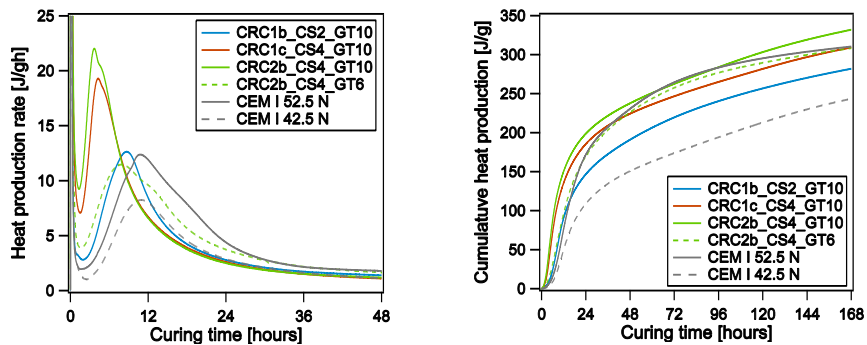
Figure XII.1 – Heat production rate (left) and cumulative heat production (right) of hydrating CRC and commercial cement pastes.

After 7 days, the cumulative hydration heat of most CRC cements is comparable to the one of a commercial cement (CEM I 52.5 N), namely about 310 J/g. CRC2b_CS4_GT10 has slightly higher result, about 330 J/g, probably related to a higher alite content in combination with a higher fineness. The lower value for CRC1b_CS2_GT10, about 280 J/g, can be explained by its lower alite content and thus a lower hydration heat potential.

A.2. TG analysis

i. Decision on the methodology

CRC1b_CS2_GT10 was used to make decisions on the final method to be used for the analysis of the other CRC samples. Both freeze drying and solvent exchange were used to stop hydration. Also both analysis techniques were applied to quantify the portlandite content by TG analysis, namely the mere weight loss method and the tangential method. The results are presented in Figure XII.2.
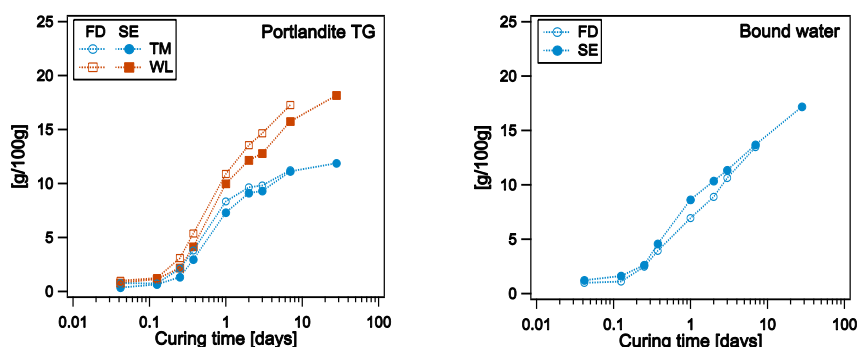
Figure XII.2 – Portlandite (left) and bound water (right) content of a hydrating CRC cement paste (CRC1b_CS2_GT10) determined by TG analysis; comparing both analysing techniques (TM = tangent method; WL = mere weight loss method) for portlandite determination and both methods for arresting cement hydration (SE = solvent exchange; FD = freeze drying) for quantifying both the portlandite and bound water content.

The effect of the drying technique on the TG measurements is shown in Figure XII.3, where the initial weight loss is higher using the solvent exchange method. However regarding both the bound water and the portlandite content, the effect of how hydration was stopped seems not to have a significant impact (see Figure XII.2). At first, the effect of the applied method for arresting hydration on the portlandite content seems to be depending on the method used for quantification, and smaller differences are noted using the tangent method. However, the bigger differences observed when the portlandite content is quantified by the mere weight loss, are possibly related to the higher absolute values obtained. In the end, the solvent exchange method was chosen for further analysis because of the benefits for XRD/Rietveld analysis (see chapter XII.A.3).

While the effect of the different methods to arrest the hydration process remains limited, the portlandite content is significantly influenced by the analytical method used. The reasoning after the tangential method seems most accurate, as the concurrent weight loss due to other cement hydrates is considered separately. However, comparing the results with the values obtained from XRD/Rietveld analysis (see Figure XII.5), it seems that there is a better correlation with the results calculated from the mere weight

loss. For this reason it was decided to continue TG analysis with the mere weight loss method for quantification of the portlandite content.
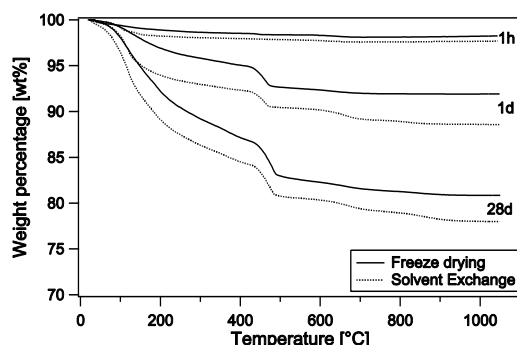
Figure XII.3 - TG data after 1h, 1d and 28d of hydration after freeze drying (full line) or solvent exchange (dotted line) [CRC1b_CS2_GT10].

ii. Results

The results of the bound water and portlandite contents are presented in Figure XII.4. Taking CEM I 52.5 N as a reference for our CRC cements it is seen that the high reactivity of CRC1c_CS4_GT10 and CRC2b_CS4_GT10 results in a higher amount of bound water and portlandite within the first day of hydration. For CRC1b_CS2_GT10, with a lower alite content, the initial values for the bound water content are similar to the ones of CEM I 52.5 N up to one day. The values of the portlandite contents are more comparable to CEM I 42.5 N. For the other CRC cement, namely CRC2b_CS4_GT6, the results are comparable to the reference cement (CEM I 52.5 N), although a higher portlandite content was measured after 28 days of hydration.
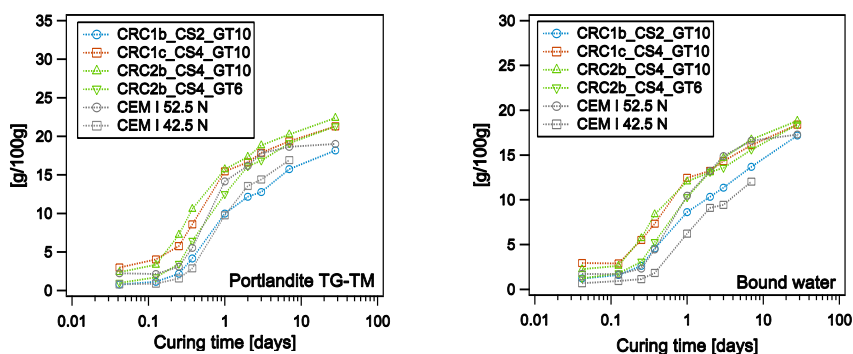
Figure XII.4 – Portlandite (left) and bound water (right) content of hydrating CRC and commercial cement pastes determined by TG analysis after arresting hydration using solvent exchange.

As an obvious difference between CEM I 52.5 N and CEM I 42.5 N was noted regarding their hydration heat, also the portlandite and bound water contents are dissimilar. The results of the bound water content seem to be affected more than the portlandite content. As explained earlier, this is on the one hand due to a lower fineness of CEM I 42.5 N resulting in a lower reactivity. On the other hand the differences in mineralogy of both cements will also affect the hydration process.

A.3. XRD/Rietveld analysis

i. Decision on the methodology

Also regarding XRD/Rietveld analysis, CRC1b_CS2_GT10 was used to decide whether freeze drying or solvent exchange is the preferred method to be used for arresting the cement hydration process. Furthermore, the results for the portlandite content from XRD analysis were used to evaluate the analysis methods of the TG data. Additionally, the portlandite content was calculated from the decrease of the alite and belite content and the following reactions [Taylor (1997); Scrivener et al. (2004)]:

$$C_3S + 5.3H \rightarrow C_{1.7}SH_4 + 1.3CH \qquad\qquad\text{(XII-13)}$$
$$C_2S + 4.3H \rightarrow C_{1.7}SH_4 + 0.3CH \qquad\qquad\text{(XII-14)}$$

Looking at the XRD/Rietveld results in Figure XII.5, it is seen that the freeze drying technique is too aggressive for the gypsum and ettringite phases. Due to freeze drying ettringite and gypsum lose their crystallinity whereby detection by XRD measurements is impossible (see Figure XII.6) as no peaks are observed. Due to this loss of crystallinity, the solvent exchange method was chosen over the freeze drying technique to stop hydration.

Due to the effect of freeze drying on some crystalline phases, the amount of 'other' phases is higher after freeze drying compared to solvent exchange. When the results of the 'other' phases, gypsum, ettringite and kuzelite are summed, still the amount of poorly or non-crystalline phases is higher after freeze drying up to 2 days of hydration. Maybe also other phases, such as alite or belite, are partly affected by the freeze drying technique, increasing the amount of other phases. It indeed seems that there is a trend to obtain lower values of alite and belite using freeze drying to stop hydration. The significance of this trend can however be questioned knowing the measurements were done on cement pastes from different batches and taking into account the accuracy of XRD/Rietveld analysis.

Kuzelite was detected from 2 and 7 days onwards after respectively freeze drying and solvent exchange. It should be noted here that after stopping hydration by solvent exchange, monosulphate tends to be converted to some amorphous phases quite rapidly, and the actual monosulphate contents might thus be underestimated. To avoid this effect the samples should be measured directly after stopping the hydration by solvent exchange.
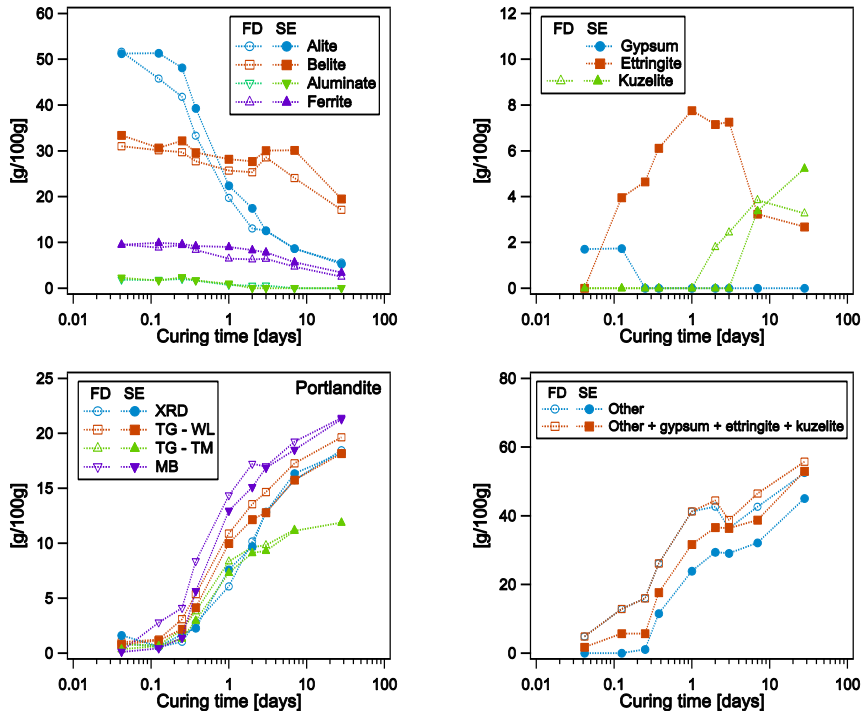
Figure XII.5 – Results of XRD/Rietveld analysis performed on CRC cement pastes (CRC1b_CS2_GT10) of which hydration was stopped by freeze drying (FD) or solvent exchange (SE). The portlandite content was quantified by XRD/Rietveld analysis (XRD), mass balance calculations (MB) or TG analysis using the tangent method (TG-TM) or the mere weight loss (TG-WL).
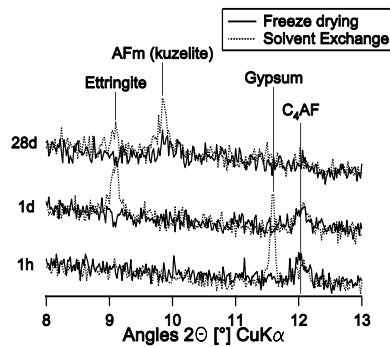
Figure XII.6 - Observed XRD patterns of a hydrated CRC cement paste (CRC1b_CS2_GT10) between 8 and 13 °2θ (CuKα) for 1h, 1d and 28d of hydration after freeze drying (full line) or solvent exchange (dotted line).

Finally, the portlandite content was quantified in two ways from XRD analysis, by Rietveld quantification of the portlandite phase and by mass balance calculations from the decrease of the alite and belite content. TG analysis was performed by the tangent or mere weight loss method. The effect of the method for arresting hydration seems minimal for all quantification techniques. The mass balance calculations result in the highest values, while the tangent method used on the TG data results in the lowest values, from 3 days onwards. The mere weight loss method on the TG data results in slightly higher results compared to those of the XRD/Rietveld analyses. Due to the significant underestimation of the portlandite content after 3 days of hydration using the tangent method on the TG data, it was decided to continue the portlandite quantification from TG analysis using the mere weight loss.

ii. Results

The hydration of the calcium silicate phases as determined by XRD/Rietveld analysis are presented in Figure XII.7. It is seen that alite and to a smaller extent also belite are consumed in time to form portlandite. Also a C-S-H gel is formed, but due to its poorly crystalline nature, an indication of the formation of this C-S-H gel can only be obtained from the increasing amount of 'other' phases quantified by using an internal standard. This amount of 'other' phases however also contains the poorly or non-crystalline hydration products from the hydration of aluminate and ferrite, namely the AFm phases (calcium monosulfoaluminate and calcium hemi- or monocarboaluminate) and hydrogarnets.

Initially, after 1 hour of hydration, the alite values vary between about 50 (CRC1b_CS2-GT10) and 75 (CRC2b_CS4) wt%. As can be expected from the isothermal calorimetry, mostly alite hydrates within the first day. After this first day, alite hydration slowly continues to result in an alite content of about 5-10 wt% after 28 days. It is seen that cements with a higher fineness and alite content (CRC1c_CS4_GT10, CRC2b_CS4_GT10 and CEM I 52.5 N) have the biggest drop in the alite content between 6 and 9 hours of hydration, indicating their higher reactivity.

The amount of the belite phase slowly decreases in time. Remarkable is the drop in the belite content between 7 and 28 days for CRC1b_CS2_GT10, which seems to be accompanied with an increase of the 'other' phases. It seems that the high belite content in combination with an ending alite hydration results in an increased reactivity of the belite. It is indeed found in literature that the solution concentrations produced by hydrating alite inhibit the dissolution of belite [Scrivener and Nonat (2011)]. The effect on the portlandite content is limited, which can be expected comparing reaction XII-12 and XII-13 where it is seen that the hydration of belite results in a lower amount of portlandite in comparison with alite.

In disregard of the differences in mineralogy of the cements, the variation on the amount of portlandite and 'other' phases after 28 days of hydration is rather limited. While initial values for alite and belite vary between 50-75 and 10-32 wt% respectively, the

Figure XII.7 – XRD/Rietveld results of hydrating CRC and commercial cement pastes after arresting hydration using solvent exchange: overview of the hydration of the calcium silicate phases

values for portlandite and 'other' phases are more comparable. For portlandite the highest values are obtained by mass balance calculations (20-26 wt%) and the lowest values by XRD/Rietveld analysis (16-21 wt%). The results from TG analysis for the portlandite quantification are with values of 17-23 wt% intermediate between the other quantification techniques. After 28 days of hydration, the amount of 'other' phases amounts to about 45-55 wt%.

The hydration of the aluminate and ferrite phases is presented in Figure XII.8. While the aluminate phases will dissolve completely, the ferrite phase will decrease from 7-12 wt% after 1 hour of hydration up to 3-6 wt% after 28 days of hydration. For CRC1c_CS4_GT10, the aluminate phase dissolved completely within the first 9 hours. For the other cements aluminate was observed by XRD analysis up to 1 day, and for CEM I 52.5 N with the highest aluminate content even up to 3 days.

Upon hydration of the aluminate phase, and to a smaller extent also the ferrite phase, gypsum is consumed within the first day for the formation of ettringite. The calcium sulphate added to the CRC cements (2/3 hemihydrate and 1/3 anhydrite) immediately formed gypsum upon contact with water, while for the commercial cements anhydrite remained present in the hydrating cement pastes up to 9 hours. For all cements ettringite remained present up to 28 days. After one week kuzelite, a crystalline calcium monosulfoaluminate, was observed for CRC1b_CS2_GT10 and CRC2b_CS4_GT6. For CRC1c_CS4_GT10 and CRC2b_CS4_GT10 it was only observed after 28 days, while for the commercial cements low amounts were detected from 9 hours onwards.

A.4. Compressive strength

In Table XII.3 the compressive strengths of mortars produced with CRC cement CRC1b_CS2_GT10 and the reference cements are shown. As seen in this table, the strength of the CRC cement is significantly lower after 2 days of hydration. After 7 days the obtained strength for CRC is similar to CEM I 42.5 N. After 28 days of curing, the strength is significantly higher compared to CEM I 42.5 N and comparable with CEM I 52.5 N. It can thus be concluded that the later strength (28 days) of the CRC cement is good. To obtain a higher early strength, the content of the most reactive clinker phase alite can be increased, besides increasing the fineness of the cement which would increase the hydration rate of the cement (i.e. cements regenerated from CRC1c and CRC2b, which were however not tested for their compressive strength).
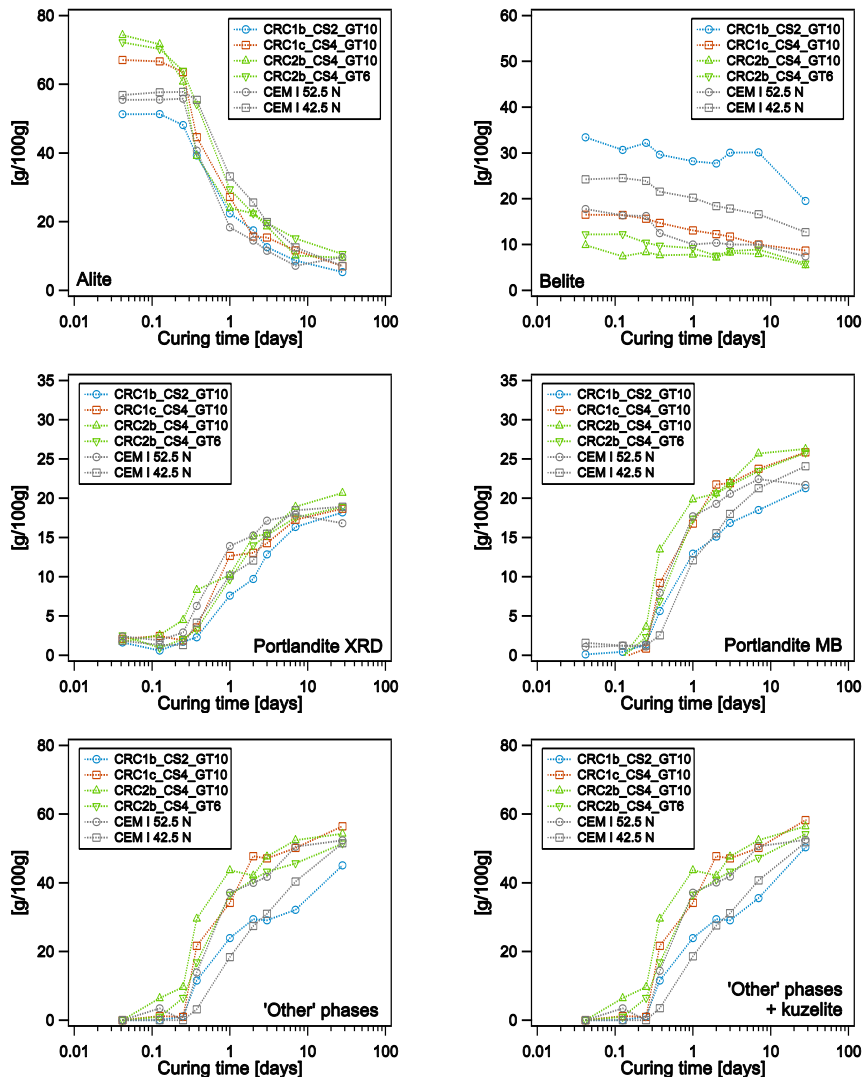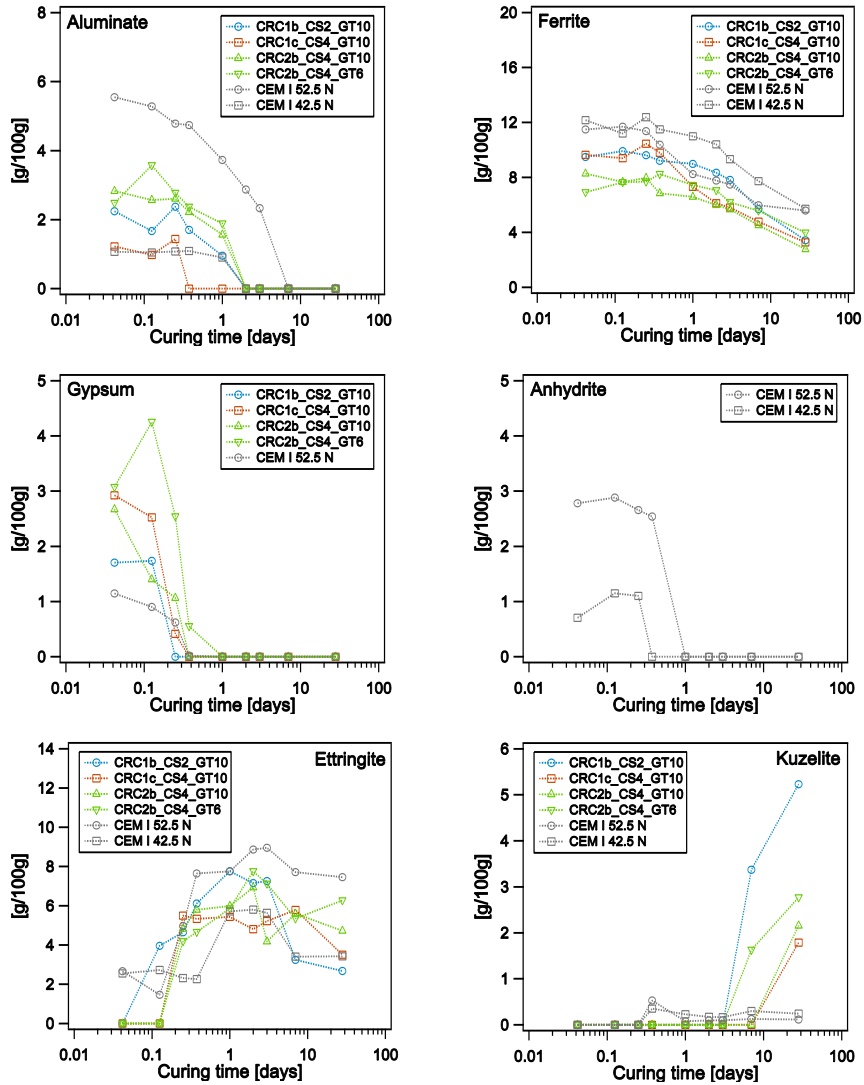
Figure XII.8 – XRD/Rietveld results of hydrating CRC and commercial cement pastes after arresting hydration using solvent exchange: overview of the hydration of the aluminate and ferrite phases

Table XII.3 - The compressive strength [N/mm^2] of standard mortar samples prepared with CRC (CRC1b_CS2_GT10) and commercial (CEM I 52.5 N and CEM I 42.5 N) cements. Standard errors on the mean values are added between parentheses

Curing age	CRC1b_CS2_GT10	CEM I 52.5 N	CEM I 42.5 N
2 days	15.59 (0.49)	38.53 (0.92)	19.55 (0.73)
7 days	34.24[A] (2.83)	61.34 (0.45)	37.01[A] (0.24)
28 days	64.56[B] (0.80)	66.54[B] (0.30)	60.86 (0.61)

[x] by a capital superscript the groups are indicated for which the mean values do not differ significantly

B. Modelling CRC cement hydration

B.1. Input data

The OPC hydration model used is described in chapter IX.B.2. As input, the mineralogy as determined by XRD analysis was used from Table XI.3 and Table XII.2 for CRC and commercial cement respectively. Besides the main clinker phases, calcite and periclase were considered, the alkali sulphates were however neglected in the modelling. For the CRC cements, the calcium sulphate added, as presented in Table XII.1, was used as input for the anhydrite content. The specific surface area, representing the fineness of the cements, was taken from Table XII.1 and Table XII.2 for the CRC and commercial cements respectively.

B.2. Modelling versus experimental results

In Figure XII.9, visualizing the experimental data obtained by XRD/Rietveld analysis and the modelled data, it is seen that the model follows the trend of the experimental data, although there is no perfect fit. The latter is however not expected as errors related to the experimental procedures cannot be avoided, and the fact that a model is never perfect.

For the cements with a higher reactivity (such as CRC1c_CS4_GT10, CRC2b_CS4_GT10 and CEM I 52.5 N), the data of the silicate phases are not fitted well within the first day of hydration, and the modelled hydration is running slower. Indeed, comparing the modelled data for CRC2b_CS4_GT10 and CRC2b_CS4_GT6 having the same composition with different finenesses (SSA of 410 and 350 m^2/kg respectively), it seems that the modelled hydration process is almost not affected by a difference in cement fineness.

Comparing the XRD/Rietveld data with the modelled data of the commercial cements, it is seen that while anhydrite was observed in the XRD patterns, anhydrite did not seem stable from the modelled data. In commercial cements, often natural anhydrite is used, which shows slow hydration kinetics. However, in the modelling, all anhydrite will convert to gypsum immediately. The presence of anhydrite was also observed in the cements tested by Lothenbach and Winnefeld (2006). The analysis of their pore
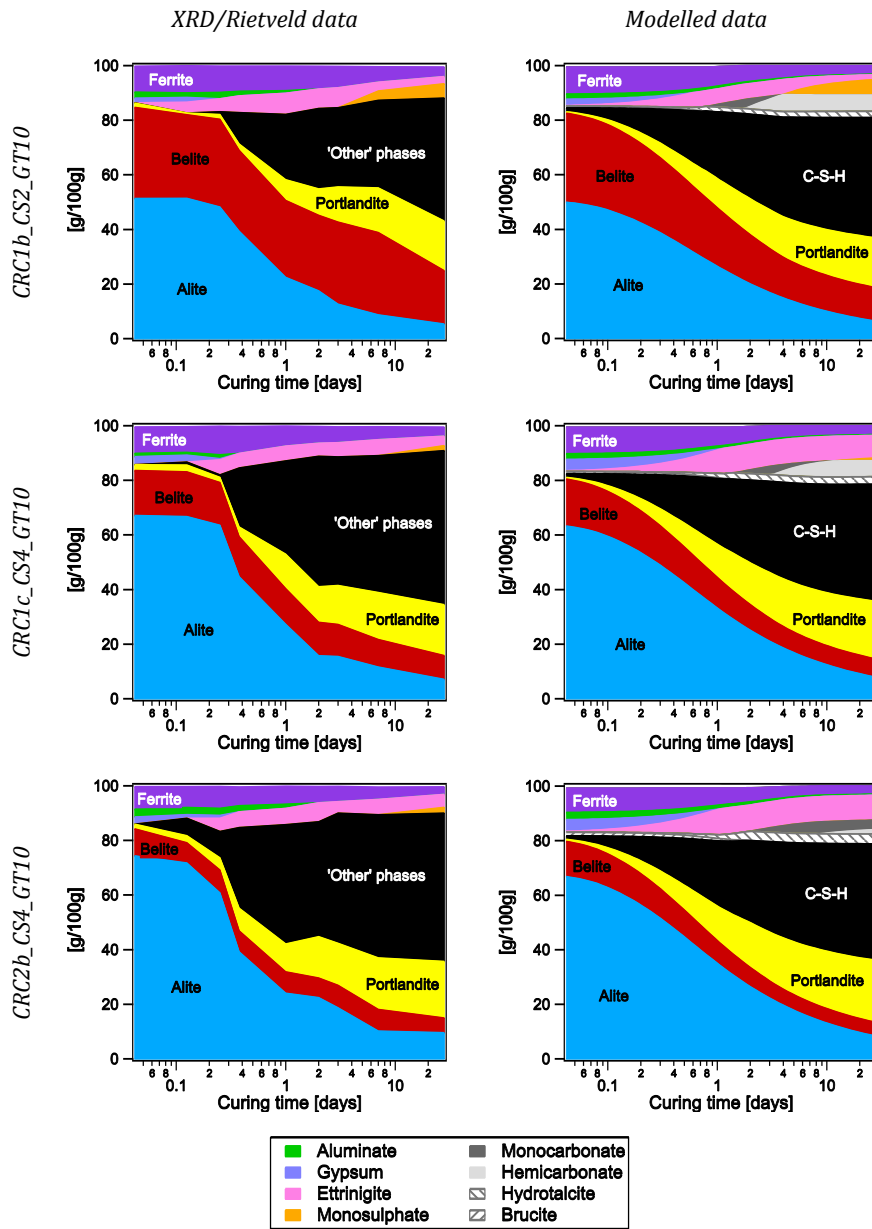
Figure XII.9a – Overview of the experimental data and modelled data of the cement hydration process for CRC and commercial cements
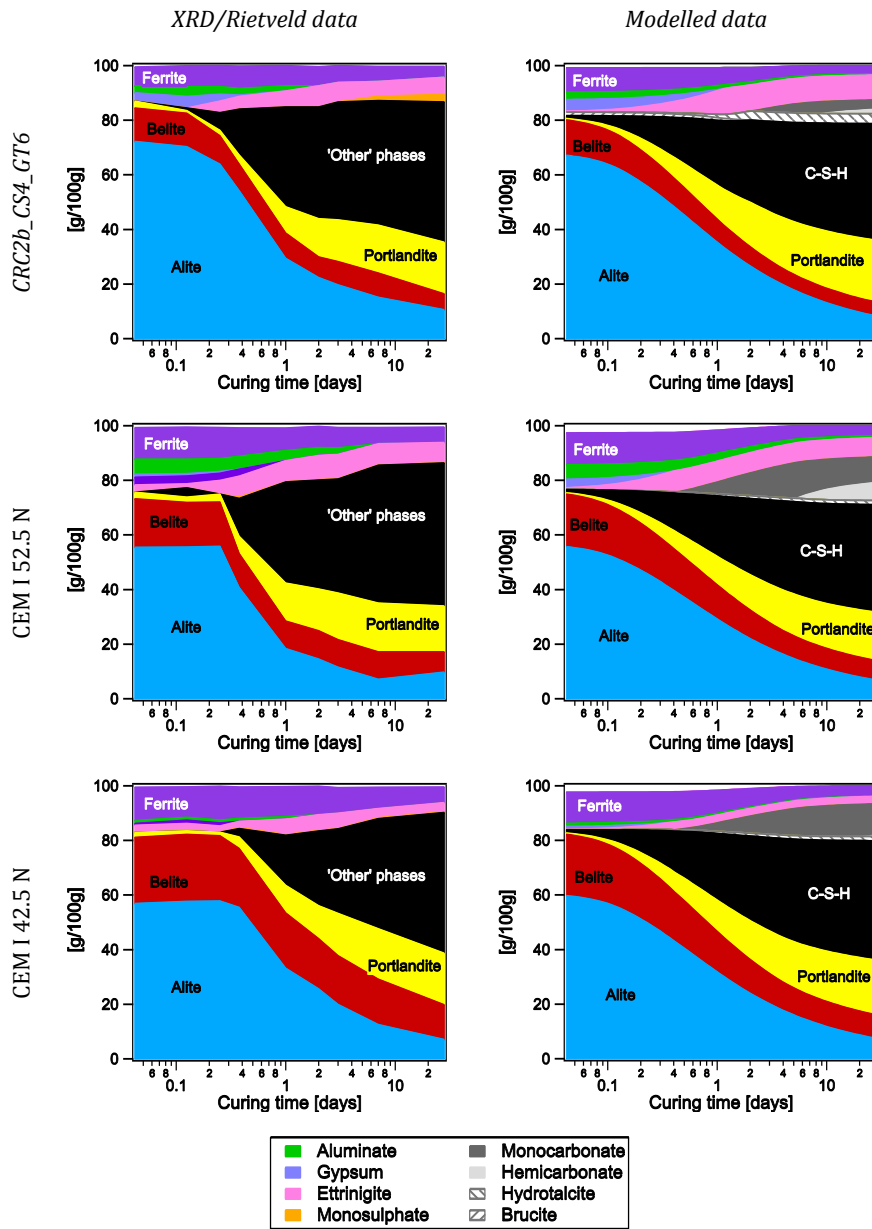
Figure XIV.9b – Overview of the experimental data and modelled data of the cement hydration process for CRC and commercial cements

solutions showed an oversaturation with respect to gypsum, portlandite and ettringite during the first 12 hours, and equilibrium with the dissolution of anhydrite. As for the dissolution of the main clinker phases, a more precise prediction of the early hydration of anhydrite would be obtained by considering a kinetic model of nucleation and precipitation.

The modelled data enables a prediction of the composition of the 'other' phases. For the hydration of the silicates, the modelled data might be interesting in giving an indication of the amount and composition of C-S-H that would precipitate. However, an indication of the amount of C-S-H can also be obtained by mass balance calculations from the reducing alite and belite contents in time. In GEMS the composition of the C-S-H phase is modelled using the solid solution model developed by Kulik and Kersten (2001), which describes the C-S-H phase as a system of two concurrent solid solution systems. The solid solution CSH-I has the end-members $SiO_2(am)$ and Tobermorite (Tob-I: $(Ca(OH)_2)_2(SiO_2)_{2.4} \cdot (H_2O)_2)$. Jennite $((Ca(OH)_2)_{1.5}(SiO_2)_{0.9} \cdot (H_2O)_{0.9})$ and tobermorite (Tob-II: $(Ca(OH)_2)_{1.5}(SiO_2)_{1.8} \cdot (H_2O)_{1.5})$ are the end members of the other solid solution CSH-II. The ultimate solid solution that is expected to be formed within this model depends on the CaO to SiO_2 ratio of the system.

Regarding the hydration of the aluminate and ferrite phases, which is much more complex, the modelled data is far more interesting. For both CRC and commercial cements, ettringite was observed up to 28 days for both the experimental and modelled data. While the crystalline calcium monosulfoaluminate phase kuzelite was observed in the CRC cements and to a smaller extent also the commercial cements, it was only obtained in the modelled data for CRC1b_CS2_GT10. In addition to these crystalline phases, 'amorphous' AFm phases were obtained from the hydration model. Both calcium mono and hemi-carboaluminate (in the figures named as mono- and hemicarbonate respectively) are expected to be present. For all CRC cements monocarbonate is expected to be the first formed AFm phase. Upon hydration a transformation towards hemicarbonate and later on, once the monocarbonate phases have completely disappeared, monosulphate is expected. Depending on the mineralogy, the composition of the AFm phases after 28 days of hydration will be dominated by monocarbonate (CRC2b_CS4 and CEM I 42.5), hemicarbonate (CRC1c_CS4_GT10), monocarbonate and hemicarbonate (CEM I 52.5) or monosulphate and hemicarbonate (CRC1b_CS2_GT10). Hydrogarnets (a solid solution between C_3AH_6-C_3FH_6-C_3AS_3-C_3FS_3) are not expected to be present looking at the modelled data. It is however also a phase that is not found as a major hydration product in modern Portland cements.

Additionally in all cements some brucite $(Mg(OH)_2)$ and hydrotalcite $(Mg_{1-x}(Al,Fe)_x(OH)_2 \cdot [A^{n-}]_{x/n} \cdot mH_2O$; with A^{n-} being an anion) might be expected to be present from the hydration of periclase, but were not experimentally proven in the XRD/Rietveld analysis. Due to their low concentration these phases are probably present below the detection limits. In case of hydrotalcite also its poor crystallinity makes it impossible for detection by XRD analysis.

C. Conclusion

TG and XRD/Rietveld analysis performed on cement pastes with different curing ages visualize the dissolution of the main clinker minerals and the formation of the (crystalline) hydration products in time. The hydration of the cement paste is preferably stopped by solvent exchange, as freeze drying affects the crystallinity of ettringite and gypsum. To calculate the portlandite content from the obtained TG data, the mere weight loss method is preferred over the tangent method. Using the latter analysing technique, the obtained portlandite content is underestimated in comparison of the XRD data. In general it can be concluded that the CRC cements have a hydration process similar to the commercial cements that were used as reference.

In addition to the obtained TG and XRD data, isothermal calorimetry clearly confirmed that the higher fineness of cement increases its reactivity. However, the effect did not come forward in the modelled data. Also the clinker mineralogy will affect the reactivity of cement. It was observed that the reduced reactivity expected from cement with a lower alite content can be compensated by increasing its fineness.

In addition to the obtained experimental data, the modelled data can be interesting in predicting the composition of the 'other' phases obtained from Rietveld analysis. On the one hand it is possible to predict the composition of the C-S-H phase. Regarding the rather complex hydration process of the aluminate and ferrite phases it is possible to indicate the distribution of the non- or poorly crystalline hydrate phases (AFm phases and hydrogarnets), which are expected to be present besides ettringite and kuzelite (a crystalline AFm phase) as observed in the XRD/Rietveld analysis.

References

Amathieu, L., T. A. Bier and K. L. Scrivener (2001). Mechanisms of Set Acceleration of Portland Cement Through CAC Addition. International conference on Calcium Aluminate Cements (CAC), Edinburgh, Scotland**:** 303-317.

Aouad, G., A. Laboudigue, N. Gineys and N. E. Abriak (2012). "Dredged sediments used as novel supply of raw material to produce Portland cement clinker." Cement and Concrete Composites 34(6): 788-793.

Aranda Usón, A., A. M. López-Sabirón, G. Ferreira and E. Llera Sastresa (2013). "Uses of alternative fuels and raw materials in the cement industry as sustainable waste management options." Renewable and Sustainable Energy Reviews 23(0): 242-260.

Babushkin, V. I., G. M. Matveyev and O. P. Mchedlov-Petrossyan (1985). Thermodynamics of Silicates. Springer-Verlag. Berlin.

Baert, G. (2009). Physico-Chemical Interactions in Portland Cement - (High Volume) Fly Ash Binders. PhD Thesis. Ghent, Ghent University. PhD.

Bentz, D., G. Sant and J. Weiss (2008). "Early-Age Properties of Cement-Based Materials. I: Influence of Cement Fineness." Journal of Materials in Civil Engineering 20(7): 502-508.

Bish, D. L. and S. A. Howard (1988). "Quantitative phase analysis using the Rietveld method." Journal of Applied Crystallography 21(2): 86-91.

Borges, P. H. R., J. O. Costa, N. B. Milestone, C. J. Lynsdale and R. E. Streatfield (2010). "Carbonation of CH and C–S–H in composite cement pastes containing high amounts of BFS." Cement and Concrete Research 40(2): 284-292.

Campbell, D. H. (1999). Microscopical Examination and Interpretation of Portland Cement and Clinker, 2nd edition, Portland Cement Association.

Chatterjee, A. K. (2011). "Chemistry and engineering of the clinkerization process — Incremental advances and lack of breakthroughs." Cement and Concrete Research 41(7): 624-641.

Coelho, A. A., Topas Academic version 4.1.

Commission Chimique du CETIC (1978). "Détermination de la composition minéralogique du clinker par analyse microscopique et dissolution sélective des phases." Ciments Bétons Platres Chaux(4/78 (713)): 205-210.

De Schepper, M., K. De Buysser, I. Van Driessche and N. De Belie (2013). "The regeneration of cement out of Completely Recyclable Concrete: Clinker production evaluation." Construction and Building Materials 38: 1001-1009.

De Schepper, M., R. Snellings, K. De Buysser, I. Van Driessche and N. De Belie (2014). "The hydration of cement regenerated from Completely Recyclable Concrete." Construction and Building Materials 60(0): 33-41.

De Schutter, G. (1999). "Hydration and temperature development of concrete made with blast-furnace slag cement." Cement and Concrete Research 29(1): 143-149.

Department of Science and Industrial Research, Ministry of Science and Technology and Government of India (1988). Precalcinator Technology in Indian cement Industry. New Delhi.

Gadayev, A. and B. Kodess (1999). "By-product materials in cement clinker manufacturing." Cement and Concrete Research 29(2): 187-191.

Glasser, F. P. (2004). Advances in Cement Clinkering. Innovations in Portland Cement Manufacturing. J. I. Bhatty, F. M. G. Miller and S. H. Kosmatka. Skokie, IL, Portland Cement Association**: 331-368.

Gruyaert, E. (2011). Effect of Blast-Furnace Slag as Cement Replacement on Hydration, Microstructure, Strength and Durability of Concrete. Faculty of Engineering and Architecture. Ghent, Ghent University. PhD.

Gutteridge, W. A. (1979). "On the dissolution of the interstitial phases in Portland cement." Cement and Concrete Research 9(3): 319-324.

Herfort, D., G. K. Moir, V. Johansen, F. Sorrentino and H. B. Arceo (2010). "The chemistry of Portland cement clinker." Advances in Cement Research 22(4): 187-194.

Hewlett, P. C. (1998). Lea's Chemistry of Cement and Concrete (Fourth Edition). Oxford, Butterworth-Heinemann.

Holcim Belgium, De fabricatie van cement (The production of cement) (2013a); Available from: http://www.holcim.be/nl/holcim-belgie/de-fabricatie-van-onze-producten/de-fabricatie-van-cement.html (accessed January 2014)

Holcim Belgium (2013b). Productfiche (Product info sheet).

Horkoss, S., R. Lteif and T. Rizk (2011). "Influence of the clinker SO_3 on the cement characteristics." Cement and Concrete Research 41(8): 913-919.

Hummel, W., U. Berner, E. Curti, F. J. Pearson and T. Thoenen (2002). Nagra/PSI Chemical Thermodynamic Data Base 01/01. Nagra Technical Report NTB 02-16. U. Universal Publishers/uPUBLISH.com. Wettingent, Switzerland.

Jawed, I. and J. Skalny (1977). "Alkalies in cement: A review I. Forms of Alkalies and their effect on clinker formation." Cement and Concrete Research 7(6): 719-729.

Kakali, G. and S. Tsivilis (1993). "The effect of intergrinding and separate grinding of cement raw mix on the burning process." Cement and Concrete Research 23(3): 651-662.

Kocaba, V. (2010). Development and evaluation of methods to follow microstructural development of cementitious systems including slags, EPFL.

Kulik, D. A. and M. Kersten (2001). "Aqueous Solubility Diagrams for Cementitious Waste Stabilization Systems: II, End-Member Stoichiometries of Ideal Calcium Silicate Hydrate Solid Solutions." Journal of the American Ceramic Society 84(12): 3017-3026.

Kulik, D. A., T. Wagner, S. V. Dmytrieva, G. Kosakowski, F. F. Hingerl, K. V. Chudnenko and U. Berner, GEM-Selektor geochemical modeling package: Numerical kernel GEMS3K for coupled simulation codes.

Le Saoût, G., V. Kocaba and K. Scrivener (2011). "Application of the Rietveld method to the analysis of anhydrous cement." Cement and Concrete Research 41(2): 133-148.

Lothenbach, B., G. Le Saout, E. Gallucci and K. Scrivener (2008a). "Influence of limestone on the hydration of Portland cements." Cement and Concrete Research 38(6): 848-860.

Lothenbach, B., T. Matschei, G. Möschner and F. P. Glasser (2008b). "Thermodynamic modelling of the effect of temperature on the hydration and porosity of Portland cement." Cement and Concrete Research 38(1): 1-18.

Lothenbach, B. and F. Winnefeld (2006). "Thermodynamic modelling of the hydration of Portland cement." Cement and Concrete Research 36(2): 209-226.

Martín-Márquez, J., A. G. De la Torre, M. A. G. Aranda, J. M. Rincón and M. Romero (2009). "Evolution with Temperature of Crystalline and Amorphous Phases in Porcelain Stoneware." Journal of the American Ceramic Society 92(1): 229-234.

Matschei, T., B. Lothenbach and F. P. Glasser (2007). "Thermodynamic properties of Portland cement hydrates in the system $CaO–Al_2O_3–SiO_2–CaSO_4–CaCO_3–H_2O$." Cement and Concrete Research 37(10): 1379-1410.

Möschner, G., B. Lothenbach, J. Rose, A. Ulrich, R. Figi and R. Kretzschmar (2008). "Solubility of Fe–ettringite ($Ca_6[Fe(OH)_6]_2(SO_4)_3 \cdot 26H_2O$)." Geochimica et Cosmochimica Acta 72(1): 1-18.

Möschner, G., B. Lothenbach, F. Winnefeld, A. Ulrich, R. Figi and R. Kretzschmar (2009). "Solid solution between Al-ettringite and Fe-ettringite ($Ca_6[Al_1 – xFe_x(OH)_6]_2(SO_4)_3 \cdot 26H_2O$)." Cement and Concrete Research 39(6): 482-489.

Mostafa, N. Y. and P. W. Brown (2005). "Heat of hydration of high reactive pozzolans in blended cements: Isothermal conduction calorimetry." Thermochimica Acta 435(2): 162-167.

Odler, I., S. Abdulmaula, P. Nudling and T. Richter (1981). "Mineralogical and oxidic composition of industrial Portland-cement clinkers." Zement-Kalk-Gips 34(9): 445-449.

Pane, I. and W. Hansen (2005). "Investigation of blended cement hydration by isothermal calorimetry and thermal analysis." Cement and Concrete Research 35(6): 1155-1164.

Parrot, L. J. and D. C. Killoh (1984). "Prediction of Cement Hydration." Br. Ceram. Proc. 35: 41-53.

Pradip, D. Vaidyanathan, P. C. Kapur and B. N. Singh (1990). "Production and properties of alinite cements from steel plant wastes." Cement and Concrete Research 20(1): 15-24.

Rampelberg, G., M. Schaekers, K. Martens, Q. Xie, D. Deduytsche, B. De Schutter, N. Blasco, J. Kittl and C. Detavernier (2011). "Semiconductor-metal transition in thin VO2 films grown by ozone based atomic layer deposition." Applied Physics Letters 98(162902).

Rodriguez-Carvajal, S. (1993). "FULLPROF: A program for Rietveld Refinement and Pattern Matching Analysis." Physica B. 192(55).

Roduit, N., JMicroVision: Image analysis toolbox for measuring and quantifying components of high-definition images, Version 1.2.2. (2008); Available from: http://www.jmicrovision.com/ (accessed December 8th, 2011)

Schmidt, T., B. Lothenbach, M. Romer, J. Neuenschwander and K. Scrivener (2009). "Physical and microstructural aspects of sulfate attack on ordinary and limestone blended Portland cements." Cement and Concrete Research 39(12): 1111-1121.

Schmidt, T., B. Lothenbach, M. Romer, K. Scrivener, D. Rentsch and R. Figi (2008). "A thermodynamic and experimental study of the conditions of thaumasite formation." Cement and Concrete Research 38(3): 337-349.

Schoon, J., L. Van der Heyden, P. Eloy, E. M. Gaigneux, K. De Buysser, I. Van Driessche and N. De Belie (2012). "Waste fibrecement: An interesting alternative raw material for a sustainable Portland clinker production." Construction and Building Materials 36(0): 391-403.

Scrivener, K. L., T. Füllmann, E. Gallucci, G. Walenta and E. Bermejo (2004). "Quantitative study of Portland cement hydration by X-ray diffraction/Rietveld analysis and independent methods." Cement and Concrete Research 34(9): 1541-1547.

Scrivener, K. L. and A. Nonat (2011). "Hydration of cementitious materials, present and future." Cement and Concrete Research 41(7): 651-665.

Snellings, R., M. De Schepper, K. De Buysser and I. Van Driessche (2012). "Clinkering reactions during firing of recyclable concrete." Journal of the American Ceramic Society: Accepted for publication.

Sorrentino, F. (2011). "Chemistry and engineering of the production process: State of the art." Cement and Concrete Research 41(7): 616-623.

Stinton, G. W. and J. S. O. Evans (2007). "Parametric Rietveld refinement." Journal of Applied Crystallography 40: 87-95.

Taylor, H. F. W. (1997). Cement Chemistry. London, Thomas Telford Publishing.

Thoenen, T. and D. Kulik (2003). Nagra/PSI chemical thermodynamic database 01/01 for GEM-Selektro (V.2-PSI) geochemical modeling code. PSI. Villingen.

Torréns-Martín, D. and L. Fernández-Carrasco (2013). "Effect of sulfate content on cement mixtures." Construction and Building Materials 48(0): 144-150.

Weritz, F., A. Taffe, D. Schaurich and G. Wilsch (2009). "Detailed depth profiles of sulfate ingress into concrete measured with laser induced breakdown spectroscopy." Construction and Building Materials 23(1): 275-283.

Wikipedia, Hot clinker (2009); Available from: http://en.wikipedia.org/wiki/File:Hot_Clinker_2.jpg (accessed January 2014)

Winnefeld, F. and B. Lothenbach (2010). "Hydration of calcium sulfoaluminate cements — Experimental findings and thermodynamic modelling." Cement and Concrete Research 40(8): 1239-1247.

Yang, J. and C. Roy (1999). "Using DTA to quantitatively determine enthalpy change over a wide temperature range by the "mass-difference baseline method"." Thermochimica Acta 333(2): 131-140.

Zhang, J. and G. W. Scherer (2011). "Comparison of methods for arresting hydration of cement." Cement and Concrete Research 41(10): 1024-1036.

PART IV
CRC Evaluation

XIII - Life cycle assessment of CRC

CRC is designed to reduce the impact of concrete on the environment, and its benefit for the environment should thus be proven through Life Cycle Assessment (LCA). The standard method for LCA is set down by the International Organization for Standardization in the standards ISO 14040 (2006) and ISO 14044 (2006). According to these standards a life cycle assessment occurs in four steps. First the goal and scope of the life cycle assessment are defined. In a second step an inventory is made for the different areas in the production process, together with their environmental impact. With these results the impact of a product's whole life cycle can be calculated in step three. Finally the interpretation of the obtained results occurs by critically analysing them within step four.

A. Goal and scope definition

A.1. Goal

The aim of this study is to quantify the impact of CRC on the environment. The final compositions made, CRC1c and CRC2b, are chosen for this assessment. Their impact will be evaluated in comparison with the reference concrete mixture T(0.50) or T(0.45), depending on the considered environment.

The idea for CRC came from the finiteness of natural resources and wants to optimize concrete recycling opportunities by designing it as an ultimate raw meal for cement production. It is thus hoped that the implementation of CRC will reduce the demand for primary raw materials. Furthermore it is hoped to decrease the global warming potential due to the use of by-products such as fly ash and blast furnace slag, reducing the clinker content of the concrete.

A.2. Scope

To perform a proper study regarding the environmental impact of products, it is essential to make an unambiguous definition of its scope. In this study the whole life cycle of concrete will be considered (see Figure XIII.1), starting with the exploitation of the raw materials and ending with the recycling or disposal of the demolished concrete, taking into account the (positive) impact of avoiding the use of natural raw materials. The environmental impact of the application field and repair of the structure are considered into the functional unit which takes into account the strength and durability performance of the concrete mixtures. However, the environmental impact related to the use phase, e.g. the effect on the energy consumption for heating of the building, is not considered.

A.3. Functional unit

The functional unit is seen as the reference unit of the product system for which the environmental impact will be calculated [Desmyter and Martin (2001); Van den Heede

and De Belie (2012); ISO 14044 (2006)]. Within this study it was decided not to compare 1 m^3 of traditional concrete with 1 m^3 of CRC, but to compare the total amount of concrete necessary to deliver 1 MPa of strength and 1 year of service life. This definition of the functional unit is analogous to the definition of the binder intensity proposed by Damineli et al. (2010), for which an adaption was suggested by Van den Heede and De Belie (2012) to obtain a unit of functional performance on two levels, namely strength and durability/service life.
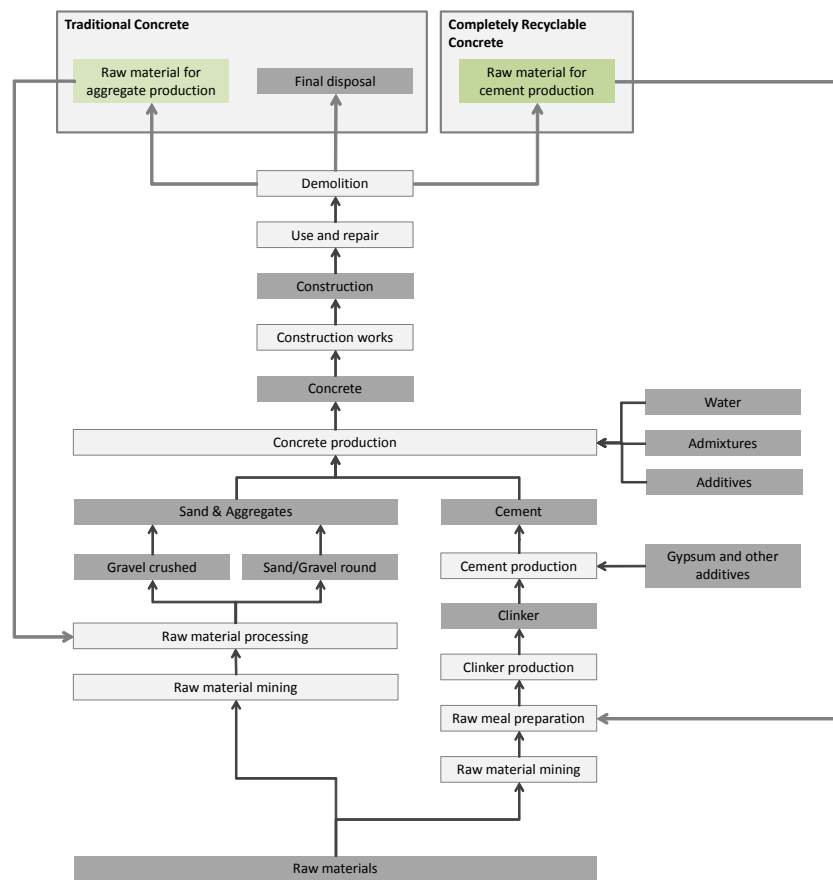
Figure XIII.1 - Life cycle of concrete

i. Strength performance

Using concrete with a higher strength could reduce the amount of concrete needed to obtain the same performance of a certain construction. Nonetheless it should be noted that the amount of concrete that can be saved is highly dependent on the type of the structural element. By Habert and Roussel (2009) it was found that for a concrete structure, a vertical element is the most environment friendly. The compressive strengths of CRC1c, CRC2b, T(0.50) and T(0.45) can be found in Table VI.1.

ii. Durability/service life

Both CRC and traditional concrete mixtures were designed according to NBN EN 206-1 (2001). The reference mixtures T(0.50) and T(0.45) were produced as reference for the environmental classes XC4 (carbonation induced corrosion in a cyclic wet and dry environment) and XS3 (chloride induced corrosion from sea water in tidal, splash and spray zones) respectively. For both CRC mixtures, the k-value concept is applicable, whereby their performance is expected to be comparable to T(0.45). Their application is thus allowed in both environmental classes XC4 and XS3. For this reason, with an appropriate concrete cover and field of application (XC4 and/or XS3 environment), a service life of 100 years should be guaranteed for all four concrete mixtures. Nonetheless durability tests were performed to verify the potential service life for concrete exposed to carbonation or chlorides, whereby rebar corrosion can be initiated (see chapter VI).

Service life in case of chloride induced corrosion

Although the same range of chloride depths was measured for both CRC mixtures and T(0.45), no solid conclusions could be drawn from the conducted diffusion test. The effect of curing time observed seems not to be consistent and the better performance for fly ash mixtures as found in literature [Sumranwanich and Tangtermsirikul (2004); Chindaprasirt et al. (2007); Cheewaket et al. (2010)] was not observed for all curing times. An improved performance of the CRC mixtures compared to T(0.45) could only be seen after 3 months curing. After 1 year curing, the performance of CRC2b was comparable with T(0.45), but for CRC1c a higher chloride ingress was measured. Additional study is thus required and for an appropriate service life prediction a more extensive test program (using profile grinding according to NT Build 443 (1995)) or a chloride migration test (NT Build 192 (1999)) should be conducted. In the following it is thus assumed that, as both CRC mixtures and reference mixture T(0.45) are designed according to NBN EN 206-1 (2001), the measured chloride penetration depths are within the same range and a better performance regarding chloride diffusion might be expected from literature, a service life of 100 years is valid for all three mixtures.

Service life in case of carbonation induced corrosion

Another image is obtained regarding the carbonation resistance of the CRC and traditional concrete mixtures. While for the CRC mixtures carbonation was observed from the first measurement onwards, no carbonation was observed for the traditional

concrete mixtures within the time frame of the experiments. Also Van den Heede and De Belie (2014) observed almost no carbonation in case of traditional concrete. From their experiments it can be concluded that rebar corrosion in a construction with traditional concrete is not to be expected within a life span of 100 years, as indeed the requirements of NBN EN 206-1 (2001) are fulfilled.

For the CRC mixtures, although the k-value concept from NBN EN 206-1 (2001) was applied, it might be interesting to actually predict their service life due to the observed carbonation. The service life is assumed to end at the moment that the carbonation ingress exceeds the concrete cover on the reinforcement. At this moment, the reinforcement is depassivated and corrosion will be initiated. The time needed for the carbonation front to reach the reinforcement will be calculated by using the experimentally determined carbonation coefficients from chapter VI.

As explained in chapter VI.A.2, the carbonation coefficients were determined by plotting the carbonation depths measured not in function of the square root of time (conventional model) but in function of $t^{0.4}$. This to take into account the reduction of the gas diffusivity as the carbonation reaction blocks the air pores in concrete. As the service life predicted will be longer using $t^{0.4}$ instead of the conventional $t^{0.5}$, $t^{0.5}$ will be used to evaluate the effect on service time. An overview of the carbonation coefficients is given in Table XIII.1.

Table XIII.1 – Overview of the carbonation coefficients used for the prediction of the service life of CRC mixtures

Concrete mixture	Curing time	$x = k_{acc,0.4} \cdot t^{0.4}$		$x = k_{acc,0.5} \cdot t^{0.5}$	
		$k_{acc,0.4}$	R^2	$k_{acc,0.5}$	R^2
	2 months	5.09±0.25	0.84	4.19±0.20	0.85
CRC1c	4 months	5.90±0.29	0.84	4.76±0.23	0.86
	1 year	1.92±0.16	0.67	1.53±0.13	0.65
	2 months	3.46±0.10	0.94	2.81±0.09	0.93
CRC2b	4 months	3.01±0.10	0.92	2.43±0.08	0.91
	1 year	1.00±0.08	0.69	0.80±0.06	0.66

To predict the carbonation depth under field conditions, the k-value under environmental conditions k_{env} can be calculated as followed [Sisomphon and Franke (2007)]:

$$\frac{k_{acc}}{k_{env}} = \sqrt{\frac{c_{acc}}{c_{env}}}$$

(XIII-1)

with k_{acc} the k-value under (accelerated) test conditions and c_{acc} and c_{env} the CO_2 concentrations during the accelerated test and under environmental conditions respectively. The CO_2 concentration under environmental conditions was chosen to be

0.05% according to the Fib Bulletin 34 [Fib (2006)], which considers an expected increase in atmospheric CO_2 concentrations with time.

In Van den Heede and De Belie (2014) it was found that calculation of the obtained k_{env} strongly depends on the CO_2 concentration of the accelerated test. For the High Volume Fly Ash (HVFA) concrete mixtures tested it was shown that the calculated field carbonation coefficient from an accelerated test with a CO_2 concentration of 10 vol% was only 55% of the one obtained after exposure to a CO_2 concentration of 1 vol%. For this reason it was decided to correct the calculated k_{env} by a factor 1/0.55. The service life $t_{service}$ of the CRC mixtures was thus calculated as followed:

$$t_{service} = \left(\frac{x_{cc}}{k_{env,n}/0.55} \right)^{1/n} \qquad \text{(XIII-2)}$$

with x_{cc} the concrete cover, which was considered to be 35 mm, which is required for a concrete construction in the simulated XC3 environment with a service life of 100 years [NBN EN 1992-1-1 (2010)] and n = 0.4 or 0.5. From the service times predicted in Table XIII.2 it can be concluded that when using the carbonation model as set by Sisomphon and Franke (2007) with n = 0.4, a service life of at least 100 years is expected for all CRC mixtures, independent from the curing time prior to the accelerated testing. On the other hand, when using the conventional model, wherein the carbonation depth is taken proportional to the square root of time, rebar corrosion might be expected after 81 and 63 years for CRC1c using the carbonation coefficients determined after 2 and 4 months curing respectively. It should be noted here, that in fact durability of both CRC concretes should not be questioned since the requirements for the k-value concept are fulfilled for both concretes.

Table XIII.2 - Overview of the service life predictions of CRC mixtures

Concrete mixture	Curing time	$k_{env,0.4}$	$t_{service,0.4}$ [years]	$k_{env,0.5}$	$t_{service,0.5}$ [years]
CRC1c	2 months	0.65	402	0.54	81
	4 months	0.76	278	0.61	63
	1 year	0.25	>1000	0.20	606
CRC2b	2 months	0.44	>1000	0.36	181
	4 months	0.39	>1000	0.31	242
	1 year	0.13	>1000	0.10	>1000

Calculation of the Functional Unit

As the service life of all concrete types is now known, the functional units can be calculated. For the calculations, the service life was given a maximum value of 100 years since this is the demanded minimum life span. The results are presented in Table XIII.3.

Table XIII.3 - Overview of the calculated Functional Units

Concrete mixture	Compressive strength [MPa]	$t_{service}$ [years]	Functional Unit [m³ concrete per MPa per year service life]
CRC1c with $k_{env,0.5}$ after 2 months curing	65.1	81	$1.90 \cdot 10^{-4}$
CRC1c with $k_{env,0.5}$ after 4 months curing	65.1	63	$2.44 \cdot 10^{-4}$
CRC1c from all other calculations	65.1	100	$1.53 \cdot 10^{-4}$
CRC2b	84.2	100	$1.19 \cdot 10^{-4}$
T(0.50)	57.8	100	$1.73 \cdot 10^{-4}$
T(0.45)	69.3	100	$1.44 \cdot 10^{-4}$

B. Life cycle inventory

Most of the data used in this study were taken from the ecoinvent 2.0 database [Frischknecht and Jungbluth (2007)], which was built by the Swiss Centre for Life Cycle Inventories and is commonly used in combination with the LCA software used (SimaPro, see chapter XIII.C). As adaptations were necessary to take into account e.g. the recycling of CRC within the clinker manufacturing process, an overview of the used input data is given hereafter. The actual data can be found in Appendix A.

B.1. Cement production process

Within the ecoinvent 2.0 database, the cement production process is divided into two sub processes, namely the clinker production (burning of the clinker raw materials) and the actual cement production (milling of the cement raw materials). The data for both Ordinary Portland Cement (see Table A.1) and Blast Furnace Slag Cement (see Table A.2) were taken from the ecoinvent 2.0 database.

The clinker production process was split into the raw material delivery (see Table A.3) and the actual clinker production (see Table A.4) to enable the recycling possibilities of CRC within the clinker production process (see chapter XIII.B4). Within the raw material delivery process, not only the raw material extraction and transport were considered, but also the CO_2 emissions related to the chemical decarbonation of limestone.

B.2. Concrete production process

The process 'Concrete, normal, at plant/CH U' from the ecoinvent 2.0 database was adapted to the concrete compositions of CRC1c, CRC2b, T(0.45) and T(0.50) (see Table A.5). Data regarding the superplasticizer were obtained from environmental declarations published by the European Federation of Concrete Admixture Associations (EFCA) [EFCA (2006)].

The life cycle inventory considered for the fly ash is presented in Table A.6 and is based on Van den Heede and De Belie (2012). Fly ash is a by-product from coal fired furnaces (e.g. for the production of electricity). The environmental impact of the coal fired furnaces should thus be partitioned between the electricity produced on the one hand and the fly ash obtained on the other hand. The partitioning of the impact can occur through allocation by mass or by economic value. In case of fly ash, a mass or economic allocation coefficient of respectively 12.4% or 1% should be applied. In this study, the economic allocation was chosen over the mass allocation since this principle takes into account the (economic) value of the products. Of course the results of the life cycle assessment will be influenced by the allocation percentage for the fly ash. A sensitivity analysis regarding the choice of the allocation coefficient can be found in Appendix B.

As mentioned in chapter I, the replacement of 20-30% of natural concrete aggregates by recycled concrete aggregates will have no significant impact on the durability performance of concrete. For this reason, the aggregate composition of T(0.45) and T(0.50) is divided into a first part that can be replaced by recycled aggregates (25% of the total aggregate content), and a second part that cannot be replaced, to guarantee the concrete durability (75% of the total aggregate content). The aggregate production process for the recycled concrete aggregates is also divided into the actual aggregate production process (see Table A.7) and the raw material delivery (see Table A.8).

B.3. Construction and use phase

The concrete produced at the concrete mixing plant is subsequently transported to the construction site. According to De Herde and Evrard (2005), the average distance from the concrete mixing plant to a construction site is 50 km and thus an additional input of 120 tkm 'Transport, lorry 20-28t, fleet average/CH U' from the ecoinvent 2.0 database for 1 m^3 concrete was considered. The energy needed for placing and compaction of the concrete was neglected according to De Herde and Evrard (2005). It should however be mentioned that the energy needed for compaction of concrete can be avoided when using self-compacting concrete. For a producer of concrete products this can result in significant savings on a yearly basis. De Schutter et al. (2010) estimated that a concrete pipe factory can save annually about 1GWh of energy when the shift is made from traditional concrete to SCC. The impact related to repair and maintenance activities is considered in the functional unit (see chapter XIII.A.3).

B.4. Demolition and end-of-life scenario

The data for demolition of the construction and sorting of the waste was taken from the ecoinvent 2.0 database, namely 'Disposal, building, concrete gravel, to sorting plant/CH U'. Necessary adaptations were related to transport and the products that are avoided due to recycling opportunities. For both CRC and traditional concrete, a different waste scenario was defined.

For CRC, all concrete waste is recycled within the cement production process. The life cycle inventory of this waste treatment is presented in Table A.9. Since the geographical

spread of concrete mixing plants and sorting plants was found comparable, the average distance between the construction site and a sorting plant was also assumed to be 50 km. The average minimum distance from a Flemish sorting plant to a cement plant was calculated to be 90 km. Since the environmental impact of the end-of-life scenario is highly depending on the transport distances, a sensitivity analysis regarding these transport distances was conducted and can be found in Appendix B.

Due to the presence of non-carbonate CaO, mainly from the cement, a lower raw material CO_2 emission is expected within the regeneration process of cement from CRC instead of a traditional cement raw meal. TG analysis of CRC raw meal showed a total mass loss of about 35 wt%. The weight loss of 30 wt% between 600 and 900 °C was considered to be CO_2. The raw material CO_2 emissions from CRC are thus expected to be 0.46 g/g clinker, which is indeed about 15% lower than 0.54 g/g clinker in case of the traditional clinker production process. In practice, part of the CRC will be carbonated, and higher CO_2 emissions can be expected. However, since this CO_2 was captured from the atmosphere during the life cycle of concrete, this additional CO_2 release was considered neutral in the life cycle assessment. Since the results of the life cycle assessment will be influenced by the CO_2 emissions released upon clinkering CRC, a sensitivity analysis towards this effect was performed and can be found in Appendix B. Finally about 1.54 kg CRC will be needed for the production of 1 kg clinker (cf. total mass loss of about 35 wt% from TG analysis).

The waste scenario of traditional concrete was analysed according to two alternative routes, namely recycling as concrete aggregate or final disposal e.g. as (sub)base material, for embankment constructions and in earth construction works. For the final disposal of concrete waste (incl. transport), the data were taken from the ecoinvent 2.0 database, namely 'Disposal, building, concrete gravel, to final disposal/CH U' (see Table A.10). Regarding the recycling of traditional concrete as aggregate raw material (see Table A.11), the 'Disposal, building, concrete gravel, to sorting plant/CH U' process in the ecoinvent 2.0 database needs an additional input. Compared to round gravel, recycled concrete aggregates require a crushing process. The extra data needed were obtained from the difference between the 'Gravel, crushed, at mine/CH U' process and the 'Gravel, round, at mine/CH U' process from the ecoinvent 2.0 database. Again, a transport distance of 50 km between the construction site and sorting plant was taken into account.

C. Life cycle impact assessment

For the impact assessment the LCA software SimaPro was used. This software is developed by PRé Consultants (Product ecology Consultants) in the Netherlands and it contains the complete ecoinvent 2.0 database. The assessment was performed according to the CML 2002 problem oriented impact method. For each impact category, a category indicator can be calculated based on the applicable characterisation model and the characterisation factors derived from the underlying model. An overview of the

considered baseline impact categories and their characterisation factor is given in Table XIII.4.

Table XIII.4 - Overview of the considered impact categories within the life cycle assessment according to the CML 2002 impact method

Impact category	Characterisation factor [Unit]
Abiotic depletion	*Abiotic depletion potential (ADP)* [kg Sb eq]
	Depletion of natural non-living resources (minerals and fossil fuels)
Acidification	*Acidification potential (AP)* [kg SO_2 eq]
	Covers all impacts on soil, water, organisms, ecosystems & materials by acidifying pollutants (e.g. SO_2, NO_x, NH_x)
Eutrophication	*Eutrophication (EP)* [kg PO_4^{3-} eq]
	Covers all impacts of excessively high environmental levels of macronutrients (N, P) causing a shift in species composition and an elevated biomass production in aquatic and terrestrial ecosystems
Climate change	*Global warming potential (GWP 100[*])* [kg CO_2 eq]
	Deals with all GHGs that may cause the earth's temperature to rise and have an adverse effect on the ecosystem and human health and material welfare
Stratospheric ozone depletion	*Ozone depletion potential (ODP)* [kg CFC-11 eq]
	The ozone depletion produced by e.g. CFCs
Human toxicity	*Human toxicity potential (HTP)* [kg 1.4-DB eq]
	Covers the impact on human health of all toxic substances emitted to air, water and soil
Ecotoxicity	*Fresh water aquatic, marine aquatic and terrestrial ecotoxicity (FAETP, MAETP and TETP)* [kg 1.4-DB eq]
	Covers impacts on aquatic & terrestrial ecotoxicity of all toxic substances emitted to air, water and soil
Photo-oxidant formation	*Photochemical ozone creation potential (POCP)* [kg C_2H_4]
	Indicates the potential capacity of a volatile organic substance to produce ozone

[*] Global warming potential calculated over a time interval of 100 years

C.1. Cement production process

The results of the life cycle impact assessment of the cement production process for the different impact categories are presented in Figure XIII.2. Three processes are visualized: the clinkering process and the manufacturing of Ordinary Portland Cement and Blast Furnace Slag Cement. The environmental impact of recycling CRC in the clinker production process is considered in the end-of-life scenario for CRC. The different categories related to the environmental impact of the clinker used for the manufacturing of OPC and BFSC are grouped and presented as 'clinker in cement production' in Figure XIII.2.
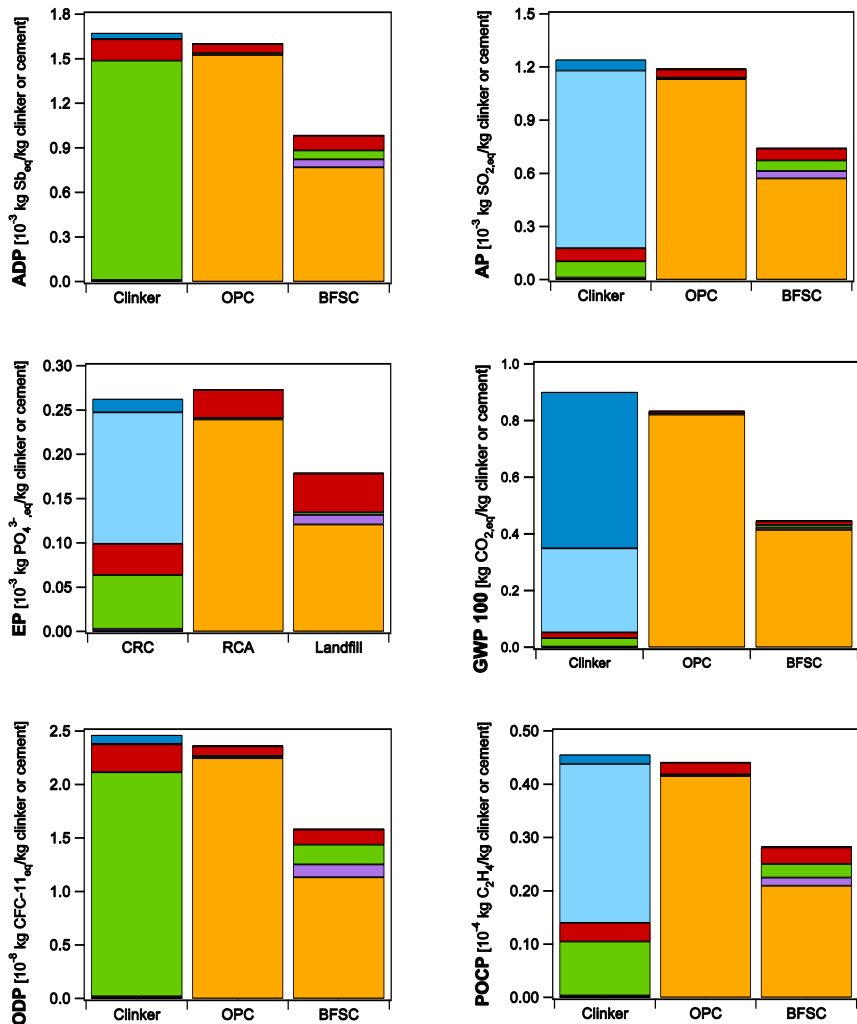
ADP: Abiotic Depletion Potential
AP: Acidification Potential
EP: Eutrophication
GWP 100: Global Warming Potential
ODP: Ozone Depletion Potential
POCP: Photochemical Ozone Creation Potential
HTP: Human Toxicity Potential
TETP: Terrestrial EcoToxicity Potential
FAETP: Fresh water Aquatic EcoToxicity Potential
MAETP: Marine Aquatic EcoToxicity Potential

Legend:
- Raw materials for 1 kg clinker (incl. raw material CO_2 emissions)
- Emissions clinkering process (excl. raw material CO_2 emissions)
- Operation of the cement plant (excl. fuels)
- Fuels
- Transport
- Clinker ready for cement production

Figure XIII.2a – Life Cycle Impact Assessment of 1 kg clinker or cement
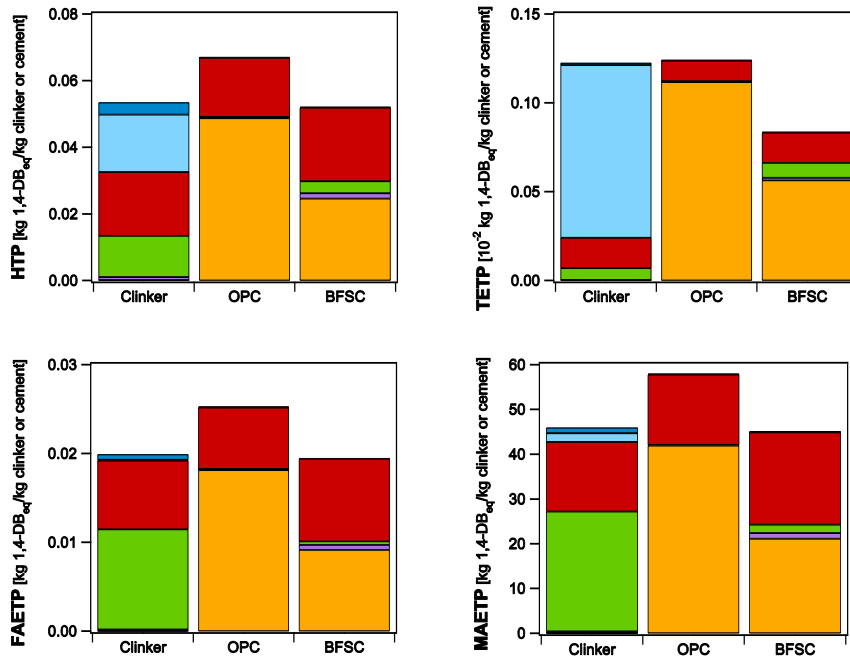
Figure XIII.2b – Life Cycle Impact Assessment of 1 kg clinker or cement

Taking a first look at the results, it is seen how the environmental impact of the cement production process can be reduced by incorporating supplementary cementitious materials, such as Blast Furnace Slag. Depending on the considered impact category, the environmental impact of the cement production can be reduced with 22-47% by making use of BFSC instead of OPC. When replacing part of the clinker by BFS, only some heat (from fuels) and additional energy for grinding (in operation of the cement plant) is required for its pre-treatment. The environmental impact of this treatment is of course significantly lower compared to the whole clinkering process, explaining the reduced environmental impact of BFSC.

The cement production process is known for its high CO_2 emissions, related primarily to the clinkering process. Looking at Figure XIII.2, it is seen that 61% of the CO_2 emissions for clinker production are related to the decarbonation process of the raw materials ('raw materials for 1 kg clinker (incl. raw material CO_2 emissions)'). Additionally 36% is related to the burning of fuels; 33% from alternative fuels of which the CO_2 contribution is added to the clinkering process ('emissions clinkering process (excl. raw material CO_2 emissions)' in Figure XIII.2) and 3% from fossil fuels ('Fuels' in Figure XIII.2). By using BFSC instead of OPC, the Global Warming Potential of cement can be reduced by 47%.

For the other impact categories, it is seen that the environmental impact is dominated by the use of fuels and the air emissions related to the clinkering process. Furthermore the required electricity (mainly for milling of the raw materials and cement) and the consumables (e.g. ammonia, lubricating oil, refractory bricks, ...) necessary for the operation of the cement plant contribute significantly to the human toxicity and aquatic ecotoxicity, and to a smaller extent also to the terrestrial ecotoxicity and eutrophication of the environment.

C.2. Concrete production process

In Figure XIII.3, the results of the life cycle impact assessment of the different concrete mixtures for 1 m^3 at a construction site are shown. The Functional Unit is thus not considered yet, but the transport from the concrete plant to the construction site is incorporated into the calculations.

It is seen that depending on the considered impact category, both CRC and traditional concrete mixtures can have the lowest environmental impact. The main advantage of using CRC2b is related to the global warming potential, which is 30-34% lower compared to the traditional concrete mixtures. The good performance of CRC2b regarding the global warming potential is due to its reduced clinker content by using both fly ash and Blast Furnace Slag Cement. Considering global warming, the environmental impact of CRC1c and the traditional concrete are comparable.

Regarding the Ozone layer depletion, CRC2b has a slightly better performance compared to the reference concrete mixtures, with a reduction of 6-10%. Again, the result for CRC1c is comparable with the traditional concrete mixtures. While the global warming potential is strongly related to the cement content of the concrete, the ozone layer depletion is not only related to the cement content, but also to the required transport of the materials.

The environmental impact of the concrete mixtures regarding the other impact categories is mainly related to their cement and fly ash content and the required transportation. To a smaller extent also the sand and aggregates, the superplasticizer, if needed, and the operation of the concrete mixing plant contribute to these impact categories. In case of abiotic depletion, acidification, photo-oxidant formation and the terrestrial ecotoxicity, the environmental impact of CRC2b, T(0.45) and T(0.50) are comparable, while the impact of CRC1c is 8-26% higher. The environmental impact considering eutrophication, human toxicity and aquatic ecotoxicity of both CRC mixtures is worse compared to the traditional concrete mixtures. The impacts are 25-47%, 18-25% and 53-72% higher, respectively.

C.3. Demolition and end-of-life scenario

The results of the impact assessment of the end-of-life scenarios for both CRC and traditional concrete mixtures are presented in Figure XIII.4. The negative impacts observed are related to the avoidance of natural raw materials by the recycling of

concrete. For the final disposal of concrete e.g. as (sub)base material, for embankment constructions and in earth construction works, no benefit was considered since it is more a useful disposal than real recycling of the concrete waste. For the recycling of CRC as raw material for the clinker production and traditional concrete as raw material for the aggregate production, their environmental impact is lowered by 8-24% and 4-15% respectively, depending on the considered impact category ('Avoidance of raw materials' in Figure XIII.4).

The results regarding global warming definitely stand out for the CRC recycling opportunity. Although the $CO_{2,eq}$ emissions are indeed several times higher when CRC is recycled in the clinkering process, the release of a significant amount of CO_2 is also avoided. Indeed, for each 1 kg $CO_{2,eq}$ released upon the recycling of CRC in a clinker kiln, the emission of 1.08 $CO_{2,eq}$ related to the burning of traditional cement raw meal is avoided. The latter will reduce the impact on global warming of the CRC concrete mixtures significantly.

Nonetheless, for the other impact categories, the recycling of the concrete waste seems not always better compared to its final disposal. The main contributor to the environmental impact of the recycling of both CRC and traditional concrete is the transport of the materials. In total 140 and 50 km of road transport was considered for the recycling of CRC and traditional concrete, respectively, while the ecoinvent 2.0 data used for the final disposal of concrete takes into account a transport distance of only 15 km. Indeed, concrete rubble is often disposed in the neighbourhood as (sub)base material, for embankment constructions and in earth construction works. Depending on the considered impact category, the transport contributes for 57-88% and 24-66% to the environmental impact of the recycling of CRC and traditional concrete respectively, while it only amounts to 10-25% in case of the mere final disposal of the concrete waste. It will thus be beneficial for both recycling of CRC and traditional concrete to reduce the environmental impact of the transport by minimizing road transport and maximizing rail and barge transport. As can be expected, the main impact of the final disposal of concrete is related to its disposal to an inert material landfill (47-69%).

The impact of the demolition process is identical for all end-of-life scenarios and amounts to 8-27%, 5-32% and 16-41% in case of CRC recycling, recycling of traditional concrete as aggregates or final disposal of concrete waste respectively. The additional processing needed to sort the waste materials for both recycling options is rather limited, except for the impact categories eutrophication, human toxicity, aquatic ecotoxicity and terrestrial ecotoxicity, wherein contributions of 5-38% and 9-45% were calculated for CRC and traditional concrete recycling respectively. The additional processing that should be considered for the aggregate production in case of the recycling of traditional concrete varies between 8 and 41%, depending on the considered impact category.
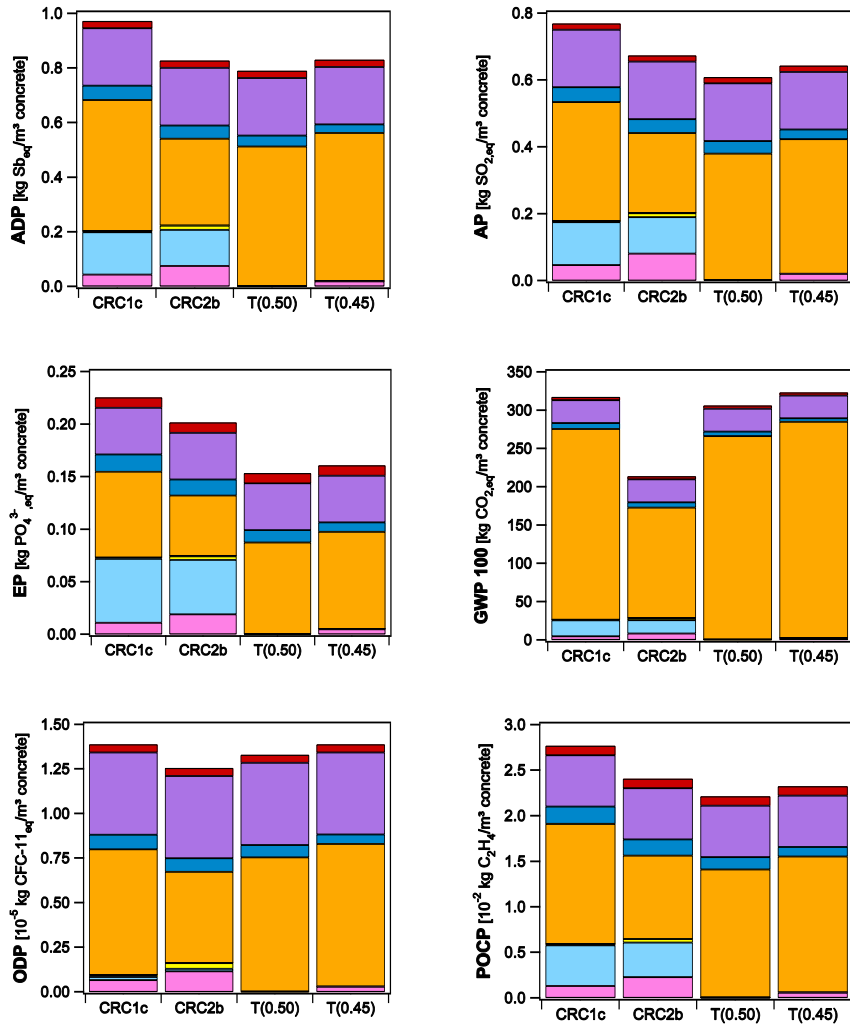
ADP: Abiotic Depletion Potential
AP: Acidification Potential
EP: Eutrophication
GWP 100: Global Warming Potential
ODP: Ozone Depletion Potential
POCP: Photochemical Ozone Creation Potential
HTP: Human Toxicity Potential
TETP: Terrestrial EcoToxicity Potential
FAETP: Fresh water Aquatic EcoToxicity Potential
MAETP: Marine Aquatic EcoToxicity Potential

Figure XIII.3a – Life Cycle Impact Assessment of 1 m³ concrete
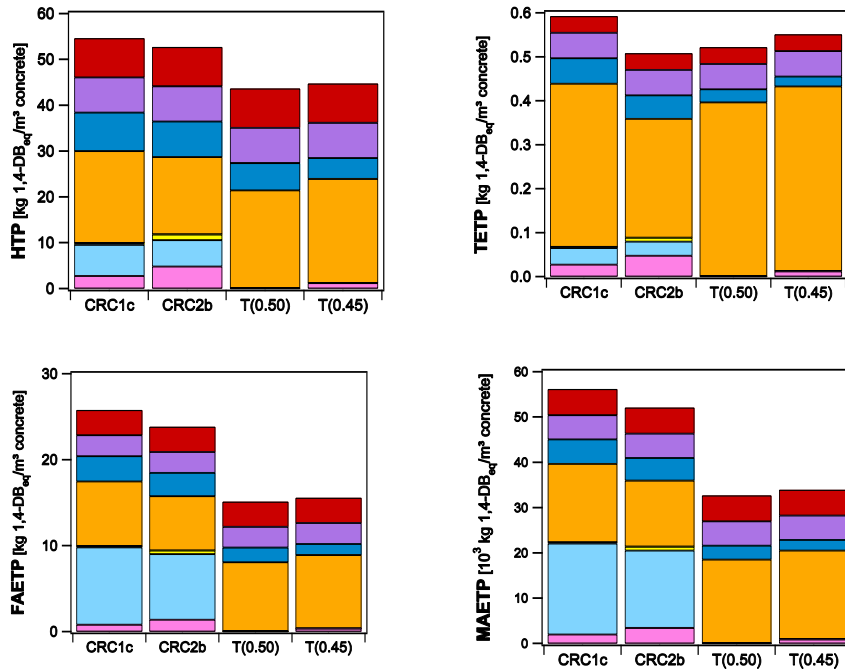
Figure XIII.3b – Life Cycle impact Assessment of 1 m³ concrete

D. The environmental impact of CRC vs. traditional concrete

In the previous part of this chapter it was seen that most impact categories of the concrete production process are dominated by the cement manufacturing process and the required transportation. In case of abiotic depletion, acidification, eutrophication, photo-oxidant formation, human toxicity and aquatic toxicity, the environmental impact of fly ash might not be underestimated. The environmental impact of the sand and aggregates used in concrete is limited.

The underlying cause of the huge environmental impact of the cement production is the clinkering manufacturing. Indeed, high amounts of raw materials and fuels are needed for this process, which goes along with high CO_2 emissions. The main goal for the development of a sustainable concrete is thus minimizing its clinker content (reducing the environmental impact of 1 m³ concrete), while still obtaining a high performance (lowering total amount of concrete needed to deliver 1 MPa of strength and 1 year of service life).

Additionally, the recycling possibilities of concrete will affect its sustainability. It was seen that additional transport and processing costs are needed for the recycling of
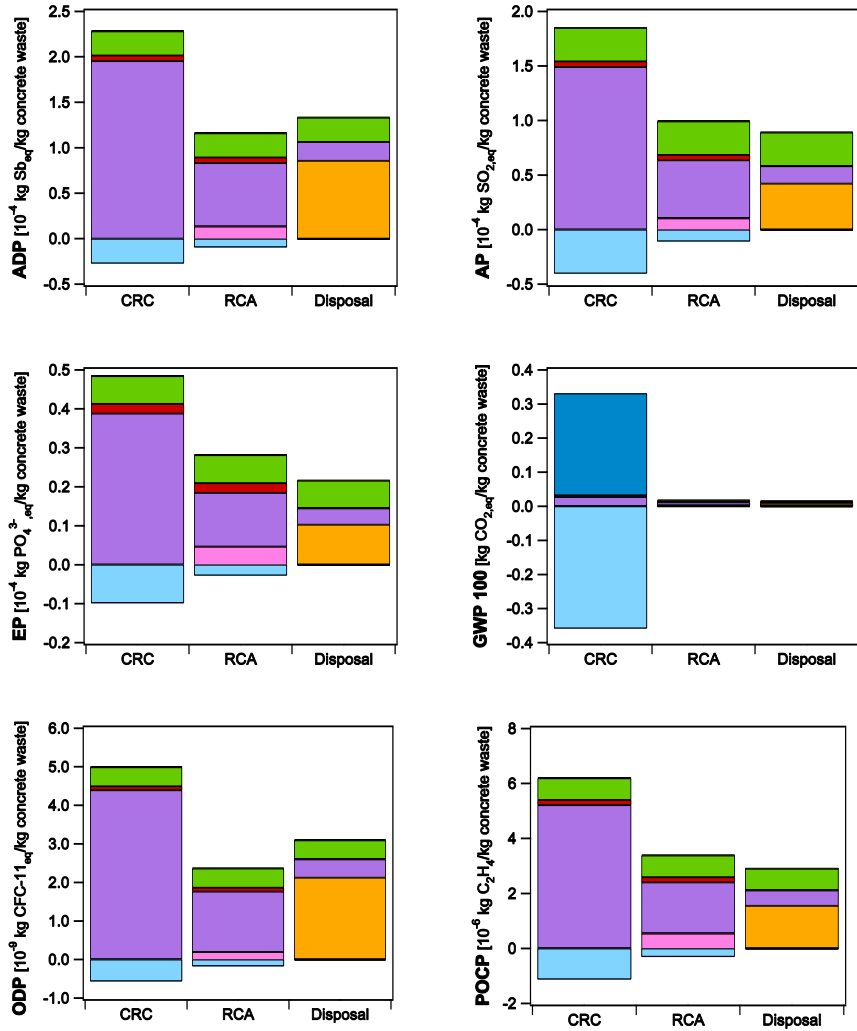
ADP: Abiotic Depletion Potential
AP: Acidification Potential
EP: Eutrophication
GWP 100: Global Warming Potential
ODP: Ozone Depletion Potential
POCP: Photochemical Ozone Creation Potential
HTP: Human Toxicity Potential
TETP: Terrestrial EcoToxicity Potential
FAETP: Fresh water Aquatic EcoToxicity Potential
MAETP: Marine Aquatic EcoToxicity Potential

Figure XIII.4a – Life Cycle Impact Assessment of the different waste scenarios: CRC = Completely Recyclable Concrete; RCA = Recycling of traditional concrete as Recycled Concrete Aggregates; disposal = disposal of traditional concrete waste
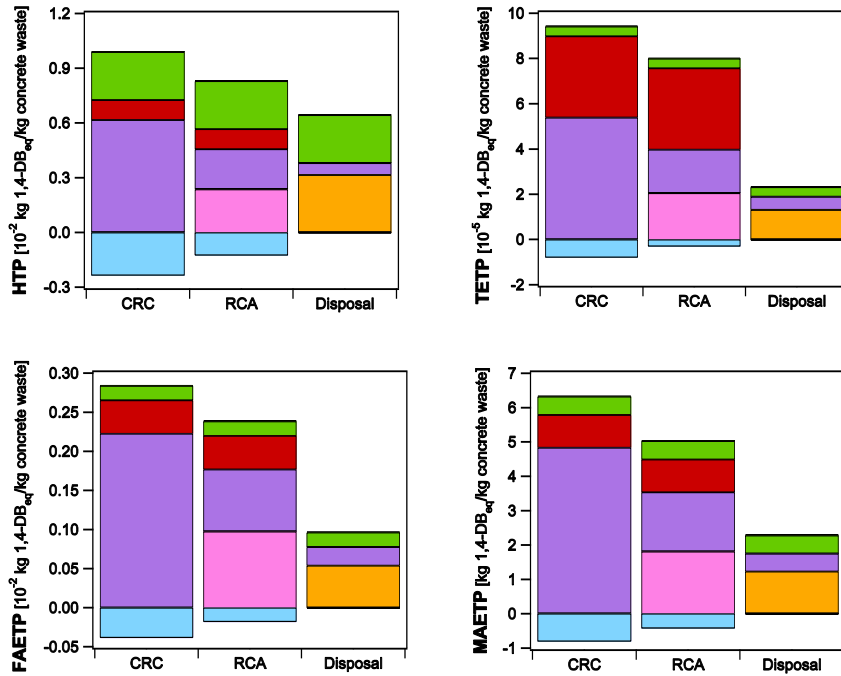
Figure XIII.4b – Life Cycle impact Assessment of the different waste scenarios: CRC = Completely Recyclable Concrete; RCA = Recycling of traditional concrete as Recycled Concrete Aggregates; disposal = disposal of traditional concrete waste

concrete, nonetheless, natural resources will be saved and waste disposal is avoided. Comparing the recycling of CRC and traditional concrete, it was observed that although the global warming potential is lower, mainly the longer transport distances in case of CRC increase its environmental impact.

The question thus remains whether the whole CRC concept is indeed sustainable, when looking at its whole life cycle. The life cycle impact assessments of the different stages in the life cycle of concrete described in chapter XIII.C were assembled for each concrete type, and subsequently multiplied by the corresponding functional unit calculated in chapter XIII.A.3. The obtained results are presented in Figure XIII.5 and are used for the final assessment of the (potential) sustainability of CRC.

Looking at the results for traditional concrete, it is seen that the environmental impact in case of both recycling as aggregate or the disposal of the concrete is comparable regarding most impact categories (abiotic depletion, acidification, eutrophication, global warming, photo-oxidant formation and human toxicity). The impact of concrete disposal is higher when looking at the ozone layer depletion, while the impact on the ecotoxicity is higher for the recycling as concrete aggregate.
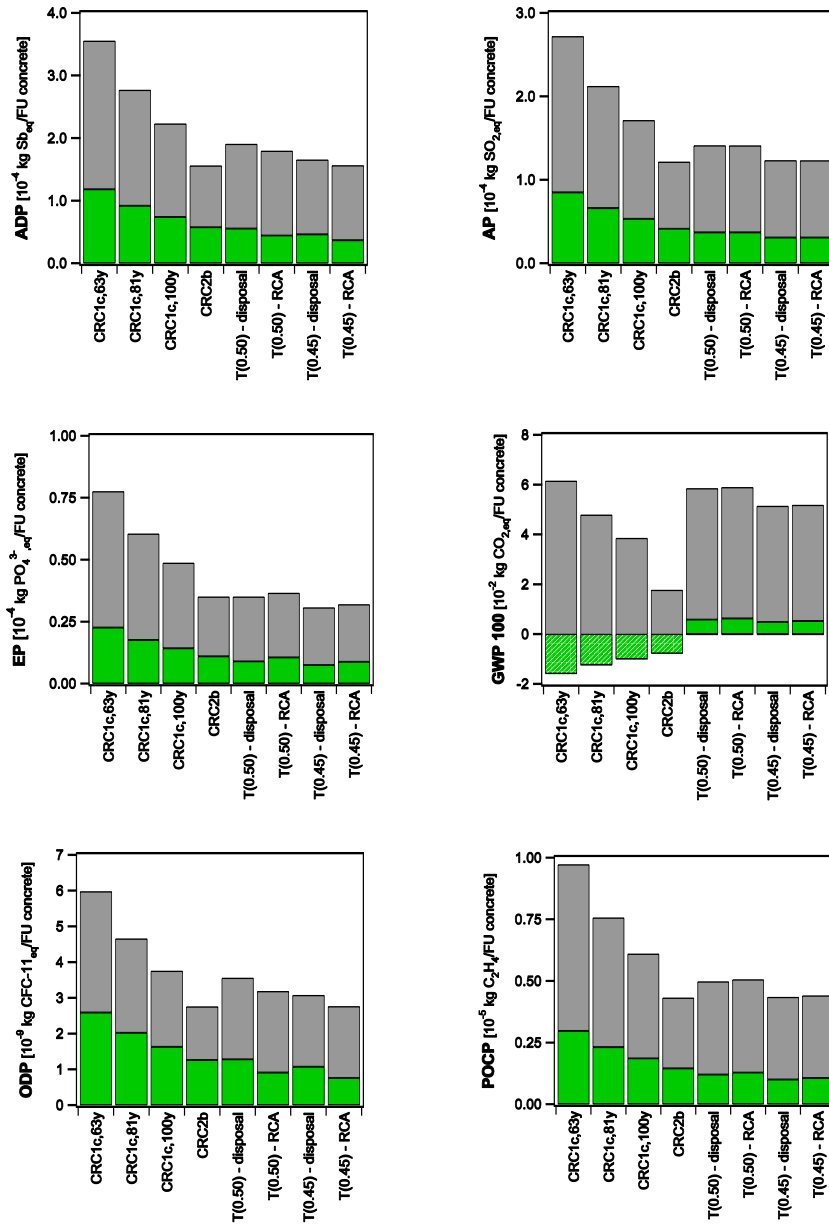
Figure XIII.5a – Cradle-to-cradle Life Cycle Impact Assessment of 1 FU concrete
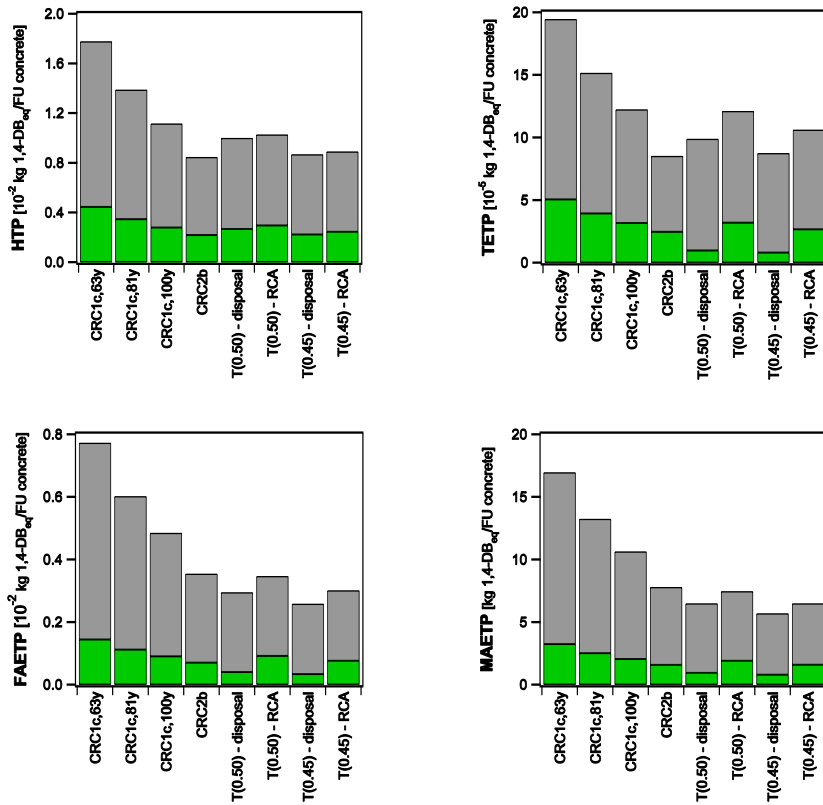
ADP: Abiotic Depletion Potential
AP: Acidification Potential
EP: Eutrophication
GWP 100: Global Warming Potential
ODP: Ozone Depletion Potential
POCP: Photochemical Ozone Creation Potential
HTP: Human Toxicity Potential
FAETP: Fresh water Aquatic EcoToxicity
Potential
MAETP: Marine Aquatic EcoToxicity Potential
TETP: Terrestrial EcoToxicity Potential

- Concrete production
- End-of-life scenario
- Saved CO_2 emissions upon clinkering CRC

Figure XIII.5b – Cradle-to-cradle Life Cycle Impact Assessment of 1 FU concrete

Both the low clinker content and the good strength performance of CRC2b compensate for the additional environmental costs related to its recycling as cement raw meal for most impact categories (abiotic depletion, acidification, eutrophication, global warming, ozone layer depletion, photo-oxidant formation, human toxicity and ecotoxicity). While in most cases, the impact of CRC2b is comparable to the traditional concrete mixtures, the benefits regarding the global warming potential are significant and a reduction of 66-70% was calculated. The lower global warming potential for the CRC mixtures is the result of the lower CO_2 emission of CRC raw material compared to traditional cement raw meals due to the presence of CO_2 free lime in a CRC cement raw meal. The clinker content and strength performance of CRC1c are, however, not low or high enough, respectively, to obtain a lower environmental impact compared to the traditional concretes. Depending on the obtained service life, the environmental impact will be 5-88% (100 years), 31-134% (81 years) or 68-200% (63 years) higher compared to the disposal of concrete and 1-64% (100 years), 26-104% (81 years) or 61-161% (63 years) in comparison with recycling concrete as aggregate. Only regarding the global warming potential, the environmental impact might be 7-35% lower if a service life between 81 and 100 years can be obtained. With a service life of 63 years, the global warming potential is 4-20% higher compared to T(0.50) and T(0.45).

XIV - Conclusions

A. General discussion

The intentions of the design of CRC are clear by now; Completely Recyclable Concrete is designed to be recycled as raw material for cement production. Hereby raw materials are saved and no waste is generated. These intentions are noble and for a CRC properly designed, indeed an improved sustainability is observed. Hereafter, a SWOT analysis will be used to evaluate the Strength, Weaknesses, Opportunities and Threats of the CRC concept. Herein internal (strengths and weaknesses) and external (opportunities and threats) factors that are favourable and unfavourable towards the CRC concept will be identified. The results of the SWOT analysis are presented in Table XIV.1.

Table XIV.1 - SWOT analysis of the CRC concept

	Strengths	**Weaknesses**
Internal factors	CRC Strength & durability Quality regenerated cement Global warming potential	Logistics & practicalities Overall sustainability
	Opportunities	**Threats**
External factors	Safe disposal of toxic waste Deteriorated concrete can be recycled	Other recycling possibilities Consumer interest

A.1. Strengths

i. CRC strength & durability

In Part II, the current study has proven that the requirements for the chemical composition, inherent to the CRC design, should not limit the strength and durability of CRC. Although not intended, CRC2b was found to be a high strength concrete, despite its lower clinker content compared to CRC1c. Both the applicability of the k-value concept according to NBN EN 206-1 (2001) and the improved packing due to a higher powder content are probably the reason for its good performance. The latter also shows that a high strength performance does not necessarily require a high clinker content and the sustainability of concrete can be improved in two ways. First, a higher material efficiency can be obtained by a higher strength, which will reduce the amount of material required and thus the environmental impact of the construction. Secondly, as clinker is the concrete ingredient with the highest environmental impact, a lower clinker content will reduce the environmental impact significantly.

Furthermore it was proven that the application of the k-value concept according to NBN EN 206-1 (2001) is compatible with the design of a CRC. The latter is a big benefit as this guarantees the quality and durability of the concrete. Indeed, when higher amounts of fly ashes would be required, the equal performance should be proven according to NBN

B 15-100 (2008) 'Methodology for the assessment and the validation of the fitness for use of cements or additions of type II for concrete'.

ii. Quality of regenerated cement

In Part III it was shown that the quality of clinker regenerated from CRC is comparable to the one of a traditional cement raw meal. Although the mineralogy of the cement raw meals is different, this only affects the decomposition of the initial phases, and the formation of the clinker phases is found similar to the clinkering reactions in a traditional cement raw meal found in literature. A hydration study on the regenerated cements proved that the hydration process is comparable to the one of traditional cement.

In practice, the chemical composition of the cement raw meal will be depending on the (secondary) fuels that are burned in the clinker kiln, so in fact no ideal composition for CRC is known beforehand. Furthermore it is known that OPC production asks very strict limits towards raw material composition. These issues will, however, solve themselves as no future clinker production plant will be fed with CRC only. Nonetheless, by aiming for a 100% use of CRC in laboratory studies, the potential of CRC use in the clinkering process is maximized.

iii. Global warming potential

From the LCA conducted in chapter XIII, it was concluded that the sustainability regarding CO_2 emissions is improved significantly by making use of the CRC concept. For a CRC with a low clinker content and high compressive strength, reductions of up to 66-70% were found. In case of a CRC with a higher clinker content and normal compressive strength, the saved $CO_{2,eq}$ amounted up to 7-35%. The obtained lower $CO_{2,eq}$ emissions are for one part due to the lower clinker content of the concrete, but it is mainly the avoidance of CO_2 emissions upon clinkering that affects the $CO_{2,eq}$ emitted during the life cycle of the concrete. In comparison with a traditional cement raw meal, the CO_2 free lime available in the CRC raw materials, results in less CO_2 emitted during the CRC clinkering process.

A.2. Weaknesses

i. Logistics and practicalities

At first, it should be mentioned that indeed the design process of a CRC concrete mixture will be more complex compared to a traditional one. It was however already mentioned that no clinker kiln will run on 100% CRC, and thus some last-minute fine tuning will always be possible. Also in some cases (e.g. when using CRC exposed to toxic wastes), the CRC raw meal will require some dilution, which will broaden the strict limits regarding the chemical composition of a cement raw meal.

Secondly, also the recycling process itself requires more efforts compared to recycling concrete as aggregates for new concrete. A well-considered tracking system will be

required, but should be feasible for integrated cement and concrete producers. It is important that after some decades, the information regarding mix design and location of the construction elements produced with CRC is still available. Also a selective demolition is needed; this is however also the case for recycling concrete as aggregates. Additionally, extra efforts are required for the transport of the concrete to the cement plant. Despite of these additional ecological efforts needed, it was proven that the CRC concept can, however, still be more sustainable compared to the traditional concrete.

ii. Overall sustainability

Although the global warming potential of CRC is substantially lower compared to traditional concrete (see chapter XIII), no benefits regarding other impact categories, such as abiotic depletion, acidification, eutrophication, ozone layer depletion, photo-oxidant formation, human toxicity and ecotoxicity, were obtained for the CRC mixtures. For a CRC mixture with a low clinker content and high strength performance, the obtained impacts were comparable with the one of traditional concrete. But if a concrete with a higher clinker content and normal compressive strength was studied, the environmental impact was found to be higher.

A.3. Opportunities

i. Safe disposal of toxic waste

In comparison with other recycling options for concrete, the CRC concept will have its benefits in case concrete structures were exposed to serious pollutions. The dilution factor of CRC exposed to serious pollutions will however be crucial to avoid problems related to e.g. leaching, setting or strength development. Toxic elements can be decomposed to harmless elements within the clinkering process on the one hand. The point of addition might be crucial towards this decomposition. On the other hand (limited amounts of) heavy metals can be incorporated into the clinker phases, without adverse effects on the physical properties of the cement and concrete and without exceeding the limits of the concentration of heavy metals in the leachates.

ii. Recycling of deteriorated concrete

In the introduction it was seen that one of the problems related to the recycling of concrete as aggregates for new concrete was related to contaminations by various sources of aggressive ions, like chlorides and sulphates (e.g. from de-icing salts, sewage plants or seawater), which may have a significant impact on the durability of the new concrete. In Part III it was proven that in case of CRC, the effects on the regenerated clinker will be minimal, although dilution with other raw materials might be necessary in extreme cases.

A.4. Threats

i. Other recycling possibilities

In comparison with today's recycling opportunities of concrete, the CRC concept is more complex. Indeed, the chemical compositions of the concrete raw materials should be checked for each batch produced, and from these results the batch proportions will need some adaptations. Also the issue of logistics and other practicalities handled earlier are not in favour of the CRC concept. Additionally, also the longer transport distances required make the CRC concept only sustainable if its strength and clinker content is sufficiently high and low respectively.

ii. Consumer interest

Although recycling is a hot topic, some restraints from consumers might be expected. When CRC will be recycled, it will, in all likelihood, not be the only ingredient in the cement production process and the latter is thus not expected to trouble the consumer. What might, however, cause some distrust, is the quality of the concrete as it contains fly ash and maybe also some other waste materials such as copper slag. Avoiding this lack of trust from the consumer is another reason to design CRC according to the available standards (e.g. the k-value concept from NBN EN 206-1 (2001)), and not to use higher fly ash contents wherefore additional testing will be needed. Notwithstanding the fact that higher fly ash contents will increase the sustainability of the concrete mixtures.

B. Main research findings

A design methodology for CRC was established in Part I of this thesis. Based on the requirements for a traditional cement raw meal and the chemical compositions of all concrete raw materials, a CRC can be designed for reincarnation within the cement production. It was found that the compositional parameters (lime saturation factor, silica modulus, alumina modulus and hydraulic modulus) are preferred over the Bogue formulas to evaluate the chemical composition of CRC. Indeed, the Bogue formulas are sensitive for small changes in chemical composition. The strength performance and durability of the CRC mixtures can be guaranteed by applying the k-value concept according to NBN EN 206-1 (2001) on the CRC design, of which the requirements are compatible with those of the chemical composition.

By making use of limestone aggregates and filler, cement and fly ash, with small additions of copper slag or porphyry aggregate if necessary, it was feasible to design CRC to be the only ingredient for cement production. The main issue regarding CRC's strength and durability is the use of fly ash, as the latter is known to delay the strength development and increase the carbonation rate of the concrete. The obtained 28-day strengths however were feasible for normal applications, and even a high strength concrete was produced in the study. Regarding the durability of concrete, one could apply the k-value concept according to NBN EN 206-1 (2001) or if higher fly ash

contents would be required, additional tests can be conducted according to NBN B 15-100 (2008).

For one CRC, the combination of Calcium Aluminate Cement and Blast Furnace Slag Cement resulted in fast setting, and a study towards the deceleration of the hydration process was conducted. The addition of calcium sulphate and lime, with or without an additional retarder based on gluconate, was found successful for this purpose. The delay of the setting times was observed using a Vicat needle, but could not be registered by ultrasonic transmission measurements. The latter might be related to ettringite formation, but a more in depth study of the early hydration reactions is needed. Although the measured heat of hydration was lower compared to the reference mixtures, compressive strengths sufficient for practical applications were obtained after 7 and 28 days of hydration for the mixtures with calcium sulphate and lime, with or without the retarder. Although the hydration process was slowed down successfully, the CRC mixtures combining CAC and BFSC are not preferred. An optimal combination of calcium sulphate and lime, and maybe also a retarder, should be searched for each time, making the design process more complicated.

The use of copper slag in CRC was found interesting as a source for iron. For this reason an assessment was performed to study the possible applications of this copper slag in concrete production. The use of copper slag as supplementary cementitious binder was of minor interest. The first tests conducted showed no pozzolanic reactivity of the copper slag. From literature it could additionally be concluded that high finenesses are required to reveal these properties, but high amounts of energy are needed for this purpose as these slags are not easy to grind. Far more interesting are the possibilities for use as aggregate. The effects on compressive strength, open porosity, gas permeability and resistance against carbonation and chloride ingress were found acceptable, or even an improved performance of the concrete was observed. Only the resistance to freeze-thaw attack with de-icing agents was inferior. The latter is however expected to be manageable by using an air entraining agent. The excess of water due to the lower water absorption of the copper slag was claimed to be the main parameter affecting the performance of the concrete.

Apart from the decomposition reactions of the CRC raw material mix, the main clinkering reactions (formation of the cement clinker phases) were found comparable with a traditional cement raw meal. The differentiation of the decomposition of the raw materials is indeed inherent to the composition of the raw material mixture, and it is the end product that will determine the quality of the clinker. All four traditional clinker phases (alite, belite, aluminate and ferrite) were found present in the regenerated clinkers. As many other researchers found, also in this study the experimentally determined clinker composition was found different from the one calculated using the Bogue formulas. The difference is mainly attributed to minor elements such as MgO, sulphate and alkalis, which can be incorporated in the different phases and will thus influence the composition of the clinker. By making use of the modified Bogue calculations, these minor elements in the different clinker phases are taken into account.

However, as the incorporation of the different minerals is depending on the overall chemistry of the cement raw meal, the obtained results will (almost) always differ from the experimental results.

The effect of raw material fineness on the mineralogy of the clinker was studied for CRC raw meals with R90 values ranging from 12-24%, for which no significant influence was noted. Also the differential thermal analysis conducted on these raw materials showed that no significant energy savings resulting from an improved reactivity due to a higher fineness should be expected. Only in the lower temperature range there might be a small effect as additional milling seems to result in a slightly drier raw material. Nonetheless, the possible energy savings will be undone (partially) by a higher energy consumption required for the milling of the raw materials.

When using CRC as cement raw material, the permeated acids and salts in deteriorated concrete will have an effect on the clinkering process. While the amounts of MgO should be limited to avoid a potential delayed expansion in hardened concrete, the amounts of chlorides, sulphates and alkali should be mainly limited to avoid problems in the kiln system. Due to the volatility of these elements, cycles of evaporation and condensation will be established in the clinker kiln. As a result of these cycles, the preheater might get clogged or kiln rings might appear on the kiln walls, both requiring periodic maintenance of the kiln system. Nonetheless, if properly balanced, magnesium, chlorides, sulphates and alkali can have a positive effect on the clinkering process (e.g. stabilisation of more reactive phases and decreasing the melt viscosity) and the use of deteriorated CRC raw meals is possible if properly diluted.

The assessment of the hydration process of cements regenerated from CRC showed a comparable behaviour to Ordinary Portland Cement. The tests revealed that a higher fineness results in a higher reactivity of cements, which is interesting for cements with a rather low alite content. Regarding the methodology for studying the hydration of the cement pastes it was found that for XRD/Rietveld analysis, hydration is preferably stopped by solvent exchange, as freeze drying affects the crystallinity of ettringite and gypsum. An established hydration model [Lothenbach & Winnefeld (2006)] combining an empirical clinker dissolution model [Parrot & Killoh (1984)] and the thermodynamic equilibrium model GEMS [Kulik et al. (2013)] was used to model the hydration reactions of the cement regenerated from CRC. As the hydration of CRC and OPC cement was found comparable, also the model was found applicable. Only the increased reactivity related to the higher fineness of the cement did not come forward in the modelled data.

The sustainability of the CRC concept regarding its global warming potential was proven through a Life Cycle Assessment. It was found that a reduction of 66-70% is possible when a high strength CRC with low clinker content is designed. In case of a normal strength CRC with a higher clinker content, the reductions can be up to 7-35% if a sufficient service life can be obtained. For most other impact categories (abiotic depletion, acidification, eutrophication, ozone layer depletion, photo-oxidant formation, human toxicity and ecotoxicity) only the performance of a high strength CRC with low

clinker content could compensate for the additional transport required in the recycling process.

C. Perspectives

The service life of concrete is a major parameter regarding its sustainability. Today, durability assessments become more and more important, due to the increasing use of alternative raw materials as supplementary cementitious binders or as aggregates, which might affect the concrete durability and thus its service time. Mostly accelerated durability tests are used to evaluate the durability performance of concrete and later on predict its service time. Indeed, 'in situ' durability tests can be time consuming, certainly keeping in mind that service times of (at least) 50 to 100 years are aimed for. It is however not always easy, or better say accurate, to relate the results of accelerated durability tests with service times. A lot of research on the durability of concrete containing alternative raw materials in relation with is service life is ongoing. It is hoped that in the (near) future also straight-forward standards will be developed describing accelerated tests for concretes in view of service life prediction and thus not only to check the concrete quality (e.g. NBN B 15-100 (2008)).

The study towards the deceleration of the reaction of CAC in combination with BFSC was approached from the engineering viewpoint, and the effect of several admixtures was tested. A more scientific approach, and thus an in depth study of the reaction mechanism might facilitate a controlled setting of the mixture.

As mentioned in the introduction, there are many recycling opportunities of solid wastes in concrete. For some solid wastes the effects on concrete are well known (e.g. recycled concrete aggregates, blast furnace slag, fly ash and silica fume), for others scientific studies are required and should be encouraged. The benefits of supplementary cementitious materials are twofold: not only material efficiency is increased, but also CO_2 emissions are avoided as the clinker content of concrete can be reduced. The use of solid waste as cementitious binder is thus preferred. However, for solid wastes without hydraulic or pozzolanic properties, the possibilities for its application as aggregate or filler when having a fine particle size distribution, in concrete can be assessed. In the end also the possibilities of its use as clinker raw material or as fuel can be verified. The latter can be of great importance for toxic wastes, as toxic elements might be decomposed into harmless elements, or heavy metals might be incorporated into the clinker phases, if properly diluted, without arising problems related to leaching of the produced concrete. In case of the use of solid wastes as clinker raw material, a higher CO_2 free lime content will result in additional environmental advantages.

Finally it should be mentioned that also research towards alternatives for the Ordinary Portland Clinker can help to enhance the sustainability of the construction sector. An example of an alternative to Ordinary Portland Clinker is calcium sulphoaluminate cement. Chemically less CaO is required and thus less CO_2 will be released from the decarbonation reaction of the raw materials. Furthermore a lower clinkering

temperature is required reducing the amount of fuels needed. Also for these clinkers the CRC concept might be feasible, if the requirements for its chemical composition can be combined with requirements related to its strength and durability performance.

References

Cheewaket, T., C. Jaturapitakkul and W. Chalee (2010). "Long term performance of chloride binding capacity in fly ash concrete in a marine environment." Construction and Building Materials 24(8): 1352-1357.

Chindaprasirt, P., C. Chotithanorm, H. T. Cao and V. Sirivivatnanon (2007). "Influence of fly ash fineness on the chloride penetration of concrete." Construction and Building Materials 21(2): 356-361.

Damineli, B. L., F. M. Kemeid, P. S. Aguiar and V. M. John (2010). "Measuring the eco-efficiency of cement use." Cement and Concrete Composites 32(8): 555-562.

De Herde, A. and A. Evrard (2005). Dossier cement: Beton en rationeel energiegebruik. Brussel, Febelcem. 35.

De Schutter, G., D. Feys and R. Verhoeven (2010). Ecological profit for a concrete pipe factory due to self-compacting concrete technology. The second international conference on suitstainable construction materials and technologies, Ancona, UWM Center for By-Products Utilization**:** 1281-1287.

Desmyter, J. and Y. Martin (2001). "De milieuimpact van bouwmaterialen en gebouwen." WTCB-tijdschrift(winter): 3-13.

EFCA (2006). Environmental Declaration Superplasticizing Admixtures.

Fib (2006). CEB-FIP Fib bulletin 34. Model code for service life design. The International Federation for structural concrete. Task Group 5.6. Lausanne.

Frischknecht, R. and N. Jungbluth (2007). Overview and methodology. Final Report ecoinvent v2.0 No.1. St-Gallen, Swiss Center for Life Cycle Inventories.

Habert, G. and N. Roussel (2009). "Study of two concrete mix-design strategies to reach carbon mitigation objectives." Cement and Concrete Composites 31(6): 397-402.

Sisomphon, K. and L. Franke (2007). "Carbonation rates of concretes containing high volume of pozzolanic materials." Cement and Concrete Research 37(12): 1647-1653.

Sumranwanich, T. and S. Tangtermsirikul (2004). "A model for predicting time-dependent chloride binding capacity of cement-fly ash cementitious system." Materials and Structures 37(6): 387-396.

Van den Heede, P. and N. De Belie (2012). "Environmental impact and life cycle assessment (LCA) of traditional and 'green' concretes: Literature review and theoretical calculations." Cement and Concrete Composites 34(4): 431-442.

Van den Heede, P. and N. De Belie (2014). "A service life based global warming potential for high-volume fly ash concrete exposed to carbonation." Construction and Building Materials 55(0): 183-193.

APPENDIX A
Life Cycle Inventory Data

The data used for the life cycle inventory was taken from the ecoinvent 2.0 database [Frischknecht and Jungbluth (2007)], built by the Swiss Centre for Life Cycle Inventories and commonly used in combination with the LCA software used (SimaPro). As adaptations were necessary to take into account e.g. the recycling of CRC within the clinker manufacturing process, an overview of the used input is given in chapter XIII.B. The actual input data is given hereafter.

Abbreviations

BE   Belgium
CH   Switzerland
DE   Germany
GLO   Global
I   Infrastructure
RER   Europe
U   Unit process
WEU   Western Europe

Units

kg   Mass
kWh   Energy
m   Length
m^2 Area
m^2a Land use
m^3 Volume
MJ   Energy
p   Amount
tkm   Transport

Table A.1 - Life cycle inventory for the production of 1 kg Ordinary Portland Cement taken from the ecoinvent 2.0 database

Input - Materials & Fuels	Value	Unit
Cement plant/CH/I U	5.36E-11	p
Clinker, at plant/CH U[a]	9.12E-01	kg
Electricity, medium voltage, at grid/CH U	4.85E-02	kWh
Ethylene glycol, at plant/RER U	3.50E-04	kg
Steel, low-alloyed, at plant/RER U	6.00E-05	kg
Transport, lorry 3.5-20t, fleet average/CH U	4.40E-03	tkm
Output - Emissions to air	**Value**	**Unit**
Heat, waste	1.75E-01	MJ
Output - Products	**Value**	**Unit**
Portland cement, strength class Z 52.5, at plant/CH U	1.00E+00	kg

[a] The process 'Clinker, at plant/CH U' from the ecoinvent 2.0 database was split into the raw material delivery and actual clinker production process to enable the recycling of CRC concrete waste

Table A.2 - Life cycle inventory for the production of 1 kg Blast Furnace Slag Cement taken from the ecoinvent 2.0 database

Input - Materials & Fuels	Value	Unit
Ethylene glycol, at plant/RER U	5.50E-04	kg
Clinker, at plant/CH U[a]	4.60E-01	kg
Cement plant/CH/I U	5.36E-11	p
Electricity, medium voltage, at grid/CH U	7.83E-02	kWh
Steel, low-alloyed, at plant/RER U	1.10E-04	kg
Heavy fuel oil, burned in industrial furnace 1MW, non-modulating/CH U (Drying of granulated blast furnace slag)	1.03E-01	MJ
Transport, lorry 3.5-20t, fleet average/CH U	2.70E-02	tkm
Output - Emissions to air	**Value**	**Unit**
Heat, waste	2.82E-01	MJ
Output - Products	**Value**	**Unit**
Blast furnace slag cement, at plant/CH U	1.00E+00	kg

[a] The process 'Clinker, at plant/CH U' from the ecoinvent 2.0 database was split into the raw material delivery and actual clinker production process to enable the recycling of CRC concrete waste

Table A.3 - Life cycle inventory of the raw materials needed for 1 kg clinker based on the ecoinvent 2.0 database

Input - Materials & Fuels	Value	Unit
Calcareous marl, at plant/CH U	4.66E-01	kg
Clay, at mine/CH U	3.31E-01	kg
Limestone, crushed, for mill/CH U[a]	8.41E-01	kg
Sand, at mine/CH U	9.26E-03	kg
Lime, hydrated, loose, at plant/CH U	3.92E-03	kg
Bauxite, at mine/GLO U	1.20E-04	kg
Transport, lorry 3.5-20t, fleet average/CH U	8.61E-05	tkm
Transport, lorry 20-28t, fleet average/CH U	2.68E-03	tkm
Transport, lorry >28t, fleet average/CH U	2.11E-03	tkm
Transport, barge/RER U	7.22E-03	tkm
Transport, freight, rail/CH U	1.77E-02	tkm
Output - Emissions to air	**Value**	**Unit**
Carbon dioxide, fossil	5.43E-01	kg
Output - Products	**Value**	**Unit**
Raw materials for 1 kg clinker[b]	1.00E+00	kg

[a] As CRC still needs to be milled, all milling processes should be considered in the clinkering process. For this reason the input of the 'Limestone, milled, loose, at plant/CH U' process from the ecoinvent 2.0 database is added to the clinkering process in Table A.4, except for the raw material 'Limestone, crushed, for mill/CH U' which is considered in this table.

[b] The process 'Clinker, at plant/CH U' from the ecoinvent 2.0 database was split into the raw material delivery and actual clinker production process to enable the recycling of CRC concrete waste

Table A.4 - Life cycle inventory of the production of 1 kg clinker based on the ecoinvent 2.0 database

Input - Resources	Value	Unit
Water, unspecified natural origin/m^3	1.62E-03	m^3

Input – Materials & Fuels	Value	Unit
Ammonia, liquid, at regional storehouse/CH U	9.08E-04	kg
Lubricating oil, at plant/RER U	4.71E-05	kg
Refractory, basic, packed, at plant/DE U	1.90E-04	kg
Refractory, fireclay, packed, at plant/DE U	8.21E-05	kg
Refractory, high aluminium oxide, packed, at plant/DE U	1.37E-04	kg
Cement plant/CH/I U	6.27E-12	p
Diesel, burned in building machine/GLO U (Internal transport)	1.34E-02	MJ
Industrial machine, heavy, unspecified, at plant/RER/I U (Round kiln)	3.76E-05	kg
Electricity, medium voltage, at grid/CH U	5.80E-02	kWh
Hard coal, at regional storage/WEU U	3.54E-02	kg
Chromium steel 18/8, at plant/RER U	5.86E-05	kg
Natural gas, high pressure, at consumer/CH U	6.81E-03	MJ
Heavy fuel oil, at regional storage/CH U	2.55E-02	kg
Light fuel oil, at regional storage/CH U	3.74E-04	kg
Petroleum coke, at refinery/RER U	3.91E-03	kg
Transport, van <3.5t/CH U	7.09E-05	tkm
Transport, freight, rail/RER U	7.09E-03	tkm
Tap water, at user/RER U	3.40E-01	kg
Light fuel oil, burned in boiler 100kW, non-modulating/CH U[a]	1.26E-03	MJ
Industrial machine, heavy, unspecified, at plant/RER/I U[a]	1.89E-04	kg
Heat, light fuel oil, at industrial furnace 1MW/CH U[a]	7.55E-02	MJ
Electricity, medium voltage, at grid/CH U[a]	1.35E-02	kWh
Electricity, hydropower, at run-of-river power plant/CH U[a]	1.35E-02	kWh
Raw materials for 1 kg clinker[b]	1.00E+00	kg

Output - Emissions to air	Value	Unit
Ammonia	2.28E-05	kg
Antimony	2.00E-09	kg
Arsenic	1.20E-08	kg
Beryllium	3.00E-09	kg
Cadmium	7.00E-09	kg
Carbon dioxide, biogenic	1.51E-02	kg
Carbon dioxide, fossil	2.96E-01	kg
Carbon monoxide, fossil	4.72E-04	kg
Chromium	1.45E-09	kg

Cobalt	4.00E-09	kg
Copper	1.40E-08	kg
Dioxin, 2,3,7,8 Tetrachlorodibenzo-p-	9.60E-13	kg
Heat, waste	3.62E+00	MJ
Hydrogen chloride	6.31E-06	kg
Lead	8.50E-08	kg
Mercury	3.30E-08	kg
Methane, fossil	8.88E-06	kg
Nickel	5.00E-09	kg
Nitrogen oxides	1.08E-03	kg
NMVOC, non-methane volatile organic compounds, unspecified origin	5.64E-05	kg
Particulates, < 2.5 um	2.41E-05	kg
Particulates, > 10 um	5.66E-06	kg
Particulates, > 2.5 um, and < 10um	7.92E-06	kg
Selenium	2.00E-09	kg
Sulfur dioxide	3.55E-04	kg
Thallium	1.30E-08	kg
Tin	9.00E-09	kg
Vanadium	5.00E-09	kg
Zinc	6.00E-08	kg
Chromium VI	5.50E-10	kg
Heat, waste[a]	9.67E-02	MJ

Output - Waste to treatment

Disposal, inert waste, 5% water, to inert material landfill/CH U	8.00E-05	kg
Disposal, municipal solid waste, 22.9% water, to municipal incineration/CH U	4.50E-05	kg

Output - Products	**Value**	**Unit**
Clinker, at plant/CH U[b]	1.00E+00	kg

[a] As CRC still needs to be milled, all milling processes should be considered in the clinkering process. For this reason the input of the 'Limestone, milled, loose, at plant/CH U' process from the ecoinvent 2.0 database is added to the clinkering process in this table, except for the raw material 'Limestone, crushed, for mill/CH U' which is considered in Table A.3.

[b] The process 'Clinker, at plant/CH U' from the ecoinvent 2.0 database was split into the raw material delivery and actual clinker production process to enable the recycling of CRC concrete waste

Table A.5 - Life cycle inventory for the production of 1 m³ concrete based on the ecoinvent 2.0 database

Input - Materials & Fuels	Value	Unit
Concrete mixing plant/CH/I U	4.57E-07	p
Diesel, burned in building machine/GLO U	2.27E+01	MJ
Electricity, medium voltage, at grid/CH U	4.36E+00	kWh
Heavy fuel oil, burned in industrial furnace 1MW, non-modulating/CH U	3.09E+00	MJ
Light fuel oil, burned in industrial furnace 1MW, non-modulating/CH U	1.33E+01	MJ
Lubricating oil, at plant/RER U	1.19E-02	kg
Natural gas, burned in industrial furnace low-NOx >100kW/RER U	1.16E+00	MJ
Steel, low-alloyed, at plant/RER U	2.38E-02	kg
Synthetic rubber, at plant/RER U	7.13E-03	kg
Transport, barge/RER U	4.92E+01	tkm
Transport, freight, rail/CH U	6.82E+00	tkm
Transport, lorry 3.5-20t, fleet average/CH U	9.98E-01	tkm
Transport, lorry 20-28t, fleet average/CH U	9.44E+00	tkm
Input - Materials & Fuels – CRC1c specific	**Value**	**Unit**
Gravel, crushed, at mine/CH U	1.74E+03	kg
Portland cement, strength class Z 52.5, at plant/CH U	3.00E+02	kg
Tap water, at user/CH U	1.53E+02	kg
Limestone, milled, loose, at plant/CH U	5.30E+01	kg
Fly ash	1.00E+02	kg
Superplasticizer	4.40E+00	kg
Input - Materials & Fuels – CRC2b specific	**Value**	**Unit**
Gravel, crushed, at mine/CH U	1.62E+03	kg
Blast furnace slag cement, at plant/CH U	3.25E+02	kg
Tap water, at user/CH U	1.54E+02	kg
Limestone, milled, loose, at plant/CH U	1.77E+02	kg
Fly ash	8.50E+01	kg
Superplasticizer	7.67E+00	kg
Input - Materials & Fuels – T(0.50) specific	**Value**	**Unit**
Sand, at mine/CH U	7.14E+02	kg
Gravel, round, at mine/CH U	8.90E+02	kg
Portland cement, strength class Z 52.5, at plant/CH U	3.20E+02	kg
Tap water, at user/CH U	1.60E+02	kg
Gravel, round, at mine/CH U-to be recycled[a]	2.97E+02	kg
Input - Materials & Fuels – T(0.45) specific	**Value**	**Unit**

	Value	Unit
Sand, at mine/CH U	7.15E+02	kg
Gravel, round, at mine/CH U	8.90E+02	kg
Portland cement, strength class Z 52.5, at plant/CH U	3.40E+02	kg
Tap water, at user/CH U	1.53E+02	kg
Superplasticizer	1.87E+00	kg
Gravel, round, at mine/CH U-to be recycled[a]	2.97E+02	kg
Output – Emissions to air	**Value**	**Unit**
Heat, waste	1.57E+01	MJ
Output – Waste to treatment	**Value**	**Unit**
Disposal, concrete, 5% water, to inert material landfill/CH U	1.69E+01	kg
Disposal, municipal solid waste, 22.9% water, to municipal incineration/CH U	9.51E-02	kg
Treatment, concrete production effluent, to wastewater treatment, class 3/CH U	1.43E-02	m^3
Output – Products	**Value**	**Unit**
Concrete, normal, at plant/CH U	1.00E+00	m^3

[a] The process 'Gravel, round, at mine/CH U' from the ecoinvent 2.0 database was split into the raw material delivery and actual aggregate production process to enable the recycling of traditional concrete waste

Table A.6 – Life cycle inventory for 0.052 kg Fly Ash based on Van den Heede and De Belie (2012)

Input – Electricity/heat	Value	Unit
Electricity, hard coal, at power plant/BE U	1.00E+00	kWh
Output – Products	**Value**	**Unit**
Fly ash (with an economic allocation of 1%)	5.20E-02	kg
Electricity (with an economic allocation of 99%)	1.00E+00	kWh

Table A.7 – Life cycle inventory of the raw materials needed for 1 kg gravel based on the ecoinvent 2.0 database

Input – Natural resources	Value	Unit
Gravel, in ground	1.04E+00	kg
Occupation, mineral extraction site	2.88E-04	m^2a
Occupation, water bodies, artificial	6.27E-05	m^2a
Transformation, to mineral extraction site	2.88E-05	m^2
Transformation, to water bodies, artificial	6.27E-06	m^2
Transformation, from unknown	3.51E-05	m^2
Input – Materials, fuels, electricity & heat	**Value**	**Unit**
Mine, gravel/sand/CH/I U	4.75E-11	p
Recultivation, limestone mine/CH U	1.27E-06	m^2
Diesel, burned in building machine/GLO U	1.43E-02	MJ
Output – Avoided products	**Value**	**Unit**
Raw materials for 1 kg gravel[a]	1.00E+00	kg

[a] The process 'Gravel, round, at mine/CH U' from the ecoinvent 2.0 database was split into the raw material delivery and actual aggregate production process to enable the recycling of traditional concrete waste

Table A.8 - Life cycle inventory of the production of 1 kg round gravel based on the ecoinvent 2.0 database

Input – Natural resources	Value	Unit
Water, unspecified natural origin/m3	1.35E-03	m^3

Input – Materials, fuels, electricity & heat	Value	Unit
Building, hall, steel construction/CH/I U	2.85E-06	m^2
Conveyor belt, at plant/RER/I U	9.51E-08	m
Electricity, medium voltage, at grid/CH U	9.06E-03	kWh
Heat, light fuel oil, at boiler 10kW, non-modulating/CH U	4.91E-03	MJ
Industrial machine, heavy, unspecified, at plant/RER/I U	9.51E-05	kg
Lubricating oil, at plant/RER U	2.50E-06	kg
Steel, low-alloyed, at plant/RER U	5.10E-05	kg
Synthetic rubber, at plant/RER U	4.00E-06	kg
Tap water, at user/RER U	1.22E-02	kg
Transport, lorry 3.5-20t, fleet average/CH U	2.92E-06	tkm
Transport, lorry 20-28t, fleet average/CH U	1.72E-05	tkm
Transport, van <3.5t/CH U	1.55E-05	tkm
Raw materials for 1 kg gravel[a]	1.00E+00	kg

Output - Emissions to air	Value	Unit
Heat, waste	3.26E-02	MJ
Particulates, < 2.5 µm	4.00E-10	kg
Particulates, > 10 µm	5.60E-09	kg
Particulates, > 2.5 µm, and < 10 µm	2.00E-09	kg

Output – Waste to treatment		
Disposal, municipal solid waste, 22.9% water, to municipal incineration/CH U	2.12E-06	kg
Disposal, used mineral oil, 10% water, to hazardous waste incineration/CH U	2.50E-06	kg

Output - Avoided products	Value	Unit
Gravel, round, at mine/CH U[a]	1.00E+00	kg

[a] The process 'Gravel, round, at mine/CH U' from the ecoinvent 2.0 database was split into the raw material delivery and actual aggregate production process to enable the recycling of traditional concrete waste

Table A.9 - Life cycle inventory for the recycling of 1.54 kg CRC as raw material for the clinkering production

Input – Waste material	Value	Unit
CRC	1.54E+00	kg
Input – Materials, fuels, electricity & heat	**Value**	**Unit**
Diesel, burned in building machine/GLO U[a]	6.25E-02	MJ
Excavation, hydraulic digger/RER U[a]	7.95E-04	m^3
Electricity, low voltage, at grid/CH U[a]	5.29E-03	kWh
Transport, lorry 20-28t, fleet average/CH U [b]	1.39E-01	tkm
Transport, lorry 20-28t, fleet average/CH U [c]	7.70E-02	tkm
Sorting plant for construction waste/CH/I U[a]	1.43E-10	p
Output - Emissions to air	**Value**	**Unit**
Particulates, < 2.5 μm[a]	2.37E-05	kg
Particulates, > 2.5 μm, and < 10 μm[a]	9.07E-05	kg
Particulates, > 10 μm[a]	1.19E-04	kg
Heat, waste[a]	1.90E-02	MJ
Carbon dioxide, fossil[d]	4.60E-01	kg
Output - Avoided products	**Value**	**Unit**
Raw materials for 1 kg clinker	1.00E+00	kg

[a] Data from the 'Disposal, building, concrete gravel, to sorting plant/CH U' process from the ecoinvent 2.0 database
[b] Transport between the sorting plant and the cement factory, assumed to be 90 km
[c] Transport between the construction site and sorting plant, assumed to be 50 km
[d] Raw material CO_2 emissions within the clinkering process

Table A.10 - Life cycle inventory for the disposal of 1 kg concrete waste

Input – Waste material	Value	Unit
Traditional concrete	1.00E+00	kg
Input – Materials, fuels, electricity & heat	**Value**	**Unit**
Diesel, burned in building machine/GLO U	4.37E-02	MJ
Transport, lorry 20-28t, fleet average/CH U	1.50E-02	tkm
Output - Emissions to air	**Value**	**Unit**
Particulates, < 2.5 µm	1.66E-05	kg
Particulates, > 2.5 µm, and < 10 µm	6.34E-05	kg
Particulates, > 10 µm	8.35E-05	kg
Output – Waste to treatment	**Value**	**Unit**
Disposal, inert waste, 5% water, to inert material landfill/CH U	1.00E+00	kg

Table A.11 - Life cycle inventory for the recycling of 1.04 kg traditional concrete as raw material for the production of aggregates

Input – Waste material	Value	Unit
Traditional concrete	1.04E+00	kg

Input – Materials, fuels, electricity & heat	Value	Unit
Diesel, burned in building machine/GLO U[a]	4.54E-02	MJ
Excavation, hydraulic digger/RER U[a]	5.78E-04	m^3
Electricity, low voltage, at grid/CH U[a]	3.85E-03	kWh
Building, hall, steel construction/CH/I U[b]	2.35E-06	m^2
Electricity, medium voltage, at grid/CH U[b]	6.34E-03	kWh
Heat, light fuel oil, at boiler 10kW, non-modulating/CH U[b]	2.47E-03	MJ
Industrial machine, heavy, unspecified, at plant/RER/I U[b]	8.39E-05	kg
Lubricating oil, at plant/RER U[b]	6.50E-07	kg
Steel, low-alloyed, at plant/RER U[b]	3.80E-05	kg
Synthetic rubber, at plant/RER U[b]	2.00E-06	kg
Tap water, at user/RER U[b]	2.10E-03	kg
Transport, lorry 3.5-20t, fleet average/CH U[b]	2.04E-06	tkm
Sorting plant for construction waste/CH/I U[a]	1.04E-10	p
Transport, lorry 20-28t, fleet average/CH U[c]	5.20E-02	tkm

Output - Emissions to air	Value	Unit
Particulates, < 2.5 μm[a]	1.73E-05	kg
Particulates, > 2.5 μm, and < 10 μm[a]	6.59E-05	kg
Particulates, > 10 μm[a]	8.68E-05	kg
Heat, waste[a]	1.38E-02	MJ

Output - Avoided products	Value	Unit
Raw materials for 1 kg gravel	1.00E+00	kg

[a] Data from the 'Disposal, building, concrete gravel, to sorting plant/CH U' process from the ecoinvent 2.0 database

[b] Compared to round gravel, recycled concrete aggregates need to be crushed; the additional input therefore is obtained from the difference between the 'Gravel, crushed, at mine/CH U' process and the 'Gravel, round, at mine/CH U' process from the ecoinvent 2.0 database

[c] Transport between the construction site and sorting plant, assumed to be 50 km

LCA Sensitivity Analysis

The life cycle assessment conducted in chapter XIII is based on a deterministic approach. In order to see the influence of data uncertainty on the conclusions and verify the robustness of the conclusions, a sensitivity analysis was performed. This sensitivity analysis was performed for three assumptions made in the life cycle inventory: the allocation of the environmental impact of the fly ash production, the avoided CO_2 emissions by recycling CRC and the transport distances upon recycling.

A. LCA sensitivity towards the allocation of the environmental impact of fly ash

When a production process results in more than one product, the environmental impact of this process should be divided over the different end products. Since fly ash is today considered as a by-product from the production of electricity, it seems reasonable to divide the environmental impact of the electrical power plant over both the electricity and fly ash produced. The portioning of the impact can occur through allocation by mass or by economic value. The advantage of mass allocation is that the allocation coefficient remains constant over a long period of time. However, enormous environmental impacts are imposed to the by-products which may discourage the concrete industry to continue applying them as cement replacement. By economic allocation lower environmental impacts are imposed to the by-products, but the allocation coefficient will fluctuate due to price instability.

In Table B.1, an overview of the allocation coefficients for fly ash are given. In chapter XIII the economic allocation coefficient was based on a price of 20 euro/ton fly ash and 0.10 euro/kWh electricity. Since fly ash becomes more and more accepted as a concrete product, its price also increases (e.g. 35 euro/ton fly ash). In the meantime the price for electricity decreased in Belgium since the energy market was privatized (e.g. 0.06 euro/kWh electricity). Hereby the economic allocation coefficient for fly ash increases from 1% up to 3%.

Table B.1 – Allocation coefficients by mass and economic value for fly ash based on Van den Heede (2012)

Product	Mass	Price (1)	Price (2)
Value			
Fly ash	0.052 kg	20 euro/ton	35 euro/ton
Electricity	1 kWh*	0.10 euro/kWh	0.06 euro/kWh
Allocation coefficient [%]			
Fly ash	12.4	1	3
Electricity	87.6	99	97

* 1 kWh electricity = 0.67 kg hard coal

To evaluate the effect of the allocation of the environmental impact of fly ash on the concrete production process, calculations were made using no allocation as a minimum (fly ash is an avoided waste from the electrical power plants) and 12.4% allocation as a

maximum (mass allocation). The results are presented in Figure B.1 as error bars on the results that were presented in chapter XIII (see Figure XIII.3).

If no allocation would be used for the fly ash, the environmental impact of the CRC mixtures would be 2-39% lower depending on the considered impact category. When using the mass allocation, the environmental impact of the CRC mixtures increases drastically for all impact categories. The aquatic ecotoxicity is affected the most and the values are 5 times higher. The lowest effect is found regarding the ozone layer depletion.

Based on mass allocation, the use of fly ash in concrete would not be beneficial for the environmental impact of concrete. However it is still better to use fly ash in concrete instead of landfilling it. For this reason it was decided to use the 3% allocation coefficient (economic allocation) as the maximum when calculating the effect of the allocation of fly ash on the whole life cycle of CRC. The results of these calculations are presented in Figure B.2.

Similar to the effect on the concrete production, the environmental impact of the CRC life cycle would reduce if no allocation would be used. The obtained values are 1-29% lower. When using a 3% allocation coefficient (economic allocation), the environmental impact of the CRC mixtures increases significantly for almost all impact categories. Again the aquatic ecotoxicity is affected the most and the values increase with about 50%. The effect on the ozone layer depletion was found negligible.
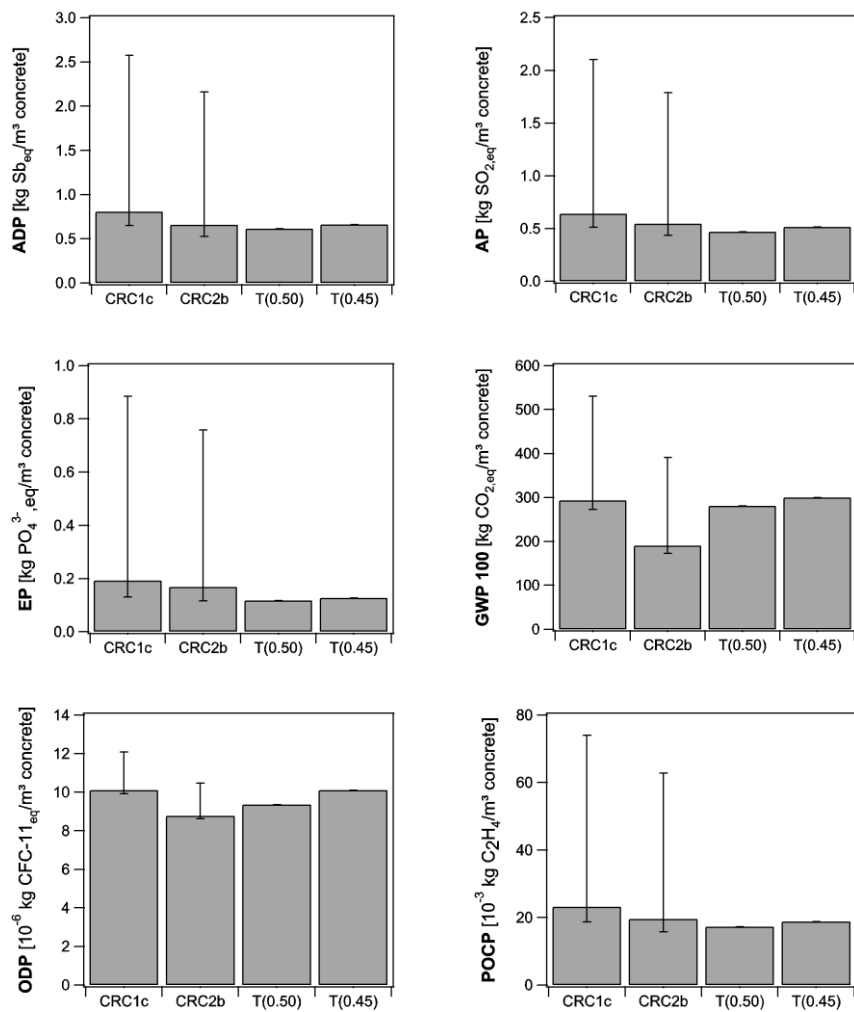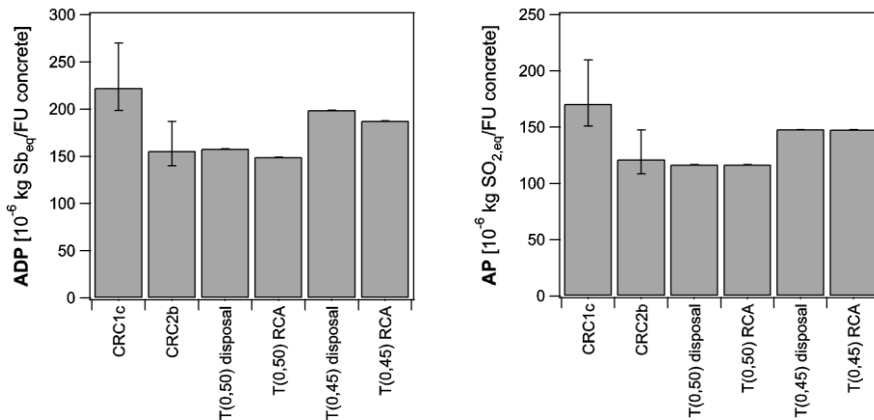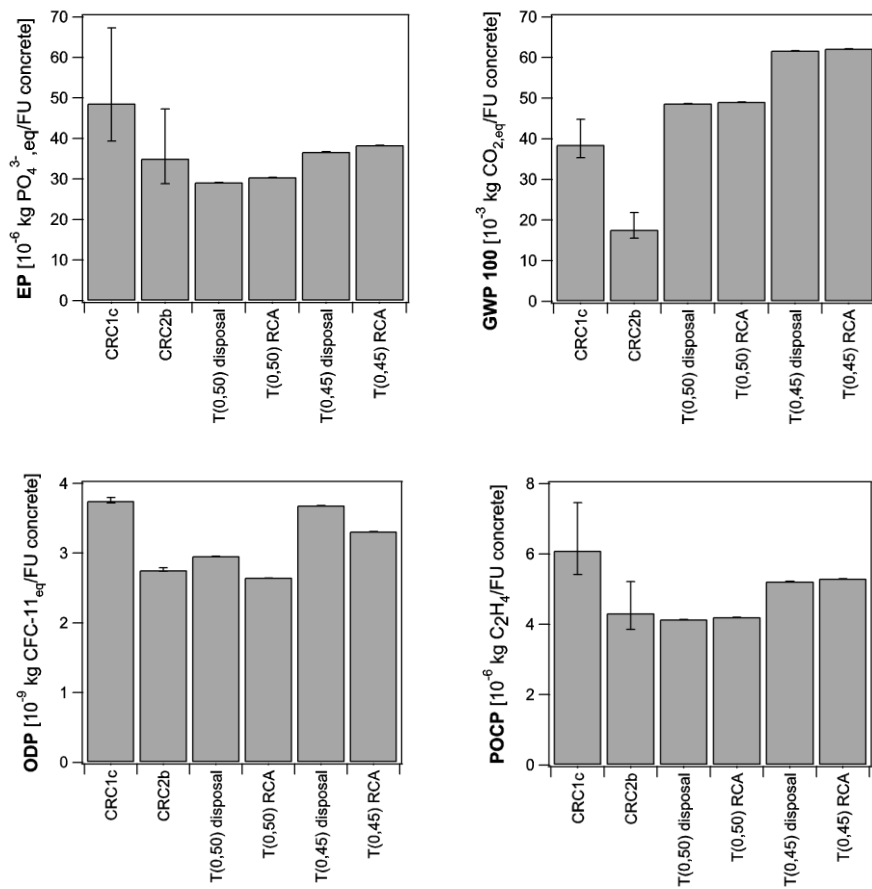
Figure B.1a – Life Cycle Impact Assessment of 1 m³ concrete with the effect of the allocation of the environmental impact of fly ash indicated by error bars. For the lower values no allocation for the fly ash was considered. For the higher values an allocation coefficient of 12.4% was used (mass allocation).
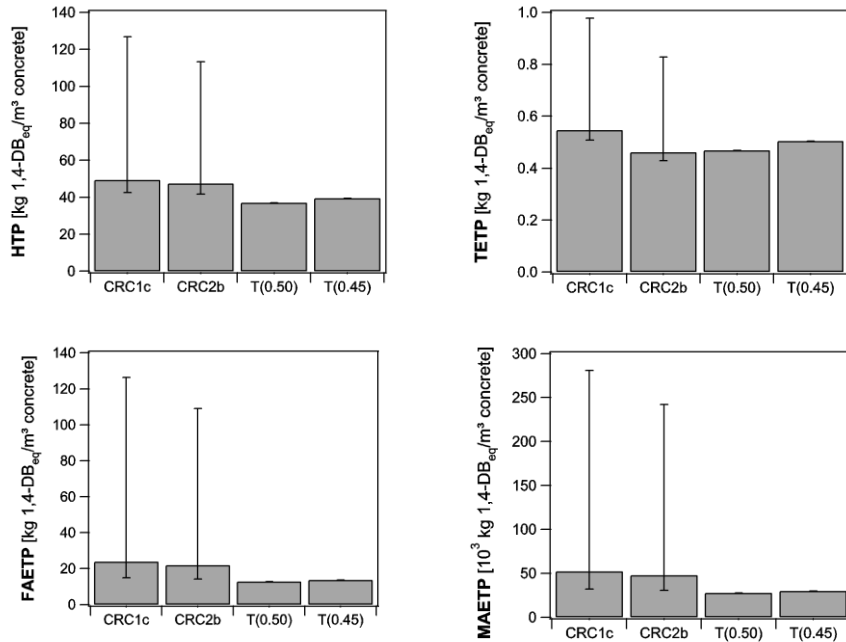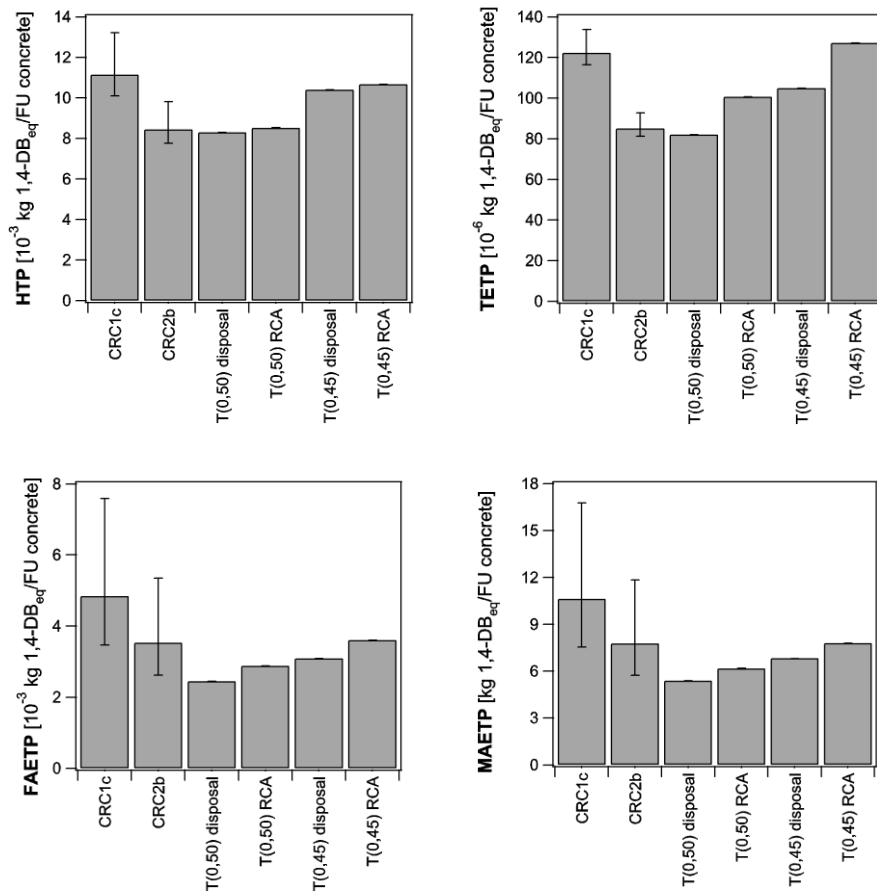
Figure B.1b – Life Cycle Impact Assessment of 1 m³ concrete with the effect of the allocation of the environmental impact of fly ash indicated by error bars. For the lower values no allocation for the fly ash was considered. For the higher values an allocation coefficient of 12.4% was used (mass allocation).

Figure B.2a – Cradle-to-cradle Life Cycle Impact Assessment of 1 FU concrete with the effect of the allocation of the environmental impact of fly ash indicated by error bars. For the lower values no allocation for the fly ash was considered. For the higher values an allocation coefficient of 3% was used (economic allocation).

Figure B.2b – Cradle-to-cradle Life Cycle Impact Assessment of 1 FU concrete with the effect of the allocation of the environmental impact of fly ash indicated by error bars. For the lower values no allocation for the fly ash was considered. For the higher values an allocation coefficient of 3% was used (economic allocation).

Figure B.2c – Cradle-to-cradle Life Cycle Impact Assessment of 1 FU concrete with the effect of the allocation of the environmental impact of fly ash indicated by error bars. For the lower values no allocation for the fly ash was considered. For the higher values an allocation coefficient of 3% was used (economic allocation).

B. LCA sensitivity towards avoided CO_2 emissions

The advantage regarding the global warming potential of the CRC mixtures is strongly related to the avoided CO_2 emissions upon clinkering. In chapter XIII, the CO_2 emissions upon clinkering of CRC were expected to be 46 g/100g clinker from TG analysis. Of course some spread on the results might be expected depending on the cement content of the CRC mixtures. In Table B.2 the theoretical expected CO_2 emissions for the different CRC mixtures are calculated. A minimum and maximum value of 40.5 and 43.1 g/100g clinker, respectively, were calculated.

Table B.2 – Theoretical values for the expected CO_2 emissions of the different CRC mixtures produced in this study

CRC mix	CO₂ max *Based on CaO content [g/100g clinker]*	CO₂ cement *Avoided, based on CaO delivered by cement [g/100g clinker]*	Expected CO₂ *CO₂ max – CO₂ cement [g/100g clinker]*
CRC1a	51.1	9.8	41.3
CRC1b	49.9	9.4	40.5
CRC1c	51.5	9.4	42.1
CRC2a	51.3	8.2	43.1
CRC2b	51.7	9.0	42.7
CRC3a	51.0	8.2	42.7
CRC3b	51.1	8.3	42.8

These results are lower compared to the 46 g/100g clinker measured by TG analysis. The difference between the theoretical and experimental value can be explained by different reasons. At first only CaO is expected to be bound to CO_2 but also other oxides, mainly MgO, are expected to be present as a carbonate. Additionally it is possible that the CRC sample tested was carbonated upon storage and handling. This uptake of CO_2 is also expected to be present when CRC would be applied in practice. As already mentioned in chapter XII, this CO_2 is however considered neutral in the LCA since this CO_2 was captured from the atmosphere and temporarily stored in the concrete. Finally there is also the error related to the experimental procedure.
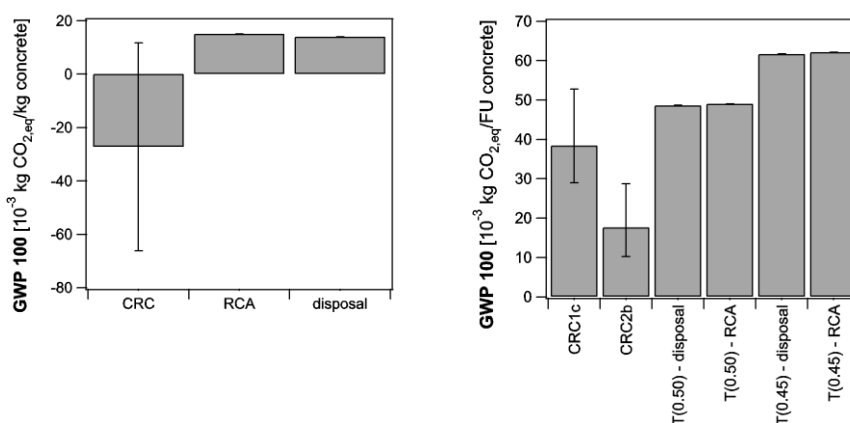
Since the avoided CO_2 emissions are strongly related to the cement content of the concrete, an additional calculation was made to estimate the expected CO_2 emissions of a CRC mixture depending on its cement content. The results of these calculations are presented in Table B.3. For a cement content varying between 260 and 360 kg/m³ concrete, the expected CO_2 emission varies between 37.7 and 41.6 g/100g clinker.

Based on the results presented above, the minimum and maximum value was set at 40 and 52 g/100g clinker respectively. The minimum value is based on the minimum value of the expected CO_2 emissions calculated in Table B.2. The maximum value was taken worst case by adding the difference between the experimental and minimum value (46 g/100g clinker – 40 g/100g clinker = 6 g/100g clinker) to the experimental value (46

g/100g clinker + 6 g/100g clinker = 52 g/100g clinker). The results of the sensitivity calculations are presented in Figure B.3.

Table B.3 – Theoretical values for the expected CO_2 emissions for concrete with CRC mixtures with different cement contents

Cement content [kg/m³]	CO_2 max *Based on CaO content* [g/100g clinker]	CO_2 cement *Avoided, based on CaO delivered by cement* [g/100g clinker]	Expected CO_2 CO_2 max – CO_2 cement [g/100g clinker]
260	51.0	9.4	41.6
280	51.0	10.2	40.8
300	51.0	10.9	40.1
320	51.0	11.7	39.3
340	51.0	12.5	38.5
360	51.0	13.3	37.7

Figure B.3 – Sensitivity analysis of the avoided CO_2 emissions by clinkering CRC. Left: effect upon the waste scenario. Right: effect upon the total life cycle.

Considering the waste scenario itself, it is seen that the negative global warming potential may become positive, and thus a contribution to the global warming potential instead of a saving might be expected upon the recycling of CRC concrete. Looking at the total life cycle of the concrete mixtures, the global warming potential is expected to vary around the initial value calculated in chapter XIII by about 25% and 40% for CRC1c and CRC2b respectively. In case of CRC2b the global warming potential will still be significantly lower by 60-90% and 40-90% compared to T(0.50) and T(0.45) respectively. In the best case, the impact on global warming of CRC1c will be 60% and 50% lower compared to T(0.50) and T(0.45). In the worst case, the impact of CRC1c will be 25% lower compared to T(0.45), and comparable with T(0.50).

C. LCA sensitivity towards transport distances upon recycling

The impact on the environment of material transport in the life cycle of concrete is highly depending on the geographical location of not only the cement and concrete plant, the construction site and the sorting plant, but also on transportation method. Optimization of the transport system in the concrete life cycle will thus have a significant impact on the results. The latter was however outside the scope of this study. Nonetheless, since especially the environmental impact of the end-of-life scenario of concrete is highly depending on the transport distances, a sensitivity analysis regarding these transport distances was conducted.

For the calculation of the transport distances between the construction site and the sorting plant the distance between the Magnel laboratory in Ghent and the Flemish sorting plants associated to the FPRG (Federatie van Producenten van Recycling Granulaten – Federation of producers of recycling aggregates) was measured using Google Maps. The average distance was found to be 50 km, with a minimum and maximum of 10 and 150 km respectively. The distance between the sorting and cement plant was measured using the minimum distance between the sorting plant and one of the cement plants (with clinker production) in Belgium. An average value of 90 km was found with a minimum and maximum of 40 and 150 km respectively.

The minimum and maximum values were used to evaluate the impact of transport distances on the recycling scenario. These results are presented as error bars, on the results obtained in chapter XIII, in Figure B.4. In these graphs it is seen that the sensitivity of the environmental impact of the recycling waste scenarios is enormous. For both recycling opportunities the environmental impact is twice as high in the worst case scenario. A significant decrease is however obtained when the transport distances are strongly reduced. It can thus be concluded that the optimization of the transport system of a recycling scenario is crucial to increase its sustainability.

Finally also the sensitivity of the complete life cycle towards transport distances upon recycling was calculated and shown in Figure B.5. In the worst case scenario, the environmental impact of CRC or traditional concrete increases by about 20-50% and 10-40% in case of CRC and RCA recycling respectively. In the best case scenario, the environmental impact of CRC and traditional concrete can be reduced by about 10-30% and 5-15% in case of CRC and RCA recycling respectively. Thus the optimization of the transport system will not only affect the sustainability of the end-of-life scenario, but also in the whole concrete life cycle the results will be affected significantly.
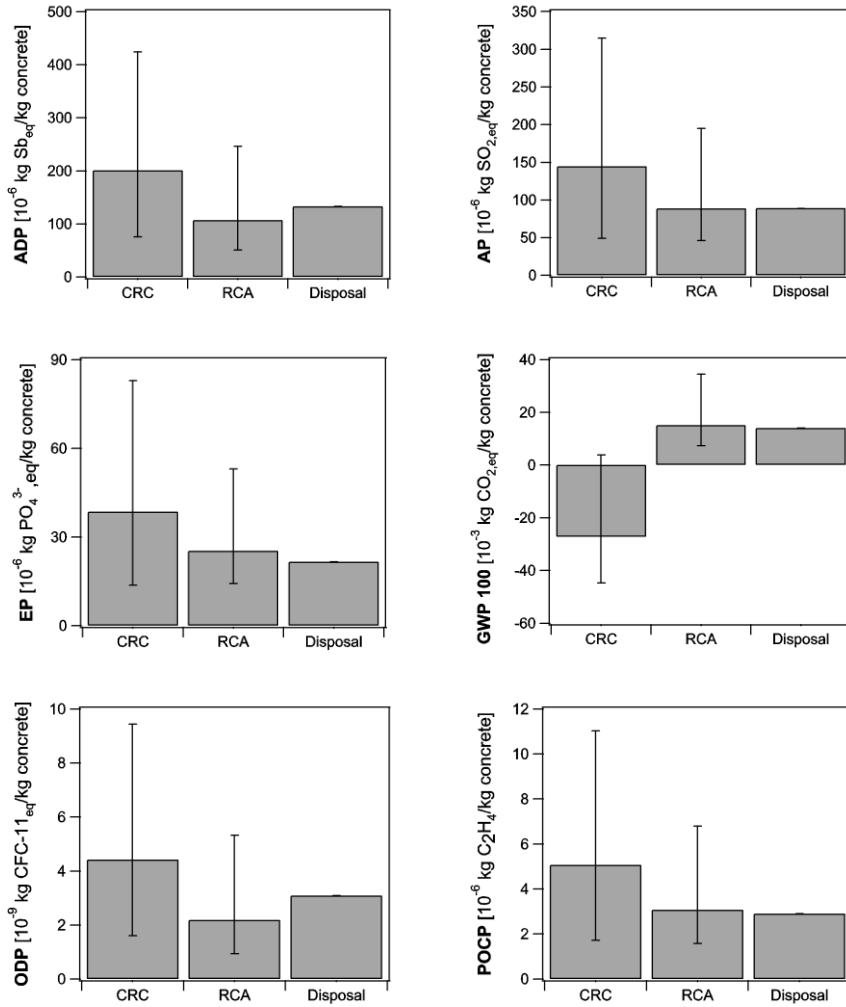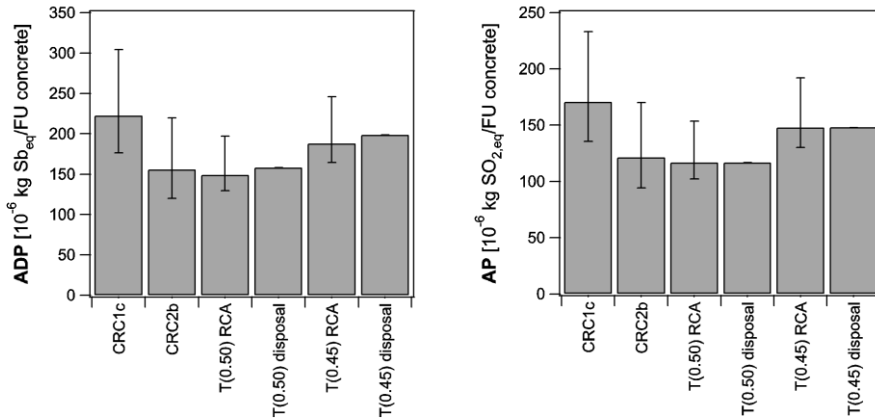
Figure B.4a – Life Cycle Impact Assessment of the different waste scenarios with the effect of transport distances upon recycling indicated by error bars.
CRC = Completely Recyclable Concrete; RCA = Recycling of traditional concrete as Recycled Concrete Aggregate; disposal = disposal of traditional concrete waste.
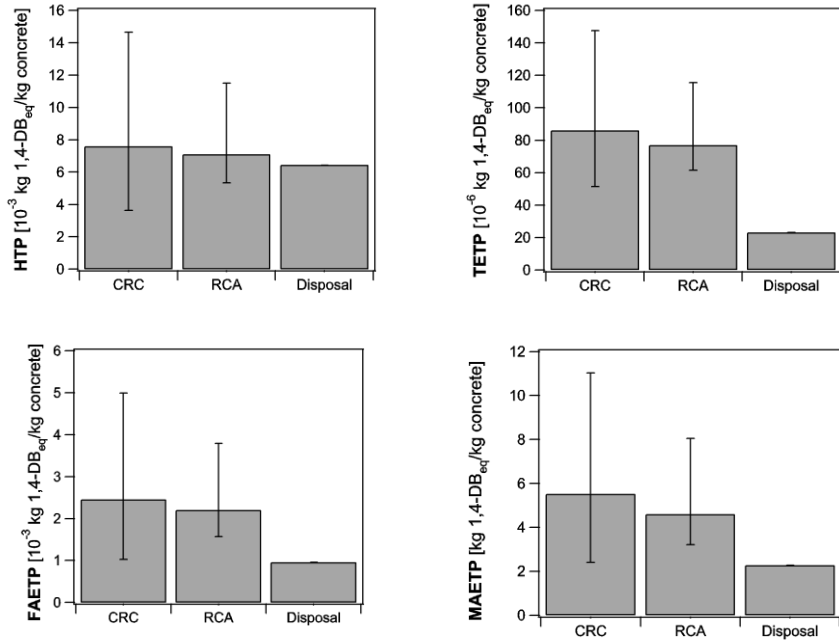
Figure B.4b – Life Cycle Impact Assessment of the different waste scenarios with the effect of transport distances upon recycling indicated by error bars. CRC = Completely Recyclable Concrete; RCA = Recycling of traditional concrete as Recycled Concrete Aggregate; disposal = disposal of traditional concrete waste.
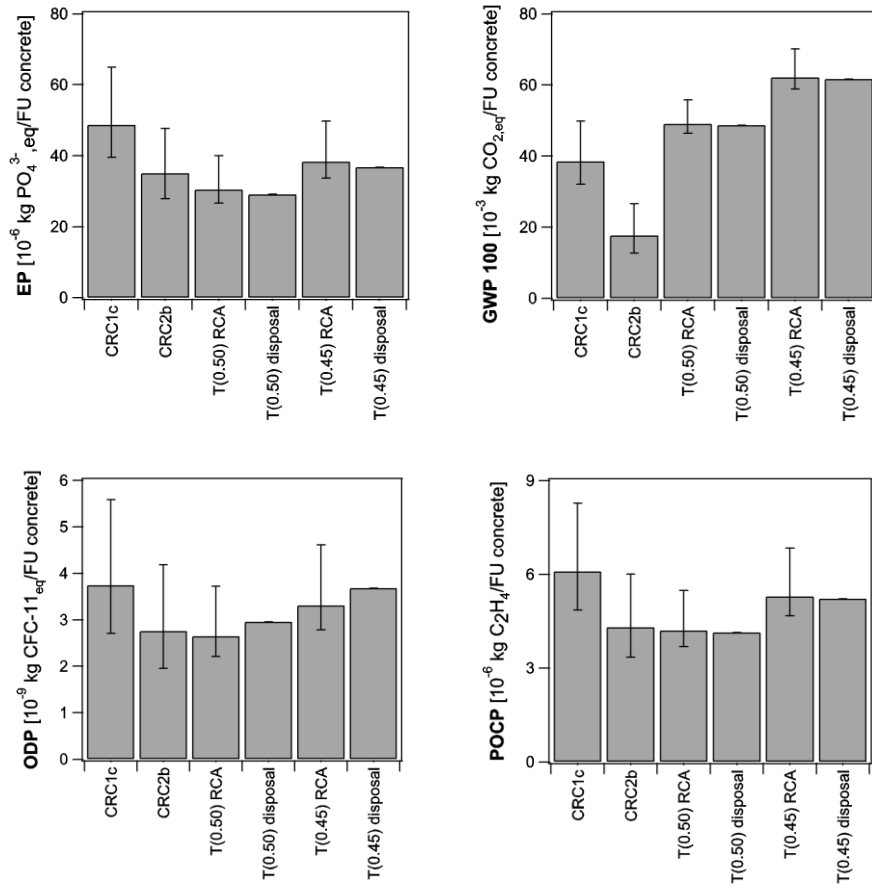

Figure B.5a – Cradle-to-cradle Life Cycle Impact Assessment of 1 FU concrete with the effect of transport distances upon recycling indicated by error bars. CRC = Completely Recyclable Concrete; RCA = Recycling of traditional concrete as Recycled Concrete Aggregate; disposal = disposal of traditional concrete waste.
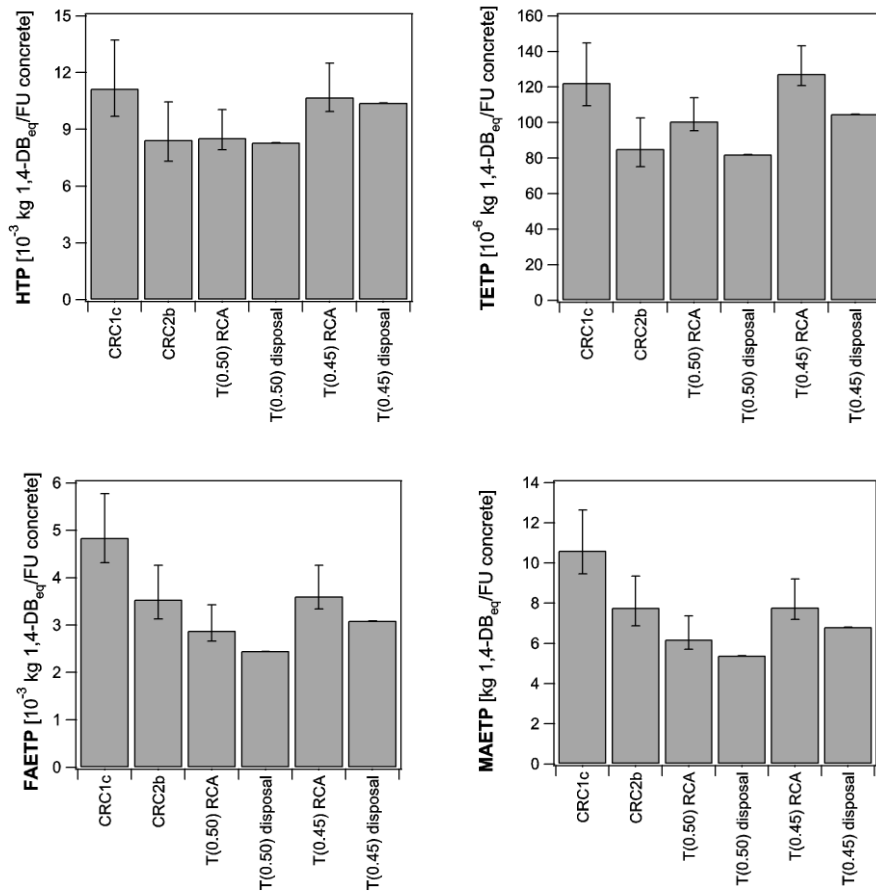
Figure B.5b – Cradle-to-cradle Life Cycle Impact Assessment of 1 FU concrete with the effect of transport distances upon recycling indicated by error bars. CRC = Completely Recyclable Concrete; RCA = Recycling of traditional concrete as Recycled Concrete Aggregate; disposal = disposal of traditional concrete waste.

Figure B.5c – Cradle-to-cradle Life Cycle Impact Assessment of 1 FU concrete with the effect of transport distances upon recycling indicated by error bars. CRC = Completely Recyclable Concrete; RCA = Recycling of traditional concrete as Recycled Concrete Aggregate; disposal = disposal of traditional concrete waste.

CURRICULUM VITAE

Mieke De Schepper

Curriculum vitae

Personal information

Name	Mieke De Schepper
Date of birth	August 30th, 1986
Place of birth	Beveren, Belgium
E-mail	midschep.deschepper@ugent.be

Education

<u>2009-2014</u> *Doctor in Civil Engineering*
Ghent University – PhD thesis 'Completely Recyclable Concrete for a More Environment-Friendly Construction'

<u>2004-2009</u> *Master of Science in Civil Engineering: Architecture* (Magna cum laude)
Ghent University – Master thesis 'Completely Recyclable Concrete for a More Environmental Friendly Construction'
  Awards: Honourable mention at the ENCI study award (2009) and short list for the KVIV engineers awards (2010)

<u>1998-2004</u> *Science-Mathematics (8 hours mathematics)*
Onze-Lieve-Vrouw-Presentatie (OLVP) – Sint-Niklaas

Additional courses

<u>2012</u> *Communication Skills: basics, negotiation skills, meeting skills, networking skills*
Doctoral schools – Ghent University

<u>2011</u> *General Didactics & Communication*
Specific teacher training – CVO Panta Rhei de Avondschool – Ghent

<u>2011</u> *Training for assistants*
Office for Educational Quality Control – Ghent University

<u>2011</u> *Crystal Chemistry*
Faculty of Sciences – Ghent University

<u>2010-2011</u> *Italian level 1*
Het perspectief – Ghent

<u>2010</u> *Advanced Academic English: Conference Skills*
UCT – Ghent University

<u>2010</u> *Thermodynamic Modelling in Cementitious Systems (3rd GEMS Workshop)*
Empa – Switzerland

<u>2010</u> *Concrete Microscopy Course*
TU Delft – The Netherlands

<u>2009</u> *Advanced Academic English: Writing skills*
UCT – Ghent Univeristy

Work experience

<u>2009-2014</u> *PhD student with SBO scholar ship (IWT)*
Faculty of Engineering & Architecture – Ghent University
> *Teaching activities*: Exercise classes in 'Concrete technology' and the lab sessions of 'Engineering project II' (Civil engineering).
> *Services for industry*: tests on hardened concrete and studies related to her research area

<u>2008</u> *Internship*
Bureau Bouwtechniek – Antwerp
> Designing technical installations for buildings

Scientific publications

A1 – Snellings R., <u>De Schepper M.</u>, De Buysser K., Van Driessche I. and De Belie N. (2012).
*C*linkering reactions during firing of recyclable concrete.
Journal of the American ceramic society. 95(5). p. 1741-1749.

A1 – <u>De Schepper M.</u>, De Buysser K., Van Driessche I. and De Belie N. (2013).
The regeneration of cement out of Completely Recyclable Concrete: Clinker production evaluation.
Construction and building materials. 38. p. 1001-1009.

A1 – <u>De Schepper M.</u>, Snellings R., De Buysser K., Van Driessche I. and De Belie N. (2014).
The hydration of cement regenerated from Completely Recyclable Concrete.
Construction and Building Materials. 60. p. 33-41.

A1 – <u>De Schepper M.</u>, Verlé P., Van Driessche I. and De Belie N..
The use of secondary slags in Completely Recyclable Concrete.
Journal of Materials in Civil Engineering. Accepted for publication May 2014.

A4 – <u>De Schepper M.</u> and De Belie N. (2010).
Cement, een grondstof voor betonproductie! Beton, een grondstof voor cementproductie?
Het ingenieursblad. 79(5). p. 50-53.

C1 – <u>De Schepper M.</u>, Van den Heede P., Windels C. and De Belie N. (2011).
The resistance of completely recyclable concrete to carbonation, chloride penetration and freeze-thaw attack with de-icing agents.
Proceedings of the 12th international conference on durability of building materials and components. Porto, 12-15 April 2011. Volume IV. p. 2061-2068.

C1 – <u>De Schepper M.</u>, Van den Heede P., Windels C. and De Belie N. (2011).
Life cycle assessment of completely recyclable concrete.
Proceedings of the 4th international conference on Non-traditional cement & concrete.
Brno, 27-32 June 2011. p. 67-76.

C1 – <u>De Schepper M.</u>, Vernimmen L., De Belie N., De Buysser K. and Van Driessche I. (2011).
The assessment of clinker and cement regenerated from completely recyclable concrete.
Proceedings of XIII ICCC International congress on the chemistry of cement. Madrid, 3-8 July 2011. p. 67 in abstract book, full paper on CD.

C3 – <u>De Schepper M.</u>, Snellings R., De Buysser K., Van Driessche I. and De Belie N. (2012).
Completely Recyclable Concrete: how does the cement paste behave during reclinkering?
Proceedings of the 3rd international conference on concrete repair, rehabilitation and retrofitting (ICCRRR). Cape Town, 3-5 September 2012. p. 484-485 in abstract book, full paper on CD-ROM.

C1 – <u>De Schepper M.</u>, Arvaniti E., Van Haute S., De Buysser K., Van Driessche I. and De Belie N. (2013)
Influence of raw material fineness on clinker produced from Completely Recyclable Concrete.
Proceedings of the first international conference on the chemistry of construction materials. Berlin, 7-9 October 2013. p. 19-22.

C1 –Arvaniti E., <u>De Schepper M.</u>, De Buysser K., Van Driessche I. and De Belie N. (2013)
The effect of chloride and sulfate on Completely Recyclable Concrete.
Proceedings of the first international conference on the chemistry of construction materials. Berlin, 7-9 October 2013. p. 465-468.

C1 – <u>De Schepper M.</u>, De Buysser K., Van Driessche I. and De Belie N..
Quantification of cement hydration by XRD/Rietveld analysis.
Proceedings of the 5th international conference on Non-traditional cement & concrete. Brno, 16-19 June 2014. Accepted May 2014.

P1 – <u>De Schepper M.</u>, Van den Heede P. and De Belie N. (2010).
The use of fly ash in completely recyclable concrete.
Rilem Proceedings. PRO 77. p. 35-43.